



University of HUDDERSFIELD

University of Huddersfield Repository

Charlton, Phillip

The Application of Zeeko Polishing Technology to Freeform Femoral Knee Replacement Component Manufacture

Original Citation

Charlton, Phillip (2011) The Application of Zeeko Polishing Technology to Freeform Femoral Knee Replacement Component Manufacture. Doctoral thesis, University of Huddersfield.

This version is available at <http://eprints.hud.ac.uk/14062/>

The University Repository is a digital collection of the research output of the University, available on Open Access. Copyright and Moral Rights for the items on this site are retained by the individual author and/or other copyright owners. Users may access full items free of charge; copies of full text items generally can be reproduced, displayed or performed and given to third parties in any format or medium for personal research or study, educational or not-for-profit purposes without prior permission or charge, provided:

- The authors, title and full bibliographic details is credited in any copy;
- A hyperlink and/or URL is included for the original metadata page; and
- The content is not changed in any way.

For more information, including our policy and submission procedure, please contact the Repository Team at: E.mailbox@hud.ac.uk.

<http://eprints.hud.ac.uk/>

THE APPLICATION OF ZEEKO POLISHING TECHNOLOGY TO FREEFORM FEMORAL KNEE REPLACEMENT COMPONENT MANUFACTURE

MR. PHILLIP CHARLTON BENG (HONS), MSC

A thesis submitted in partial fulfilment of the requirements of the University of Huddersfield
for the degree of Doctor of Philosophy

June 2011

ACKNOWLEDGEMENTS

The author of the thesis would like to acknowledge his parents Colin and Angela for financial and moral support as well as other close friends and family for their moral support throughout the studies.

A significant mention should be made to my Director of Studies Prof. Liam Blunt and my second supervisor Prof. Xiangqian (Jane) Jiang. Also he would like to Thank Allan Kennedy for assistance in sample preparation together with the staff at Eroda Tools Ltd. for their help and advice on fixturing.

He is also grateful to Anthony Beaucamp and all those at Zeeko Ltd. for their dedicated time in technical support and assistance to ensure his understanding of the operation of the machine.

Special gratitude goes to Cath Hardaker at Johnson & Johnson Depuy International, Leeds for supplying knee implant components for polishing and use of equipment for sample preparations.

Last but not least to all my colleagues at Huddersfield University and Hong Kong Polytechnic University that have not already been mentioned for their support, understanding and keeping me from going insane throughout the write-up of the thesis.

ABSTRACT

The purpose of this study was to develop an advanced 7-axis Computer Numerical Controlled (CNC) Polishing Machine from its successful original application of industrial optics manufacture into a process for the manufacture of femoral knee components to improve wear characteristics and prolong component lifetimes.

It was identified that the successful manufacture of optical components using a corrective polishing procedure to enhance their performance could be applied to femoral knee implant components. Current femoral knee implants mimic the natural shape of the joint and are freeform (no axis of symmetry) in nature hence an advanced CNC polishing machine that can follow the contours associated with such shapes could improve surface finish and conformity of replacement femoral knee bearing surfaces, leading to improved performance.

The process involved generating machine parameters that would optimize the polishing procedure to minimize wear of materials used in femoral knee implant manufacture. Secondly a design of a Non-Uniform Refined B-Spline (NURBS) model for control of the Polishing Machine over the freeform contours of the femoral component. Completing the process involved development of a corrective polishing process that would improve form control of the components. Such developments would improve surface finish and conformity which are well documented contributors to wear and hence the lifetime of orthopaedic implants.

By the means of comparison of this technique to that of a conventional finishing technique using pin-on-plate disc testing it was concluded that performance of the CNC polished components was an improvement on that of the conventional technique. In the case of form control there were slight indications through small decreases in peak to valley (PV) error that the process helped reduce form error and could increase the lifetime of femoral knee replacement components.

The overall study provided results that indicate that the Zeeko process could be used in the application of polishing of hard-on-hard material combinations to improve form control without compromising surface finish hence improving lifetimes of the implant. The results have their limitations in the fact that the wear test performance was only carried out on orthopaedic implant materials using a pin-on-plate wear test rig. Due to the time limitations on the thesis it can be said that further analysis of correcting form without compromising surface finish on entire implant systems under full joint simulator testing which would provide more realistic conditions would a more definitive answer be achieved.

LIST OF FIGURES

Figure 2.1 Schematics of Osteoarthritis	8
Figure 2.2 Schematic an X-Ray of Osteolysis.....	9
Figure 2.3 Degrees of Freedom of the Human Knee Joint.....	12
Figure 2.4 TKR movements that mimic the Human Knee Joint	13
Figure 2.5 Phases and Periods of the Human Gait Cycle.....	15
Figure 2.6 Normal (a) and Normal v OA (b) Knee Flexion Angle Plots.....	17
Figure 2.7 Flexion of Normal (a) PCL retained (b) & PCL Substituted (c) Knee	18
Figure 2.8 Pre TKR Designs.....	20
Figure 2.9 Uni-compartmental design replacing one femoral condole.....	23
Figure 2.10 Fixed Bearing Condylar Knee Design.....	24
Figure 2.11 LCS Complete Mobile Knee Replacement.....	26
Figure 2.12 Examples of Polyethylene Wear	29
Figure 2.13 Schematic (a) and X-ray (b) of Aseptic Loosening of a TKR	30
Figure 2.14 Schematic of instability (a) leading to TKR revision (b)	31
Figure 2.15 Infection in a TKR causing revision surgery	32
Figure 2.16 MRI Image of Arthrofibrosis	33
Figure 2.17 Schematic of Varus (a) and Valgus (b) misalignment	35
Figure 2.18 X-Ray of Malpositioning (a) & retrieved Tibial Tray component (b)	35
Figure 3.1 Flow Chart of the Manufacture of an Orthopaedic Implant Component	50
Figure 3.2 Milling (a) and Grinding (b) of defects after investment casting	53
Figure 3.3 Fanuc Robots Grinding Knee Implants in an Acme Manufacturing Robotic Cell	58
Figure 3.4 Schematic of the Fixed Abrasive Self Sharpening Process.....	61
Figure 3.5 Loose Abrasive and Carrier Components of Material Removal Mechanisms	64
Figure 3.6 Sharp Cutting leading to microchip generation on the surface.....	65
Figure 3.7 Rolling Grit causing micro fractures and cracking on the surface.....	66
Figure 3.8 Magnified Surface showing micro-cracks and micro fracture cavities	66
Figure 3.9 Blunt Ploughing of Abrasive Particles in the Finishing Process	67
Figure 3.10 Various Abrasive Granule Shapes.....	67
Figure 3.11 Monocrystalline (a) and Polycrystalline Granules (b)	68
Figure 3.12 Various Carrier Materials	69
Figure 3.13 Examples of Engineered Freeform Surfaces	71

Figure 3.14 Freeform Femoral Knee, Knee Cap and Tibial Tray Insert.....	71
Figure 4.1 Examples of Metrology for manufacture of a femoral knee component.....	75
Figure 4.2 Principles of Contact Measurement	80
Figure 4.3 Complexity of Freeform Femoral Knee Implant Components	87
Figure 5.1 Final Surface Roughness Ra (a) and Ra versus polishing time (b).....	95
Figure 5.2 Comparison of (a) Conventional and (b) Precessions Tool Marks	96
Figure 5.3 (a) Zeeko IRP200 and (b) 7-Axis Schematic	97
Figure 5.4 Uniform & Symmetrical I.F. on BK7 using the 1st IRP Machine	99
Figure 5.5 Examples of Polishing Modes on the Zeeko IRP Polishing Machines	103
Figure 5.6 Errors caused by incorrect relocation	106
Figure 5.7 Fixture Design to Eliminate Positional Errors	107
Figure 5.8 Problem Areas For Polishing of a Freeform Femoral Implant Component	107
Figure 5.9 Patented 10mm Radius Tool For Polishing Problem Areas	108
Figure 6.2 3M CR39 Glass Mineral Smoothing 12µm Yellow Cloth	115
Figure 6.3 Schematic of 316L Stainless Steel Samples Used For Taguchi Testing	116
Figure 6.12 Telum™ Nickel Bonded Diamond Polishing Pad from KGS Diamond Int.....	125
Figure 6.13 New & Used KGS Telum™ Nickel Bonded Diamond Cloth at 40x Mag.....	127
Figure 6.14 Best (a) and Worst (b) Cases of Nickel Bonded Diamond at 40x Mag.	127
Figure 6.15 Non Woven Abrasive Mats under a laboratory standard microscope.....	129
Figure 6.16 Lower influence function variations compared to KGS Bonded Diamond.....	130
Figure 6.17 Mechanical and FluidJet Material removal Mechanisms	131
Figure 6.18 Microscope Images After 1 st Run of Hybrid (a) and Fluidjet Only (b).....	134
Figure 7.1 Basics of Freeform Corrective Polishing Procedure	140
Figure 7.2 Design New Part Function with 40mm Flat Plano Design.....	141
Figure 7.3 Imported Part in ZeeCAD with Non Linear Correction Parameters.....	141
Figure 7.4 Generate DIF function in ZeeCAD	142
Figure 7.5 Influence Functions on 40mm Plano Cobalt Chrome Sample.....	142
Figure 7.6 2D Surface Profile Measurement of a Machine Influence Function.....	143
Figure 7.7 Imported Influence Function in Precessions 3D Software	144
Figure 7.8 Desired geometry of a freeform femoral knee implant component section	145
Figure 7.9 Taylor Hobson PGI 1240.....	146
Figure 7.10 Error Map Imported to Metrology Toolkit from Taylor Hobson PGI 1240.....	147
Figure 7.11 Precessions 3D Software for Optimised Corrective Polishing Process.....	148

Figure 7.12 Measured Data (a) and Designed Surface Matching (b)	148
Figure 7.13 Measurement Areas Images Before and After Corrective Polishing	151
Figure 7.14 Error Maps Before (a) and After (b) Corrective Polishing Process	153
Figure 7.15 Influence Function Generations on CoCr Sample.....	154
Figure 8.1 Schematic of Pin-on-Disc Wear Simulator Equipment.....	156
Figure 8.2 Cobalt chrome pin component CAD drawing showing dimensions	157
Figure 8.4 Positioning of Wear Test Pins in 3-Jaw Chuck on Zeeko IRP200 Machine	160
Figure 8.5 Best Machine and Hand Polished Pin Surfaces Pre-Wear Testing	161
Figure 8.6 Weight Loss of UHMWPE (Plastic) during Co-Cr Pin on Disc Testing	163
Figure 8.7 Inverse wear track profile of machine polished pin after 2 million cycles.....	164
Figure 8.8 Inverse wear track profile of machine polished pin after 2 million cycles.....	165
Figure 8.8 Sample Disc Manufactured from Forming Tool.....	166
Figure 8.9 Setup for polishing sample discs on Zeeko IRP200 Machine	167
Figure 8.10 Teer Coatings Pin-on-Plate Wear Test Rig.....	169
Figure 8.11 Modified Pin-on-Plate Wear Test Rig Setup	169
Figure 8.12 Interferometer process to determine wear volume loss of test discs	170
Figure 8.13 Comparison of methods for effect of disc edge radius on wear volumes.....	171
Figure 8.14 Comparison of methods for effect of surface roughness on wear volumes.....	172
Figure 6.1 Taguchi Orthogonal Array Selection Table.....	I
Figure 6.4 One way ANOM of 3D Surface Roughness Sa (nm) for Head Speed (RPM)	IV
Figure 6.5 One way ANOM of 3D Surface Roughness Sa (nm) for Head Pressure (Bar)	IV
Figure 6.6 One way ANOM of 3D Surface Roughness Sa (nm) for Precess Angle (°)	V
Figure 6.7 One way ANOM of 3D Surface Roughness Sa (nm) for X-Y Spacing (mm)	V
Figure 6.8 Main effects Plot of Sq	VI
Figure 6.9 Main effects Plot of Spk	VI
Figure 6.10 Main Effects Plot of Sk	VII
Figure 6.11 Main Effects Plot of Svk.....	VII

LIST OF TABLES

Table 2.1 Statistics Related to Knee Joint Loading during Various Activities	14
Table 2.2 A Summary of Pre TKR Designs	21
Table 2.3 Comparison and Advantages/Disadvantages of Condylar v Mobile TKR's	27
Table 2.4 Common failure mechanisms and % presence in 212 Revision TKRs	28
Table 2.5 Advantages and Disadvantages of Bearing Surfaces of Prosthetics	36
Table 2.6 Comparison of common ceramic-ceramic/UHMWPE bearing combinations.....	40
Table 3.1a Comparison of ISO and CAMI Standards for Macro Grits	59
Table 3.1b Comparison of ISO and CAMI Standards for Micro Grits.....	60
Table 3.2 Forms of Fixed Abrasive Bonding Materials.....	62
Table 3.3 Chemical Compositions of Materials and Loose Abrasives	67
Table 3.4 Summary of Research into Prediction of Free Abrasive Metal Removal.....	69
Table 4.1 Standards information for the metrology of TKRs	76
Table 4.2 Surface Metrology Guidelines for Articulating THR Surfaces.....	77
Table 4.3 Surface Metrology Guidelines for Articulating TKR Surfaces.....	78
Table 4.4 Contact/ Non-contact Measurement Equipment used in Implant Applications.....	81
Table 4.5 Some 3D Surface S-Parameters with Implant Manufacturing Applications	85
Table 4.6 Some 3D Surface V-Parameters with Implant Manufacturing Applications.....	86
Table 4.7 Summary of Fitting Techniques for Freeform Rough Stage Fitting	88
Table 4.8 Summary of Wear Test Simulation Techniques for Implants.....	90
Table 4.9 Summary of Wear Measurement Techniques for Implants	91
Table 5.1 Form error of components machined using Zeeko Software Packages.....	98
Table 5.2 Zeeko Machine Parameters	101
Table 6.1 Factors with their assigned levels for the Taguchi testing	114
Table 6.4 Statistical data of combined averages of Taguchi Test Runs 1 & 2.....	117
Table 6.5 General Analysis of 3D Measurements Conclusions for 12 μ m Cloth	119
Table 6.6 Two run average filtered Sa values used in ANOM.....	120
Table 6.8 ANOM Closest Values to Upper and Lower 99.9% C.L. and Mean Values.....	121
Table 6.9 Summary of effects of machine parameters on Sq values	122
Table 6.10 Summary of effects of machine parameters on Spk values	123
Table 6.11 Summary of effects of machine parameters on Sk values	123
Table 6.12 Summary of effects of machine parameters on Svk values	124

THE APPLICATION OF ZEEKO POLISHING TECHNOLOGY TO FREEFORM
FEMORAL KNEE REPLACEMENT COMPONENT MANUFACTURE

Table 6.13 Rankings of Factors for 3D Parameters Sq, Spk, Sk and Svk.....	124
Table 6.15 Sample 1 Parameters – Hybrid Polishing (Mechanical and FluidJet).....	132
Table 6.16 Sample 2 Parameters – FluidJet Polishing.....	133
Table 6.17 Analysis after 1 st Polishing Run for Samples 1 and 2	134
Table 6.18 Analysis after 2nd Polishing Run for Samples 1 and 2	135
Table 6.19 Analysis after 4 th Polishing Run for Samples 1 and 2	135
Table 6.20 Summary of ANOM Technique Results.....	138
Table 7.1 Influence Function Parameters and Dwell Map for Corrective Polish.....	152
Table 7.2 Surface Roughness Measurements Before and After Corrective Polishing	152
Table 7.3 Parameters for Influence Functions on CoCr Curved Samples	154
Table 7.4 Influence functions Generated on Curved CoCr Sample Surface	154
Table 8.1 Summary of Zeeko IRP200 Form Corrected Used in Wear Tests.....	159
Table 8.2 Machine (MP) and Hand Polished (HP) Pin Surfaces Pre-Wear Testing	161
Table 8.3 Summary of 2D Stylus Trace Averages for Pins after Wear Testing.....	165
Table 6.2 Taguchi L16b Orthogonal Array with Factors Assigned to Columns.....	II
Table 6.3 Random Run Number, Test Number & Filtered Sa Values for Taguchi Tests	III

TABLE OF CONTENTS

ACKNOWLEDGEMENTS.....	i
ABSTRACT.....	ii
LIST OF FIGURES.....	iii
LIST OF TABLES	vi
TABLE OF CONTENTS	viii
1 INTRODUCTION	1
1.1 Hypothesis	2
1.2 Aims and Objectives.....	2
1.3 Structure of the Thesis.....	4
1.4 Contributions to Knowledge	5
1.4.1 Optimisation of Surface Roughness of Implant Materials.....	5
1.4.2 Performance of Zeeko polished orthopaedic implant materials.....	6
1.4.3 Form correction of a freeform femoral knee joint component	6
2 HISTORY AND CURRENT STATUS OF KNEE IMPLANTS.....	7
2.1 Introduction to Knee Implants	7
2.1.1 Osteoarthritis.....	7
2.1.2 Total Knee Replacement	11
2.1.3 Why TKR Implants Fail.....	26
2.1.4 Current Developments in TKRs Materials to Prevent Implant Failures.....	34
2.2 New materials.....	42
2.3 The Tribology of Wear	43
2.4 Summary.....	46
3 MANUFACTURING OF KNEE IMPLANT COMPONENTS	48
3.1 Manufacture of Knee Implants	48
3.1.1 Initial Casting/Forging.....	51
3.1.2 Machining.....	52
3.2 Final Finishing of Biological surfaces	54
3.2.1 Manual process	55
3.2.2 Semi and Fully Automated.....	56
3.3 Polishing Media	58
3.3.1 Fixed Abrasive	60
3.3.2 Loose Abrasive and Carrier Material.....	63
3.4 Basic Material Removal Mechanisms in Final Finishing.....	64
3.4.1 Sharp Cutting	64
3.4.2 Rolling Grit	65
3.4.3 Blunt Ploughing.....	65
3.5 Simple modelling of material removal mechanism in final finishing	66
3.6 Why Freeform Surfaces in Knee Implant Design?	70
3.6.1 Need for Freeform Surfaces	70
3.6.2 Freeform Femoral and Tibial Insert Knee Components	71
3.7 Summary.....	72

THE APPLICATION OF ZEEKO POLISHING TECHNOLOGY TO FREEFORM
FEMORAL KNEE REPLACEMENT COMPONENT MANUFACTURE

4	METROLOGY & TEST METHODS FOR IMPLANT MEASUREMENTS.....	74
4.1	Metrology needs of implant surface manufacture	75
4.1.1	Standards for Measurement	76
4.1.2	Instrumentation.....	79
4.1.3	Surface Characterisation of implant surfaces.....	80
4.1.4	Simulation Tests.....	88
4.1.5	In-vivo reviews.....	89
4.2	Summary.....	92
5	ZEEKO IRP200 7-AXIS CNC POLISHING MACHINE.....	95
5.1	Developments of the Zeeko IRP machines in the optics industry	98
5.2	Types of polishing processes available on the Zeeko IRP machines	99
5.3	Machine parameters.....	100
5.3.1	Polishing Modes	102
5.3.2	Feed Rate	103
5.4	Development to Freeform Surfaces and Improved Biological Implants	103
5.4.1	Tool path generation.....	104
5.4.2	Surface Quality.....	104
5.4.3	Form Error Reduction	105
5.4.4	Fixturing Issues	105
5.4.5	Polishing Issues	106
5.4.6	Metrology Issues	108
5.4.7	Adaption of an optimized process to other materials	109
5.5	Summary.....	109
6	OPTIMISING PARAMETERS FOR 316L STAINLESS STEEL	111
6.1	Taguchi Testing for One Stage of the Polishing Process	112
6.1.1	Selection of Zeeko IRP200 machine parameters for Taguchi tests.....	113
6.1.2	Selection of number of levels for machine parameters	113
6.1.3	Selection of the appropriate orthogonal array.....	114
6.1.4	Assignment of the factors and/or interactions to columns	114
6.1.5	Conducting tests.....	115
6.1.6	Analysis of Results	116
6.2	Study of Diamond and Non-Wooven Alumunia Oxide Polishing Pads.....	125
6.3	Capability Study : FluidJet and Hybrid FluidJet/Mechanical Polishing	131
6.4	Summary.....	136
7	ZEEKO CORRECTIVE POLISHING METHOD.....	139
7.1	Influence Function Creation	140
7.2	Corrective Polish CNC file generation	143
7.2.1	Influence Function Data.....	144
7.2.2	CAD Model modification and NURBS conversion.....	145
7.2.3	Measured Surface Topography of Component to be corrected.....	146
7.3	Optimizing corrective polish procedure.....	147
7.4	Form Correction of an area of a Freeform Femoral Knee Component	147
7.4.1	Corrective Polishing Results.....	150
7.5	Summary.....	155

THE APPLICATION OF ZEEKO POLISHING TECHNOLOGY TO FREEFORM
FEMORAL KNEE REPLACEMENT COMPONENT MANUFACTURE

8	PERFORMANCE OF ZEEKO POLISHED ORTHOPAEDIC MATERIALS..	156
8.1	Zeeko form correction polished pins vesus hand polished polished	157
8.1.1	Sample Preperation.....	157
8.1.2	Simulator Test Parameters	162
8.1.3	Analysis of Results	163
8.2	Pin on disc testing for Diamond Like Coatings (DLC's).....	166
8.2.1	Sample Preperation.....	166
8.2.2	Simulator Test Parameters	168
8.2.3	Analysis of Results	171
8.3	Summary.....	172
9	OVERALL DISCUSSION.....	174
9.1	Surface Roughness Optimisation.....	174
9.2	Form Correction of a Freeform Femoral Knee Implant Component.....	177
9.3	Wear Performance of Zeeko Polished Implant Materials	181
10	CONCLUSIONS	184
11	FUTURE WORK.....	186
	REFERENCES	187
	SELECTED LIST OF PUBLICATIONS.....	208
	APPENDIX.....	I

CHAPTER 1: INTRODUCTION

1 INTRODUCTION

Current manufacture of freeform femoral knee implant component is proving to be a difficult task due to the non uniform and non symmetrical nature of surfaces. The components are firstly cast or formed, machined to micron level form error and then super finished to low level nanometre surface roughness whilst maintaining or improving the form achieved from post machining.

McGloughlin and Kavanagh (2000) [1] studied surface topography, third-body debris, load, contact mechanics and material quality in the wear process. The combination of form and surface finish is critical in future developments of knee implants as witnessed by a tribological study by McCann et al (2009) [2].

Whereas maintaining form and surface finish of freeform femoral knee replacement surfaces is in comparison a new research area with the need for in depth research. Such research areas include not only the manufacturing of freeform surfaces but also the instrumentation and measurement standards used to ensure correct tolerances are achieved and maintained throughout manufacture.

The present research targets secondary form correction and super finishing of a freeform femoral knee implant surface through the use of advanced CNC machining and current instrumentation devices and measurement standards.

Current practice uses a combination of highly skilled hand polisher's or limited axis CNC polishing machines which can achieve surface finishes in the region of nanometres that current standards dictate. Even with a great eye for detail these skilled humans can not maintain the low levels of form control that could significantly reduce wear characteristics of knee replacements to substantially higher than that currently being achieved.

1.1 Hypothesis

The wear particles generated when the two load bearing surface associated with knee implants come into contact are problematic due to the adverse reaction they have on the human body. Such particles cause premature rejection and in most cases premature failure of the implant which becomes a traumatic experience to the patient, requiring further surgery.

Determining aims and objectives for this thesis defines the potential capability of the Zeeko polishing process to improve the lifetime of femoral knee implants through enhanced surface finish and form correction at the final stages of the manufacturing process.

The overall goal being demonstration that the Zeeko machine process can create better conformance, clearance and surface finish, reducing the wear between mating parts, hence increasing the lifetime of the prosthesis by the reduction of catastrophic failures associated with wear particle generation.

The ability to correct and finish components to CAD design specifications by a Computer Numerical Control (CNC) finishing process, highlights the capability to develop the Zeeko polishing machine into a manufacturing processes of the future, especially with the accelerating trends of freeform components such as knee implants.

1.2 Aims and Objectives

The aim of the present study is to develop an advanced 7-axis CNC polishing machine manufactured by Zeeko Ltd. to machine Cobalt Chrome (CoCr) based alloy implants enhancing the manufacturing process and also bringing economic benefits to manufacturing companies as well as a better quality of life to the patient after implantation.

Due to the success of the Zeeko polishing process in the optics industry the question that arose and brought about this study was “could it be applied to other industrial applications and in particular in the case of this thesis could it be used to improve the lifetime of prosthetic hip and knee replacements by improving surface finish and form?”

The specific aims and objectives are given below: -

Aims

- Investigate and develop the Zeeko polishing process to final finish a free form knee joint bearing surface.
- Demonstrate improved functional performance of Zeeko machined polished femoral implant materials (collaborative company results to be used here).
- Develop an understanding of material removal mechanism when form correcting and polishing bio-compatible materials.

Objectives

- Use the Zeeko machine to attain surface roughness levels required.
- Use the Zeeko machine to obtain improved geometrical control of femoral knee specimens.
- Implement Taguchi methodologies to optimise the machining process.
- Use Zeeko software for final finishing of femoral knee implant components.
- Analyse and investigate associated metrology for checking femoral knee joint implant geometry.
- Carry out wear performance using pin-on-plate testing.
- Develop an understanding of the material removal mechanisms in, “grolishing” polishing and fluidjet process for femoral knee implant materials.
- Develop the process for other bio-materials.

1.3 Structure of the Thesis

The structure of this thesis is as follows: -

Chapter 1 introduces the thesis and the work carried out throughout its duration.

Chapter 2 reviews literature that has been published related to the topics of this thesis. Topics include an introduction to orthopaedic implants, the history of Total Hip Replacements (THR) and Total Knee Replacements (TKRs), implant failure mechanisms and current developments in the prevention of implant failures.

Chapter 3 covers the manufacturing process of hip/knee implant components from initial casting/forging through to final finishing and the polishing media. An introduction to freeform surfaces and their use in orthopaedic implants concludes the chapter.

Chapter 4 aims to identify the methodologies and test methods required for measurement of implant manufacture including measurement standards, contact and non-contact measurements and simulation (in-vivo) trials of orthopaedic implants before implantation.

Chapter 5 introduces the Zeeko 7-axis CNC polishing machining including the machine parameters and development to freeform surfaces and the improvement of the lifetimes of orthopaedic implants.

Chapter 6 covers the research associated with optimising machine parameters for polishing orthopaedic implant materials using conventional and fluid jet polishing processes as well as testing of a hybrid process involving both techniques.

Chapter 7 incorporates the research into the corrective polishing process that was trialled for the possible improvement of form control of a femoral knee implant component that could help reduce wear and improve lifetimes of the joint.

Chapter 8 covers the simulation testing of implant materials through pin-on-plate testing to determine whether or not the Zeeko polishing process can perform better than that of a conventional technique.

Chapter 9 is an overall discussion/critical analysis of the project.

Chapter 10 is a conclusion of the findings from the thesis.

Chapter 11 includes some indications for future work.

1.4 Contributions to Knowledge

The contributions to knowledge produced by this PhD thesis include the following: -

- Optimisation of surface roughness of implant materials using Zeeko Bonnet, Zeeko Fluidjet and combinational Hybrid processes.
- Assessment and reporting of the performance of Zeeko polished orthopaedic implant materials.
- Use of the Zeeko machine, Zeeko software and metrology for form correction of a freeform femoral knee joint component.

These contributions to knowledge have been reported in several publications and at international conferences throughout the duration of this PhD as seen in the publications list and contained in the Appendix.

1.4.1 Optimisation of Surface Roughness of Implant Materials

Using Taguchi analysis techniques the surface roughness of 316L Stainless Steel and Cobalt Chrome implant materials were optimised.

Use of Taguchi techniques eliminates the time consuming and expensive trial and error methods currently used in optimisation the manufacturing process of orthopaedic implants. Zeeko conventional and Zeeko fluid jet optimisation methods have been compared.

1.4.2 Performance of Zeeko polished orthopaedic implant materials

Using the knowledge gained from the optimisation of the polishing process samples of uncoated and Diamond Like Carbon (DLC) coated cobalt chrome were prepared. A cobalt chrome on UHMWPE (pin-on-disc) and DLC coated cobalt chrome on uncoated cobalt chrome (modified pin-on-disc) wear simulation tests were performed. The results obtained were used to analyse the performance of Zeeko machine to reduce wear in orthopaedic implant materials.

1.4.3 Form correction of a freeform femoral knee joint component

The Zeeko corrective polishing process used for form correction of optical glasses was adapted to the correction of a freeform femoral knee joint component. The process included the use of Zeeko software to develop a known material removal for cobalt chrome gathered from measurement data retrieved from suitable metrology equipment. This information was transformed in to a CNC program allowing material removal at a controlled rate over the freeform femoral knee joint component surface improving the form of the component. This process would aid in validating the Zeeko machine as a possible candidate for manufacture of orthopaedic implants in the future.

CHAPTER 2: History and Current Status of Knee Implants

2 HISTORY AND CURRENT STATUS OF KNEE IMPLANTS

This chapter of the thesis is intended to give the reader a background into the history and current status of orthopaedic implants with an emphasis on the load bearing joints of knee replacements.

2.1 *Introduction to Knee Implants*

It is a well documented fact that in the developed world the general population is aging and the percentage of elderly people (over 65 years old) is growing rapidly. The result of this demographic change is an increasing demand on healthcare. One of the major concerns in the ageing population is that of arthritic conditions in particular osteoarthritis being the main cause of problems in the load bearing surfaces of knee joints.

2.1.1 *Osteoarthritis*

Osteoarthritis (OA) as seen in Figure 2.1 is the progressive degeneration of the natural cartilage tissue which plays a critical part in the load bearing function of the knee joint. Commonly it is the main cause of the initial problems associated with the need for medical implants. [3] OA caused 8.5 million cases of disability alone in the UK in 2009. [4]

OA develops over time through everyday activities but more critically heavy duty work and sporting activities which create excessive strain on the load bearing joints of the knee causing excessive cartilage damage. Such damage cannot be regenerated by the body which leads to bone on bone contact (Brandt 2008) [5]. Siddique and Laborde (2008) [6] report that in such cases contact of Suchondral bone generate eburnation areas of dense bone which is termed as osteoarthritis and is diagnosed by symptoms of inflammation, joint pain, tenderness, stiffness, creaking and locking of joints.

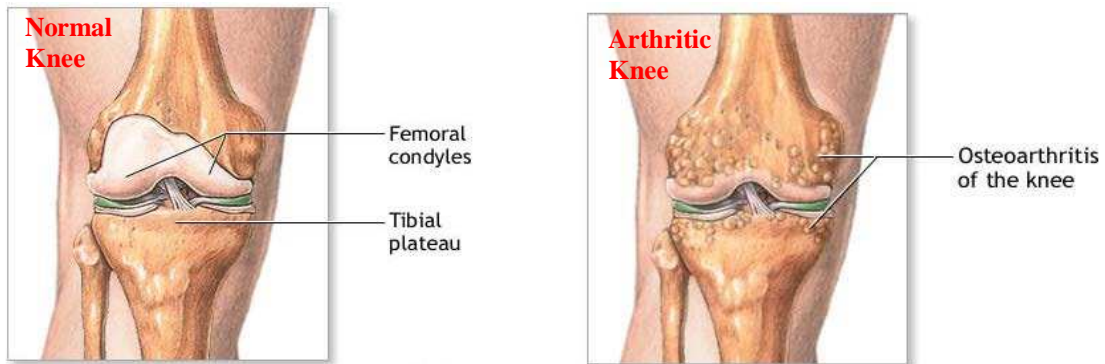


Figure 2.1 Schematics of Osteoarthritis [7]

OA is diagnosed as either Primary or Secondary. Primary OA involves chronic degeneration of the joint which is related to, but not necessarily caused by aging. Secondary OA is caused by factors other than that of aging cartilage i.e. ligament damage [8], diabetes [9], septic infections [10] and obesity [11].

Solutions to both Primary and Secondary OA problems require initial administration of anti-inflammatory drugs to suppress the pain and reduce swelling. If not successful as observed in most advanced cases then replacement of all or part of the joint with artificial components is essential.

The National Joint Register in England and Wales records knee joint replacements carried out each year. Data collection began in April 2003 they recorded 71,527 primary knee surgeries were recorded in the current period (April 2008-March 2009) [12]. The department of health quotes a cost of £6,182 in 2008 [13] for a knee surgery with its new fixed price surgery costs, giving a total cost of approximately £442.17 million for the year 2008-2009. Worldwide, the total number of all types of implants is approaching 1 million. [14] Over many years considerable research has been conducted concerning the design and function of artificial joint systems. Today the life expectancy of such systems can range from 5-15 years.

Currently the most common medical implant system comprises of a metallic component running on a polymeric bearing surface. Throughout the lifetime of the joint wear occurs, although this is normally within acceptable levels. However in some joints ranging between 0-10 years after the joint is implanted [15-18] a process of aseptic loosening occurs causing joint failure. In these defective systems considerable wear occurs at this interface generating wear particles which in turn trigger an immune response called Osteolysis (Figure 2.2). Such a response produces osteoclasts which attack and break down bone surrounding the implant (causing bone resorption) leading to loosening of the joint [19-21]. Once at this stage, the joint is deemed to have failed and is replaced prematurely.

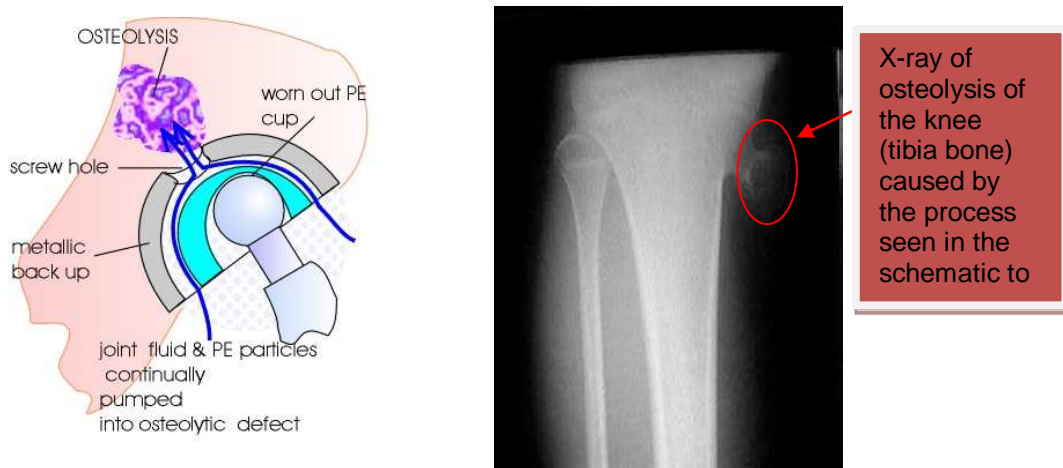


Figure 2.2 Schematic an X-Ray of Osteolysis [22, 23]

The development of medical implants has evolved over the past 300 years. However, much of the medical breakthroughs have been in the past 30 years albeit many of the theories associated with these developments date back to surgeons who designed and performed the first implant surgeries. Their theories could not be proven due to limited knowledge/advances in manufacturing techniques and materials used in the design and implantation of medical implants at that time.

The development of new materials to counteract the generation of wear particles resulting from the loading and motions of the medical implant is a current hot research topic. The thrust of much recent research in the field of joint replacements is the use a hard on hard bearing couples using metal-on-metal, metal-on-ceramic or combinations rather than the traditional metal-on-Ultra High Molecular Weight PolyEthelene (UHMWPE) and the tackling the problems associated with them to increase their potential alternative bearing surfaces for implants. [24-32]

Difficulties surrounding the manufacture of hard on hard bearings include: -

1. Surface Roughness – defined as the transcendent irregularities in the texture of the surface normally relating to the manufacturing process used to generate the surface i.e. grinding, turning, polishing etc. The most common way to represent surface roughness is through the two dimensional reference value (Ra) which is an arithmetic average of the deviation of the sum of all peaks and valleys in single trace measurement. Ra is normally measured in micrometres or for smoother surfaces Ra is defined in nanometres. The surface roughness of biological surfaces especially those of orthopaedic implant load bearing surfaces i.e. hip and knee implants can greatly affect the wear resistance and characteristics of the materials. Minimising roughness increases the likelihood of full fluid film lubrication.

It has been well documented that the lower the surface roughness value (Ra) of the load bearing materials the less wear particle generation will be created, [33-35] hence reducing the chances of particle induced aseptic loosening of the orthopaedic implant components. With the optimum goal of increased implant lifetimes manufacturers are constantly striving to maintain surface roughness values in and below the 20nm guidelines set by International Standards Organisations.

2. Form Control – defined as keeping the deviation from a controlled shape to as minimal as possible i.e. in the case of a hip joint the form will be controlled to within $\pm 50\mu\text{m}$ from a sphere of a given diameter stipulated in the CAD model drawing of the femoral head. The form of bearing components has been

investigated by Price et al (2005) [36] showed that better form control of the components could enhance clearances creating the correct volume of lubrication to fill the bearing surface gap and reduce wear particle generation. The area filled by synovial fluid is known as the thin film lubrication layer and achieving the correct level of thin film lubrication can reduce friction and minimise wear characteristics of the bearing surfaces investigated by Wang et al (2008) [37].

Supporting the manufacture of hard-on-hard bearing combinations requires an extremely low surface roughness and excellent conformances of the mating parts. Such necessities can only be achieved using advanced manufacturing techniques.

The above requirements can be achieved in the case of simple geometry implants e.g. the hip although not without some difficulties (Harrysson et al (2008), Mitsuyoshi et al (2004) and Novikov et al (2005)) [38-40]. For more complicated medical implant surfaces e.g. those which can not be determined through geometric shapes or symmetry i.e. knee systems; the use of hard on hard bearings has up till now been precluded by the need to obtain the conformance and roughness constraints on the effectively freeform knee surfaces. As such even simple development work has been very difficult.

A review of the evolution of the knee will be discussed in the sections to develop an understanding of where the research associated with this thesis has evolved.

2.1.2 Total Knee Replacement

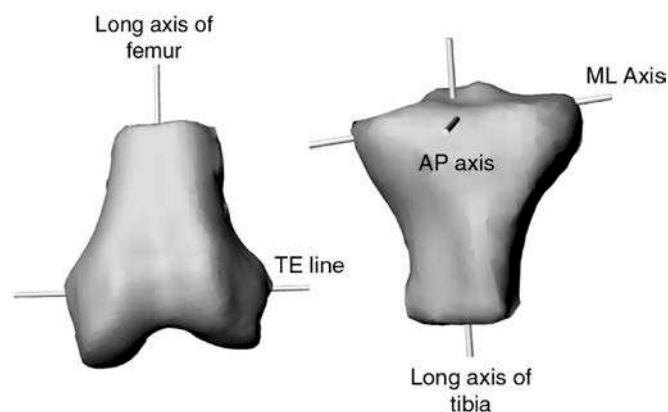
2.1.2.1 Freedom of the Human Knee Joint

Due to flexibility of the cartilage which lies between the bone surfaces of the human knee joint the joint itself is allowed to move freely in six degrees of freedom consisting of one translational and one rotational plane along the Anterior-Posterior and Medial-Lateral Axes which intersect with the long axis of the tibia as well as the

Transepicondylar Line which intersects with the long axis of the femur as outlined in Figure 2.3.

The degrees of freedom of a TKR need to match the movements of the human knee joint as seen in the TKR shown in Figure 2.4

The degrees of freedom shown in Figures 2.3 and 2.4 need to be considered in not only the initial design of the TKR but also considered in the design and manufacture of the equipment used to test/simulate the TKR performance before release into the market. Not only degrees of freedom need to be considered but the factors of loading, forces and gait cycle mentioned in the preceding sections have to mimic that witnessed by that of a human knee joint.



AP = Anterior-Posterior ML = Medial-Lateral and TE = Transepicondylar

Figure 2.3 Degrees of Freedom of the Human Knee Joint [41]

2.1.2.2 Loading of the Knee Joint

Loading of the knee joint is dependent on the activity undertaken with research existing for such activities as uphill and downhill walking, sitting to standing through to sporting activities.

Load bearing of the knee joint is the force applied to the knee joint during the activity and is usually measured in multiples of body weight with sometimes statistical

information relating to contribution of the loading i.e. ground reaction force, bone on bone compressive force etc. Values taken from research carried out on load bearing of the knee joint during various

activities can be seen in Table 2.1 with reference to multiples of body weight in terms of maximum bone on bone compression forces.

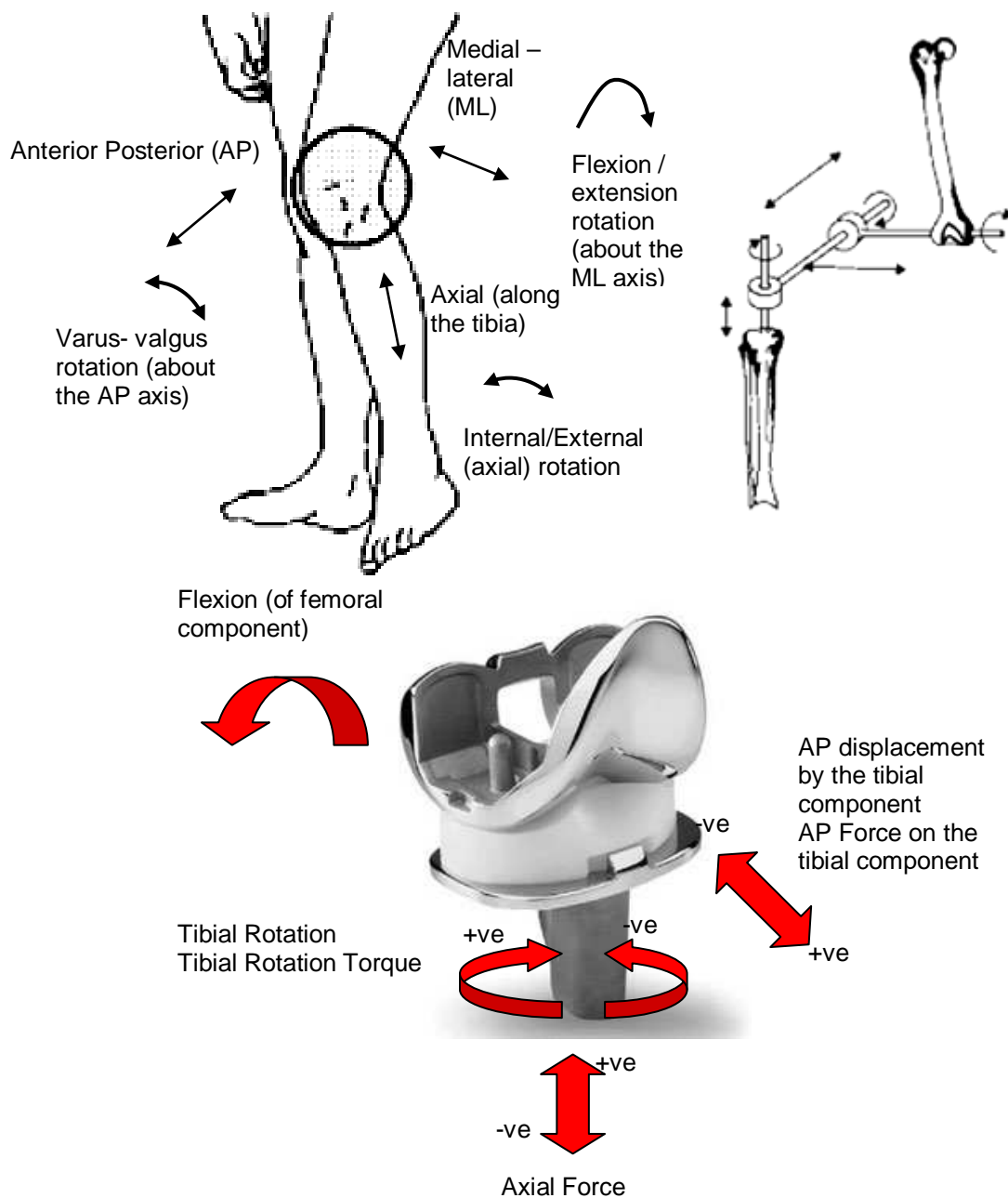


Figure 2.4 TKR movements that mimic the Human Knee Joint [42]

Research shows that in the majority of cases loading statistics related to the knee joint increases in knees that are deformed or disease infected. Besier et al (2009) [43] reported that patella femoral pain patients witnessed higher joint contact forces and stresses than those of pain free patients during walking and running activities.

Whereas Henriksen et al (2006) [44] conclude that even when using pain relief medication in treatment of mild medial knee OA increased joint loads during the final phase of walking gait were witnessed, albeit less compressive force was evident through pain relief treatment than that of the control group. Increased joint loads could cause enhanced progression of the disease a theory also backed by studies carried out Baliunas et al (2002). [45]

Table 2.1 Statistics Related to Knee Joint Loading during Various Activities [46-50]

Research	Activity	Maximum Bone on Bone Compression Force (x Body Weight)	
Kuster et al (1997)	Level Walking	3.4 (Male)	3.7 (Female)
	Downhill Walking	7 (Male)	8 (Female)
Costigan et al (2002)	Stair Climbing	3-5 (Mixed Sex)	
Christina & Cavanagh (2002)	Stair Decent	1.4 – 1.48 (Mixed Sex aged 21-27)	1.48-1.50 (Mixed Sex aged 71-75)
Nisell and Ericson (1992)	Jogging	12 (Male)	
	Running	7.5 (Male)	
Rodosky et al (1989)		Right Knee (Mixed Sex aged 20-35)	Left Knee (Mixed Sex aged 20-35)
	Rising from chair 65% of Knee Heel Height	2.3	4.0
	Rising from chair 80% of Knee Heel Height	3.6	5.4
	Rising from chair 100% of Knee Heel Height	4.8	6.6
	Rising from chair 115% of Knee Heel Height	5.2	6.6

2.1.2.3 Gait Cycle of the Knee Joint

Gait cycle is defined as the time from which the heel of one foot touches the ground to the time it touches the ground again as seen in Figure 2.5. In the case of the knee joint one of the most common forms of analysis is that of flexion angle measured during the gait cycle (Figure 2.5). The knee flexion during phases of the gait cycle of a normal function knee should conserve energy through resisting forces (gravity, inertia and muscle contractions), maintain balance by avoiding a collapse and project the body in the intended direction through correct movement of the centre of mass.

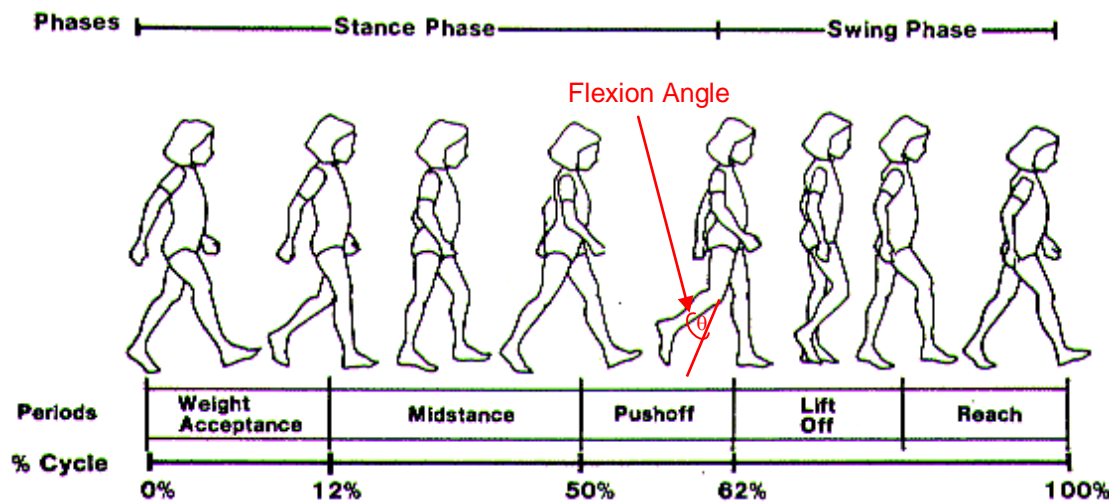


Figure 2.5 Phases and Periods of the Human Gait Cycle [51]

The knee flexion over 100% gait cycle plots of a normal knee and that of a normal knee versus an osteoarthritis knee can be seen in Figure 2.6. It can be seen from Figure 2.6a that the normal knee joint cycle witnesses a sinusoidal period of flexion angle of almost equal amplitude and frequency through the stance stage which incorporates weight acceptance, midstance, and push-off (Figure 2.5). There is a step rise towards the end of the stance phase where the flexion angle increases to 60° at 75% of the gait cycle lowering at a steady rate to almost 0° within the swing phase which incorporates lift-off and reach (Figure 2.5) completing 100% of the gait cycle.

Figure 2.6b shows several flexion angles of an osteoarthritis infected knee versus a normal knee. It can be observed that the normal knee shows little variation between repeated gait cycles with only one case not following the normal pattern (possibly caused by a slight loss of balance) observed in Figure 2.6a. This is not the case for the osteoarthritis diseased knee which shows great variation amongst repeated gait cycles, where flexion angles are permanently lower than those of the normal knee during the same phases of the gait cycle. The greatest variation is witnessed in the stance phase where over half of the cycles witness no sinusoidal pattern for the extension of the osteoarthritis infected knee which stays close to either lower than 0% or above 20%.

Figure 2.7 shows the flexion angle during the gait cycle for a normal knee (a) and TKR replacements using retention (b) and substitution (c) of the Posterior Cruciate Ligament (PCL) used to prevent posterior translation of the tibia on the femur. It can be seen that the flexion angles are closely matched in the TKR's compared to that of the normal knee joint. Such research investigating loading and gait cycles after a TKR operation justifies the use of TKR's to alleviate the pain and discomfort caused by such increased loading and abnormal flexion during the gait of an osteoarthritic or diseased knee.

2.1.2.4 History of Total Knee Replacement

The history of Total Knee Replacements (TKR's) can be separated into two periods: -

- Pre TKR's (resurfacing, replacement bearing surfaces) Early 40's to Pre 1960's
- Modern TKR's (Total Knee Replacement's (TKR's)) – Post 1960's

2.1.2.5 Pre Total Knee Replacements

Professor Themistocles Gluck of Berlin can be accredited with the first TKR back in 1891 [54] which was constructed from Ivory and cemented in place with cement made up from a mixture of gypsum and colophony pumice. Most of the principles and theories being applied to modern day prosthetics designs used today had already been thought of or realized by Gluck including stable fixation of the artificial joint [55-59], modular construction of artificial joints [60-62], choice of material to match bone properties [63, 64], allografts [65-68], fixation methods in bone marrow tracts [69-71] and bio-compatibility of materials [72-77]. Thus leading to Gluck being accredited as an unrecognised genius in a publication by Eynon-Lewis (1992) over a century later [78].

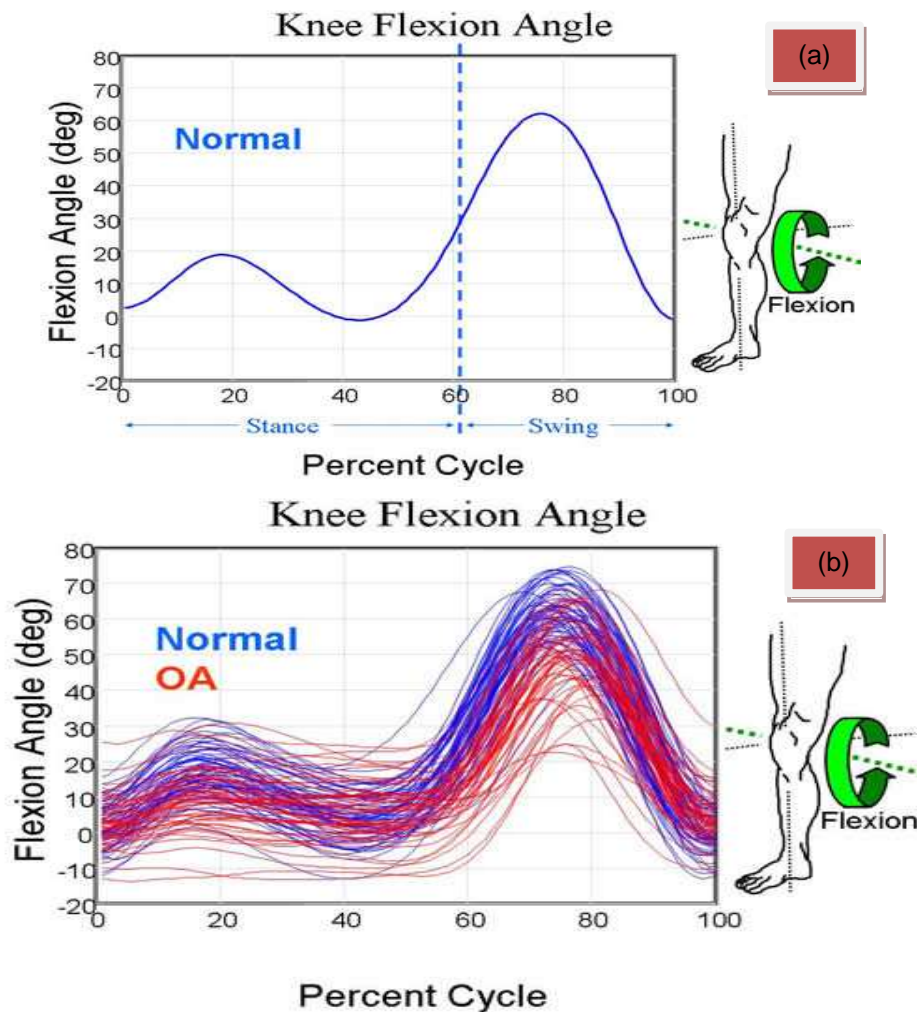


Figure 2.6 Normal (a) and Normal v OA (b) Knee Flexion Angle Plots [52]

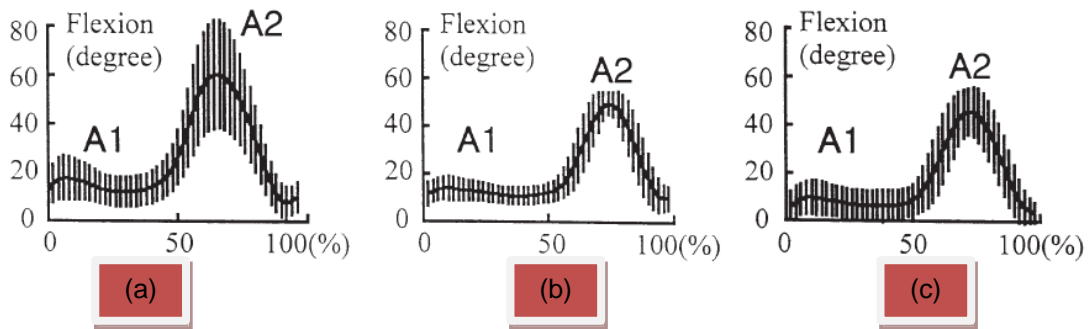


Figure 2.7 Flexion of Normal (a) PCL retained (b) & PCL Substituted (c) Knee [53]

A design that understood and replicated knee joint movement and used hard materials came some 60 years after the Gluck Ivory design in 1951 in the form of the Wallidus design [80-82]. The design consisted of a cobalt chrome hinge joint linking cemented femoral and tibial stems. Shiers (1953) [83] further developed hinge joint designs with femoral and tibial stems longer than the Wallidus design enabling better alignment of the stems. McKee [84] incorporated the same stem lengths as Wallidus but used fixation screws rather than cement in his design. Later he changed the design to incorporate cemented fixation using a tri-fin stem. A group of French designers developed a design named after their group called the GUEPAR hinge prosthesis but lack of consideration to complex forces of the knee joint led to catastrophic failures.

Furthermore orthopaedic surgeons McKeever and then Macintosh attempted the principal of using a metal spacer/bearing surface. The spacer designs developed and lead to the introduction of a uni-compartmental athroplasty and replaced the bearing surfaces on either the medial or lateral side of the joint on both the tibial and femoral bone components. A design by Gunston [85] was made of metal and semi-circular in shape. The design was not fixed to the tibia component allowing more freedom of movement to that of the hinged joint thus accounting for some of the more complex forces experience by the knee joint. Images of the pre TKR designs can be seen in Figure 2.8 and a summary of pre TKRs are given in Table 2.2

2.1.2.6 *Modern TKR's*

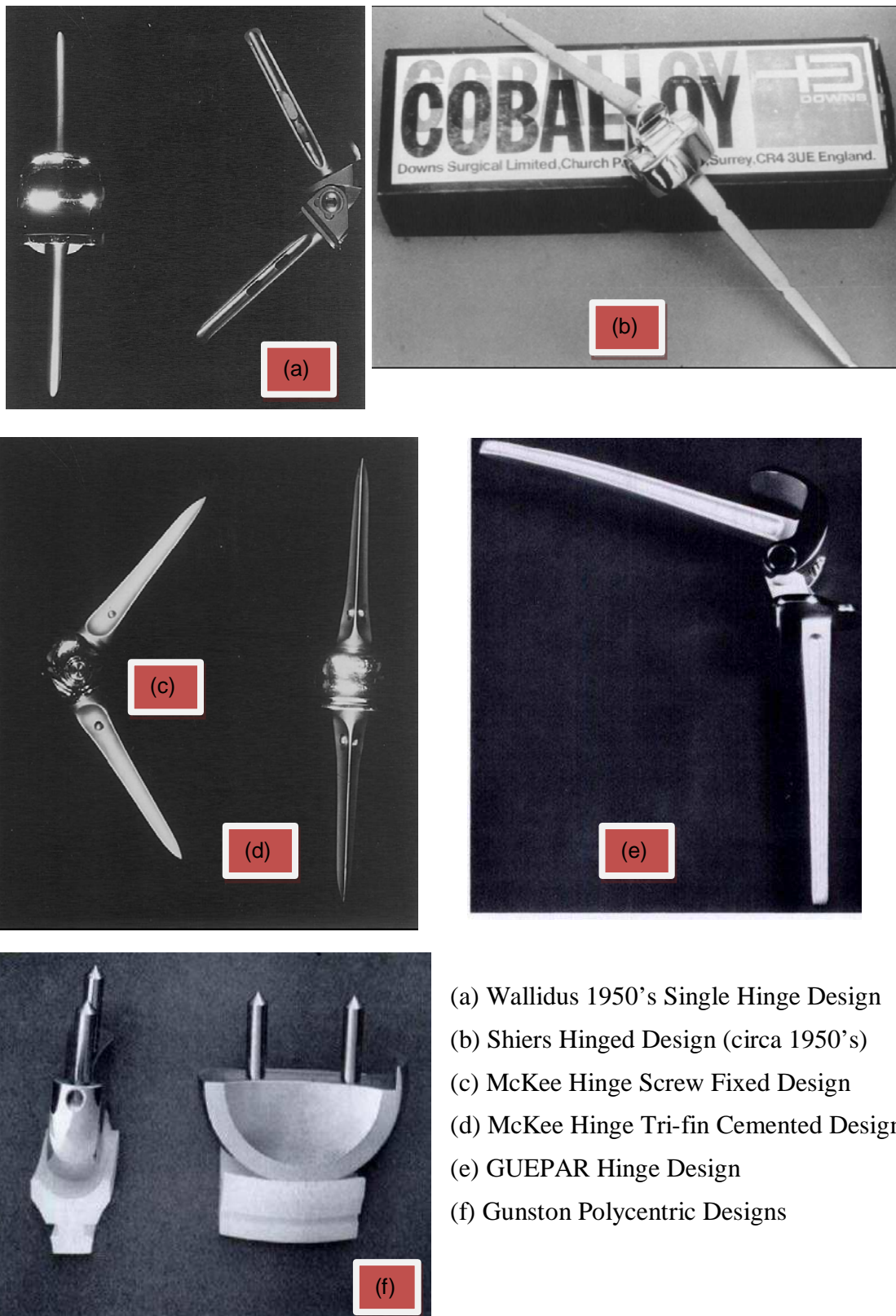
Unlike hip replacements, the pre-modern TKR's had "astronomical" failure rates, Miller (2002) states "The knee rotates in more directions than the hip, and the artificial joint needs to be more complicated. Since the first knee replacements in the 60s, the joint has been redesigned to mimic the real joint, and now success rates are similar to those for hips." [86]

The early problem occurred as the bearing surfaces were manufactured from metal causing a rubbing action that produced wear debris and the muscles and ligament forces loosened the implants during physical movement. These problems lead to high failure rates and clinical problems including aseptic loosening and other mechanisms of failure which require revision surgery and are described in section 2.2.3.

In the early to mid seventies better implants, called condylar total knee implants, were designed. The condylar knee implant allowed for knee rotation. They came in only two sizes and were solid pieces. Initially, orthopaedic surgeons were cautious about using the new knee implants because of their experience with hinges, but as good results were recognized, more surgeons performed the operations. [87]

Marmors 1972 design became one of the most successful uni-compartmental designs (Figure 2.9) but the main flaw in the design was the technicality of fixing the prosthesis accurately in place especially if there were degenerative changes on the medial and lateral sides.

THE APPLICATION OF ZEEKO POLISHING TECHNOLOGY TO FREEFORM FEMORAL KNEE REPLACEMENT COMPONENT MANUFACTURE



(a) Wallidus 1950's Single Hinge Design
 (b) Shiers Hinged Design (circa 1950's)
 (c) McKee Hinge Screw Fixed Design
 (d) McKee Hinge Tri-fin Cemented Design
 (e) GUEPAR Hinge Design
 (f) Gunston Polycentric Designs

Figure 2.8 Pre TKR Designs [85, 86]

THE APPLICATION OF ZEEKO POLISHING TECHNOLOGY TO FREEFORM
FEMORAL KNEE REPLACEMENT COMPONENT MANUFACTURE

Table 2.2 A Summary of Pre TKR Designs

Knee Type	Design	Motion	Stress / Wear	Advantages	Disadvantages
Gluck	Hinge Mechanism constructed from Ivory Material	Forwards and Backward, No rotational movement	High stress due to lack of load bearing surface (stress on pin in hinge) high wear properties of ivory	First attempt of TKR which lead to accelerated developments of today's modern TKR's	Although knowledge was available the lack of research and development of biocompatible material and surgical procedures led to downfall of the Gluck design
Walldius	Hinge Mechanism constructed from Acrylic then metal	Forwards and Backward, No rotational movement	High stresses on acrylic design lead to fracture of material. Lower wear properties in replacement metal design with acrylic bearing surfaces	Breakthrough in understanding of the load bearing function of the knee rather than just a replacement of the knee itself	Short stems (10cm) on both femoral and tibial components lead to fixation problems due to lack of surface area on which bone regrowth could be dispersed.
Shiers	Hinge Mechanism constructed from metal with acrylic roller bearing	Forwards and Backward, No rotational movement	High stress on local surface areas (screws). Wear reduced due to larger range of movement through 3.6mm bridged gap from using roller bearing design hence better alignment of components.	Stem length increased (15cm) to reduce the affects of failure due to loosening of the femoral and tibial components.	Fixation using screws lead to failure due to the load being distributed through a the single screw rather than the whole surface area of the stem

THE APPLICATION OF ZEEKO POLISHING TECHNOLOGY TO FREEFORM
FEMORAL KNEE REPLACEMENT COMPONENT MANUFACTURE

Knee Type	Design	Motion	Stress / Wear	Advantages	Disadvantages
McKee / GUEPAR	Hinge Mechanism constructed from metal with acrylic roller bearing	Forwards and Backward , No rotational movement	Reduced stress on local surface areas due to the use of bone cement rather than fixation by screws. Hence the reduction of wear as complex forces disperses through areas other than the contacting surfaces.	The diversity of loads experienced by the knee joint were dispersed over the surface area of the stem by incorporating fins on the stem which allowed the use of bone cement creating the larger areas compared to that of smaller areas by using screwed fixation method.	Limited knowledge of bone cement and fixation methods with bone cement lead to premature failure due to misalignment when cementing the femoral and tibial stems into bone canals. Lack of attention to increasing the range of movement lead to the downfall of the hinged design principle.
Gunston	Hinge Mechanism constructed from metal with separate tibial and femoral components	Forwards and Backwards with limited rotational movement	Stresses on joint reduced with increased motion due to separating the components allowing limited rotational movement hence reducing wear due to dispersion of loads from a range of movements	Knowledge of the increased range of movements and complex forces witnessed by the knee joint lead to detachment of the components to increase movement to rotational as well as forwards and backwards.	Limited knowledge of the geometry required to increase rotational movement lead to increased wear from non compliant metal components fouling during movement hence increasing the chances of premature failure.

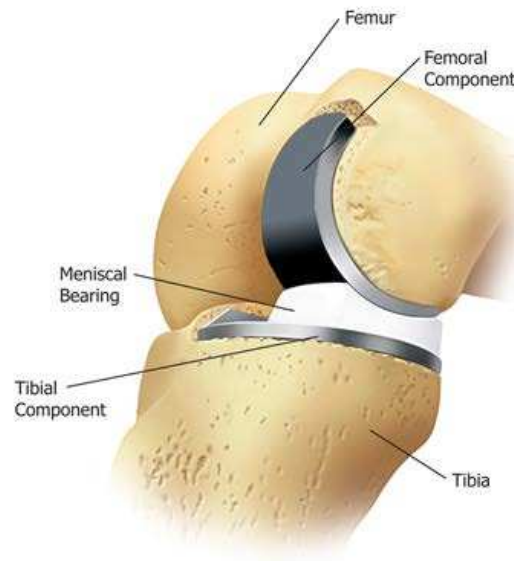


Figure 2.9 Uni-compartmental design replacing one femoral condole [88]

By 1976 designs which used metal on UHMWPE bearings to replace the bone surfaces, were introduced to attempt to overcome some of the limitations of the previously described hinges. These designs required more precise surgery as well as medical incisions, where ligaments and muscles had not suffered irreparable damage caused by the disease.

The invention of the condylar prosthesis design by John Goodfellow, a Surgeon, and John O'Connor, a bio-engineer (Oxford) [89] was a great leap forward as it wraps around the front of the femur and incorporates the original patella-femoral articulation. Their design was unique in the fact it was something that none of the previous designs had accounted for at all or very inadequately, hence survival rates of these designs were substantially greater. The development of condylar prosthesis (Figure 2.10) continued and the design improvements including development of fixation devices and the refinement of surgical jigs for more accurate bone cutting have increased joint lifetimes. This design more closely mimics the 6 degrees of freedom movement of a natural knee.



Figure 2.10 Fixed Bearing Condylar Knee Design [90]

Typical design improvements were the addition of enhanced fixation features between the tibial component and the tibia [91, 92] and reduction of conformity to reduce cold flow and creep of the polymer [93, 94]. By the late 1980s and early 1990s designs had evolved from highly conforming surface type designs to highly non-conforming, surface type designs with metal reinforced tibial components. Despite this remarkable progress significant engineering problems still remain in the search for implants which provide long term trouble-free performance in the human body.

One of the modern designs to be introduced and developed is that of mobile bearing which as well as its differences has its advantages and disadvantages over that of the condylar design these can be seen in Table 2.3.

One particular design that has increasingly become popular is that of the Low Contact Stress (LCS) Complete Knee replacement. Designed by DePuy Johnson & Johnson, this mobile bearing joint has proven survivorship rates of greater than 96% after 20 years post operation. [95]

The LCS complete knee system has four main components: -

1. **Tibial Tray:** This component made from a metal alloy replaces and covers the top of the tibia (shinbone).
2. **Tibial Insert (bearing component):** This disk shaped component inserts into the tibial tray and lies between the femoral bearing component and tibial tray. The insert is made from low wear/ low coefficient of friction polymer, Ultra High Weight Molecular Polyethylene (UHMWPE).
3. **Femoral Component:** A metal alloy component that replaces the two boney ridges at the end of the femur (femoral condyles) and also the grove in the original femur that the kneecap (patella) would run against.
4. **Patellar Component:** Replacing the boney surface on top of the knee cap. This UHMWPE component is domed shaped and mimics the natural kneecap and runs in a grove along the bottom of the thighbone (femur).

Figure 2.11 shows an example of a LCS Complete Knee Replacement with the components labelled. Using the recognised designs (Table 2.3) as a baseline knee major implant manufacturing companies continued working towards improved designs with an emphasis on ease of implantation. Improved designs were also supported by a range of medical devices that made the surgery more reproducible. With these devices in place the total knee replacement went into the nineties as an acceptable operation for the relief of pain caused by arthritis in ageing patients.

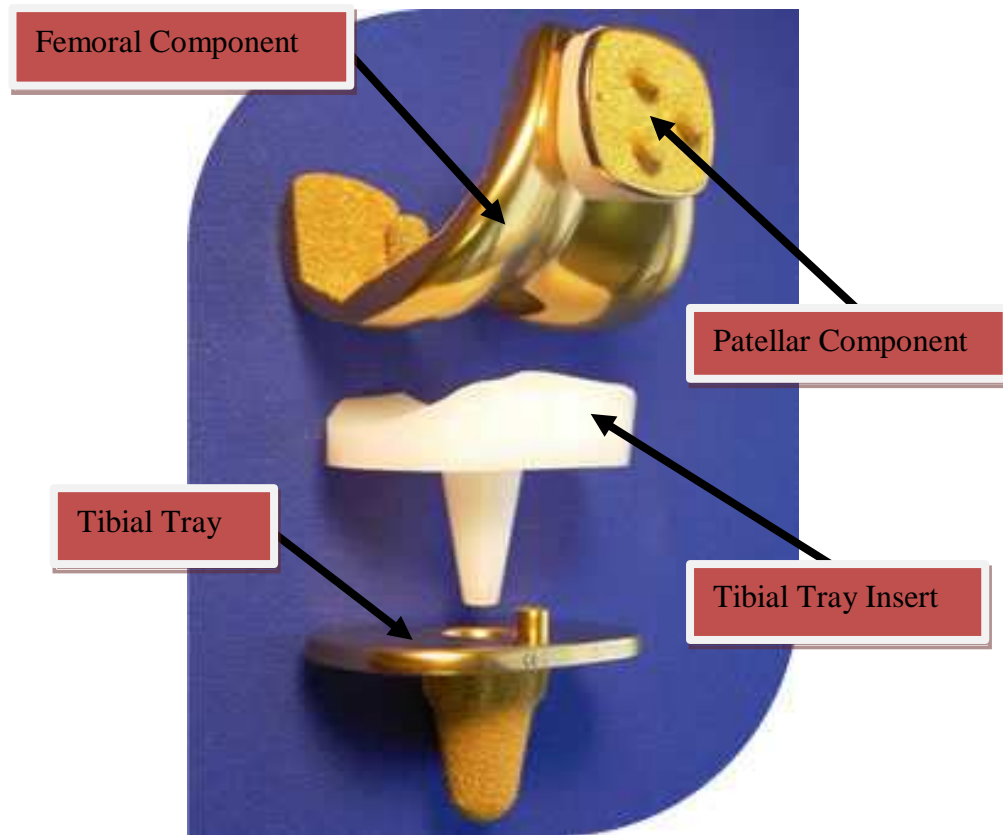


Figure 2.11 LCs Complete Mobile Knee Replacement

[96]

2.1.3 Why TKR Implants Fail

In the UK alone they were 3,897 TKRs revised in 2009 accounting for approximately 5% of 75,629 TKR surgeries performed in the same year [97]. Some of the more common mechanisms and their presence in the 212 patient revision surgery cases for early (< 2 years after surgery) and late revisions (> 2 years after surgery) of TKRs reported by Sharkey et al (2002) [98] are seen in Table 2.4. An explanation and examples of these common TKR failure mechanisms will be discussed.

Table 2.3 Comparison and Advantages/Disadvantages of Condylar v Mobile TKR's

Knee Type	Design	Motion	Stress / Wear	Advantages	Disadvantages
Condylar TKR	Tibial component is supported with a flat metal piece that securely holds the polyethylene insert	When the knee is in motion, the femoral component glides over the polyethylene	Natural shape of a condyle is not a perfect circle: Different amounts of stress are exerted on the insert at different points.	The main advantages of the fixed-bearing condylar replacement are its simplicity and its reliability with good to excellent function in the large majority of cases. Cruciate ligaments can be revived in most cases.	Restricted movement especially in activities that required the rotational movement of the knee e.g. sports climbing stairs etc. Less freedom for surgeon error on location due to fixed position of polyethylene insert.
Mobile TKR	The polyethylene insert can rotate slightly, which gives knee implant a more natural interface between the surface of femoral component and the polyethylene	Both gliding and rotating motion can be achieved	Since PE can rotate, contact with Femoral Condyle is more even, less stresses and wear	Many components of mobile-bearing knee are same as traditional fixed knee implants Same proven surgical procedures can be used Currently used preoperative and postoperative routines for patient are also same	Particles from polyethylene wear - Can lead to aseptic loosening and osteolysis - Can destroy a tibial inlay in less than 10 years - Can cause infection - Can cause possible unexplained pain - Reduced flexion

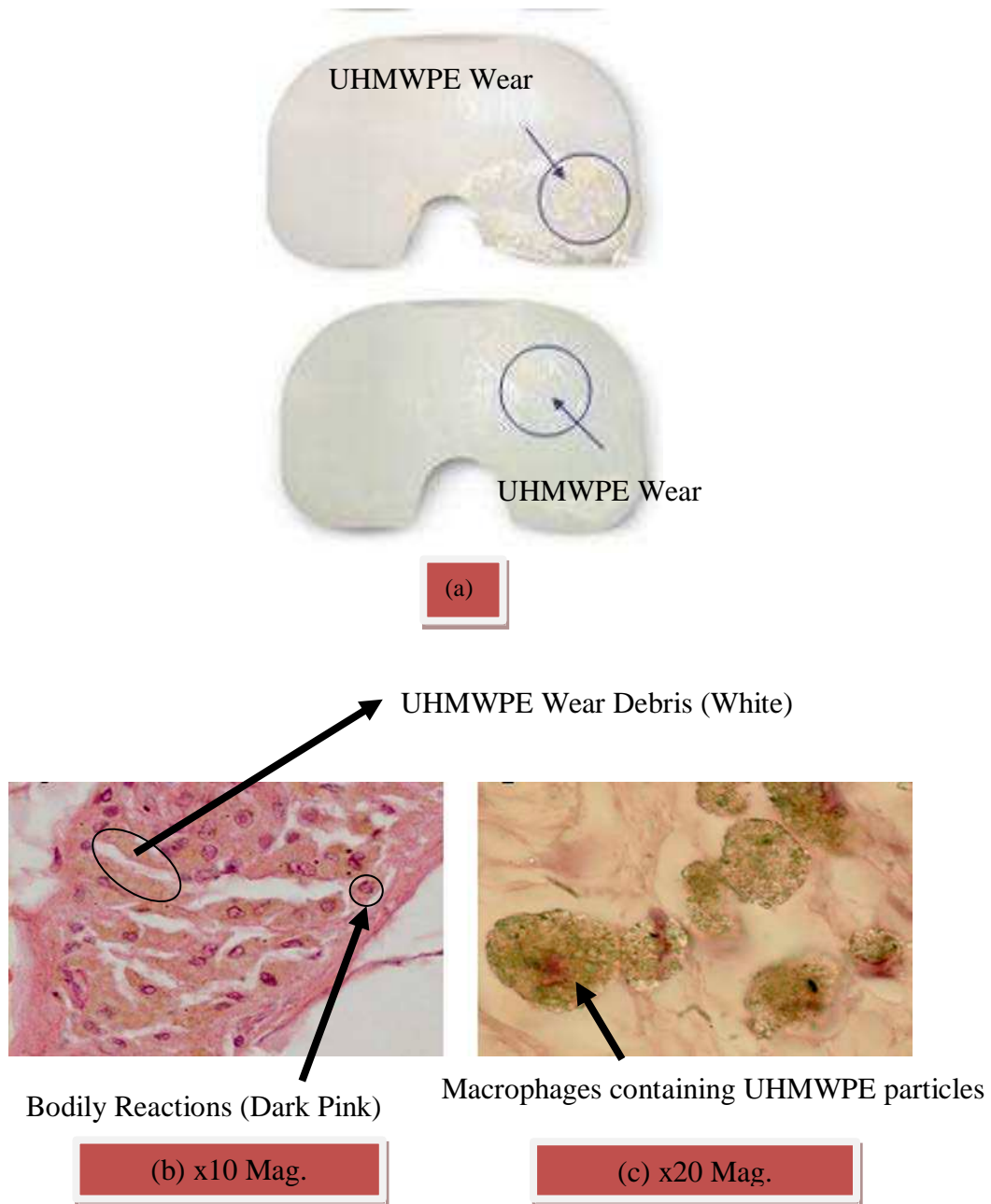
Table 2.4 Common failure mechanisms and % presence in 212 Revision TKRs [98]

Failure Mechanism	Presence in patient population (%)		Overall contribution to TKR Revisions (%)
	Early TKR Revision	Late TKR Revision	
Polyethylene Wear	11.8	44.4	25
Aseptic Loosening	16.9	34.4	24.1
Instability	21.2	22.2	21.2
Infection	25.4	7.8	17.5
Arthrofibrosis	16.9	12.2	14.6
Malalignment or malposition	11.9	12.2	11.8
Others	19	10	13.8

2.1.3.1 Polyethylene Wear

Polyethylene wear occurs due to articulation with the harder load bearing surface of the TKR implant. An image of a TKR insert witnessing polyethylene wear caused by the wear particles being entrapped in between the load bearing surfaces can be seen in Figure 2.12 (a). More severe consequences happen when the wear particles are released into tissue surrounding the bone joint interface causing (Figure 2.12 (b and c)) causing bodily reactions i.e. microphages and micro-haemorrhages etc.

Although polyethylene wear is seen as more of a major contributor in late revision surgery (44%) compared to early revision (11.8%) of Sharkey et als research the wear particles generated initiate some of the other mechanisms i.e. infection and aseptic loosening.



(a) Worn TKR inserts, (b) Bodily Reactions to UHMWPE,
(c) Macrophages containing UHMPE Particles

Figure 2.12 Examples of Polyethylene Wear [99, 100]

2.1.3.2 Aseptic Loosening

Wear particles of UHMWPE, metallic material and bone cement caused by articulation or broken away from the joint or left over from surgery are released into the body. The UHMWPE attracts cells called macrophages which attack and try to digest these particles believing them to be bacteria due to them being of similar dimensions.

These wear particles interact with the macrophages releasing enzymes and chemicals which leading to bone re-absorption around the bone joint interface causing the implant to fail due to movement of the implant in the cavities left behind (Figure 2.13a). White arrows indicate luceny (lower absorbed X-Ray areas) indicated by the white arrows in Figure 2.13b showing the cavity left behind from the bone absorption and the movement of the knee implant within the cavity is clearly visible.

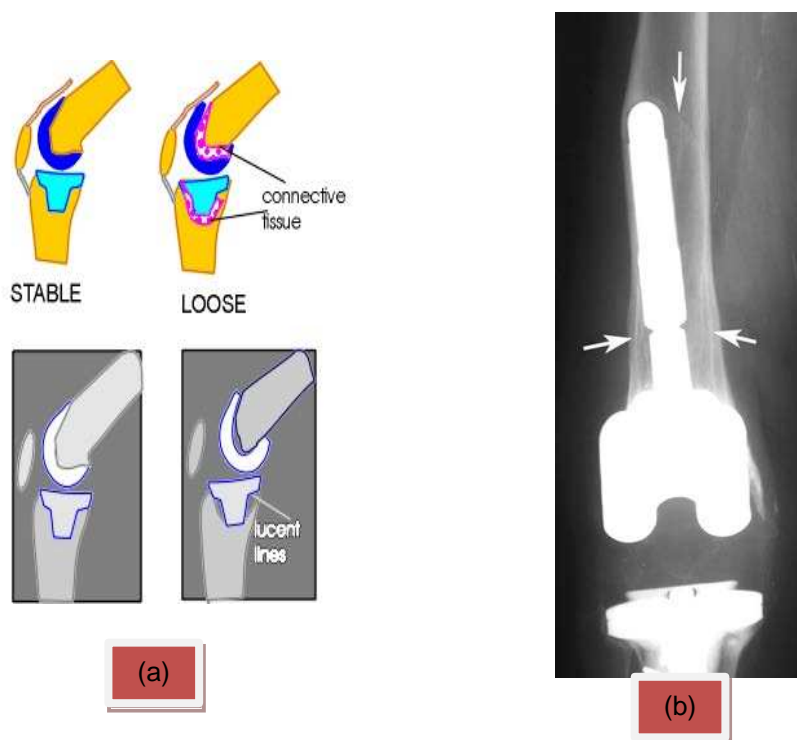


Figure 2.13 Schematic (a) and X-ray (b) of Aseptic Loosening of a TKR [101, 102]

2.1.3.3 Instability

Instability is caused by TKR components that are not perfectly aligned or positioned and therefore become unstable. Fehring and Valadie (1994) [103] observed 25 revision surgery cases concluding instability was related to the lack of surgeon's experience or the inadequate instrumentation available to aid the surgeon in positioning the TKR correctly. It was found that only a few cases of instability were found to be caused due to inferior designs.

TKR studies by Mitts et al [104] showed that the amount of patients with instability from a cruciate retaining TKR design could have been reduced by using a cruciate substituting design rather than the cruciate retaining design under investigation. A schematic of instability can be seen in Figure 2.14.

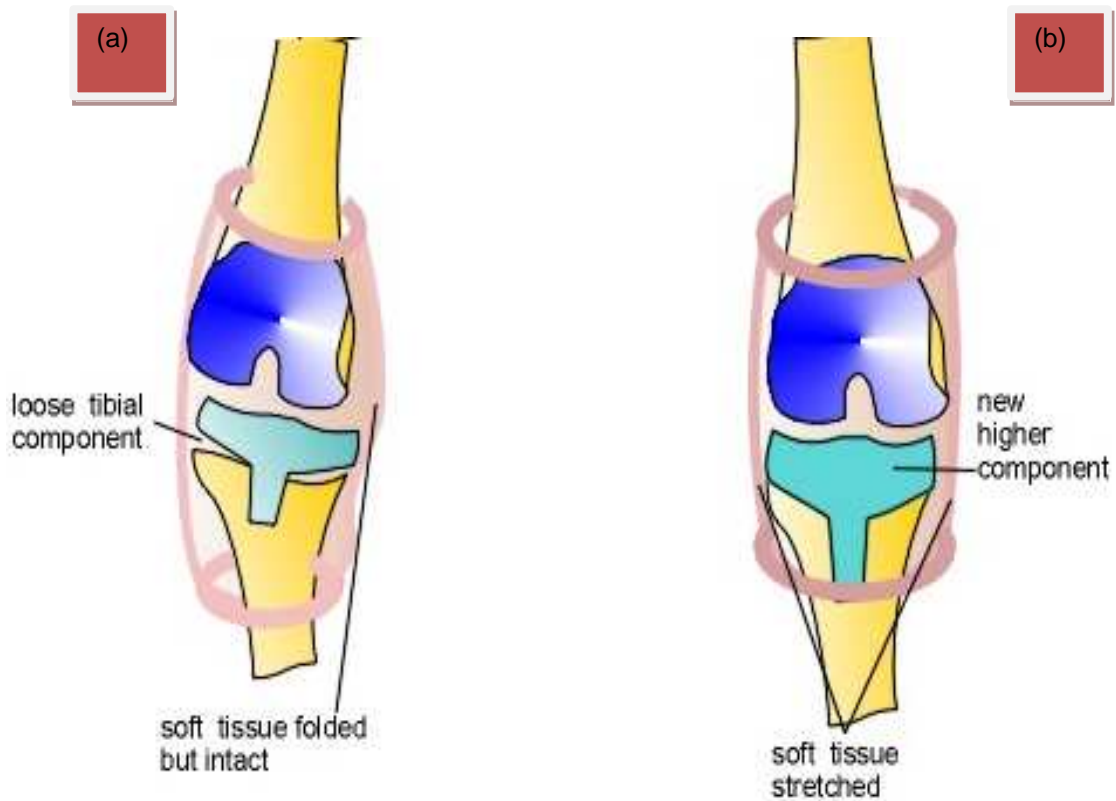


Figure 2.14 Schematic of instability (a) leading to TKR revision (b) [105]

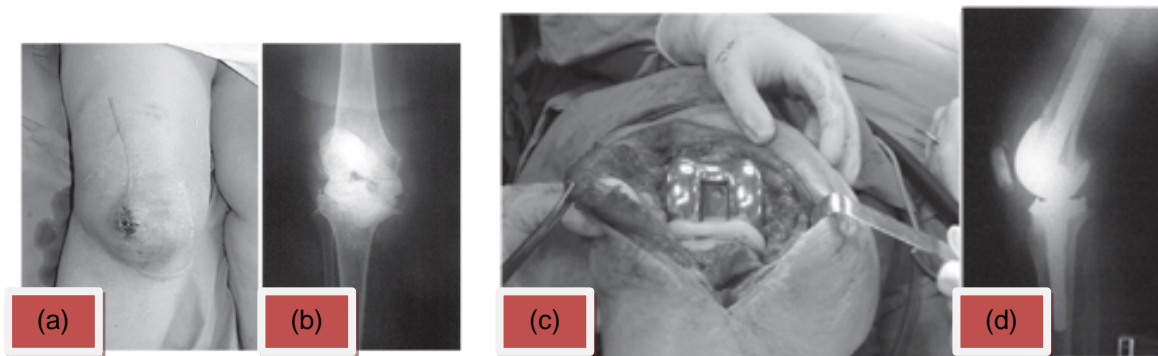
2.1.3.4 Infection

Infection can happen either during surgery or after surgery. Infections caused during surgery are most common and occur when organisms present in the operating theatre enter the body during the TKR operation. Whereas organisms in the blood stream known as bacteraemia

settling in an around the joint after surgery are less common. It is inevitable that bacteria during surgery will happen but limiting the bacteria can reduce the chances of infection.

This can be achieved by an experienced surgeon performing the operation with sterilised instruments in a clean environment as quickly as possible and covering the patient in antibiotic covers. In some cases of surgery involving cemented fixation antibiotics are added to the cement to aid in preventing infection [106]. Post-operation infections can also be limited by administration of antibiotic drugs after completion of the surgery.

Due to the complexity of the TKR procedure if infection procures it causes great pain and discomfort through swelling and loss of movement for the patient. In the large majority of cases the TKR is removed, the infection is then treated and revision surgery is carried out as seen in Figure 2.15



(a) Infection causing swelling and discharge, (b) X-Ray of infection with temporary insert to alleviate discomfort (c) Revision surgery and (d) X-Ray of revision surgery with infection removed

Figure 2.15 Infection in a TKR causing revision surgery [107]

2.1.3.5 *Arthrofibrosis*

TKR surgery complications can cause vast scar tissue responses which in turn lead to excessive pain and restricted knee motions in either flexion and or extension of the patient's knee. The diagnosis of this excessive scar tissue response is known as Arthrofibrosis where the scar tissue enters the joint and surrounding areas of the tissue and remains there even after rehabilitation. Over a period of time muscle weakness leads to a displacement of the patella which damages the TKR joint surfaces.

The TKR becomes encapsulated with the scar tissue and the patient has little to no movement of their knee.

If recognized early, extensive therapy can reduce the need for revision surgery although in most cases revision surgery is required to remove the TKR, dissect the Arthrofibrosis then perform revision surgery. An X-ray cannot determine Arthrofibrosis but due to advances in radiology and especially the introduction of Magnetic Resonance Imaging (MRI) a visual image of the full knee joint can be used to diagnose Arthrofibrosis indicated by the red arrow as seen in Figure 2.16

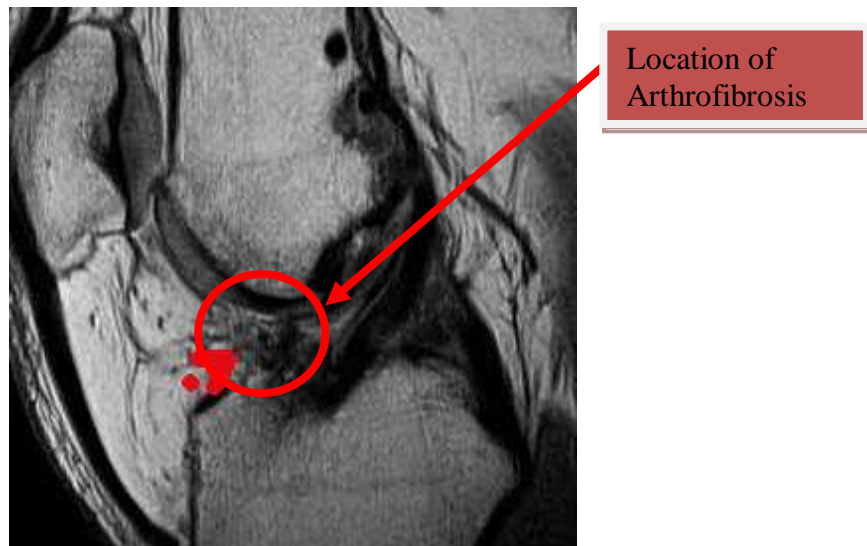


Figure 2.16 MRI Image of Arthrofibrosis [108]

2.1.3.6 Malalignment or malpositioning

Misalignment or malpositioning either valgus or varus (Figure 2.17) of a TKR causes the stress distribution of the implant components to increase either medially or laterally due to the weight bearing being unevenly distributed.

The worst cases cause catastrophic failures from fractured UHMWPE components or in most cases excessive wear that leads to other problems such as aseptic loosening or infection mentioned previously. Malalignment or malpositioning of TKRs is less of an issue in modern TKR surgery than back in the days of the first TKR operations.

Such a statement can be justified by comparing the amount of revision surgery cases caused by misalignment (Table 2.4) to that discovered by Lotke and Eckler (1977) [109].

Lotke and Eckler stated that from all the patients that receiving TKR surgery between May 1972 and June 1974 at the Hospital University of Pennsylvania, Philadelphia only 10% received a perfectly aligned TKR. The increase in yearly TKR operations since then has increased the experience of surgeons leading to published guidelines for TKR surgeons [110].

Research and development of computer assisted surgery to aid the surgeon in making the correct cuts to ensure correct location of TKR components [111] have addressed points made by Lotke and Eckler for reduction of failures due to malalignment or malpositioning. A pre-revision radiograph and an image of a retrieved tibial insert showing excessive wear to a 10° rotational misalignment between the tibial and femoral components can be seen in Figure 2.18.

2.1.4 Current Developments in TKRs Materials to Prevent Implant Failures

The current choice of orthopaedic implant materials for TKRs is that of a cobalt chrome femoral component and a UHMPE tibial insert bearing combination. Although a highly polished metal surface articulated against a polyethylene surface produces low friction hence less wear particle generation there is still a significant research effort to lower friction bearing combinations compromised of hard-on-hard combinations.

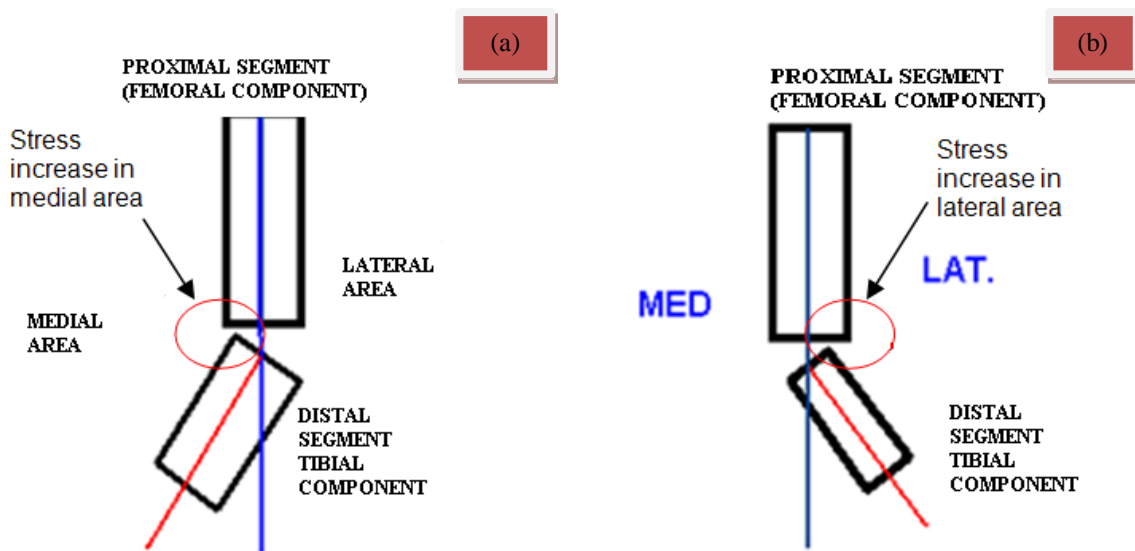


Figure 2.17 Schematic of Varus (a) and Valgus (b) misalignment

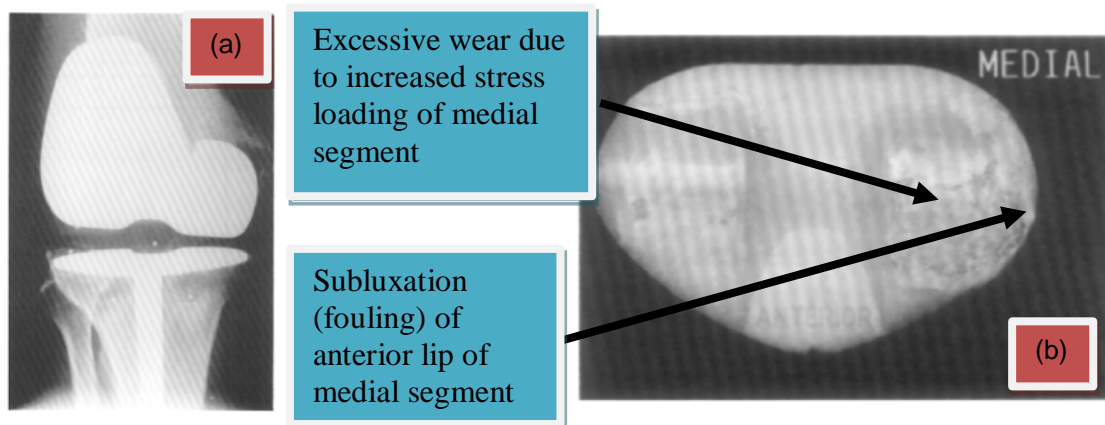


Figure 2.18 X-Ray of Malpositioning (a) & retrieved Tibial Tray component (b) [112]

Two of the alternative bearing surfaces combinations under current research are: -

- Metal-on-Metal
- Ceramic-on-Ceramic
- Metal-on-Ceramic

A summary of the advantages and disadvantages of hard-on-soft and hard-on-hard bearing combinations can be seen in Table 2.5.

A further alternative being investigated is Diamond Like Carbon (DLC) Coatings which are applied to the hard surface component to produce a very smooth and low frictional intermediate surface between the metal and the UHMWPE component.

At the time of publication of this thesis the FDA had just passed approval of the first hip implant combination of a metal-on ceramic manufactured by Johnson & Johnson Depuy called the PINNACLE [113] although there are concerns about adverse events and ion concentration in the body which will be closely monitored.

Table 2.5 Advantages and Disadvantages of Bearing Surfaces of Prosthetics

Bearing Surfaces	Advantages	Disadvantages
Metal on Polyethylene	High Wear Resistance No Toxicity Low Cost	Increase in bio particles hence more cases of prosthesis loosening
Metal on Metal	Low wear rates Osteolysis reduction Improved surface finish hence lower frictional torque Fisher et al (2000) research showed good results	Relatively new and no long term results yet. Particle release Increase in metal ions within the erythrocytes Increase in Urine ion levels Local & global Allergic reactions Carcinogenic concern
Ceramic on Ceramic	Lowest wear rates No toxicity Good long-term results	Position sensitivity Liner chipping Risk of impact fracture of bearing surfaces

If successful it will almost certainly become the best choice of bearing combination due to pre-clinical trials producing the lowest recorded wear rates and performing up to 100 times better than that of any current combination [114].

2.1.4.1 Metal-on-Metal Bearing Surfaces

Metal-on-metal bearings are not new to being used as bearing surfaces for orthopaedic implants with a successful application in THRs in the 1960-1970s although as the

introduction of metal-on- UHMWPE bearings gained popularity with surgeons due to its clinical results being superior to that of the metal-on-metal counterpart it succeeded.

The demise of the metal-on-metal bearing was believed to be due to the following:

1. **Lack of implant design knowledge** – Bad designs caused fouling of surfaces outside the desired contact area known as subluxation leading to excessive wear and aseptic loosening.
2. **Manufacturing Processes** – Poor grain size control and lack of inspection caused problems with the quality of cast materials used in manufacture affecting the mechanical properties of the TKR components causing premature failure.
3. **Poor metallurgy** – Surface material testing/ inspection tools were limited during this period restricting the research into new tougher more wear resistant alloy materials. Wear analysis was limited to unidirectional movement in which UHMWPE outperformed metals.

With improvement in all three of these areas the research and use of metal-on-metal bearing combinations are starting to advance in the fight to overcome those of metal-on-UHMWPE. Implant design knowledge has been increased with the use of computer aided design and finite element analysis (FEA) packages available to assess the performance of designs before manufacture [115] with the McKee design being one that was particularly successful.

Quality control as well as introduction of Near Net Shape manufacturing [116] using cast alloy materials and the ability to control grain size [117] has increased the mechanical properties of metals hence increasing their performance in load bearing surfaces through advances in real life (in vivo) equipment [118] that can fully mimic the movement of the TKRs.

Improved metallurgy in the form of mechanical property testing, surface measurement and form have allowed the performance of metal-on-metal bearing surfaces to be compared to that of other bearing combinations proving that physical properties, surface quality, and conformance of mating metal-on-metal TKR surfaces could enhance wear resistance.

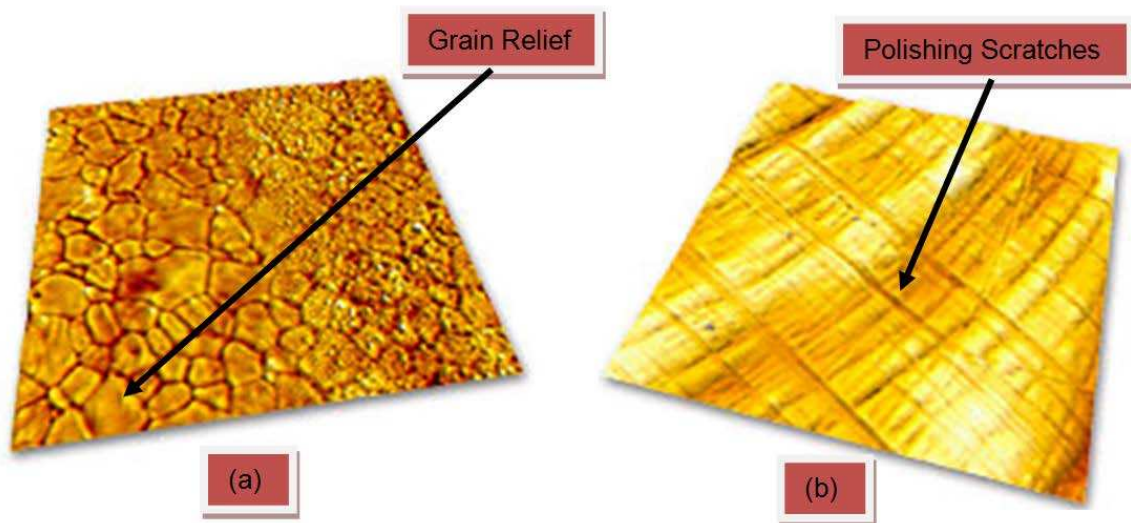
According to penetration results published by Semlitsch and Willert [119] metal-on-metal implant bearing surfaces produced lower penetration rates (50 $\mu\text{m}/\text{year}$) compared to that of most commonly used bearing combination of metal-on-UHMWPE (100 $\mu\text{m}/\text{year}$) and although ever slightly higher wear rate than ceramic-on-ceramic both these combinations show penetration of $< 10 \mu\text{m}/\text{year}$ proving hard-on-hard alternative bearing surfaces are becoming more common in implant manufacture. The knowledge of metal processing techniques over that of ceramic manufacture means they have the added advantage of producing better conformity due to the lower tolerances as well as reduced costs associated with ceramic manufacture. Cumulative wear loss over long term results compared to that other combinations also makes them prime candidates.

Albeit all these advances surgeons are still concerned over the release of ionic debris of that of other bearing combinations especially in the case of resurfacing of hips where a larger head size relates to increased wear [120] increasing the amount of chromium and cobalt levels in the bodily fluids [121]. The recent withdrawal of the Depuy ASR design due to metallosis or metal poisoning causing inflammation, pain, tumours, blood loss, birth defects, and even certain cancers [122] is a defining example of such complications.

2.1.4.2 Ceramic-on-Ceramic Bearing Surfaces

Alumina-ceramics in implant surgery have been used since the mid 1980's. They have the advantage of being more wear resistant as a bearing surface with steady state wear rates of $>$

$0.014\text{mm}^3/10^6$ cycles reported by Clarke et al for combinations of $\text{Al}_2\text{O}_3\text{-Al}_2\text{O}_3$, $\text{ZrO}_2\text{-Al}_2\text{O}_3$ and $\text{ZrO}_2\text{-ZrO}_2$ although their long term cumulative wear is not as good as metal-on-metal (CoCr-CoCr) combination [123]. Due to their hardness ceramics can be polished to extremely smooth surface finishes whilst remaining fairly scratch resistant when implanted into the human body [124]. An example of a polished ceramic surface compared to a metal alloy surface can be seen in Figure 2.19.



Images courtesy of Nanosurf (www.nanosurf.com)

Figure 2.19 Images of Polished Ceramic (a) and Polished Metal Alloy (b)

Despite being scratch resistant the major disadvantage of ceramic-on-ceramic bearings is their brittleness which makes them prone to fracture [125] especially in high stress large range motions associated with hip and socket components [126] therefore making them inadequate for patients who wish to continue in physical activities. Advances in chemical purity [127] and smaller grain sizes [128] and ceramic manufacture have seen fracture cases reduced.

Ceramics have a longer history in hip heads with alumina [129] and zirconia [130] based ceramics being used for several decades although only recently has oxidised zirconia been introduced as an orthopaedic material in both hip and knee manufacture articulated against UHMWPE with early results showing superb wear resistance [131].

The performance of some common Ceramic on Ceramic/UHMWPE combinations can be seen in Table 2.6 listing coefficients of friction, advantages and disadvantages of each combination. The variance in co-efficient of friction values is due to results of research performed under various combinations of lubrication, temperature and direction of motion i.e. lower values are obtained with a lubricated uni-directional movement and higher values are associated with a multi-directional movement and dry conditions.

Table 2.6 Comparison of common ceramic-ceramic/UHMWPE bearing combinations

Bearing Combination	Coefficient of Friction	Advantages	Disadvantages
Zirconia-UHMWPE	0.040 ± 0.01 (R) - 0.082 ± 0.005	No advantages have been found with wear rates highest in comparison to other ceramic bearing combinations. [132]	Changes its crystalline structure which reduces toughness and increases susceptibility to wear. [133]
Alumina-UHMWPE	0.044 ± 0.005 - 0.115 ± 0.02	Decrease in wear rates and osteolysis cases compared to metal alloy on UHMWPE cases [134]	Only midterm results and limited comparison to other bearing combinations available for knee joints [135].
Oxinum (Oxidised Zirconium) - UHMWPE	0.47 ± 0.06	Modified zirconium metal alloy makes an alloy with the advantage of surface properties of ceramic (harder, smoother and less friction) with decreased chances of fracture. [136]	Positive but only short term results available for femoral knee implant components [137]
Alumina-Alumina	0.002 - 0.05 ± 0.01	Excellent wear resistance and minimal fractures in younger patients (no evidence of osteolysis and non measurable wear) [138]. Follow-up results show good wear resistance in hip applications. [139]	Squeaking of the surface witnessed by various studies including one particular study concluding that in 20% of cases witnessed audible squeezing levels under normal motion after surgery. [140] No follow-up studies for knee implant use.

(Table adapted from: Banchet et al (2007) [141], Scholes (2000) [142], Hall and Unsworth (1997) [143], and Illinois University (2005) [144])

An image of a ceramic-on-ceramic TKR made from Biolox delate ® a new ceramic material can be seen in Figure 2.20

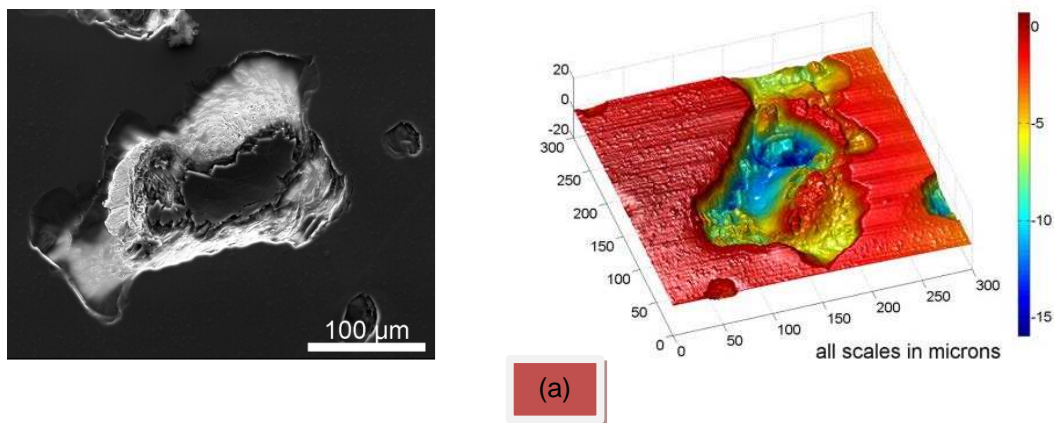


Figure 2.20 Biolox delta ® Ceramic-on-ceramic TKR [145]

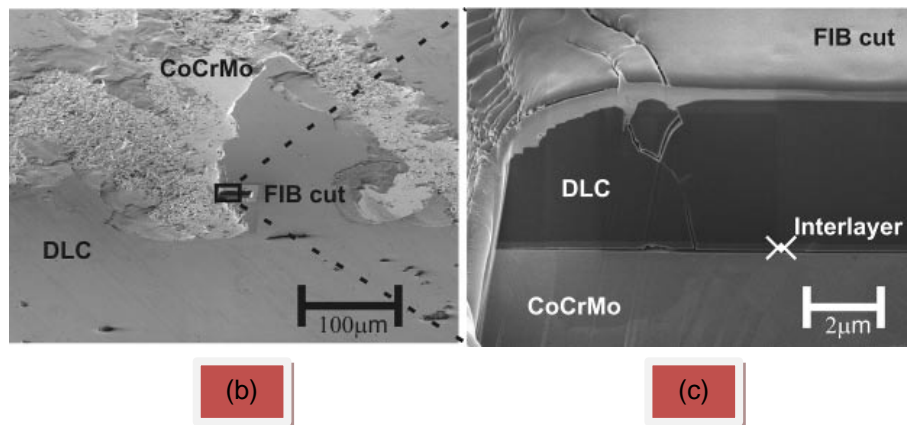
2.1.4.3 Diamond Like Carbon (DLC) Coatings

DLC coatings in biomedical applications have been reviewed by various researchers [146-150]. Roy et al (2007) [151] concludes that for their application as coatings on bearing surfaces they not only reduce wear during hip and knee joint simulation they help reduce corrosion leading to less wear particle debris.

He also comments due to vast variation in results of various aqueous solutions that for long term and commercial use that careful examination of issues as delamination and corrosion should be examined in extensive in-vivo and in-vitro studies for long term use of DLC coatings on a commercial. Examples of delamination and corrosion of DLC coatings can be observed in Figure 2.21.



(a) AF Microscope and 3D Profilogram of Mechanical Delamination of a DLC Coating



(b) Stress Cracking and Crevice (c) Corrosion Mechanisms in Failure of a DLC Coating

Figure 2.21 Delamination (a) and Corrosion (b & c) of DLC Coatings [152, 153]

2.2 New materials

The design of medical implants detailed in chapter 2 of this thesis followed the story of implants from early Gluck Designs through to current day designs. Knee implant design is being carried through to the 21st century by implementing TKR designs with ceramics [154] and hard on hard bearing surfaces [155]. Despite these introductions the new materials that are available are restrictive and manufacturers are reluctant to use them without significant bio-compatible testing and because of the tribological properties associated with these tests, results in compromises being made.

Scholes and Unsworth (2009) [156] researched the reduction of the wear volume to minimise the affect of particle induced Osteolysis by pin on plate testing of a new materials. These materials were Polyetheretherketone (PEEK-OPTMIA) and carbon fibre reinforced Polyetheretherketone (PEEK-OPTIMA) and their performance was evaluated using various combinations of Cobalt Chromium Molybdenum (CoCrMo) to assess their potential as orthopaedic implants.

Scholes and Unsworth concluded from the results that: -

“The PEEK/low carbon CoCrMo produced the highest wear. CFR-PEEK against high carbon or low carbon CoCrMo provided low wear factors. Pin-on-plate tests performed on ultra-high molecular weight polyethylene (UHMWPE) against CoCrMo (using comparable test conditions) have shown similar or higher wear than that found for CFR-PEEK/CoCrMo. This study gives confidence in the likelihood of this material combination performing well in orthopaedic applications.”

Very intriguing new material surfaces will be seen in the future of replacement hip and knee joints including such surfaces made from more variations of inorganic and organic artificial bone, diamond deposited materials and the possibility of hardened titanium as it has a smooth exterior hence less final manufacturing after the casting process. Textured surfaces may also find themselves functional i.e. pockets to promote fluid retention and trap wear particles to isolate them surrounding tissue hence reducing the chances of wear particle initiated aseptic loosening [157].

2.3 *The Tribology of Wear*

Most of the research previously reported in this literature review has emphasised the need for bearing surfaces that are smooth and conforming to reduce wear in knee implants. The purpose being that there is a thin layer between the two mating surfaces know as the film lubrication layer in which the synovial fluid of the human body lies as seen in Figure 2.22.

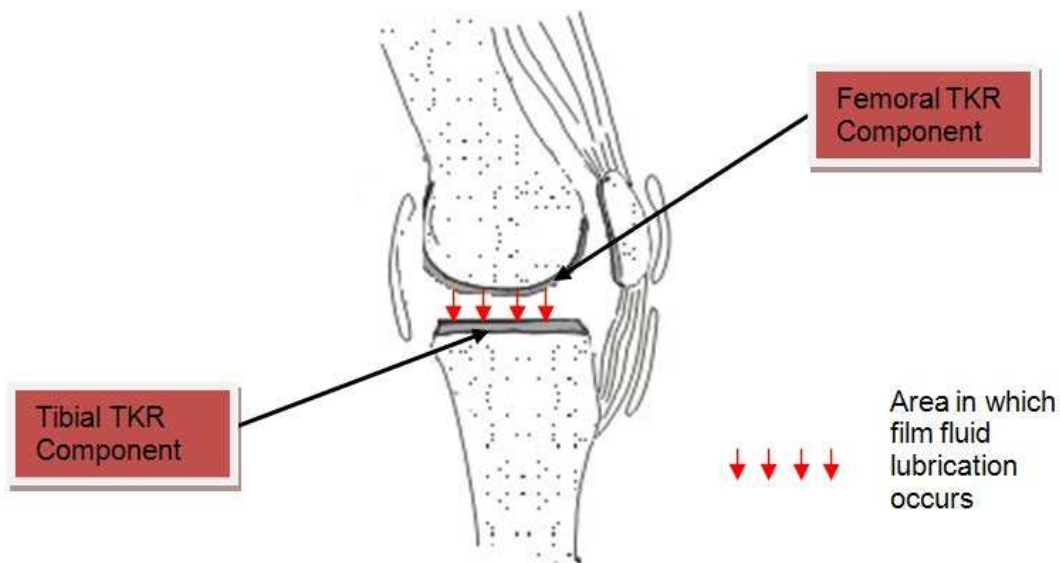


Figure 2.22 Principles of film lubrication layer in a human synovial joint

As seen in Figure 2.23 this area can exist in various conditions known as:

- Boundary regime – the two surfaces are in close contact between their asperities generating through local pressures leading to a stick-slip situation with some asperities breaking away. The synovial fluid of the knee joint reacts with surfaces to produce a high resistance boundary film across the moving surfaces supporting the load; eliminating excessive wear and catastrophic failures.
- Mixed-film regime – where there is a layer of synovial fluid carrying the body weight through external pressure (Hydrostatic Lubrication), or by the hydrodynamic forces acting in the conjunction to the joint surfaces movement and the viscous resistance of the synovial fluid (Hydrodynamic lubrication).
- Hydrodynamic regime – similar to mixed film but involves interactions of the asperities in the on the load bearing surfaces causing elastic deformation on the load bearing areas of the joint. This load is supported by the viscous resistance of the lubricant.

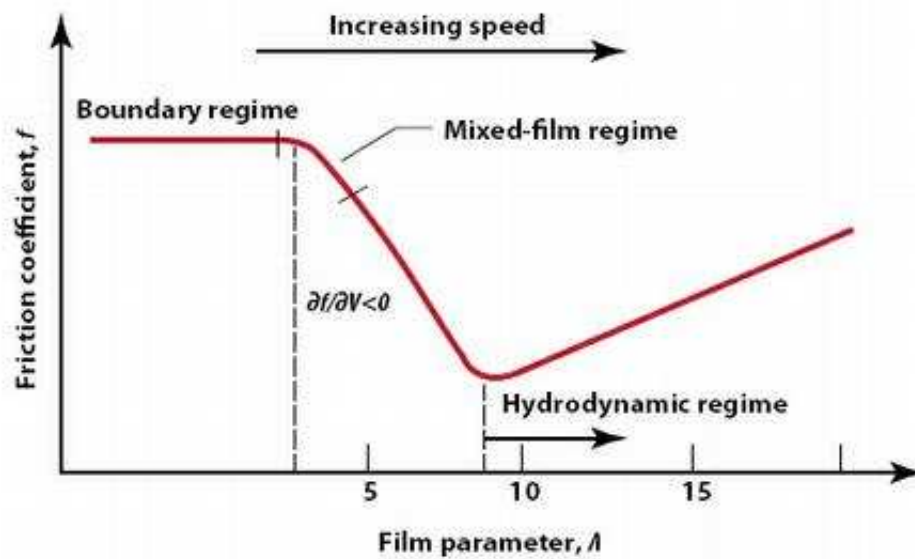


Figure 2.23 Stribeck Curve [158]

The wear performance of implant materials varies dependant on the lubrication condition in which the bearing surfaces are performing. These conditions as reported by Stribeck et al [159] and seen in Figure 2.23 are a measure of viscosity of fluid multiplied by sliding speed derived by Arnold Sommerfield [160] (film parameter) plotted against co-efficient of friction.

In the case of orthopaedic implant materials it has been seen that conformity, contact surface area and reduction of the coefficient of friction of bearing components can control the boundary condition in which the bearing surfaces operate. Careful control of these parameters can reduce wear such research has been performed by Smith et al [161] in the case of hip joints and Murikami et al [162] discovered that the boundary lubrication can change dependent upon activity in their simulation model of a TKR.

Taking this into consideration the use of high conforming metal-on-metal implants which have a low co-efficient of friction could be the way forward especially if the use of the Zeeko corrective polishing process can reduce the form without compromising the surface finish.

2.4 *Summary*

Osteology, the study of bones began in the mid to late 16th Century, developing research has found that degenerative bone diseases i.e. osteoarthritis and osteoporosis etc. have caused discomfort and pain in the skeletal joints of the aging population. The use and development of medical implants to help relieve such pain and discomfort has developed over the past 300 years. The most common medical implants being that of Total Hip Replacement (THR) and Total Knee Replacement (TKR) of which well over 1 million implants are conducted worldwide each year.

An introduction to the biomechanics of the knee joint including freedom of movement, loading and gait cycle has been discussed with reference to normal and diseased knee joints and how TKR's can aid in the almost returning diseased and deformed knee joints back to their original function. The development of TKR's began in 1891 by non-other than the famous inventor of the ivory ball and socket joint Thermistocles Gluck.

Constructed from ivory a simple hinge joint fixed with pumice and gypsum cement provided pain relief for diseased knee joint patients. Although having a lack of knowledge of raw material and mechanical properties of bone and the complex biomechanics involved with a joint that has six-degrees of freedom, Gluck developed theories that are applied to modern day TKR's including fixation in bone marrow tracts through to the understanding of compatibility of implant materials within the human body.

Designs in the early 1940's to mid 1960's (Walldius, McKee and Shiers) further developed materials and fixation methods but none of them understood the complex forces experienced by the knee joint leading to poor survivorship rates. Pre 1960 designs suffered catastrophic failure rates due to metal on metal articulation, muscle and ligament forces causing loosening of the joint during physical movements.

Modern day Post 1960 designs (condylar and mobile) would mimic the real joint patella-femoral articulation and the introduction of an intermediate bearing surface made for Ultra High Molecular Weight Polyethylene would see surgeons have more confidence in TKR's due to higher survival rates.

The key to improving the lifetime of implants especially those of orthopaedic load bearing components is to reduce the wear particle generation which in turn initiates osteolytic reactions in the human body eventually resulting in failure due to aseptic loosening.

The use of coatings such as Diamond Like Carbon (DLC) and Titanium Nitride (TiN) can be applied to these highly finished form tolerant components through Chemical Vapour Deposition (CVD) techniques which vaporise the Carbon or Titanium source and deposit it on the heated surface of the component to coat the surface in a thin micron sized layer within a pressurised gas container. These coatings have proved that they can substantially improve the wear characteristics of the bearing surface and have the added advantage of creating a barrier between the implant material and bone which reduces the affect of metal ions particles in the body. Such particles can cause Osteolysis and other forms of disease and infection that can lead to premature implant failure.

The development of new materials is an ongoing research in the field of biological implants i.e. Zirconium and Alumina based ceramics as the goal of achieving a negligible wear surface continues. New materials are constantly being developed and tested in wear simulators (in vivo) before being used in the ultimate test of clinical trials (in vitro).

The quest for further improvement in the lifetime of TKR's will see further developments in the improvement of conformity and surface finish of the mating load bearing surfaces. This is based upon the fact that with careful control of surface roughness conformity and reduced friction of bearing components the lubrication layer conditions can be controlled to reduce wear. Such developments will aid in reducing the wear associated with aseptic loosening and premature failure as well as increasing long term survivorship rates. If use of the Zeeko machine and the corrective polishing process can control conformity without compromising the surface finish then it will be seen as powerful manufacturing machine in the future development of hard-on-hard high conforming TKR implants.

CHAPTER 3: Manufacture of Freeform Knee Implant Components

3 MANUFACTURING OF KNEE IMPLANT COMPONENTS

This chapter of the thesis is intended to broaden the knowledge of the reader in the manufacture of knee implant components.

3.1 *Manufacture of Knee Implants*

The manufacture of knee implant components require precision engineering throughout each stage of the manufacture especially those component areas that act as high load bearing surfaces e.g. d the femoral and tibia components of a knee implant.

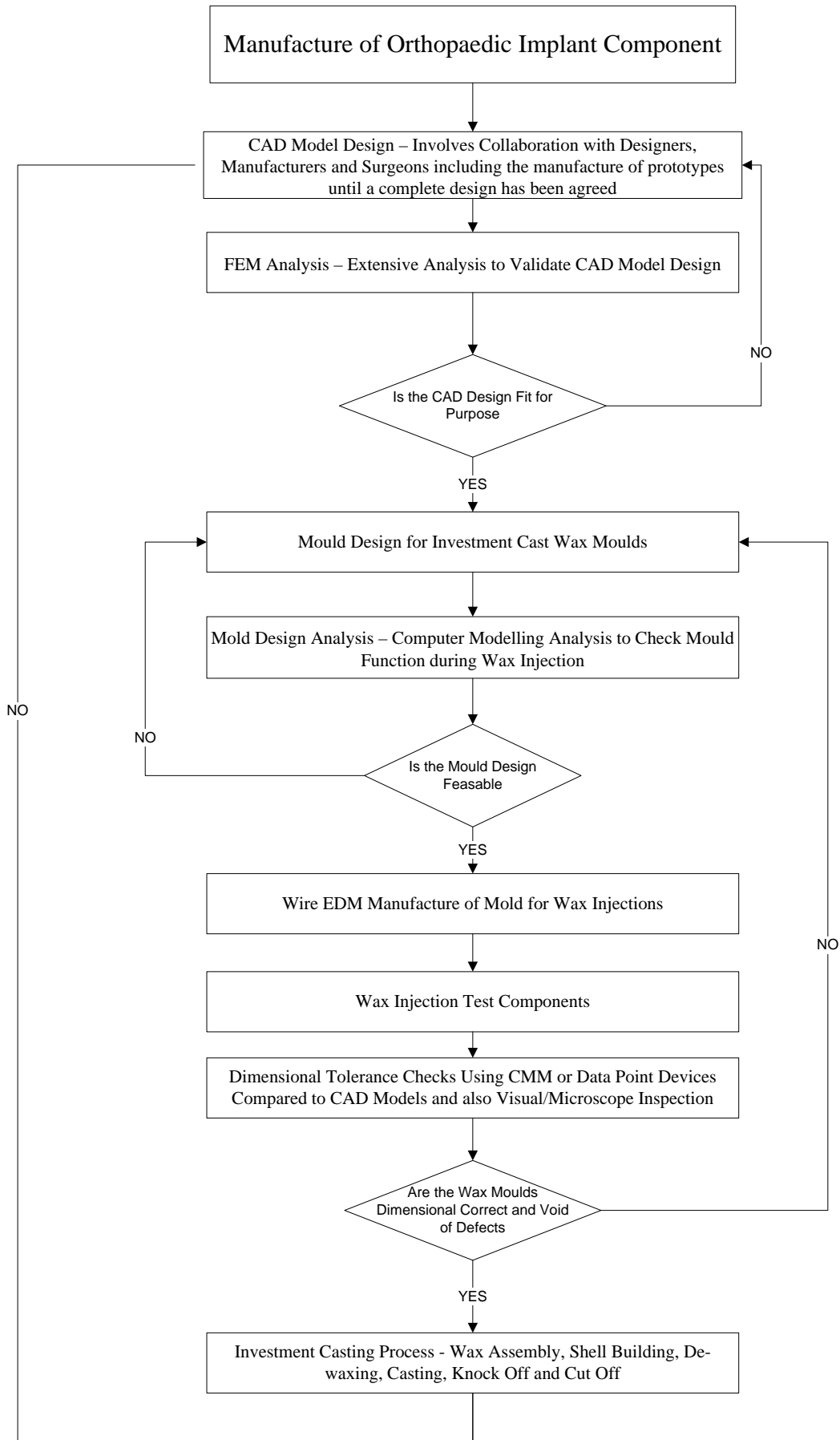
To facilitate the high performance of load bearing implants; standards were outlined including bio-compatible materials, surface finish, dimensional tolerances and clearances associated with load bearing component surfaces. The standards covering these issues are ISO 7207-1 and ISO7207-2 [163-164].

A flow chart of the manufacture of an orthopaedic implant component can be seen in Figure 3.1 the manufacturing process of an orthopaedic implant can be categorised in to several processes: -

- Initial casting/forging
- Post cast machining
- Grinding
- Final finishing of the biological surfaces of the implant

The role of each of these stages can influence the functionality and performance of the biological components directly impacting on the component lifetimes. A brief description of initial casting/forging, post cast machining and grinding will be given.

THE APPLICATION OF ZEEKO POLISHING TECHNOLOGY TO FREEFORM FEMORAL KNEE REPLACEMENT COMPONENT MANUFACTURE



THE APPLICATION OF ZEEKO POLISHING TECHNOLOGY TO FREEFORM FEMORAL KNEE REPLACEMENT COMPONENT MANUFACTURE

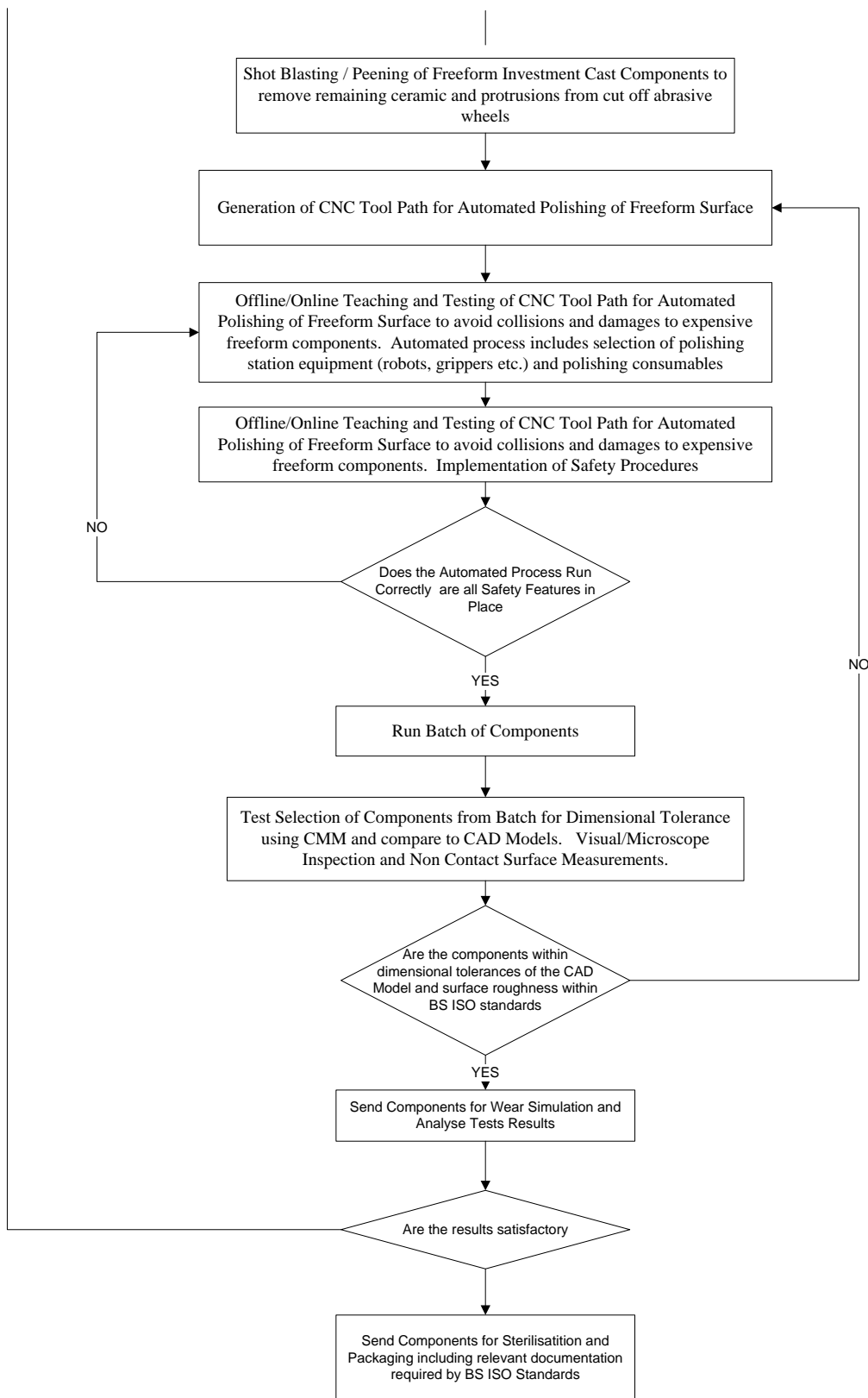


Figure 3.1 Flow Chart of the Manufacture of an Orthopaedic Implant Component

The most critical of the processes is the final finishing of the bearing surfaces of the implant although achieving the targets outlined in current standards can be difficult depending upon the precision and optimisation of previous processes. Final finishing is the main focus area of this thesis therefore it will be explained in more detail.

The introduction of freeform surfaces into medical implants has increased their performance and functionality by allowing replacement joints to mimic those of the human body (bone on cartilage) rather than relying on geometric shapes with axes of symmetry e.g. spheres cups and ellipses etc.

The drive towards improving lifetimes of other implants other than knee joints have emphasised areas such as surface finish, form correction and coatings [165-167]. These areas together with use of new material combinations such as alumina and zirconium bio-ceramics combined with current knee implant materials have provided hard on hard load bearing surfaces which show little to no wear characteristics and are being seen as the way forward in increasing the lifetimes of medical implants as well as improved functionality and performance.

3.1.1 Initial Casting/Forging

Casting and Forging are processes that give initial life to a biological implant. The processes differ in the physical state of the raw material; casting involves using molten material liquid form whereas forging uses semi-molten material which is in a state between the transitional phases of solid-liquid. The purpose of both processes is to achieve an overall shape of the component, with dimensions as close to the accepted tolerances as possible. Usually castings are within 1 μ m-1mm dependant on component size and volume of the desired component whereas dimensions of forgings are within 5 μ m-2mm.

3.1.1.1 Casting

Most casting techniques are not suitable for casting knee implants due to their complex freeform shape as the high accuracy and fine detailed reproduction required for is not achievable so all cast implant components are either investment cast or hot isostatic pressed to provide high accuracy defect free castings prior to post cast machining and finishing processes.

3.1.1.2 Forging

Wall and Hefron (2004) [168] promote the advantages of forgings which include yielding components with greater strength than other metalworking processes due to the use of high temperatures and in some cases cold working of forgings. In the case of Titanium, forgings are better due to the lack of waste material produced compared to the other processes.

Although when creating Cobalt Chrome implants that require less tensile strength e.g. femoral knee components then casting is a better solution although in the cases where high tensile strength is required e.g. hip components and tibial knee components then the ultimate tensile strength of forgings is preferred.

3.1.2 Machining

Albeit that of near-net shape forging the other processes used to create knee implant components will require some kind of post machining process These machining processes are used to acquire the upper tolerance bands of the components allowing the final finishing process to achieve the surface quality that current standards demand whilst maintaining the dimensional tolerances outlined in the same standards.

3.1.2.1 BS / ISO Machining Standards for Knee Implant Components

Whereas dimensional tolerances for hip joint bearing surfaces are available there are currently not stipulated for knees due to the complexity of the surface not having any rotationally symmetry ('freeform'). As there are no current guidelines for the tolerances of this kind of freeform shape at the time of publication of this thesis, the tolerances are driven by company standards. The only guidelines that exist are those related to the assigning of dimensions to components of the knee joint and these are very vague in BS7251-14 (ISO7207-2) and BS-7251-4 (ISO7206-2).

3.1.2.2 Machining processes used after casting/forging processes

A range of conventional and non-conventional machining process are applied to the post cast/forged components of femoral knee implants

3.1.2.2.1 Conventional Machining

Conventional machining processes used in post cast/forged knee implant components include the milling of femoral near net shape femoral knee implant components (Figure 3.2 a) and grinding of investment cast knee components (Figure 3.2 b) to remove defects/surface damage layers which occurred during contact with the mould [169]

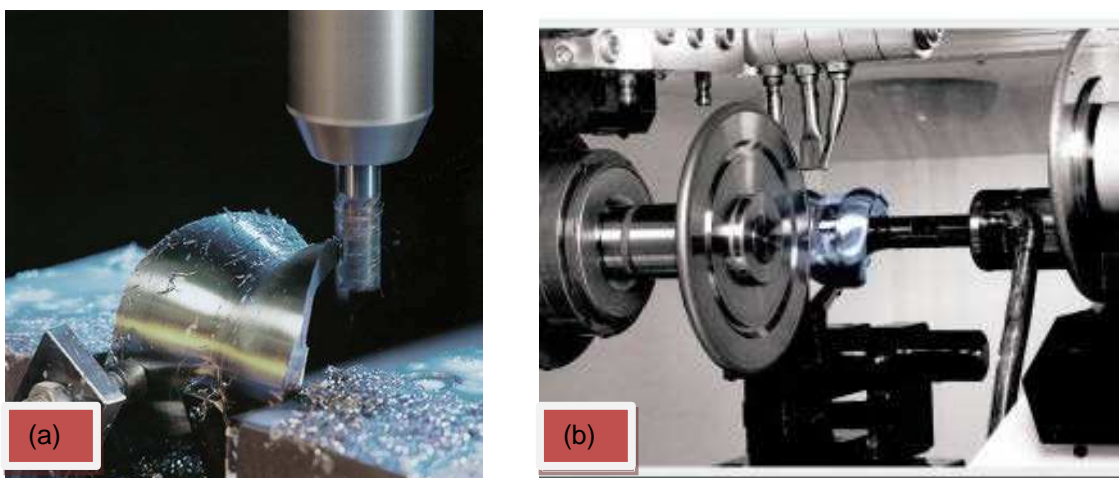


Figure 3.2 Milling (a) and Grinding (b) of defects after investment casting [169, 170]

3.1.2.2.2 Non Conventional Machining

Non conventional machining methods have been used not only to create the desired dimensions of biological implant components but in most cases to enhance the mechanical properties of the material used to manufacture the component e.g. structured surfaces for enhancing bone growth. The use of non-conventional machining processes in knee implant manufacture includes water jet cutting [171], electro chemical machining [172, 173] and ultrasonic machining [174]. Such processes help in improving surface roughness/texture, material properties and bone growth enhancement. In the case of ultrasonic machining the process lends itself to aid in difficult to secondary machine ceramics.

3.2 Final Finishing of Biological surfaces

The role of final finishing process of biological surfaces is essential to maintaining a smooth surface that reduces the friction between the contacting load bearing areas, reducing wear hence increasing the lifetime of the implant.

The types of polishing processes and media used to achieve these highly polished smooth surfaces are discussed in detail with reference to relevant research in key areas. The quality of the surface finish of load bearing knee surfaces is not the only influential factor in premature failure of medical implants. The conformance of the mating components is also a critical factor especially in more complex joints i.e. TKR where a metal femoral component articulates on a UHMWPE tibial insert [175, 176]. The knee joint with has varying radii across the components of the loading bearing surfaces with no axial symmetry is effectively a freeform shape. The chapter will further discuss the definition, needs and advantages that are offered from freeform shapes. An investigation into the improving the lifetimes of biological implants concludes this chapter.

There are many surface finishing techniques used in the manufacture of biological implants of which the processes can be separated into three categories: -

- Manual
- Semi Automated
- Automated

Each of the processes has their advantages and disadvantages for example a manual process can detect visual defects throughout the process; whereas an automated process would not see visual defects throughout the process although the volumes of finished components measured over a period of time is superior to that of a manual process.

The final finishing process of knee implants involves using polishing media and abrasives to remove minor defects or scratches in the material surface by a combination of a series of decreasing smaller grain particles of slurries/pastes and gradually softer polishing media with the overall aim of creating a mirror finish defect free surface that in most cases is superior or matches current standards [177].

The use of freeform surfaces for knee implants allows the designer the increased possibly of mimicking the original function of the body part to that of the purpose of which the implant was required [178]. This leads to better functionality but in the case of final finishing the form errors associated with freeform surfaces can cause complications. The roughness requirements stipulated in ISO 7207-2 stipulates that the measured surface finish of the metal bearing surface be $Ra < 50nm$ with consultation with knee implant component manufacturers the current Ra achieved in industry is lower than this at $Ra < 20nm$.

3.2.1 Manual process

As the name suggests a manual process is an entire process which is carried out manually making it very labor intensive. The majority of these manual finishing processes are used on areas of biological implants that do not function as frictional components.

Ever since the evolution of modern polishing techniques at the turn of the 20th Century [179] the vast majority of all polishing processes was done by hand. Today skilled manual workers are limited and even for them achieving standards of surface finish and form involving components other than that of simple geometries e.g. femoral hip heads will be difficult. Dimensional tolerances required for conformance in the mating of complicated freeform biological components found in TKR's is almost impossible by manually holding the component against a rotating buffing wheel.

3.2.2 Semi and Fully Automated

Semi automated processes involve some manual involvement by the use of electro-mechanical devices i.e. Motorized Polishing Tools, CNC Polishing Tools and Robotic Tools. Although some part of the process requires manual intervention e.g. loading/unloading of components into fixtures.

The introduction of automated polishing began in the 1950's in the way of automated buffing lines due to its simplicity of cloth and compound but only on large volume simple geometry shapes. This continued up until the 1980's where the development of CNC allowed for more complicated movements involved in the polishing of complex geometries. Precision surface finishes and form control are now processed using semi or fully automated polishing processes.

There are references in modern day literature relating to reducing costs throughout semi or fully automated finishing processes [180-183]. Today's technology will see the manual finishing process for biological implants become obsolete in the near future due to the benefits involved with automated processes including: -

- ***Reduced Labor Costs*** - Less workers are required for automated process.
- ***Reduced compensation claims*** - e.g. repetitive strain injury (RSI) caused by manual processes being eliminated.

- **Health and Safety** - Manual processes will not achieve the quality of ever demanding health and safety regulations e.g. air quality and disposal of hazardous waste etc.
- **New Manufacturing Techniques** - Automated processing lends itself to such techniques i.e. Just-In-Time (JIT) Manufacturing.
- **Quality Control** - Demands from customers can only be achieved by automated process.
- **Reduction in safety equipment costs** - Robots do not need protective clothing.
- **Reduction in media costs** - Automated quality control of condition of media reduces waste

These benefits are just a few and the list is far from exhaustive but gives the reader the idea of the rapid rate of movement towards a fully automated finishing process for biological implants.

Fully automated processes include the use of robots to implement the human functions associated with manual and semi automated finishing processes. Although robots do not have the sense and touches associated with that of skilled manual polishers they do have the capabilities of larger ranges of programmable motion that are far more repeatable than any skilled operator. An automated finishing process involves the movement of a component or components inside cells through different locations in which stages of the final finishing process will be carried out.

The key components in developing an automated finishing process include part selection, cell consideration, process head(s), end of arm tooling, cell arrangement and software etc. Careful selection/consideration in these areas at the early stages of development of an automated finishing process configuration can increase productivity, and reduce waste through scrap components. Some images of cells used in automated polishing of orthopaedic knee implants can be seen in Figure 3.3.

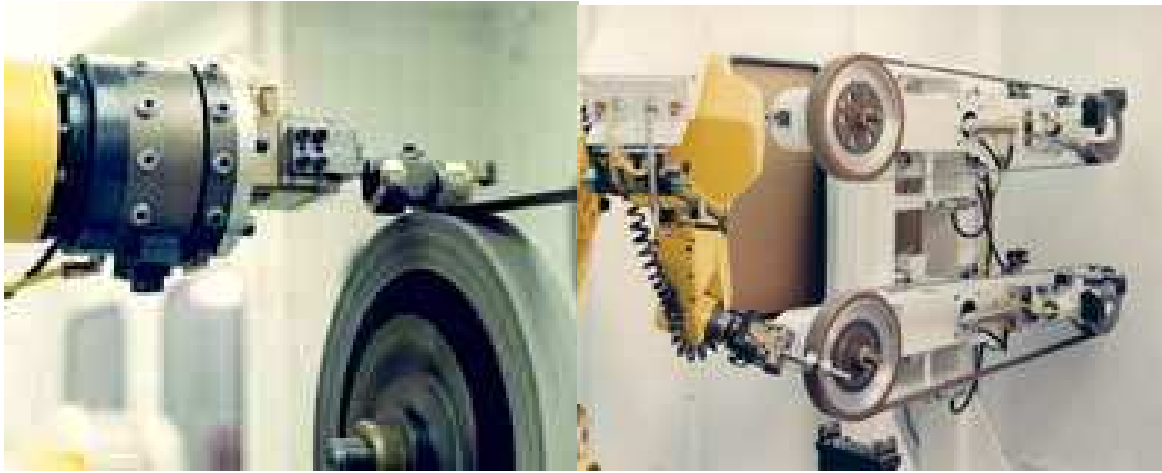


Figure 3.3 Fanuc Robots Grinding Knee Implants in an Acme Manufacturing Robotic Cell

[184, 185]

3.3 Polishing Media

Final finishing of biological implants requires the use of various polishing media for the purpose of this thesis the polishing media has been defined as one of the three following groups: -

- Fixed Abrasive
- Loose Abrasive
- Carrier Materials

The choice of polishing media is dependent on the application including material, initial conditions, desired surface finish and form control etc. The choice of abrasive will affect the amount of material removal and surface finish e.g. smaller particle abrasive will generate a better surface finish but will generate smaller amounts of material removal associated with a larger particle abrasive which generates a rougher surface finish.

Grit sizes range from 1815 μ m-68 μ m (Macrogrit) to 58.5 μ m-8.4 μ m (Microgrit) diameter particles with the most common standards being European FEPA (Federation of European Producers of Abrasives) "P" grade and United States CAMI (Coated Abrasive Manufacturers Institute, now part of the Unified Abrasives Manufacturers' Association) of which the former is the same as the ISO 6344 standard.

Table 3.1 shows a comparison of these two standards and their average particle diameter size in microns for Macro (a) and Micro (b) grits as defined in the ISO 6344 standard [186] by preparing and sieving the particles through mesh gratings. The selection of the size of grit is dependent upon the application required Figure 3.5 shows the FEPA grit sizes and the applications in which they are used.

Table 3.1a Comparison of ISO and CAMI Standards for Macro Grits

Grit Category	ISO /FEPA	CAMI	Average particle diameter (µm)	Application	
Extra Course (Very Fast Removal of Material)	P12		1815	Deburring and Cutting Off Of Implant Components After Forging/Casting Processes	
	P16		1324		
	P20		1000		
	P24		764		
		24	708		
	P30		642		
		30	632		
		36	530		
P36		538			
Coarse (Rapid Removal of Material)	P40		425		
		40	348		
	P50		336		
Medium		50	285		Grinding of Orthopaedic Implants After Forging/Casting To Remove Defects and Prepare For Finishing Process
	P60		269		
	P80		201		
		60	190		
Fine	P100		162		
		80	140		
	P120		125		
Very Fine		120	115		
	P150		100		
		150	92		
	P180	180	82		
	P220	220	68		

Table 3.1b Comparison of ISO and CAMI Standards for Micro Grits

Grit Category	ISO /FEPA	CAMI	Average particle diameter (µm)	Application
Very Fine	P240		58.5	Superfinishing of Orthopaedic Implants Before Sterilization, Packaging, Certification And Ready For Off The Shelf Products For Surgeons To Select
		240	53	
	P280		52.2	
	P320		46.2	
			40.5	
Extra Fine		320	36	
	P400		35	
	P500		30.2	
		360	28	
	P600		25.8	
Super Fine		400	23	
	P800		21.8	
		500	20	
	P1000		18.3	
		600	16	
	P1200		15.3	
Ultra Fine	P1500	800	12.6	
	P2000	100	10.3	
	P2500		8.4	

* Tables 3.1 a and b constructed from various sources [187, 188]

3.3.1 Fixed Abrasive

The term fixed abrasive as it suggests is where the abrasive used in the material removal mechanism is fixed into a matrix with a bonding material. Bonding materials are flexible or semi-flexible and include such materials as paper, cloth, resin and metal.

The purpose of a fixed abrasive is to wear away over a period of time by degradation of cutting edges of the abrasive breaking or falling away from the bonding material and exposing new sharp abrasive cutting edges as seen in Figure 3.4. This process is known as self sharpening. The fixed abrasive bonding material has many forms of which the most common can be seen in Table 3.2.

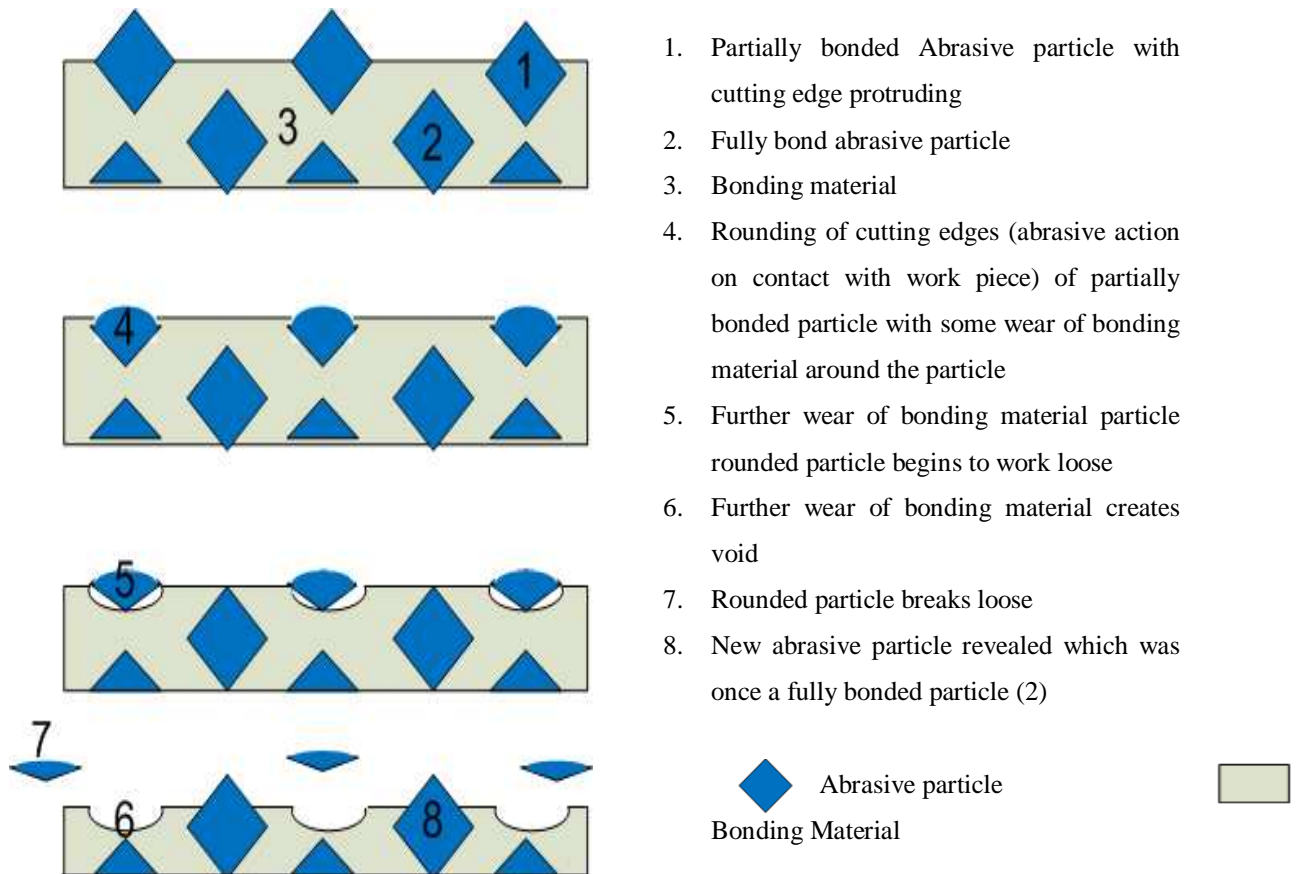


Figure 3.4 Schematic of the Fixed Abrasive Self Sharpening Process

Material removal prediction of metals especially in the cases of freeform components the material removal is diverse and equations relating to the mechanism involved in predicting material removal are uncertain as the variables associated with fixed abrasive polishing conditions as well as the geometry and mechanical properties of the tool all effect the material removal process.

Removal predictions of glass material based on the Preston equation (Equation 3.1) where the volume of material is proportional to the applied pressure times the velocity with a constant named after Preston relating to the polishing media being applied i.e. lap, grit, carrier material etc. have been documented.

THE APPLICATION OF ZEEKO POLISHING TECHNOLOGY TO FREEFORM
FEMORAL KNEE REPLACEMENT COMPONENT MANUFACTURE


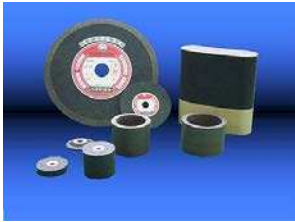
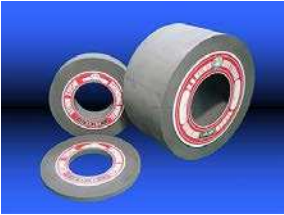

Type	Description	Advantages	Disadvantages
 Vitrified Bond	Fired materials such as feldspar or clay bond the abrasive grains together	Easy adjustment of grain and structure. Burn prevention due to numerous pores helping lubrication Not affected by lubricant choice	Low operation speeds required
 Resinoid Bond	Thermo set Bakelite is hardened around the abrasive to create the bond	Elastic, High Tensile therefore can be used in high operation applications such as cut off wheels and depressed centered wheels.	Careful choice of lubricant as can be affected by choice of oil and excessive heat
 Rubber Bond	Thermo set synthetic or natural rubber is tempered with the abrasive to create the bond	Similar to Resinoid bond but need to be used in reduced pressure applications to reduce the risk of bond breaking	Careful choice of lubricant as can be affected by choice of oil and excessive heat. Low contact pressure must be maintained.
 Foaming Method	Synthetic resins i.e. urethane are manufactured to hold the abrasive grains	Highly elastic and water resistant hence applicable for non ferrous metals e.g. aluminum. Reduce heat generation, high edge resistant with a consistent surface finish and high stock removal	Difficult to manufacture only available through experienced manufacturers.

Table 3.2 Forms of Fixed Abrasive Bonding Materials [189]

$$\frac{dz}{dt} = K_p P V_r$$

Where P is polishing pressure, V_r is the relative velocity, t is polishing time, and K_p is the Preston coefficient made up of a grain size, concentration of abrasives, workpiece and polishing tool materials

Equation 3.1: The Preston Equation

Zang et al (2003) [190] attempted to quantify the material removal by adapting the Preston equation to that of S55C steel and verified the equation with theoretical results which were closely correlated to the theoretical calculations when polishing convex/concave surfaces. Due to complexity of the equation and the amount of justification through experimental results this is by no doubt the most accurate evaluation of material removal yet. Furthermore material removal predictions for three dimensional paths of parabolic and aspherical surfaces have been derived by the principle authors of the previous paper Tam et al (2004) [191] based upon the same principles and again produced closely matched predicted and theoretical results.

3.3.2 Loose Abrasive and Carrier Material

Loose abrasive as the term suggests is loose abrasive particles which are allowed to move freely across the work piece surface creating an abrasive action and hence material removal where the sharp abrasive particles make contact with the surface. Loose abrasive needs to be applied by a carrier material or surface and the removal mechanism is dictated by the choice of abrasive and carrier material.

The components involved with material removal mechanisms that involve loose abrasive and carrier materials are described by four components by Evans et al (2003) [192]: -

- Workpiece
- Carrier Fluid
- Granule
- Lap (Rigid for lapping and Semi-Rigid/Flexible for Polishing)

These components can be seen in the Figure 3.5.

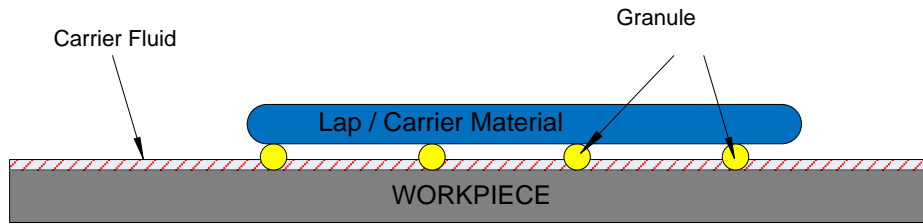


Figure 3.5 Loose Abrasive and Carrier Components of Material Removal Mechanisms

[192]

Evans et al discusses the interactions in detail and emphasises that an understanding of the interactions is required to fully understand material removal in finishing of various materials using the loose abrasive polishing process.

3.4 Basic Material Removal Mechanisms in Final Finishing

Section 3.3 discussed the polishing media used in final finishing of knee implant components. For a better understanding the basics behind the material removal mechanisms need to be understood. The interactions between the polishing media and the surface whether it be fixed or loose abrasive is defined as a three body abrasive mechanism of which the behavior of the particles used for final finishing will fall into one of three categories during the process: -

- Sharp Cutting
- Rolling Grit
- Blunt Ploughing

3.4.1 Sharp Cutting

Sharp cutting occurs when there are plenty of sharp abrasives in contact with the surface the loose or fixed abrasive will create microchips of material across the surface as seen in Figure 3.6.

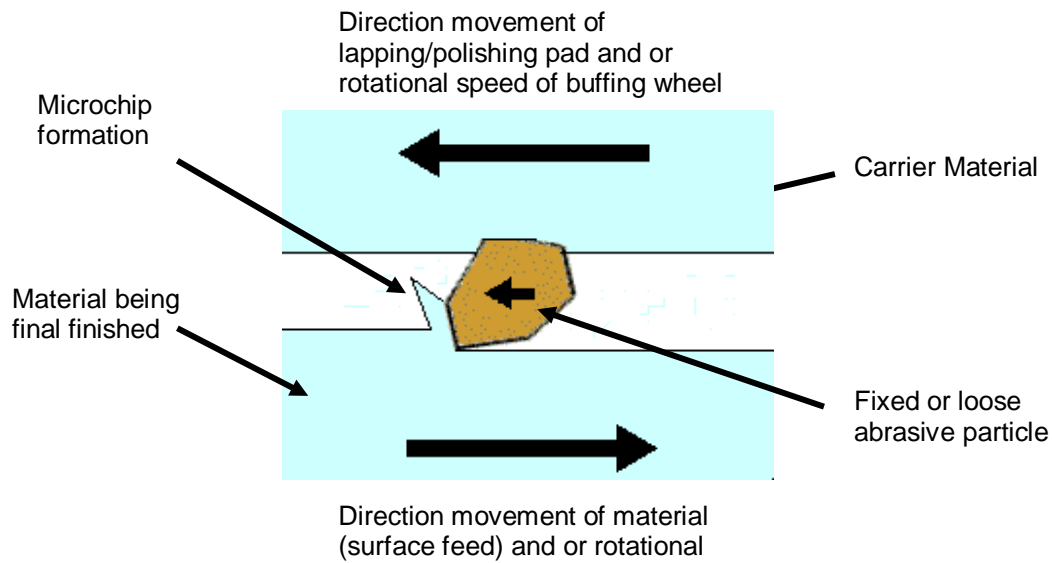


Figure 3.6 Sharp Cutting leading to microchip generation on the surface

3.4.2 Rolling Grit

Rolling grit occurs when particles become trapped between the surfaces of the carrier material and the workpiece and they roll across the surface generating material removal in the way of micro-fractures and micro cracks as seen in Figure 3.7 and in the micrograph of Figure 3.8.

3.4.3 Blunt Ploughing

Blunt ploughing occurs when the particles are coming towards the end of their physical lifetime and are blunt and rounded causing them to become fixed in the surface of the carrier material or the material being finished. Rather than cutting or fracture/cracking the surface as seen in the two other states they plough through the surface leaving a trough in the material as seen in Figure 3.9

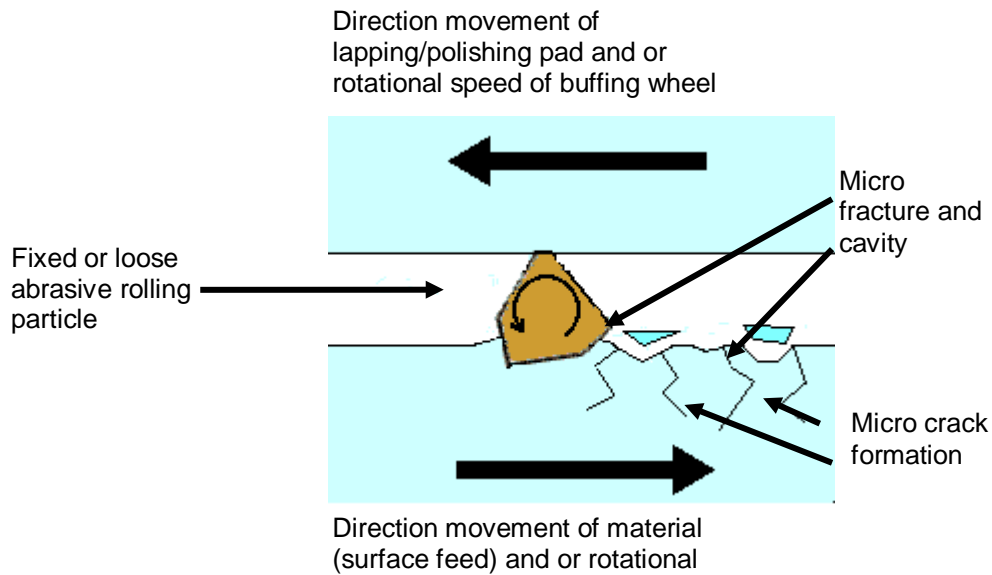


Figure 3.7 Rolling Grit causing micro fractures and cracking on the surface

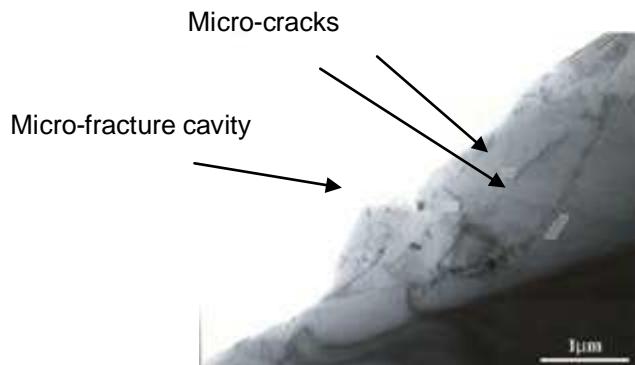


Figure 3.8 Magnified Surface showing micro-cracks and micro fracture cavities [193]

3.5 Simple modelling of material removal mechanism in final finishing

The size of the microchips, micro fractures and ploughing troughs are dependent on variables such as particle size, chemical composition of the material/abrasive (Table 3.3), shape of abrasive granule (Figure 3.10), mono-crystalline or poly crystalline granules (Figure 3.11), carrier material (Figure 3.12) etc.

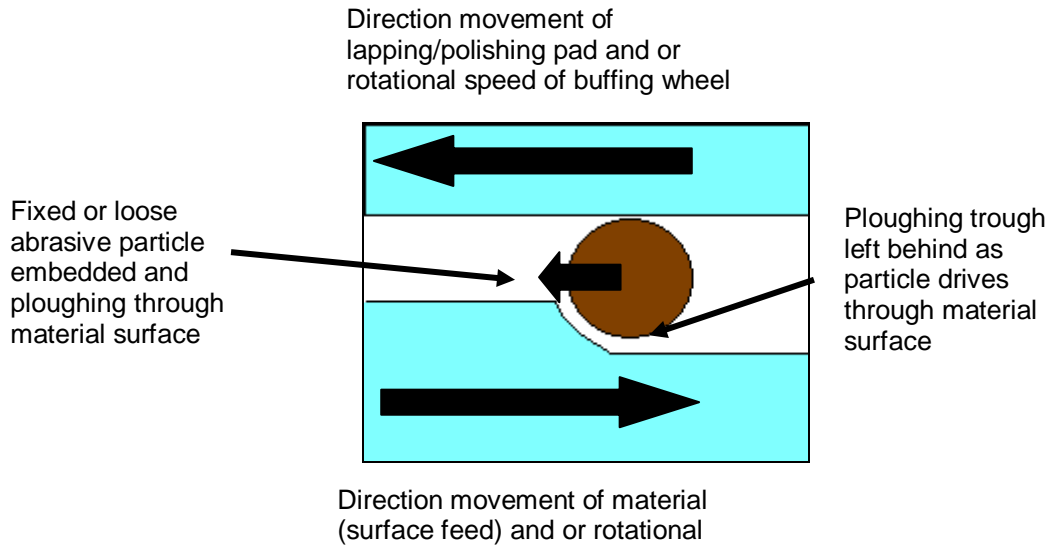


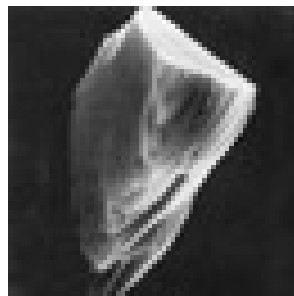
Figure 3.9 Blunt Ploughing of Abrasive Particles in the Finishing Process

Table 3.3 Chemical Compositions of Materials and Loose Abrasives

Chemical Composition	Examples
Metals	Steel, Nickel, Cobalt Chromium, Titanium etc.
Covalent Network	Silicon Nitride, Boron Carbide
Ionic Network	Quartz, Silica
Simple Ionic Network	Calcium Fluoride



Figure 3.10 Various Abrasive Granule Shapes



(a)



(b)

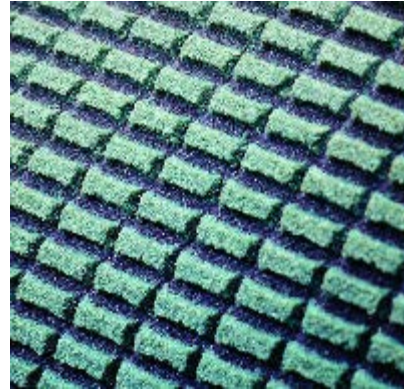
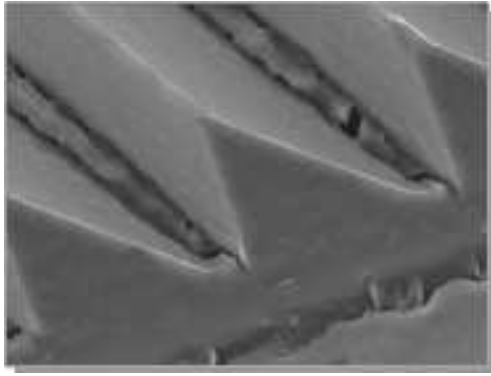
Figure 3.11 Monocrystalline (a) and Polycrystalline Granules (b)



Cast Iron Laps



Pitch and Fixed Abrasive Polishing Pad and Loose Abrasive Cloths



3M Trizact Advanced Lapping Pad

Figure 3.12 Various Carrier Materials

[194-201]

With a better understanding of basic material removal mechanisms the basis of simple modelling of the material removal can be achieved.

Xie and Bushan (1996) [202] and Trezona et al (1999) [203] produced equations to simplify the interactions between the surface and polishing media to create simplified equations of the wear index to predict material removal in free abrasive polishing a summary of which can be seen in Table 3.4.

Table 3.4 Summary of Research into Prediction of Free Abrasive Metal Removal

Authors	Equation	Comments
Xie & Bushan	$\frac{(P/E_p)(R/\sigma)^{0.5}}{(H_p/H_w)^{1.5}}$ <p>P = Contact Pressure σ = Standard Deviation of the Height of the Polish Pad E_p = Elastic Modulus of Polishing Pad H_p = Hardness of the Polishing Pad R = Particle radius H_w = Hardness of the Workpiece</p>	<p>Only positive results achieved when applied to a soft polishing pad.</p> <p>Wear index was found to approximately proportional and linear in respect to experimental testing of wear</p> <p>Surface roughness is mainly contributed to particle size and polishing pad hardness.</p> <p>If polishing harder material then to achieve a high material removal rate and a smooth surface then the performance of diamond particles over that of Al_2O_3 particles is recommended due its high resistance to deformation.</p>

Trezona et al	<p>Experimental findings in relation to Archard's wear equation</p> $\frac{V}{S} = K \frac{F}{H}$ <p>V = volume of material worn away, S = total sliding length, F = normal force i.e. the load, K = Wear Coefficient H = hardness of the worn material</p>	<p>Abrasive polishing consists of a three body situation which includes two body grooving and three body rolling mechanisms due to variations of normal load, volume fraction of abrasive in the slurry, and type of abrasive used.</p> <p>High loads and low abrasive volumes contributed to two body grooving mechanism whereas low loads and high abrasive volumes caused third body rolling mechanisms in SiC, Al₂O₃ and diamond abrasives used in validating the Archard's equation through simulation.</p> <p>The wear coefficient K, showed a transition between two body to three body mechanisms as a constant ratio of normal load to slurry volume fraction in SiC and Al₂O₃ whereas with diamond a wider variation was experienced although mean values were similar to SiC, Al₂O₃.</p> <p>A non-linear rate of abrasive wear to slurry concentration was evident with the largest variations happening at intermediate slurry concentrations.</p>
---------------	---	--

3.6 Why Freeform Surfaces in Knee Implant Design?

Looking at the dictionary the definitions for free-form and surface are: -

Free-form *adj.* - Not conforming to a regular or formal structure. [204]

Surface - The boundary of a geometric shape in three dimensions. For example, the surface of a cylinder has two circular sections and a curved surface. [205]

From these definitions therefore a freeform surface can be defined as: -

Freeform surface: - The boundary of a geometric shape in three dimensions that does not conform to a regular or formal surface

3.6.1 Need for Freeform Surfaces

Freeform shapes are used in the manufacture and design of engineering surfaces (Figure 3.13) either for aesthetics and function performance e.g. car bodies [206] or for complex fluid or air

flow dynamics e.g. turbine blades [207] or even just aesthetics everyday consumer objects e.g. sofas. [208]

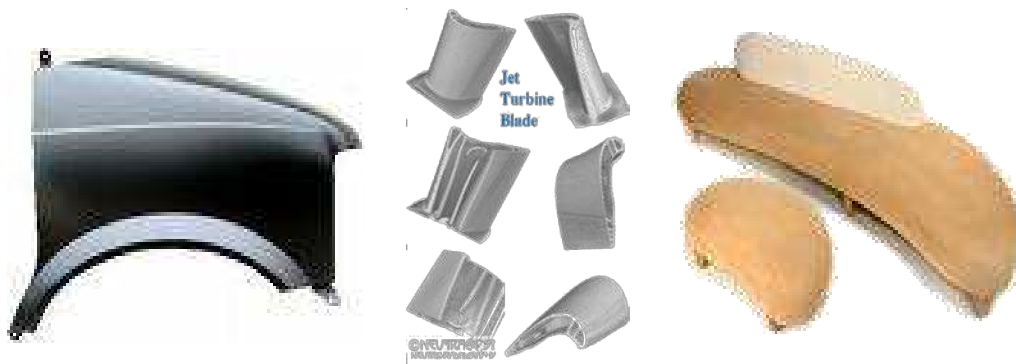


Figure 3.13 Examples of Engineered Freeform Surfaces

3.6.2 Freeform Femoral and Tibial Insert Knee Components

The freeform principle was applied in modern day TKR designs where the load bearing surfaces have been adapted to mimic that of human tibia and fibula bones by design and manufacture of femoral knee, knee cap and tibial tray insert components from freeform surfaces. An example of such designs can be seen in (Figure 3.14)

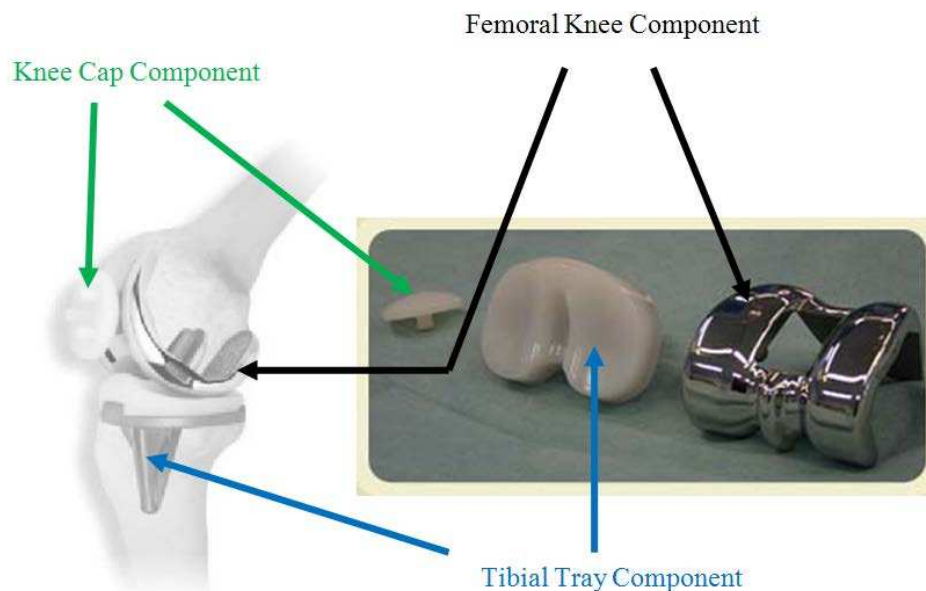


Figure 3.14 Freeform Femoral Knee, Knee Cap and Tibial Tray Insert [209, 210]

3.7 *Summary*

The manufacture of freeform implant components is a very diverse subject due to the options for material selection, post machining processes (casting, forging etc.), machining processes (grinding, milling, drilling etc.) and eventually the final finishing processes (polishing, packaging etc.) not to mention the mechanical testing and dimensional tolerance checking that is required at almost every stage of the manufacturing process.

Design standards are used as a measure of control throughout most manufacturing processes, although in the case of freeform knee implant surfaces these standards are nonexistent or extremely vague. At the time of this thesis there is an international understanding that to drive forward the control in manufacture of freeform knee implant components there is need to clarify and fully define standards.

The post machining process includes variations of casting and forging. Each of the processes has their own advantages as well as disadvantages. Forgings yield components with greater strength than other metalworking processes mainly due to grain refinement.

In the case of Titanium, forgings are better due to the lack of waste material produced compared to the other processes. Although when creating implants that require less tensile strength e.g. femoral knee components then casting is a better solution as casting can create better dimensional tolerances than those associated with forgings.

Machining processes used to remove the residual material associated with casting or forged biological components vary but their objective is to create a near net shape component for the final finishing stage of the manufacturing process. They range from traditional machining (grinding, milling etc.) to non traditional machining methods (Abrasive Waterjet, Ultra Sonic Machining etc.) which remove material in the millimetre to micron sizes.

Advances and needs in biological and freeform implant components has seen the development of traditional machining and also non-traditional machining methods to create machinery that can remove material into the submicron and nanometre ranges.

Finishing of biological and freeform implants pays a key role in improving the surface roughness which reduces wear particles. In years gone by biological implants have been finished by skilled hand polishers using combinations of loose abrasive and carrier materials as well as fixed abrasives. Although as time has advanced the technology has also with the ever rapidly increasing proportion of automated polishing lines being introduced the days of the hand polisher is becoming obsolete. The introduction of CNC operated automated finishing lines that can grind and polish the contours of freeform components to surface finishes, and form tolerances far superior to that of the hand polisher have instigated the end of a historical era of manually finished components.

Understanding material removal mechanisms in orthopaedic implant materials is an under researched topic with many attempts at predicting material removal being adapted in a simplified form from other materials such as glass. Freeform surfaces cause problems in material removal prediction as the rate of material removal constantly changes across the surface due to factors such as material properties and contact pressure of the polishing media.

**CHAPTER 4:
METROLOGY & TEST
METHODS FOR IMPLANT
MEASUREMENTS**

4 METROLOGY & TEST METHODS FOR IMPLANT MEASUREMENTS

There is a need to monitor the surface quality and geometry of the surfaces of medical implants throughout their manufacture. Dimensional tolerances are critical at the early stages of manufacture with tolerances in the region of 0.5mm-0.1mm for less critical dimensions such as fixation pin diameters to 50-100 μ m for bearing surfaces to ensure that final finishing of the mating components can be meet to requirements without excessive processing times. Final surface finishing of components requires lower tolerances of <100 μ m for geometry/conformance of load bearing surfaces to measurement of surface quality which lies in the >50 nm region.

In this chapter of the thesis standards that outline these tolerances and define the measurement methodologies will be discussed. The roles of instrumentation for both contact and non contact measurement will be outlined discussing the functionality, advantages, disadvantages and limitation involved with each type of equipment. Definitions of biological surfaces are dependant on 2D surface parameters and relevant 3D characterisation parameters together with the development of freeform metrology for complex biological surfaces; these are topics that will be discussed.

Testing of implant surfaces before implanting them in the human body is essential. This chapter will conclude with basic outlines of the various strategies ranging from pin on disc to fully instrumented simulators, to assess volumetric material loss. These test methods will be analysed through investigation of their advantages, disadvantages and limitations.

4.1 Metrology needs of implant surface manufacture

As already discussed previously inspection of biological surfaces throughout their manufacture plays an important role. The metrology needs of biological surface manufacturing process involves measurements from dimensional tolerances of moulds used to create the basic shape of the component through to final surface measurements to determine the roughness, roundness and geometry etc. Standards mentioned at the beginning of chapter 3 of this thesis will determine whether the component is fit for purpose and can be packaged and delivered to the end user. A summary of key types of metrology associated with the manufacture of femoral knee component can be seen in Figure 4.1

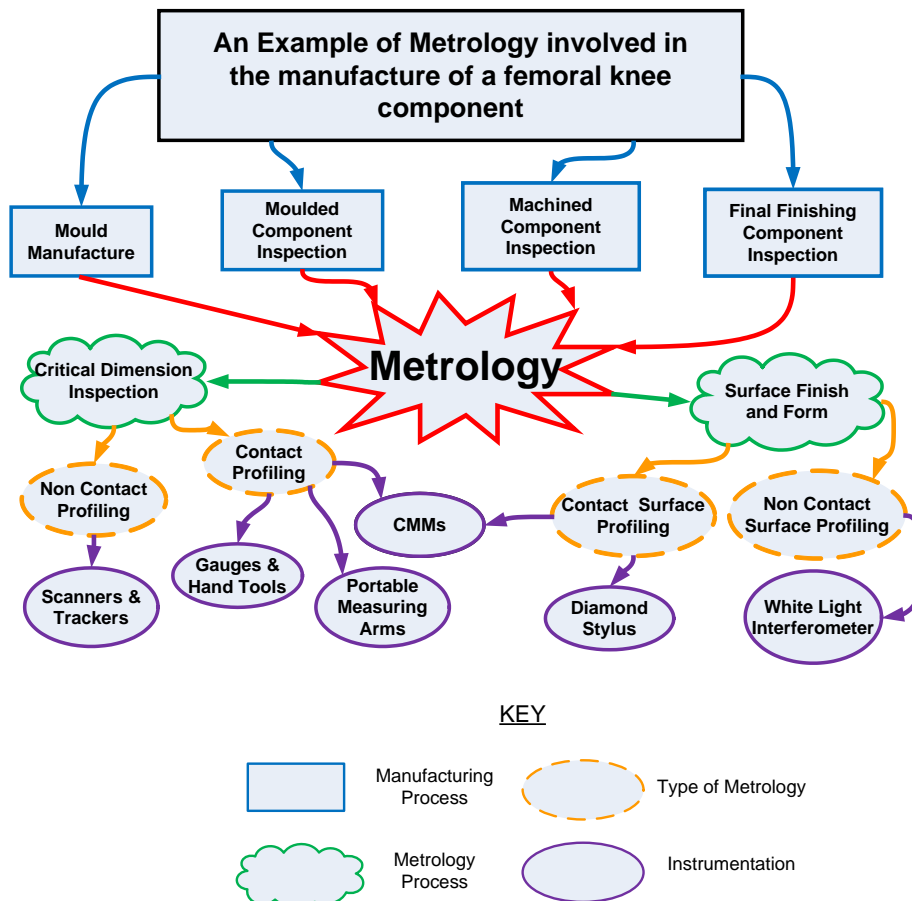


Figure 4.1 Examples of Metrology for manufacture of a femoral knee component

4.1.1 Standards for Measurement

The standards for measurement with relevant metrology information that are associated with the manufacture TKRs are defined in the standards shown in Table 4.1

4.1.1.1 Measurement Standards associated with THRs and TKRs

Recommendations for measurements taken for hip joints are specified in BS7251-3 BS7251-4 they are quoted for the femoral stem and ball, the femoral ball and the acetabular cup components. The standards associated with the metrology and surface measurements of TKR manufacture are outlined in BS 7251-2 and BS7251-14. The standards cover the metrology related to definition and dimensions of partial as well as TKR components together with the final tolerances of the finished components.

Table 4.1 Standards information for the metrology of TKRs

BS No.	ISO No.	Contents
BS7251:2 1995	ISO7207:1 1994	Specification for classification, definitions and designation of dimensions of femoral and tibial components for partial and total knee joint prostheses.
BS7251:14 1998	ISO 7207-2 1998	Components for partial and total knee-joint prostheses - Articulating surfaces made of metal, ceramic and plastics materials

It should be noted for the case of TKR's at the time of publication of this thesis that there are no recognized international standards to define the geometry of the articulating surfaces and that the surface roughness guides are a magnitude higher than what current industrial techniques for finishing of orthopedic implants are currently achieving. Hence a summary of some of the tolerances associated with THRs as well as TKRs including the metrology instrumentation used to check stipulated tolerances have been summarised in Tables 4.2 and 4.3 respectively.

THE APPLICATION OF ZEEKO POLISHING TECHNOLOGY TO FREEFORM
FEMORAL KNEE REPLACEMENT COMPONENT MANUFACTURE

Looking the information it can be seen that there are a lot more stipulated tolerances for THR's suggesting that the standards for TKR's should be reviewed and that some guidelines to surface geometry should be included with amendments to the surface roughness targets for both THR's and TKR's in respect to current industrial practices.

Table 4.2 Surface Metrology Guidelines for Articulating THR Surfaces [211]

Metrology Property	Hip Standard BS 7251-4	Metrology Instrumentation used to obtain measurement data
Roundness	5um (stainless steel/cobalt chrome alloys) 8um (Titanium alloys) in any one plane	CMM and Specific Roundness Testing Machines
Sphericity	Less than 10um (heads) and 100um (cups) of radial separation as defined from measurement	CMM and Specific Roundness Testing Machines
Surface Finish	0.05um or 50nm (stainless steel/cobalt chrome) 0.1um or 100nm (Titanium alloys)	Diamond Stylus Profilors and Non-Contact Surface Profilors i.e. White Light interferometer
Dimensional Tolerances	Spherical bearing surface diameter between 0 to -0.2um of the nominal diameter	CMM, Portable Measurement Arms and Manual Gauges/Tools
Visual Inspection	Viewing x2 magnification no embedded particles , defects with raised scratches or scores should be evident	Trained Eye of a Skilled Inspector

Table 4.3 Surface Metrology Guidelines for Articulating TKR Surfaces [212]

Type	Surface Roughness	Metrology Equipment
Metal or ceramic femoral components	<p>$Ra \leq 0.1 \mu\text{m}$ or 100nm (Cutoff = 0.08mm and stylus diameter and location of measurement should be recorded)</p> <p>Articulating Surfaces should be free of embedded particles, defects, raised edges and scratches/score marks</p>	<p>Diamond Stylus Profiler</p> <p>Trained Eye Inspection</p> <p>Microscope Inspection</p> <p>Interferometer</p>
Plastic Tibial and Patella components	<p>$Ra \leq 0.2 \mu\text{m}$ or 200nm (Cutoff = 0.08mm and stylus diameter and location of measurement should be recorded)</p> <p>Articulating Surfaces should be free of scale, embedded particles, defects, raised edges and scratches/score marks other than that from the finishing process</p>	<p>Diamond Stylus Profiler</p> <p>Trained Eye Inspection</p> <p>Microscope Inspection</p> <p>Interferometer</p>
Metal or ceramic femoral prostheses for partial knee-joint replacement	<p>$Ra \leq 0.2 \mu\text{m}$ or 200nm (Cutoff = 0.08mm and stylus diameter and location of measurement should be recorded)</p> <p>Articulating Surfaces should be free of embedded particles, defects, raised edges and scratches/score marks.</p>	<p>Diamond Stylus Profiler</p> <p>Trained Eye Inspection</p> <p>Microscope Inspection</p> <p>Interferometer</p>

4.1.2 Instrumentation

To aid the measurements involved in the dimensions and surface metrology of THR's and TKR's associated with the British Standards various instrumentation devices are required to measure critical dimensions, surface roughness and to determine whether the tolerances have been achieved to pass each manufacturing stage and end up with an off the shelf components available to surgeons worldwide. The main types of instrumentation used for the dimensional and surface metrology of THR's and TKR's are: -

- Contact Metrology
- Non Contact Metrology

Each of these types of metrology will be described and examples of the instrumentation used with reference to biological and freeform surfaces will be discussed. References are mainly THR's and TKR's orientated.

4.1.2.1 Contact and Non-Contact Measurement

The principle of contact measurement can be seen in Figure 4.2. The definition of non-contact measurement is self explanatory meaning that measurement of the surface of the component is taken without any contact with the surface hence eliminating the possible damage of the surface which can occur when using contact methods.

Several types of no-contact measurement techniques have been developed but those that are most commonly adapted to the measurement of biological components is that of the white light interferometer. A summary of the most commonly used contact and non-contact measurement equipment and their uses in hip and knee implant measurement can be seen in Table 4.4

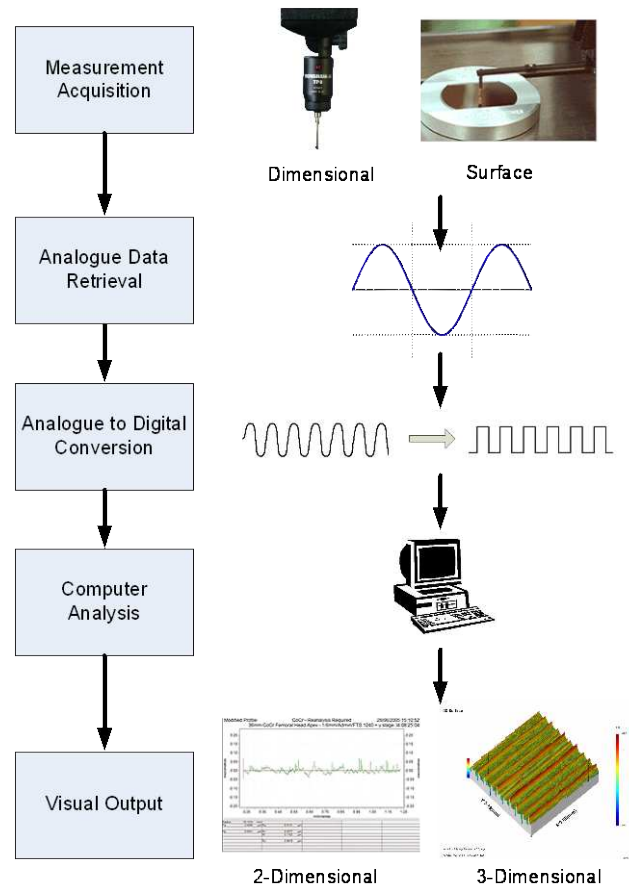
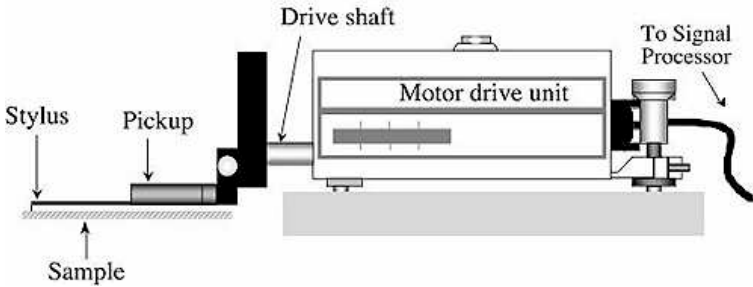
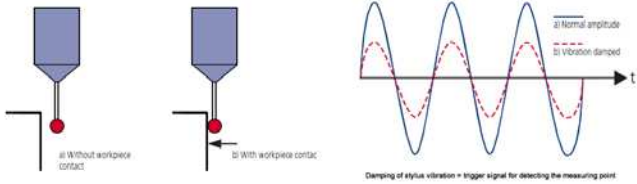


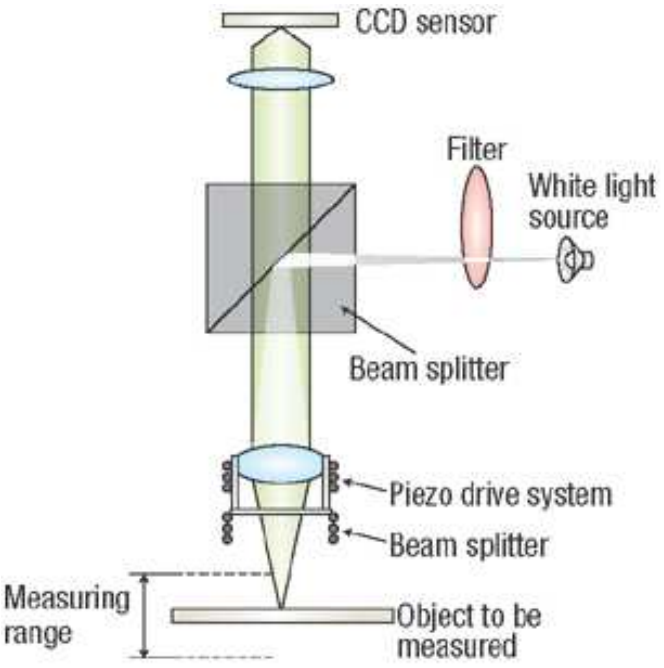
Figure 4.2 Principles of Contact Measurement

4.1.3 Surface Characterisation of implant surfaces

Using surface characterisation researchers have emphasized the importance of smoothness and form matching of load bearing surfaces of hip and knee joints [213-217]. These elements are critical if fluid film lubrication or boundary lubrication conditions are to be achieved.

Table 4.4 Contact/ Non-contact Measurement Equipment used in Implant Applications

Equipment	Brief Description	Hip/Knee Application Examples
 <p style="text-align: center;">Diamond Stylus [218]</p>	<p>Motor drive movement of pickup device (stylus) is moved across sample producing electrical signals which can be amplified and processed with the resultant output defining the surface.</p>	<ul style="list-style-type: none"> • Quality control of surface finishing of hips/knees [219]. • In-vivo [220, 221] and in-vitro [222, 223] wear measurements of hips • In vivo wear scar analysis/surface roughness measurements of knees [224, 225]
 <p style="text-align: center;">Co-ordinate Measurement Machine (CMM) [226]</p>	<p>Digital signal from probe driven at a constant force in contact with the component is picked up by resistance sensors. The X, Y and Z positions are recorded upon contact of the component using linear scales.</p>	<ul style="list-style-type: none"> • Geometric data [227] • Volumetric loss of implant retrievals [228] • Measurement of wear from in-vitro simulations [229].

Equipment	Brief Description	Hip/Knee Application Examples
 <p>White Light Interferometer [230]</p>	<p>Optical interference which splits a beam from an original source into two separate beams, the first of which is reflected from the surface to be measured, the second is used as a reference by following a constant optical path.</p> <p>Fringes caused by the difference in two recombined beams is picked up by a Charged Couple Device sensor and then converted into a representation of the surface being measured.</p>	<p>Measurement of surface roughness of final-finished hips/knees without damaging the component [231]</p> <p>Measurement of wear scar volumes of in-vitro wear simulation [232]</p>

4.1.3.1 2D Surface Parameters

The 2D centre line average roughness (CLA) [233] which was originally calculated by analogue computers from the peak to valley variations of a stylus driven over the surface to be measured. CLA born in the early 1970's would later be known as Average Roughness (Ra) and because of its use worldwide it is still commonly used today. Ra was shown to have specific limitations and additional 2D parameters were introduced to assess function.

2D surface parameters were additionally developed due to the need to determine geometric aspects of the surface roughness of a machined surface. 2D surface parameters were defined as a measure of the tolerance of the surface to its functionality using height, spacing, hybrid and volume related parameters i.e. the load bearing surface of implants [234-236].

2D parameters were developed by academic institutes in correlation with company's right up until the late 1970's. For further reading a list of 2D parameters and their definitions can be found in EN BS ISO 4287 [237]. The emergence of 3D surface parameters from the extensive and exhausted 2D parameter research is beginning to see the demise of 2D surface parameters with their 3D equivalents especially in the case of bio-engineering the most commonly used parameters will be discussed in section 4.4.3 especially those associated with knee replacements.

4.1.3.2 3D Characterisation

With the ever increasing processing power of computers through Moore's Law [238] and the transfer from the analogue to digital computer processor [239] researchers at the turn of 1980's started to see the limitations of 2D surface parameters and started to think and dream of a surface that could be defined as three dimensional through a set of three dimensional parameters. An example of such systems was developed by a team of researchers at Coventry University in the early 1980's [240].

Furthermore the same team transferred to Birmingham University and developed a set of 3D surface parameters that lead to the International Standard ISO 25178 which has grown from the definition of 14 3D surface parameters to over 30 surface parameters as well covering classification of methods for measuring surface texture. The standard covers aspects of filtering, file format and data acquisition procedures.

4.1.3.3 Parameters that define Biological Surfaces

The use of 3D parameters described in ISO 25178 and can be used to define the function of biological surfaces. The parameters outlined in the ISO 25178 standard can be defined into two categories: -

- S-parameter set (6 amplitude, 3 spacing, 3 hybrid, 1 fractal and 2 others)
- V-parameter set (5 linear areal material ratio curve, 2 void volume, 2 material volume)

An example of some of the S and V surface parameters including a brief description and relevant research and suggested applications where these parameters have been applied to orthopaedic knee and hip implant manufacture can be seen in Tables 4.5 and 4.6 respectively.

4.1.3.4 Development of Freeform Metrology

Ever since free-forms were introduced into the designs of the femoral and tibia components of TKRs there was an importance placed on the need for developments in freeform metrology. One of the arising issues in freeform metrology is the lack of available artifacts to calibrate measurement machines that have the ability to measure freeform surfaces this is especially important for CMMs.

THE APPLICATION OF ZEEKO POLISHING TECHNOLOGY TO FREEFORM
FEMORAL KNEE REPLACEMENT COMPONENT MANUFACTURE

Table 4.5 Some 3D Surface S-Parameters with Implant Manufacturing Applications

Parameter	Description	Application to Hip/Knee Implants
Sq	Root means squared deviation of the surface	Most commonly used and sample standard deviation in statistics but does not suffice as a understanding of the function of the surface
Ssk	Skewness of the surface	Comparison of Knee Implant Manufacturing Processes (Hand and Belt Polished) to determine distribution of peaks and valleys in the manufactured surface as well as using Sku to determine tight or wide height distribution of peaks and valleys (Hilario et al 2004) [241]
Sku	Kurtosis of the surface	
Sds	Density of summits in the surface	Comparison of grit blasted and grit blasted plus acid/alkaline heat treatment of the bonding strength of various cements to pure titanium. Sds determined acid treatment increased the density of summits which improved static shear strength of the bond (Fawzy and El-Askary (2008) [242].
Parameter	Description	Application to Hip/Knee Implants
Sdr	Developed interfacial area ratio of the surface	Testing of variation of tensile strength of bone cement fixation between various micro roughness surfaces of titanium using different grain sizes of TiO ₂ particles. No blasting (electropolished) upto 200µm grain sizes produced the best tensile strength with the optimum value of Sdr being at 45-55 with the largest bone to metal contact. Grain sizes between 270-300µm showed a lower Sdr value indicating lower bone to metal contact hence and reduction in tensile strength of the bond (Ronald and Ellingsen 2007). [243]
S5z	Ten point height of the surface (average of 5 lowest valley depths and 5 highest peak heights)	Check of ceramic and sapphire hip implant of hip implant heads to check the effects of anisotropy in the ceramic and partial isotropy in the sapphire which increased the stipulated 2D Ra values from between 0.006-0.020µm to a 3D Sa of 0.05-0.73µm. The S5z values were even higher determining that areal surface properties can give a better indication of wear characteristics of orthopaedic implant materials and the tooling needs to developed to maximize the potential of these low wear materials by reducing the values of contributing 3D parameters (Rozenbeg et al 2008). [244]

Table 4.6 Some 3D Surface V-Parameters with Implant Manufacturing Applications

Parameter	Description	Application to Hip/Knee Implants
Sk	Core roughness depth of the surface after peaks are worn away	Sk value can be used to estimate the contact area with a lower Sk value increasing surface contact hence a large pressure distribution reducing wear.
Spk	Peaks above working surface that are worn during the wear in period	Can be used to estimate the amount of wear that will occur during the “running in” period of orthopaedic implants. Higher Spk values will reduce the contact area an increase initial contact pressure.
Svk	Valley size of the surface after Spk has been removed	Can be used as a performance indicator for synovial fluid retention hence reducing friction which in turn will reduce wear. Larger valley sizes can entrap wear particles to reduce effects of wear particle initiated aseptic loosening.
Parameter	Description	Application to Hip/Knee Implants
Smr ₁	Fraction of the surface above the main plateau consisting of small peaks	Smr ₁ and Smr ₂ could be used to evaluate surface coatings i.e. the lower the Smr ₁ of the coating surface the less coating will be removed during the running in period hence a greater Smr ₂ value will increase the lifetime of the coating before the coating fails.
Smr ₂	Fraction of the surface that will carry the load bearing during the practical lifetime of the surface	

The research in this area is limited but without an artifact of know freeform dimension then the uncertainty and repeatability of freeform measurements cannot be determined although current standards are available and under development for evaluating CMM freeform measurements using standard artifacts i.e. cylinders and spheres. [245-247]

The need for such standards and calibration artifacts has been emphasised by by Savio and Chiffre (2002) [248] quoting: -

“In the future, improvements in manufacturing technology and the commonly increasing demand for tighter tolerances will push for more and more accurate inspection of freeform parts and, therefore, for lower measurement uncertainty.”

The cloud point data retrieved from equipment such as precision CMM's needs to be fitted to the freeform nominal data usually associated with a CAD. The fitting is normally done in two stages rough and then final fitting various techniques for rough fitting are explained by Zhang et al (2009) [249] and are summarised with advantages and disadvantages in Table 4.7.

The final fitting stage more complexed as the roughness of the surface determined by the machining process can have an effect on the technique been used. Several researchers have developed techniques for final fitting of freeform surfaces to nominal data including Zhang et al 2D interactive method which is based upon the Levenberg Marquardt combination of Gauss Newton and steepest gradient decent methods [250] and Cheung et al 3D iterative method [251] which implements rotational and translation fitting in the X, Y and Z axes. A freeform femoral component showing the complexity of the surface can be seen In Figure 4.3.

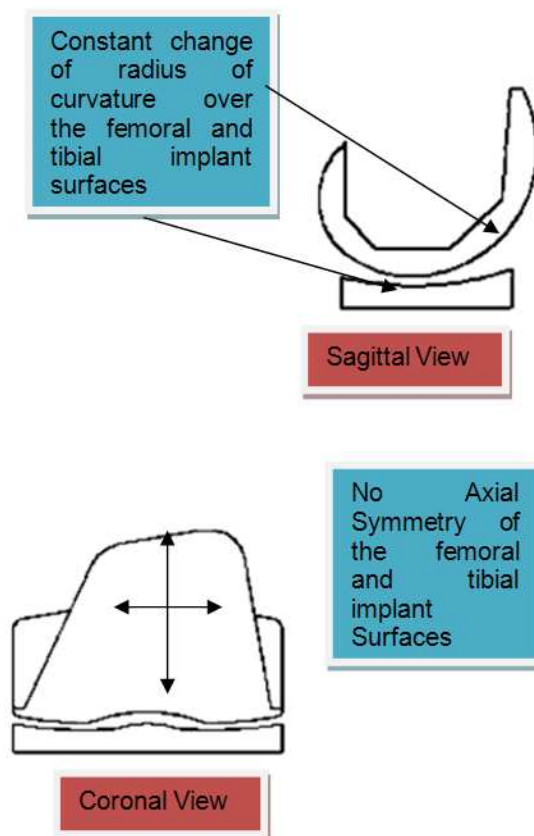


Figure 4.3 Complexity of Freeform Femoral Knee Implant Components

Table 4.7 Summary of Fitting Techniques for Freeform Rough Stage Fitting

Technique	Advantage(s)	Disadvantage(s)
Centers, Feature Lines, Five Point Method	Good results if measurement and nominal's are of identical sizes	Not compatible for partial freeform measurements in comparison to the complete nominal surface
Salient features of CAD model i.e. holes, slots, pockets etc.	Good if component has these features	Most freeform surfaces are void of such features
Mathematical features i.e moments, Fourier descriptors and correlations etc.	Good if only a single parameter or description of the entire surface	Not very descriptive of surface features important to freeform surfaces
Local features - Curvatures, shape index etc.	Good for fitting of surface measurement is free from interference	Sensitive to noise and outliers
Computerized fitting, i.e. point signature spin image etc.	Promising for partially fitting of smooth freeform surface to nominal surface	Processing power and analysis time expensive for these methods

Table constructed from techniques outlined by Zhang et al (2009) [249]

4.1.4 Simulation Tests

On completion of the manufacture of prototypes of knee implants and especially in the load bearing surface action needs to be simulated (in vitro) and the results analysed before the product becomes available to surgeons as an off the shelf product. Simulator tests are a useful aid for prediction of the material loss before the introduction (in-vivo) trials of the product commence and any redesign work can be done to reduce the material loss to acceptable levels before the effect of such wear causes catastrophic failure within a human patient.

The most commonly used simulator tests for TKRs include: -

- Pin on Disc (ASTM F 732)
- Pin on Plate (ASTM F 732)
- Hip Joint Simulators (ISO 14242)
- Knee Joint Simulators (ISO 14243)

Each of these tests is run within guidelines of the relevant ISO /ASTM standard to simulate the particular component under test. Once the tests are complete then the results have to be measured and presented in a report in a certain manner which is referenced in this standard also. The two ways in which wear is measured for the components are: -

- Weight of Material Loss (Gravimetric)
- Measurement of Material Loss (Volumetric)

A summary of the wear simulation techniques can be found in Table 4.8 and a comparison of the measurement of wear with advantages and disadvantages can be found in Table 4.9.

4.1.5 *In-vivo reviews*

The use of in-vitro testing is not fail safe and there has to be something against which the simulation results can be compared therefore clinical data called in-vivo reviews looks at the condition of patients and implants including the quality of life and the amount of wear produced in the case of failed or removed implants.

Validation of in-vitro to in-vivo has been compared by many clinical researchers. In most cases the retrieval data is comparable to that of simulation due to the design considerations to mimic the motions of the knee joint in various activities through the use of advanced simulation testers. [252-254]

Table 4.8 Summary of Wear Test Simulation Techniques for Implants

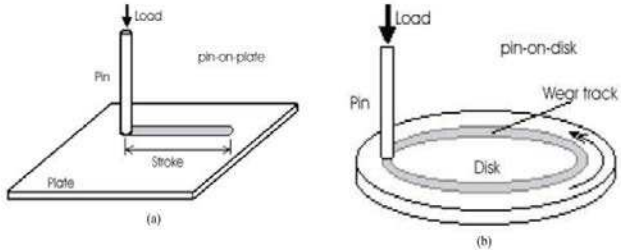


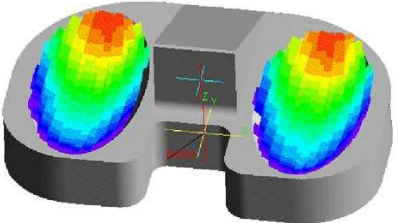
Wear Test Technique	Description	Advantages	Disadvantages
 <p>Pin-on-disc / Pin-on-plate Testing [255]</p>	<p>Reciprocation, rotational or a combination of both reciprocating and rotational movement of a pin against a plate or disc of the same or different material under controlled conditions i.e. constant force, temperature, sliding/rotational speed and stroke.</p>	<ul style="list-style-type: none"> • Results can be obtained quickly for validity of new materials for new implants [256] and coatings [257] 	<ul style="list-style-type: none"> • Limited directional movement with only multidirectional wear tracks being comparable to retrieved explants data [258-260] • Difficult to align components causing excessive wear [261]
 <p>Full Joint Simulators [262]</p>	<p>Fully mimics the movement that would occur within a healthy human body joint including degrees of freedom (3 for hips and 6 for knees), extensions, flexions, loads and displacements once the implant has been inserted. The test have controlled variables/motions and individual lubrication pockets.</p>	<ul style="list-style-type: none"> • Only acceptable testing system for hip and knee implants for Federal Drug Agency approval [263] • Multiple stations can be used in both displacement and load modes simultaneously [264] 	<ul style="list-style-type: none"> • Expensive and time consuming, tests require full joints and 5 million cycles [265] • Risk of damage to components that will effect results if cleaning procedure protocols are not fully adhered too [266]

Table 4.9 Summary of Wear Measurement Techniques for Implants

Wear Measurement Technique	Description	Advantages	Disadvantages
<p>Gravimetric [267]</p> 	<p>The weight of material loss of the bearing components is calculated using a precision balance with an accuracy of 0.001mg after every one million of cycles on either a pin-on-plate or full wear simulator testing rig.</p>	<p>Quick and easy way of measuring wear loss quantified in milligrams per million cycles using the precision balance. The reading can be converted to $\text{mm}^3/10^6$ cycles using the density of the material for a comparison to wear of retrieved components or volumetric methods.</p>	<p>Fluid can affect the weight measurement especially with UHMWPE where it is absorbed through a capillary action in the cavities of the material. Gravimetric measurement is difficult where measurement of new hard-on-hard bearing surfaces produce minimalistic wear volumes [268].</p>
<p>Volumetric [269]</p> 	<p>Measurement of Material Loss is calculated in mm^3 per million cycles using metrology equipment suitable for measuring volume of material loss e.g. a precision CMM or diamond stylus profiler.</p>	<p>Accurate measurement comparable to volumetric measurements especially when using a precision CMM [269].</p>	<p>Can overcome problems associated gravimetric measurement with low wear rates and also capillary action of lubrication fluids when using a UHMWPE bearing surface [270].</p>

Validation of in-vitro to in-vivo has been compared by many clinical researchers. In most cases the retrieval data is comparable to that of simulation due to the design considerations to mimic the motions of the knee joint in various activities through the use of advanced simulation testers. [271-273]

4.2 Summary

To ensure the quality and prolonged lifetime of orthopaedic implants and reduce the cases of failure through aseptic loosening the process of manufacture and the use of simulation techniques have to be checked. These checks and simulations are governed by international standards that cover issues including dimensional tolerances, location of measurements on load bearing surfaces to check the final quality and simulation control parameters to measurement of material or volume loss during simulation for evaluation of the wear resistance qualities of the materials.

The tolerances associated with these quality control and inspection procedures require the need for special equipment dedicated as a whole group covered under the term ‘metrology’ the equipment includes contact measurement for applications that are using hard materials which are not susceptible to scratches or are not required to be scratch free (superfinished) and non contact measurements for the delicate or easily perishable materials and surfaces that if damaged from contact measurement would affect the performance in such applications as load bearing surfaces.

Typical contact metrology devices used in biological implants are diamond stylus profilers and co-ordinate measurement machines (CMMs). Diamond stylus profilers are use to obtain 2D and more recently 3D surface roughness parameters of the surface to analysis its potential performance as a biological implant material. Advances in CMM research have produce precision CMMs eliminating the concerns associated with large uncertainty and lack of repeatability allowing accurate surface analysis of in-vitro and in-vivo wear scars of load bearing pairs of different material combinations. Results are comparable or in some cases more applicable to certain scenarios to that of its counterpart which made use of gravimetric

weight loss measurements using precisions scales (accuracy 0.001g or better) which can be affected by the capillary action of the material absorbing bodily fluids during simulation.

Non contact metrology devices that are commonly used in biological implant quality control include white light interferometers and laser CMM heads. The use of such devices eliminates the dangers of surface damage associated with contact metrology although in most cases the surface has to be reflective and below a certain level of surface roughness to achieve valid data. Whitelight interferometers are used for a rapid surface roughness parameter measurement of surfaces although this is advantageous in an industrial manufacturing scenario the measurement area is small compared to that of contact stylus profilometry typically 250µm x 250µm. New techniques are being developed to stitch measurements to create larger areas these are still in development stage and have problems.

The origin of surface measurements for use in quality control and analysis of the performance of a biological material/surface in bio-medical applications began with the use of 2D parameters as the technique was developed the understanding of academics and industrial partners alike began to realise that 2D surface analysis did not fully describe the function of the surface. The need for 3D parameters would increase the ability not only to look at the surface but also the texture of the measurement to describe it functions in its surrounding environment and the effect of the texture on how it will perform its function.

With the ability to measure the surface and texture of materials on a 3D scale the use of freeform shapes without any symmetrical features have been introduced into TKR designs for the purpose of matching the natural shape of the load bearing areas femur and tibia bone that contribute towards the knee joint movement. The use of freeform designs have placed an emphasis on freeform metrology developments for measuring and analysing errors which enhance quality control involved in the manufacture of such shapes. One way of achieving this is to develop artefacts that mimic the freeform shape to determine the uncertainty and error involved in the measurement to allow the true dimensions of the shape to be measured on the metrology equipment. Several researchers are working in this field following guidelines from international standards.

Another very significant problem associated with freeform measurement involves the fitting of the measurement to the CAD model to give the correct correlation of the measurement in terms of its desired shape from which an error map can be generated to enable freeform correction of the component. Several techniques have been developed using various stages of fitting and algorithms with current ongoing work towards an international standard.

The machining of free-form biological surfaces could benefit from applying fitting methods that have been implemented on tibia knee implant components to estimate wear scars after in-vitro testing. The method could be applied to the fitting technique for creating an error map for use in a corrective polishing procedure to reduce PV errors in knee implants to increase conformity and enhance lubrication conditions.

Biological material/surface designs which are susceptible to failure require simulation testing before being implanted into the human body especially those of load bearing surfaces. This testing can be achieved using various in-vitro techniques i.e. pin on disc/plate in the case of materials and joint simulators in the case of surface designs. The results of which must be justified by the means of comparison with in-vivo retrievals. The most commonly used technique for quantifying the amount of material loss is that of gravimetric weight loss which requires the following guidelines in international standards to minimise the effect on publishing irrelevant data from such issues as negative material loss due to lubricant absorbed by the materials during simulation.

Overall the development of metrology and simulation of biological implants needs to be accelerated to accommodate with the ever increasing demand for longer lifetimes and increased performance of biological materials to meet the demands of a longer living and aging population. In the case of this thesis the metrology techniques explained in this chapter were not only used to measure surface quality during experimental work but also used to measure surface geometries before and after freeform correction of an implant component.

**CHAPTER 5:
ZEEKO IRP200 7-AXIS CNC
MACHINE**

5 ZEEKO IRP200 7-AXIS CNC POLISHING MACHINE

The technology behind the Zeeko 7-axis CNC Intelligent Robotic Polisher (IRP) [274] was developed from a research team nucleus of Bingham, Walker, Kim and Brooks at the Optical Science Laboratory (OSL) based in University College London (UCL) concentrating on the computer controlled polishing of large optics for astronomy applications.

The patented design was later developed by Zeeko Ltd. and implemented on an innovative pressurized tool of varying size rotated at various rates to generate material removal. The patent is based on the avoidance of the zero centres caused by peripheral velocities associated with conventional spinning tools. [275]

Preliminary results showed that the surface roughness parameter Ra on a 800 Grit ground piece of Pyrex glass would progressively get better over a period of consecutive polishes as plotted in Figure 5.1 to give an eventual surface roughness of Ra equal to 2.47nm [276].

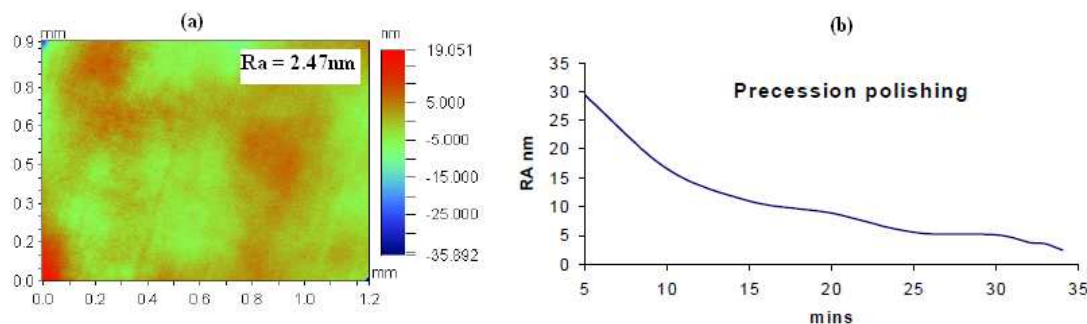


Figure 5.1 Final Surface Roughness Ra (a) and Ra versus polishing time (b) [276]

The initial development of the IRP was to overcome problems associated with work by previous researchers that used other techniques including large tooling, full scale tooling [277, 278] and a series of tools set up in an array [279]. These techniques eliminate the limitations of decreased removal rates associated with the Zeeko IRP design which uses a tool substantially smaller than the optic being polished but the cost of such large or full scale tooling is immense and application specific in which an associated problem of constant changing of the work piece shape in relevance to the tool piece. A problem that was overcome with the development work by UCL into a CNC control that can accurately manouver the tool over the work piece and together with measurement feedback between

polishing runs can compensate for the problem associated with large or full scale tools with the added bonus of the tool not being dimensionally specific to individual lens groups. Figure 5.2 shows a comparison of conventional tool removal marks to that of the patented precessions technique (influence function). The conventional tool removal has a 'w' shape profile (Figure 5.2 a) due to the influence of the zero velocity whereas the precession movement of the polishing tool removes this zero velocity effect and gives a uniform and repeatable Gaussian shape (Figure 5.2 b). The IRP200 and the schematic of the machines 7-axis of motion are shown in Figure 5.3.

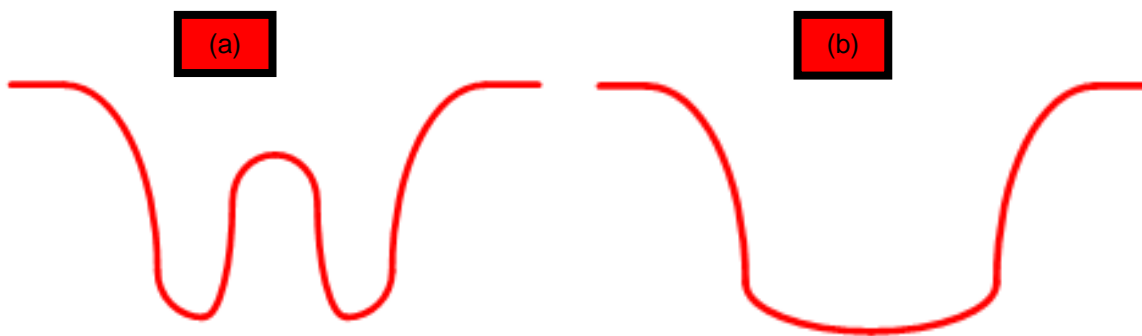


Figure 5.2 Comparison of (a) Conventional and (b) Precessions Tool Marks

With a successful CNC controller and additional software to develop the precessions process complete package was developed. Software developers at Zeeko Ltd. programmed a series of individual software which includes: -

- *Zeeko Graphical User Interface (GUI)* – A user friendly GUI that allows touch screen operation in both manual and automatic program modes (load, tool, probe etc.) making operation and preparation of work piece components easy.
- *Zeeko Tool Path Generator (TPG)* – The software incorporates and integrated surface designer, various tool path modules (raster, spiral, random etc.), on machine geometry compensation i.e. (Linear (X, Y and Z) and Rotational (A, B, and C offsets etc.), simple form correction (moderation) and 3rd party tool and machine support (i.e. metrology equipment manufacturers)

- *Precessions™* - As well as the integrated surface designer and tool path modules like TPG, *Precessions™* offers a metrology interface, an influence function database and advanced optimisation module and a 64 bit version for a parallel processing module.
- *Metrology Toolkit* - together with the integrated surface designer and metrology interface the metrology toolkit offers basic geometry manipulations, advanced data processing, data combining and analysis, point clouds and data stitching, integrated customer script editor, machining compensation and data visualization modes.

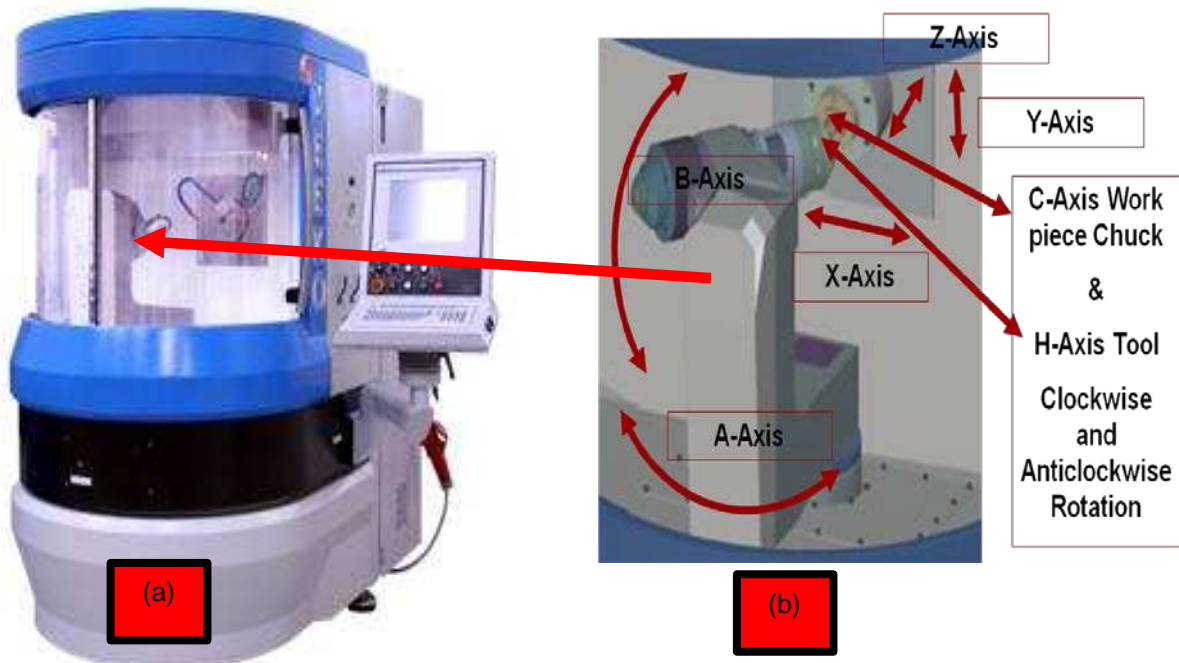


Figure 5.3 (a) Zeeko IRP200 and (b) 7-Axis Schematic [280]

The software can function individually dependent upon its application but when various combinations of the software are used then better results are achieved. The results of form on optical glass and mirror designs measured as a fraction of λ (one wavelength) commonly used in the optics industry can be seen in Table 5.1.

Table 5.1 Form error of components machined using Zeeko Software Packages [280]

Design	Error	TPG 2D + Metrology Toolkit	TPG 2D + Precessions 2D + Metrology Toolkit	TPG 2.5D + Precessions 2.5D + Metrology Toolkit	TPG 3D + Metrology Toolkit	TPG 3D + Precessions 3D + Metrology Toolkit
Sphere	Rotationally Symmetrical Error	λ	$\lambda / 3$	$\lambda / 10$	λ	$\lambda / 10$
	Non-Rotationally Symmetrical Error	n/a	n/a	$\lambda / 10$	λ	$\lambda / 10$
Circular Asphere	Rotationally Symmetrical Error	λ	$\lambda / 3$	$\lambda / 10$	λ	$\lambda / 10$
	Non-Rotationally Symmetrical Error	n/a	n/a	$\lambda/10$	λ	$\lambda / 10$
Complex Asphere	Complex Error	n/a	n/a	n/a	3λ	$\lambda / 8$
Off-Axis Asphere	Off-Axis Error	n/a	n/a	n/a	3λ	$\lambda / 4$
Freeform	Freeform Error	n/a	n/a	n/a	3λ	λ

Altogether with the software, patented tool and CNC control the complete 7-axis CNC polishing manufacturing capability was achieved and ready to be launched into the optics industry for further advances by technical experts in such fields as optics manufacture, engineering design (mechanical/electrical), mathematics and metrology etc.

5.1 Developments of the Zeeko IRP machines in the optics industry

The initial market for the Zeeko technology was the optics industry and was introduced in the Proceedings of the Large Lens and Mirrors conference in July 2001 [281] where their precessions process was incorporated into the first production machine which could position the tool to an accuracy of 10 μm . The results were demonstrated on BK7 optical glass and after initial problems with slurry delivery the accuracy of repetitive influence functions on various BK7 work pieces showed repeatability within 80-95% with a well formed and

symmetrical shape (Figure 5.4). Furthermore Zeeko presented the target of correcting the form error by 80% in a single polishing run (pass) being achieved using the Precessions software with component data, influence data and desired surface data used to calculate the CNC tool path to which the polishing head follows to correct the form.

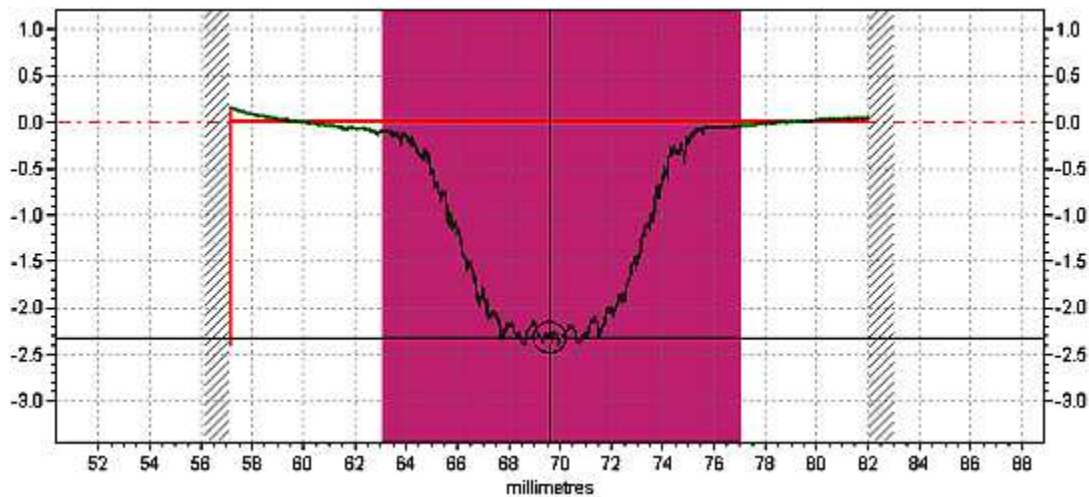


Figure 5.4 Uniform & Symmetrical I.F. on BK7 using the 1st IRP Machine [281]

The potential behind the Zeeko IRP200 machine has seen it develop into becoming a major revolution in the polishing market and especially into the manufacture of optics for major telescope projects [282, 283] through encountering and overcoming problems and challenges associated with freeform corrective polishing which were presented at various conferences and in technical publications [282-295] to create machines in sizes capable of polishing components with working areas up to 1.2m² [296].

5.2 Types of polishing processes available on the Zeeko IRP machines

Various types of polishing processes were developed to overcome the problems [297] including: -



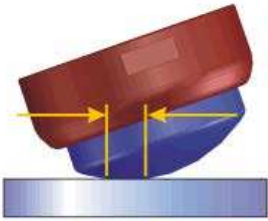
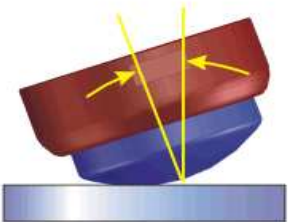
- *'Zeeko-Classic'* - This is the standard work-horse. The tool comprises an inflated membrane ("bonnet"), covered with a standard polishing 'cloth' such as polyurethane. It operates in the presence of pumped, re-circulated slurry, typically cerium oxide.
- *'Zeeko-Grolish'* (loose-abrasive) - In this case, the working surface cemented to the surface of the bonnet is hard, and typically a metal such as aluminium or copper foil. The loose-abrasive slurry is typically carborundum or diamond, and applied locally rather than by a recirculation pump.
- *'Zeeko-Grolish'* (fixed-abrasive) - Here, the bonnet is covered with a flexible backing carrying bound diamond pellets (e.g. the 3M Trizact™ product). This process is typically run within a containment vessel on the machine turntable, so that the part and the active area of the tool are submerged in coolant.
- *'Zeeko Fluidjet / Zeeko-Jet'* - In this mode, slurry is pumped at low or high pressure through jets, and removes material by direct impact with the surface of the part. Hybrid machines (such as the two 1200 mm machines built to date) accommodate both jet and bonnet based processes with a simple interchange. The fluidjet and jet polishing processes also produce Gaussian shaped influence functions like that of the head polishing technique.
- *Specialized tooling* - The standard bonnet interface (a Schunk chuck) can carry a variety of specialized tooling such as ring-laps, hard tools etc. Also, metallic buttons etc. have been successfully mounted.

5.3 *Machine parameters*

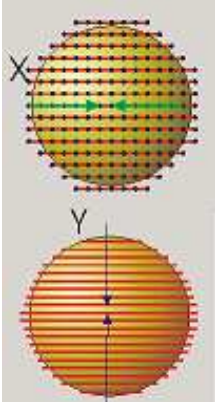
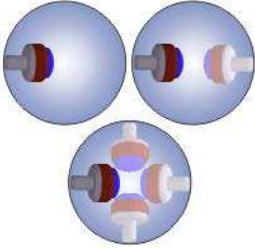
To achieve the polishing accuracies and surfaces textures there are several machine parameters that need to be adjusted to achieve optimum performance on the work piece. The settings of these parameters will vary dependant on the form and material of the workpiece. Description of these parameters can be seen in Table 5.2

THE APPLICATION OF ZEEKO POLISHING TECHNOLOGY TO FREEFORM FEMORAL KNEE REPLACEMENT COMPONENT MANUFACTURE

Table 5.2 Zeeko Machine Parameters

Parameter	Description	Units of measurement
 <p>H rpm Head Speed</p>	<p>The speed of rotation of the H-axis (tool) of the CNC machine. The axis can be either rotated clockwise or anti-clockwise.</p>	<p>Revolutions Per Minute (RPM)</p>
 <p>H Bar Head Pressure</p>	<p>The pressure behind the polishing head bonnet on the H-axis (tool) of the CNC machine. The head is supplied by a constant pressure which inflates the bonnet into a spherical shape on which the polishing media is attached.</p>	<p>Bar</p>
 <p>Spot Size</p>	<p>This parameter is determined by the size of the spot that is created when the surface of the polishing head (bonnet) comes in contact with the surface to be polished. The spot is measured in millimetres (mm).</p>	<p>Millimetres (mm)</p>
 <p>Precess Angle</p>	<p>This parameter is related to the angle at which the centre line of the bonnet and the 90 degree perpendicular between part and bonnet intersect. The unit of measure is degrees. The tool can also be used in a pole down position where there is a zero degree precess angle that mimics current lapping techniques. A 0° precess angle (pole down position) mimics current lapping techniques.</p>	<p>Degrees (°)</p>

THE APPLICATION OF ZEEKO POLISHING TECHNOLOGY TO FREEFORM FEMORAL KNEE REPLACEMENT COMPONENT MANUFACTURE

Parameter	Description	Units of measurement
 <p style="text-align: center;">X-Y Spacing</p>	<p>X spacing depicts the spacing between polishing points i.e. in a raster polish across the horizontal of the part being polished. Y spacing also determines spacing between polishing points but this time in the vertical direction of the part being polished.</p>	<p>Millimetres (mm)</p>
 <p style="text-align: center;">Precess Positions</p>	<p>This factor determines how many positional changes the tool makes for each tool path. Increasing this helps to give a uniform material removal that improves surface texture due to avoiding the zero velocity point of the polishing bonnet.</p>	<p>1, 2 or 4</p>

* Table Images Courtesy of Zeeko Ltd.

5.3.1 Polishing Modes

The polishing mode is used to designate the paths of the polishing head over the workpiece three different types of polishing mode are available these are: -

- Raster
- Spiral
- Random

An example of each of these polishing modes can be seen in Figure 5.5.

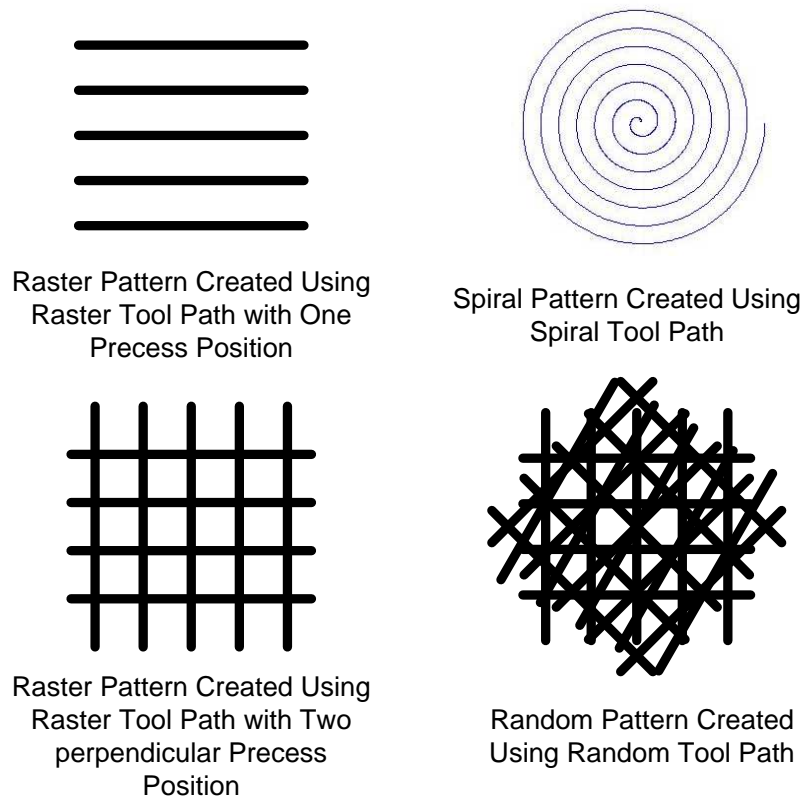


Figure 5.5 Examples of Polishing Modes on the Zeeko IRP Polishing Machines

5.3.2 Feed Rate

This parameter determines the speed at which the polishing head follows the CNC program and is stipulated in mm/min.

5.4 Development to Freeform Surfaces and Improved Biological Implants

The capability of the Zeeko IRP machines with 7-axis motion allows them to accurately follow contours of a surface making them applicable to ever rapidly developing freeform machining techniques [298-302].

The lifetime of new metal on metal freeform designs for prosthetic knee implants could be increased if the current form control (10-30 μ m) could be brought closer to the level associated with optics manufacture hence reducing the effect of micron-level high spots which cause significant pressure concentrations and premature failure due to particle initiated aseptic loosening.

The knowledge gained from the problems of development of the Zeeko manufacturing process for optics was disseminated and potential problems associated with using the machine for form correction and final finishing of freeform femoral knee implant components identified some key areas: -

- Tool path generation
- Surface quality
- Form error Reduction
- Fixturing issues
- Polishing issues
- Metrology issues
- Adaption of an optimized process to other materials

A discussion of these identified problems will be given in the following sections of the thesis.

5.4.1 Tool path generation

Consideration of a technique for generating a tool to polish the complex freeform surface was required after discussions with Zeeko Ltd. it was decided that a technique of Non-Uniform Refined B-Spline (NURBS) would be used to create a surface that followed the freeform CAD surface but added controls points for generation of CNC program within the specialized Zeeko software. The method is discussed in more detail in Chapter 7.

5.4.2 Surface Quality

To optimize surface quality initial trials were carried out to determine values of the machine parameters that would be significantly far enough apart to distinguish surface quality. The

initial trials were time consuming so a method to minimize the amount of trials and maximize the findings was investigated. It was decided that the Taguchi method approach would be used and the findings would determine the optimized parameters for obtaining the best surface roughness. After consultation with a supplier of consumables to Zeeko it was decided that a CR39 Glass Mineral Smoothing Cloth that had produced positive results on glass surfaces would be used in the Taguchi Trials. A range of particle sizes were trialed with the best results achieved using a 12µm cloth of which the Taguchi trails are described in more detail in Chapter 6.

5.4.3 Form Error Reduction

The reduction of form error would be determined using the Peak to Valley value obtained through one or more surface metrology methods that were described in Chapter 4. Investigations of the form error reduction including the form correction procedure are described in more detail in Chapter 7. It was also important that form error would be achieved without compromising surface quality as this would have a detrimental effect on the performance of the orthopedic implant material under testing procedures described in Chapter 4. The results of the testing can be found in Chapter 8 of the thesis.

5.4.4 Fixturing Issues

A major issue associated with large optic manufacture was the relocation of the optic after it was removed for metrology. The position of the optic not only on the machine but also on the metrology equipment is critical in form error correction and the correlation between the two must be identical. In correct re-positioning between polishing and metrology measurements would mean that the surface information data recorded for the generation of the CNC corrective polishing program would be incorrect. If the location of the component on the machine is different to the location on the metrology equipment (Figure 5.6) or vice versa this would incorporate positional errors (generated from translational and rotational miss location) on an already complicated freeform surface which are undesirable. The component would be effectively polished in the wrong areas having a catastrophic effect of introducing worse PV errors or reducing or not changing the PV but moving it to a different location than that of the previous measurement determined to generate the error map originally.

With this in mind a fixture to hold the freeform femoral knee implant component was designed to ensure an accurate as possible relocation on both the machine and metrology equipment. Digital images of the fixturing can be seen in Figure 5.7 mechanically clocked to ensure correct re-location. The fixture was modified from its original design after it was found that various angles were needed to polish and the entire surface area of the freeform component. The fixture was design by Eroda Tools Ltd., Penistone, UK after a consultation regarding indexing the component without having to move it from the fixture.

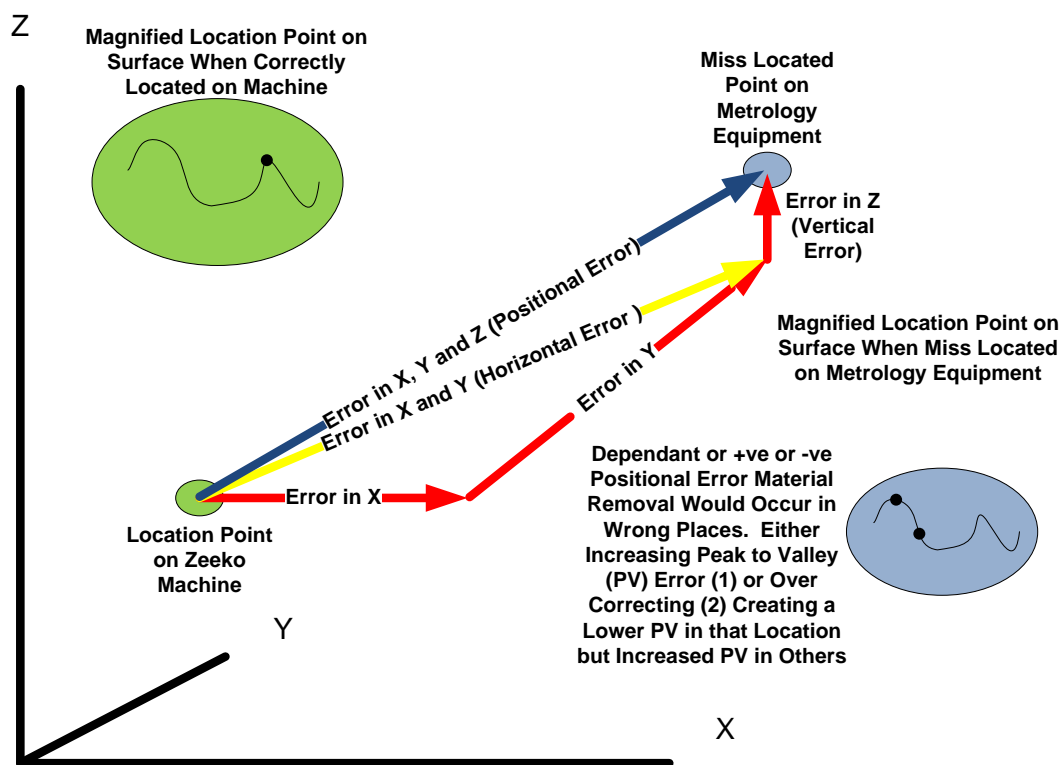


Figure 5.6 Errors caused by incorrect relocation

5.4.5 Polishing Issues

The major issue of the polishing was that problematic areas of the surface Figure 5.8 would be difficult if not impossible to polish with the standard tooling available for conventional polishing/grooving techniques developed by Zeeko.

THE APPLICATION OF ZEEKO POLISHING TECHNOLOGY TO FREEFORM FEMORAL KNEE REPLACEMENT COMPONENT MANUFACTURE

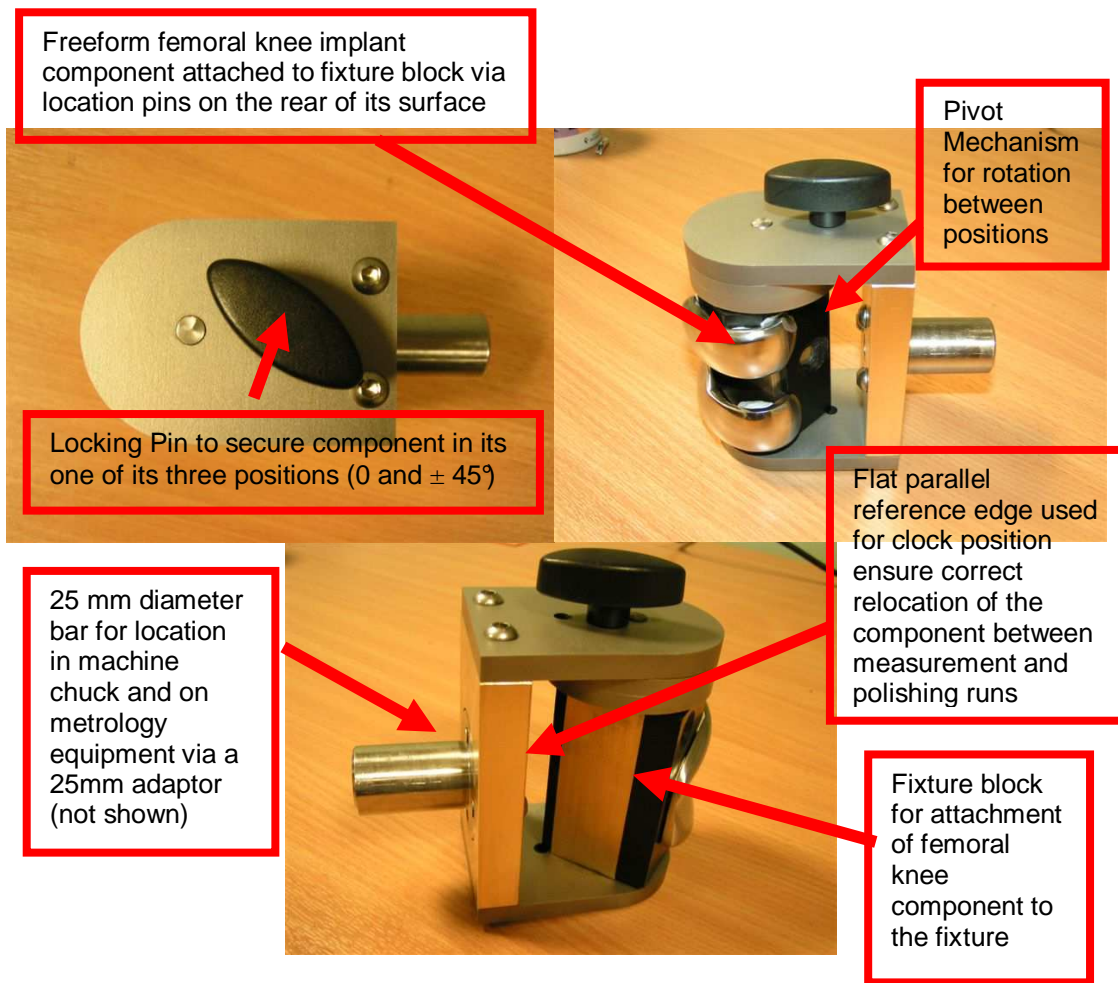


Figure 5.7 Fixture Design to Eliminate Positional Errors

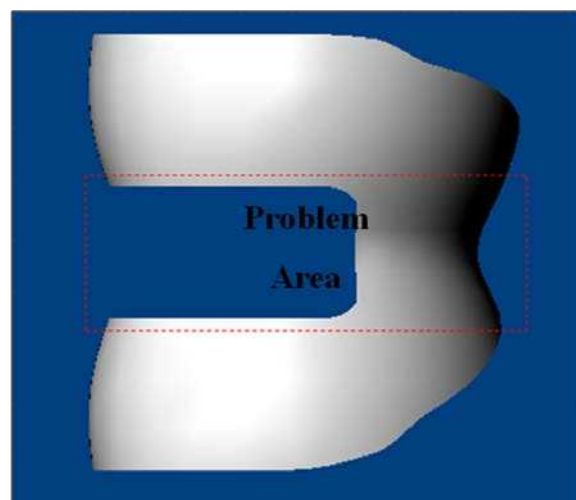


Figure 5.8 Problem Areas For Polishing of a Freeform Femoral Implant Component

The minimum tool size was a 10mm radius bonnet but this tool was still inadequate due the restrictions of it not being pressurized and the fact that its dimensions would cause it crash into the surface when performing a polish/groishing run. It was therefore determined that other tooling or investigation of the Zeeko fluid jet process was required. The Zeeko jet process and development of a patented tool design (Figure 5.9) was undertaken in collaboration with Hong Kong Polytechnic University. This would allow the problematic areas to be polished but not form corrected although this was deemed acceptable as they were not located in sections defined as critical load bearing areas (Red Box Area Figure 5.8).

5.4.6 Metrology Issues

The major factor relating to metrology equipment was would contact metrology damage the surface? In the cases of highly polished surfaces this was almost certainly going to happen, therefore it was decided that the form correction should take place before final finishing. The form correction could then be determined by contact metrology and the final surface quality could be checked using non-contact metrology alleviating the danger of surface damage. The techniques used are described in Chapters 6, 7 and 8 of the thesis.

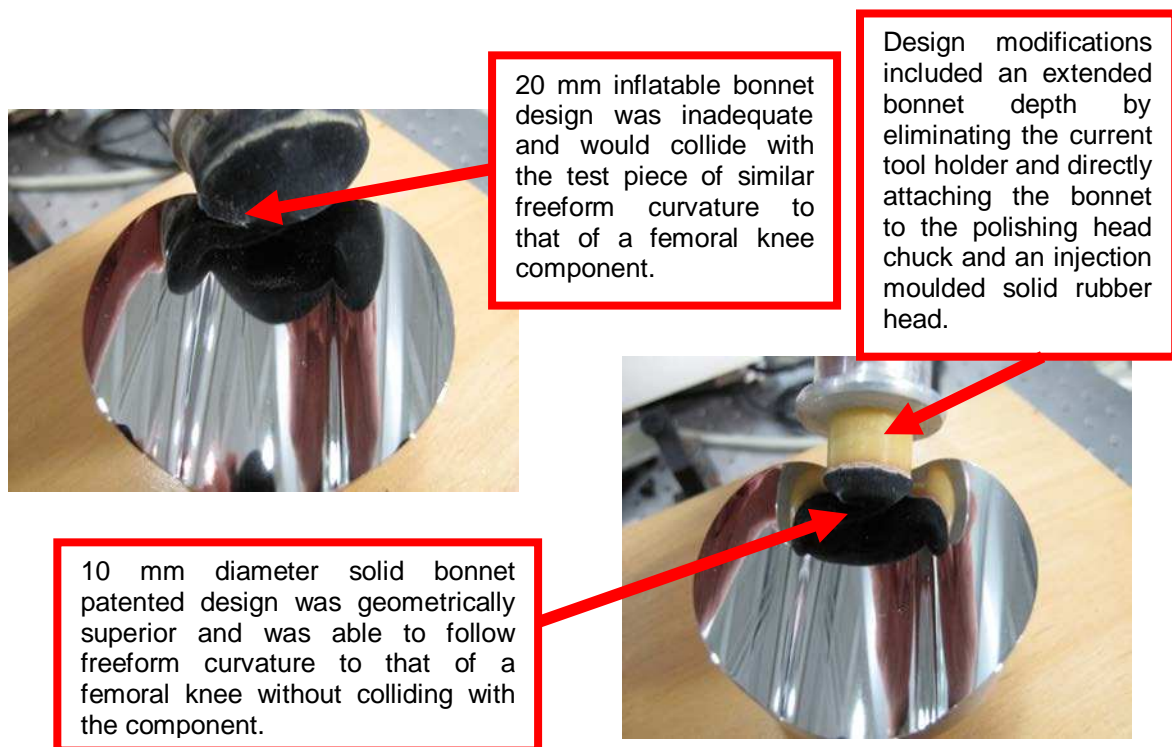


Figure 5.9 Patented 10mm Radius Tool For Polishing Problem Areas

5.4.7 Adaption of an optimized process to other materials

A critical point determined was that if a process was optimised for a certain material then would the optimised machine parameters be transferable to that of other materials.

This would be determined by using 316L stainless steel in the Taguchi trials (Chapter 6). This would be followed by using the knowledge on optimised machine parameters to form correct a Cobalt Chrome femoral knee implant component. Finally a comparison of Classic Zeeko polishing, Zeeko Fluidjet polishing and a Hybrid technique would be performed on a determining whether the application could be applied to other hips, pre coating of femoral knee implants and other freeform surfaces manufactured from titanium such as finger and shoulder and toe joints.

5.5 Summary

The Intelligent Robotic Polishing (IRP) 2000 7 –axis CNC machine manufactured by Zeeko Ltd. from an idea developed by a group of researchers at University College London lead by Dr. David Walker has been a revolution in the optics industry.

The patented polishing bonnet technique combined with software packages developed by Zeeko to generate CNC programs to accurately control the polishing head across the surface of the work piece has produced accurate and precise material removal. The precessed movement of the spot generated by depressing an air pressurised membrane into the work piece to create a contact removes the problem associated with conventional lens polishing techniques which created a zero velocity high point on the surface at the centre of the contact point. The surface finishes achieved on glass using the Zeeko IRP technology is in the nanometre range and in some cases the sub-nanometre range.

Advances in software development have allowed the form correction of glass materials to be processed by deterministic polishing, this together with an error map retrieved from metrology data can generate a CNC program to form correct the surface. The CNC program contains information from a dwell map to reduce the error by dwelling on high points (peaks) for longer than lower points (valleys) with the overall outcome of a reduction in Peak-Valley (PV) Error. It has been demonstrated that the PV of BK7 optics can be reduced to as low as 0.12λ without compromising the surface finish of the work piece.

The developing of other techniques such as Groishing and Fluidjet using loose and bonded abrasives for reducing the PV after grinding work have been proven effective in increased material removal without much of an effect on surface finish or sub surface damage.

These techniques could be used to reduce the PV error in biological implants including that of freeform femoral and tibial knee implant components. To do this knowledge disseminated from the development of the Zeeko process into a major manufacturing process for large optics manufacture were defined and addressed. The rest of this thesis demonstrates through practical results the compatibility of the Zeeko IRP polishing and corrective polishing techniques in the application of freeform femoral knee components and the possible adaption into other freeform implants made from various materials.

CHAPTER 6: OPTIMISING MACHINE PARAMETERS

6 OPTIMISING PARAMETERS FOR 316L STAINLESS STEEL

To optimize the Zeeko IRP200 machine parameters a method of analysing each parameters effect on the surface properties obtained needed to be selected. As mentioned previously in Chapter 4.3 there are several 3D surface parameters that can be used to assess the performance of biological surfaces. Selection of the most important surface parameters with respect to the wear performance of biological implants would differ amongst tribology experts [303-305]. The target parameters used optimize the machine parameters for this particular assessment were kept to a selection of particular group of surface parameters known as amplitude parameters due to time constraints and are as follows : -

- Sa – Average roughness most commonly used parameter for a general overall idea of the surface quality.
- Sq – Standard deviation of the roughness height.
- Spk – Reduced peak height is an estimate of the small peaks above the main plane of the surface and can be used to determine the amount of debris that could be worn off during the initial running in period. When Spk reduces wear particle debris generation is thought to be lower hence less wear is produced.
- Sk – Core roughness depth indicates the depth of the working part of the surface the lower the core roughness the better the wear properties after initial running in period of the bearing surfaces [307].
- Svk – estimate of the depth of the valleys after initial running in period which can be used to analyse fluid retention after initial running in period. The higher values of Svk, may indicate better performance of the bearing surface is. This is due to a higher void volume enhancing the lubrication and increasing wear particle entrapment [308].

Using these 3D measurement parameters a suitable test strategy was required. Preliminary analysis using the surface roughness parameter Sa gave an optimum setting for individual parameters of head speed, head pressure, spot size etc. for polishing a circular area of 10 mm diameter. This analysis was time consuming and exhaustive in order to gain any confidence in the results, thus indicating that to properly define the machining process and draw suitable conclusions more detailed tests were required. In order to avoid this huge experimental effort problem and to establish a framework for future process development a design of

experiments approach was considered. The primary candidate for this was the Taguchi approach which should give significant time and effort savings.

The purpose of Taguchi testing was chosen to obtain the following objectives: -

- Optimisation of the polishing process
- Minimising trials
- Statistical justifications of tests carried out
- Statistical confidence in results obtained

With these objectives in mind it was considered beneficial that the time saved in minimising trials and optimising the polishing using the Taguchi process would develop a structure that could be used not only to determine the best parameters for polishing 316L stainless steel but repeated on any other material that may be necessary.

With such a structure in place the optimal settings for various machine parameters along with a polishing time estimate was possible. Developing the Taguchi approach was initially time consuming although it yielded considerable time gains on the individual parameter analysis of previous results. This was due to the surface measurements containing information a full data set of 3D parameters hence one set of Taguchi results could be used to analyse the S_q , S_{pk} , S_k and S_{vk} values mentioned above and determine not only individual, but also machine parameter interactions that affect the performance of the surface as a biological bearing.

6.1 Taguchi Testing for One Stage of the Polishing Process

The purpose of the Taguchi testing was defined in Chapter 5.4.2 with the purpose of optimising the finishing stage of polishing of 316L Stainless Steel. There are several steps that are required to make a successful Taguchi Testing strategy these are: -

- Definition of parameters that are to be evaluated in the Taguchi testing e.g. H-axis head speed.
- The number of levels for each selected parameter e.g. for H-axis head pressure four levels consisting of 0.5, 1, 1.5 and 2 Bar could be selected.
- Selection of an appropriate orthogonal array (OA) from a Taguchi selection table (Figure 6.1 in the Appendix) e.g. an L8 OA Matrix could be selected for seven factors each having two levels.
- Assigning the factors and/or interactions of factors to the columns of the appropriate OA.
- Conducting the tests with a defined selection of the process variables (in order to avoid bias) for the individual tests carried out.

6.1.1 Selection of Zeeko IRP200 machine parameters for Taguchi tests

The following factors were used for evaluation in the Taguchi tests: -

- H-axis head speed (Factor A)
- H-axis head pressure (Factor B)
- Precess angle (Factor C)
- X-Y Spacing (Factor D)
- Spot Size (Factor E)

6.1.2 Selection of number of levels for machine parameters

With the factors selected each factor was given a number of levels and their assigned values were given as seen in Table 6.1.

Table 6.1 Factors with their assigned levels for the Taguchi testing

Factor	Factor Name	Level 1	Level 2	Level 3	Level 4
A	H-axis head speed (RPM)	500	1000	1500	2000
B	H-axis head pressure (Bar)	0.5	1	1.5	2
C	Precess Angle (Degrees)	0 (Pole Down)	5	10	15
D	X-Y Spacing (mm)	0.1	0.2	0.3	0.4
E	Spot Size (mm)	6	8	10	12

In most Taguchi testing a noise factor is added to control factors that can vary during the testing such as temperature, humidity etc. The Taguchi testing was carried out in a temperature ($\pm 0.5^{\circ}\text{C}$) and humidity ($\pm 5^{\circ}$) controlled environment with the 3D surface measurements carried out in a temperature and humidity controlled Class 10,000 clean room environment. Along with the samples being thoroughly cleaned and allowed to stabilize in the clean room environment before measurement the need for noise factor(s) was deemed unnecessary.

This left the final two machine parameters, the tool path which was set in raster mode and the surface feed rate which was kept constant at 50 mm/min.

6.1.3 Selection of the appropriate orthogonal array

It can be seen in Table 6.1 that there are 5 factors each having four levels. Using the Taguchi OA selection table as shown in the Figure 6.1 of the Appendix the appropriate orthogonal array would be a L16b.

6.1.4 Assignment of the factors and/or interactions to columns

With the appropriate OA selected the assignment of the factors and/or interactions could be placed in each column of the L16b OA which can be seen in Table 6.2 of the Appendix

together with an approximate processing time for each test determined by the X-Y spacing value as surface feed was kept constant.

6.1.5 Conducting tests

There are several different ways in which the tests could have been conducted but for simplicity and to avoid bias a complete randomisation method was used where each of the 16 individual tests (Table 6.3 in Appendix) were randomly conducted.

All the tests were conducted twice to analyse the repeatability of the results. Samples were prepared to a 1200 Grit Silicon Carbide finish. The tests were carried out using 3M CR39 glass mineral smoothing cloth (Yellow Colour 12um grit size) as seen in Figure 6.2



Figure 6.2 3M CR39 Glass Mineral Smoothing 12 μ m Yellow Cloth

In total 64 individual tests were performed using the polishing media with tap-water was used as slurry/lubricant for reduction of surface heat and prolonged life of the media. Due to the lifetime of the polishing cloths they were changed every 4 runs to ensure that enough fresh cutting grit was exposed to generate the surface texture. The tests were carried out on flat test samples of 316L Medical Grade Stainless Steel as seen in schematic in Figure 6.3.

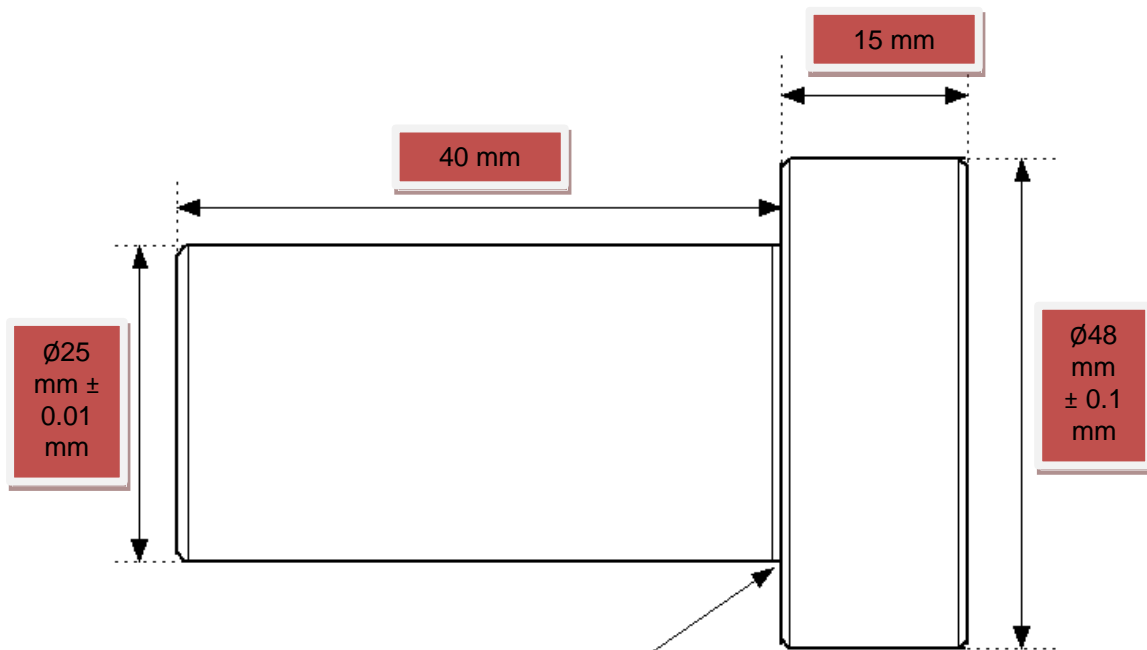


Figure 6.3 Schematic of 316L Stainless Steel Samples Used For Taguchi Testing

6.1.6 Analysis of Results

3D surface measurements were used as a means of analysing the Taguchi tests. The measurements were carried out using a WYKO NT 2000 phase shifting interferometer. The maximum capable measurement area of 4mm x 4mm was used throughout.

The results were analysed using the following methods: -

- General analysis of filtered average surface roughness of Sa Values using a paired student t-test for data set comparisons of Runs 1 and 2.
- Analysis of Mean (ANOM) for filtered two run average Surface Roughness Sa to look at the variance of the mean for machine parameters.

- Main Effects Plots – Plotted Data and Analysis of each individual parameter and its effect on the various two run average filtered 3D surface parameters (Sq, Spk, Sk and Svk)

6.1.6.1 General Analysis of Overall Results of filtered Sa Values

The results of the two runs of Taguchi tests produced 32 3D Surface Roughness (Sa) values which were obtained by taking an average of four quadrant measurements (128 measurements in total) on the surfaces of the Zeeko IRP200 manufactured test samples. The data was levelled and filtered using a Gaussian Robust Roughness Filter with $\lambda_c = 0.08\text{mm}$ in both X and Y directions. The Sa measurement data for each test sample can be seen in Table 6.3 of Appendix I.

A paired student t-test was used to compare Run 1 data (mean 9.077nm, Standard Deviation 2.179 nm) and Run 2 data (Mean 10.526 nm, Standard Deviation 1.651nm) showing that data values were not significantly different with a return $P > 0.05$. Taking this into consideration the average of the two sets of data were combined giving the data as seen in Table 6.4

Table 6.4 Statistical data of combined averages of Taguchi Test Runs 1 & 2

Statistic	Value
Mean	9.802
Standard Deviation	1.295
Standard Error of the Mean	0.324
95% Confidence Interval Levels	(9.122, 10.491)

Analysing run 1, run 2 and the two run average other conclusions include: -

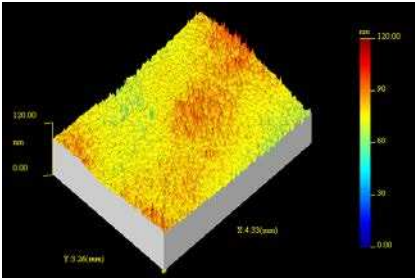
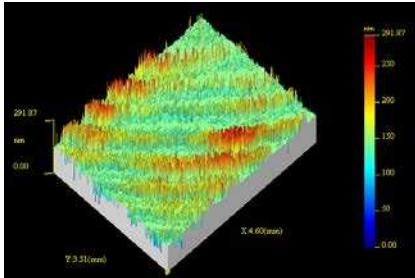
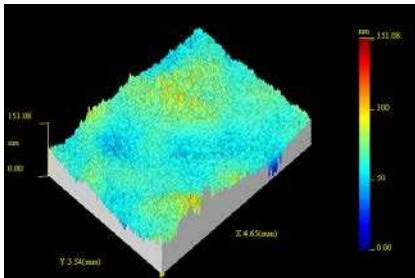
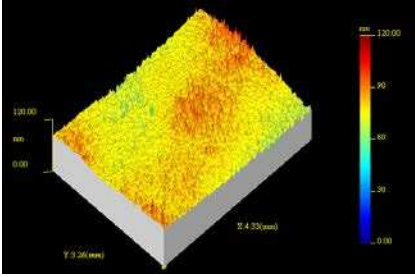
- The best result obtained from the 2 run averages was Test 16 (7.26 nm) with the best individual result being Test 4 of Run 1 (5.32 nm)
- The worst result obtained from the 2 run average was Test 4 (11.69 nm) with the worst individual result being Test 12 Run 2 (13.79 nm)
- Most of the 2nd run results are worse than that of the 1st run results
- Trend patterns are similar showing good repeatability between the 1st and 2nd runs
- The polishing time of 16 minutes (Run 1 Test 13) produced the best 2 run average albeit Run 1 test 14 produced the best individual run average of 5.32 nm.

Possible justifications behind the conclusions of best and worst finish with example data can be seen in Table 6.5

6.1.6.2 Analysis of the Mean (ANOM)

The general analysis of the results proved that Taguchi testing using filtered Sa values as a response can be an effectively quick tool to find the best parameter settings in obtaining the best manufacturing process. For a deeper understanding of the effect of the selection of parameters on manufacture of the surface ANOM testing was conducted. The averages of filtered 3D Sa Values for the two runs (Table 6.6) of the 16 Taguchi tests for each cloth were used to produce the ANOM. The one-way ANOM used had an alpha (α) value of 0.01 giving a 99% confidence level.

Table 6.5 General Analysis of 3D Measurements Conclusions for 12µm Cloth

Example	Possible Reasons
 <p data-bbox="304 667 635 725">Best Finish – Test 14 Run1qA Sa = 4.75nm*</p>	<p data-bbox="703 378 1331 521">The random run numbers was equal to 5 for meaning that the cloth was new and had plenty of sharp 12µm particles embedded ensuring a good surface finish.</p> <p data-bbox="703 539 1331 752">Head Speed and Head Pressure were at 2000 RPM and 2 Bar respectively hence giving large material which in turn removed more residual scratches from the previous 1200 Grit SiC sample preparation over a long process time. (28 minutes)</p>
 <p data-bbox="293 1099 647 1158">Worst Finish – Test 15 Run2qA Sa = 15.63nm*</p>	<p data-bbox="703 777 1331 920">Random Run Number was equal to 3 meaning the cloth had been used for 2 previous tests hence fewer sharp particles leading to less polishing work being performed on the sample.</p> <p data-bbox="703 938 1331 1081">X-Y Spacing was high which could generate patterns hence quadrant measurements could include the cavities of such patterns increasing the Sa value.</p>
 <p data-bbox="264 1467 671 1619">Best Process Time (11 Mins.) Test 16 Run2qA Sa = 6.17 nm** Versus Best Longer Process Time (28 Mins.) Test 14 Run1qA Sa = 39.96 nm**</p> 	<p data-bbox="703 1176 1331 1503">Best Process Time Result (11 minutes) had random run numbers equal to 1 and 5 respectively meaning a new cloth was used for both runs. Whereas the random run numbers for the best result using a longer process time (28 minutes) had random run numbers equal to 11 and 16, meaning that the cloth had been used on three other tests before hence the effectiveness of the 12µm cloth was reduced.</p> <p data-bbox="703 1520 1331 1848">Head Speed and Head Pressure were at 2000 RPM and 2 Bar respectively for run 16 giving higher material removal capable of removing all residual scratches left over from 1200 grit sample preparation. Thus pointing towards Head Speed and Head Pressure having a larger affect on the quality of surface finishes than that of X-Y Spacing which produces longer process times.</p>

* Examples chosen are the Best and Worst Quadrant Measurement Sa Values (Table 6.4 Appendix I)

**Examples chosen were lowest Sa quadrant value from the lowest 2 run average (Table 6.6)

Table 6.6 Two run average filtered Sa values used in ANOM

Run No.	Two Run Average (nm)
1	10.46
2	11.31
3	11.52
4	11.69
5	9.57
6	9.91
7	10.59
8	8.95
9	10.57
10	8.69
11	9.67
12	10.83
13	9.33
14	8.11
15	8.37
16	7.26

The ANOM plots for each of the machine parameters can be seen in Figures 6.4 to 6.7 (Appendix).

All plots show the overall mean of the data set as $S_a = 9.80$ nm for a confidence level of 99% ($\alpha = 0.01$) with the upper and lower decision levels varying according to the parameter being investigated. The head speed plot in Figure 6.4 shows that the highest value (500RPM = 11.25 nm) and lowest (2000RPM = 8.27 nm) of head speeds lay just inside the upper (11.50 nm) and lower decisions (nm) levels respectively indicating a larger variance from the overall mean result will be achieved when using 500 or 2000 RPM head speeds with a 99.9% confidence that the levels will fall within the upper and lower limits if the tests were repeated. The 1000 RPM head speed (9.76 nm) gives the best match to the overall mean 9.80 nm of the Taguchi Analysis.

Table 6.9 shows which set of parameters produced the closest to the upper and lower 99.9% confidence levels and closest to mean Sa results using the ANOM method: -

Table 6.8 ANOM Closest Values to Upper and Lower 99.9% C.L. and Mean Values

Parameter	Sa Level Closest to Upper 99.9% Confidence Level using ANOM Method	Sa Level Closest to Mean using ANOM Method	Sa Level Closest to Lower 99.9% Confidence level using ANOM Method
Head Speed (RPM)	11.25 nm (500)	9.76 nm (1000)	8.27 nm (2000)
Head Pressure (Bar)	10.04 nm (1.5)	9.68 nm (2.0)	9.51 (1.0)
Precess Angle (°)	10.07 nm (15)	9.79 nm (10)	9.32 (0)
X-Y Spacing (mm)	10.13 nm (0.4)	9.82 nm (0.2)	9.26 nm (0.3)
Spot Size (mm)	10.4 nm (10)	9.76 nm (12)	9.12 nm (6)

It can be concluded for a 99.9% confidence level that the best results for mean surface finish Sa (most repeatable) within the upper and lower limits would be achieved using 1000 RPM Head Speed, 2 Bar Head Pressure, 10° Precess Angle, 0.2 mm X-Y Spacing and 12 mm Spot size. Although all combinations would be within the upper and lower limits at 99.9% it would be advisable to avoid those closer to the upper and lower limits if the best repeatability is to be obtained.

6.1.6.3 Main Effects Plot for 3D Surface Parameters Affecting Wear

The ANOM results showed a better understanding of the individual parameters that effect the repeatability of the mean Sa value of the Zeeko IRP machined test components but Sa is not the only 3D surface parameter that can affect the wear performance of a material in the case of biological implant such as hip and knee joint bearing surfaces, there are many factors that can determine wear. Some of the main contributors were mentioned at the beginning of this chapter. Therefore an individual main effects plot for each of the Taguchi parameters was

THE APPLICATION OF ZEEKO POLISHING TECHNOLOGY TO FREEFORM
FEMORAL KNEE REPLACEMENT COMPONENT MANUFACTURE

analysed using Minitab 15 for the surface roughness parameters of Sq, Spk, Sk and Svk. To reduce calculation time now that the t-test proved that the data between Taguchi Runs1 and 2 was not significantly different only Taguchi Run 1 average values were used in the Main Effects and following Interaction Plots. Values of Sq, Spk and Sk as mentioned previously at the beginning of the chapter need to be reduced to minimise wear resistance with Svk needing to be increased to minimize wear the purpose of this test is to find a compromise of the machine parameters that will reduce wear.

6.1.6.3.1 Main Effects Plot for 3D Surface Parameter Sq

The main effects plot of Sq can be found in Figure 6.8 (Appendix I) with the Mean Average of the data collected for Sq being 14.35nm. A summary of the effect of each parameter on Sq can be seen in Table 6.9.

Table 6.9 Summary of effects of machine parameters on Sq values

Parameter	Comments
Head Speed (RPM)	High significance with Sq decreasing as the RPM increases
Head Pressure (Bar)	Medium significance with values <1 bar lowering Sq values
Precess Angle (°)	No significance all values produce Sq close to the overall mean
X-Y Spacing (mm)	Medium significance with Sq lowering as X-Y spacing decreases
Spot Size (mm)	No significance all values produce Sq close to the overall mean

6.1.6.3.2 Main Effects Plot for 3D Surface Parameter Spk

The main effects plots for Spk can be located in Figure 6.9 of Appendix I. The Mean Average for the Spk was 20.02nm. A summary of the effect of each parameter on Sq can be seen in Table 6.10.

Table 6.10 Summary of effects of machine parameters on Spk values

Parameter	Comments
Head Speed (RPM)	High significance with Spk decreasing as the RPM increases
Head Pressure (Bar)	Medium significance with values <1 bar lowering Spk values
Precess Angle (°)	Not much significance although a value of 5° lowers Spk below the overall mean other values of Precess Angle are close but above the overall mean.
X-Y Spacing (mm)	Medium significance with Spk lowering as X-Y spacing decreases.
Spot Size (mm)	Not much significance values of 8mm and 12 mm produce Spk close to the overall mean. A value of 6mm gives a below overall mean and a 10 mm value above the overall mean.

6.1.6.3.3 Main Effects Plot for 3D Surface Parameter Sk

The main effects plots for Spk can be located in Figure 6.10 of Appendix I. The Mean Average for the Spk was 20.41nm. A summary of the effect of each parameter on Sq can be seen in Table 6.11.

Table 6.11 Summary of effects of machine parameters on Sk values

Parameter	Comments
Head Speed (RPM)	High significance with Sk decreasing as the RPM increases
Head Pressure (Bar)	Medium significance with values <1 bar lowering Sk values
Precess Angle (°)	Not much significance although a value of 5° lowers Sk below the overall mean other values of Precess Angle are close but above the overall mean.
X-Y Spacing (mm)	Medium significance with Sk lowering as X-Y spacing decreases.
Spot Size (mm)	Not much significance values of 6mm 8mm and 12 mm produce Spk close but lower than the overall mean. A value of 10mm gives a above overall mean.

6.1.6.3.4 Main Effects Plot for 3D Surface Parameter Sv_k

The main effects plots for Sv_k can be located in Figure 6.11 of Appendix I. The Mean Average for the Sp_k was 26.29nm. A summary of the effect of each parameter on Sq can be seen in Table 6.12.

Table 6.12 Summary of effects of machine parameters on Sv_k values

Parameter	Comments
Head Speed (RPM)	Medium significance values of >2000 RPM giving an Sv _k value above the overall mean.
Head Pressure (Bar)	Medium significance with only a values >1.5 Bar giving an Sv _k value above the overall mean.
Precess Angle (°)	Not much significance all values are hovering just above or below the overall mean.
X-Y Spacing (mm)	Medium significance with Sv _k increasing as X-Y spacing increases.
Spot Size (mm)	Not much significance although a value of 10mm gives an above overall mean.

6.1.6.3.5 Comparison of Main Effects Plot for Sq, Sp_k, Sk and Sv_k

A summary of the response tables showing the rankings of factors for Sq, Sp_k, Sk and Sv_k values for both 12μ Yellow and 3μ Flesh Cloths can be seen in Table 6.13

Table 6.13 Rankings of Factors for 3D Parameters Sq, Sp_k, Sk and Sv_k

Factor	Sq Rank	Sp _k Rank	Sk Rank	Sv _k Rank	Total Ranking Score
A – Head Speed (RPM)	1	1	1	5	8
B – Head Pressure (Bar)	2	3	2	4	11
C – Precess Angle (°)	5	5	5	2	17
D – X-Y Spacing (mm)	3	2	3	3	11
E – Spot Size (mm)	4	4	4	1	15

6.2 *Study of Diamond and Non-Woven Alumunia Oxide Polishing Pads*

Although using the CR39 Glass Mineral Smoothing Cloths was deemed a success, long term use of such polishing media proved to be unsuccessful. Therefore an investigation of other polishing media was required in the search for a long lasting alternative that could generate large amounts of material removal required for stages other than that of the final finishing processes.

Described later, Influence Functions are used for corrective polishing of a work piece to correct form to the desired tolerances. In this exercise Diamond Polishing Pads manufactured by KGS Diamond (Switzerland) were used to generate Influence Functions in order to look at their potential as grolishing media for larger stock removal before final finishing of Cobalt Chrome, an Orthopaedic Implant Material. An example of the KGS diamond cloth can be seen in Figure 6.12 which shows the single crystals diamond particles grown on a cloth in layers which are held in place using a Nickel bonding. The cloths come in a range various patterns dependent upon the application. The pattern is used to distribute slurry removing loose diamond swarf and surface heat generated during the cutting mechanism. The potential of such cloths was high due to the range of grit sizes together with a resin bonded product that could be used for the final finishing process.

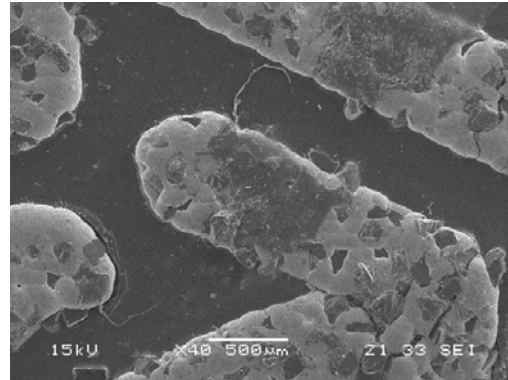
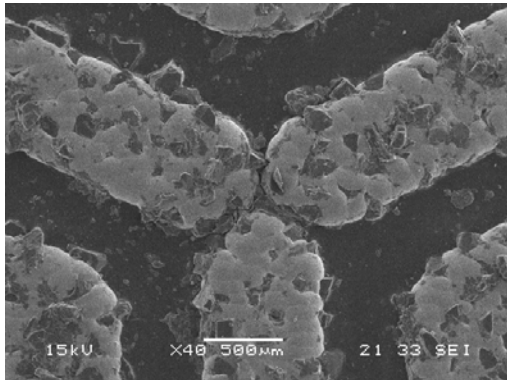


Figure 6.12 Telum™ Nickel Bonded Diamond Polishing Pad from KGS Diamond Int.

Initial attempts to polish cobalt chrome with nickel bonded diamond cloths produced very aggressive material removal with results being conclusively good on the small surface area of the pins seen later in Chapter 8. It was evident the cloth seemed to stop performing and required replacement after only one polishing run and the cause of such a lack of performance needed to be investigated. Through examination under a Scanning Electron Microscope the cloth showed evidence of a chemical reaction (Figure 6.13) similar to that witnessed in chemical aspects of tool wear in diamond turning.

It can be seen in Figure 6.13 (a) the new cloth shows sharp diamonds sitting proud of the electroplated nickel bond whereas Figure 6.13 (b) shows the cloth after one polishing run which shows rounded diamonds not sitting proud of electroplated nickel bond with several areas showing graphitisation and smeared work piece material caused by the chemical reaction mentioned previously. The effect of the chemical reaction is even clearer when visualised at 140x Mag. The images of the best and worst cases of polishing runs with the nickel bonded diamond cloths can be seen in Figure 6.14

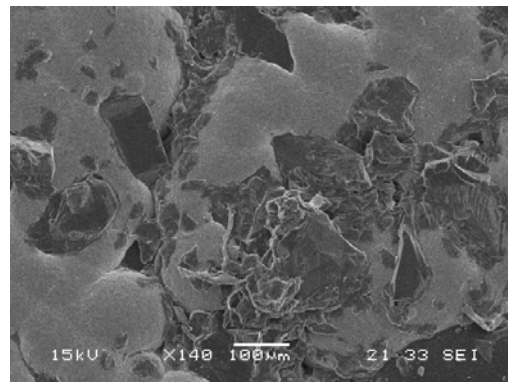
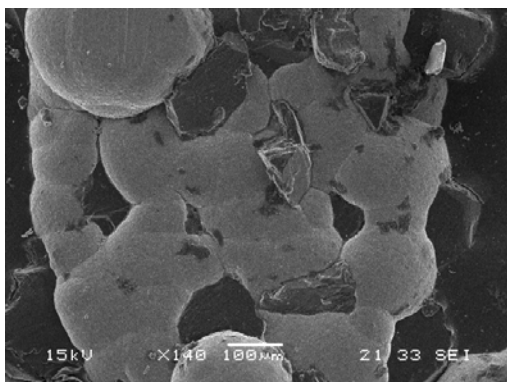
The best case Figure 6.14(a) shows cavities where diamonds have been pulled from electroplated nickel bond with some diamonds left but worn smooth. The worst case Figure 6.14(b) shows nearly all diamond removed or worn smooth with only electroplated nickel and sample swarf remaining. This worst case clearly indicates some sort of graphitisation occurred, loosening the diamond and effectively immobilising the polishing effect of the cloth as there are no diamonds left to create the material removal process. With this consideration in mind for larger surface areas of cobalt chrome knee components then the need for a polishing media that creates uniform material removal was required.



(a) New Nickel Bonded Diamond Cloth

(b) Used Nickel bonded Diamond Cloth

Figure 6.13 New & Used KGS Telum™ Nickel Bonded Diamond Cloth at 40x Mag.



(a) Best case after single grinding run

(b) Worst case after single grinding run

Figure 6.14 Best (a) and Worst (b) Cases of Nickel Bonded Diamond at 40x Mag.

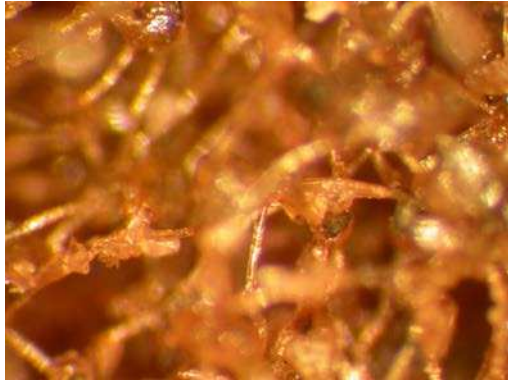
Investigation of the polishing media market discovered a product supplied by Sia Abrasives which is produced in a single process from base fibre that is carded layered and needed to form a fleece and is available as alumina oxide or silicon carbide form.

This polishing media had the following advantages: -

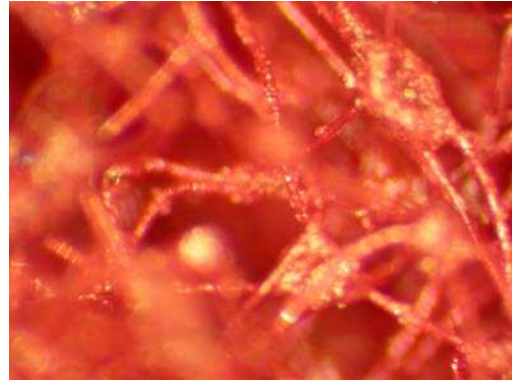
- Consistent cut and finish throughout product lifetime
- Conformable so excellent finishes are achieved without damaging or gouging the work surface
- Grit is impregnated throughout cloth so as it wears more grit is exposed increasing lifetimes
- Can be used wet or dry and will not rust

The structure of these non woven mats is best seen magnified under a laboratory standard microscope (Figure 6.15). Aggressiveness of the mats ranged from P80 heavy grit (Figure 6.15 a) to mid range grit of P320 (Figure 6.15 b) to a very fine grit P800 mat (Figure 6.15 c). The visualisation of aggressiveness of the cloth can be seen by the diameter of the particles woven into the cloth with the P80 having the largest alumina particles and the P800 have the smallest diameter alumina particles. The performance of these mats compared to that of the nickel bonded diamond cloths would determine the best polishing media to use for form correction in the future.

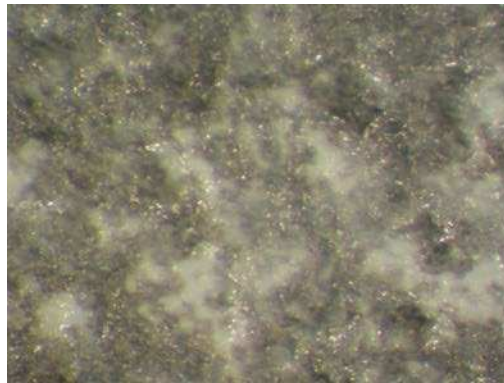
To analyse the effectiveness and repeatability of material removal a set of tests to generate four influence functions were devised each test lasting twenty minutes. Identical machine parameters were used for the tests carried out on flat samples of cobalt chrome with matching material properties as that of the pins. The results were measured in 2D on a Sominchronic Diamond Stylus Profiler. As mentioned previously the tests carried out with the nickel bonded diamond medium produced non stable material removal and decreasing influence function depths making them unsuitable for the long process time corrective polishing processes (Figure 6.16 a and b).



(a) P80 Alumina Oxide



(b) P320 Alumina Oxide



(c) P800 Alumina Oxide (very Fine)

Figure 6.15 Non Woven Abrasive Mats under a laboratory standard microscope

Although a suitable predictable material process has been achieved from using non woven abrasives the low influence function depth will increase polishing times substantially therefore the search for a non-diamond fixed abrasive substitute to decrease polishing process times was needed.

THE APPLICATION OF ZEEKO POLISHING TECHNOLOGY TO FREEFORM FEMORAL KNEE REPLACEMENT COMPONENT MANUFACTURE

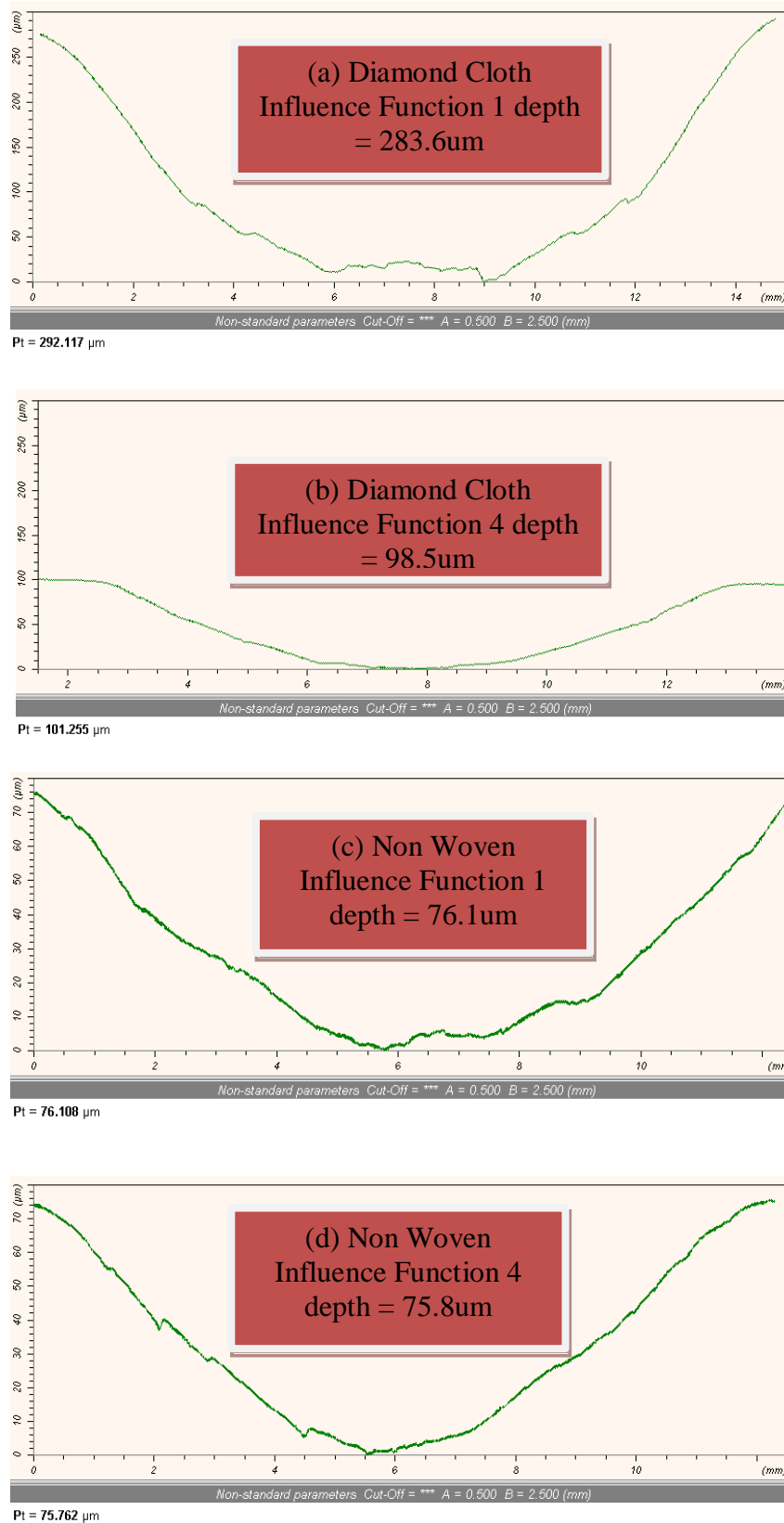


Figure 6.16 Lower influence function variations compared to KGS Bonded Diamond

6.3 Capability Study : FluidJet and Hybrid FluidJet/Mechanical Polishing

The Zeeko IRP200 has not only the ability to mechanically polish work pieces using a bulged polymer head it can also be adapted to the process of FluidJet polishing

FluidJet (Figure 6.17a) uses the same slurries as mechanical polishing (Figure 6.17b) but the tooling and material removal processes differ significantly. Mechanical polishing requires a bulged polymer head with polishing cloth attached coming in contact with a slurry flooded work piece, hence the material removal mechanism is a combination of cloth, head and slurry contact. Whereas with FluidJet polishing the slurry is delivered via a high pressure jet nozzle placed a specified distance from the work piece hence the velocity of the particles within the slurry provide the material removal mechanism.

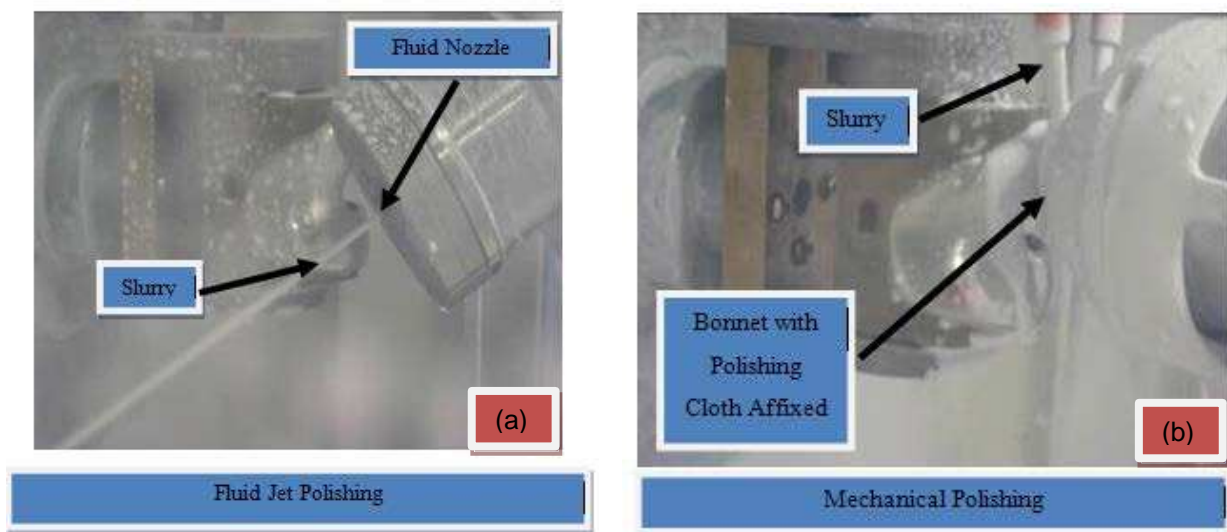


Figure 6.17 Mechanical and FluidJet Material removal Mechanisms

Due to the complications involved with fixed abrasives and the non-woven mats on cobalt chrome material it was decided to use a loose abrasive slurry and cloth for the mechanical polishing and the same loose abrasive for the Fluid Jet polishing. The material chosen for the capability study was medical grade Ti-6Al-4V ELI with samples manufactured from a 28mm diameter rod.

THE APPLICATION OF ZEEKO POLISHING TECHNOLOGY TO FREEFORM
FEMORAL KNEE REPLACEMENT COMPONENT MANUFACTURE

Rough blanks were manufactured using a conventional turning machine tool with the outcome being whether or not a hybrid process using Mechanical Polishing and FluidJet combination (Sample 1) or FluidJet Polishing only (Sample 2) could remove the turning signatures left by material cutting process. The parameters used in the capability study can be seen in Tables 6.15 and 6.16.

Table 6.15 Sample 1 Parameters – Hybrid Polishing (Mechanical and FluidJet)

Factor	Sample 1			
	1st Polishing Run - Mechanical	2nd Polishing Run - Fluid Jet	3rd Polishing Run - Fluid Jet	4th Polishing Run - Fluid Jet
Precess Angle (Deg)	0	10	10	10
Head Speed (RPM)	2000	n/a	n/a	n/a
Tool Offset (mm)	0.6	≈ 21	≈ 21	≈ 21
Tool Pressure (bar)	2	13-15	13-15	13-15
X-Y Spacing (mm)	0.4	0.4	0.4	0.4
Surface Feed (mm/min)	1500	500	500	500
Tool Size	20mm radius bonnet	2.65mm diameter nozzle	2.65mm diameter nozzle	2.65mm diameter nozzle
Polishing Cloth	Zirconium Oxide (“D” 37)	n/a	n/a	n/a
Polishing Slurry	Silicon Carbide 44µm	Silicon Carbide 44µm	Silicon Carbide 44µm	Silicon Carbide 44µm

A summary of the results after the first polishing stage are seen in Table 6.17 showing a microscope image and 3D surface roughness values (Sa) from a White Light Interferometer. It can be observed that although the measured Sa values (5x Mag.) for Sample 1 using Mechanical Polishing produced an unfiltered Sa of 48.7nm and Sample 2 using FluidJet

THE APPLICATION OF ZEEKO POLISHING TECHNOLOGY TO FREEFORM
FEMORAL KNEE REPLACEMENT COMPONENT MANUFACTURE

Polishing produced an unfiltered Sa of 43.4 nm the textures under standard microscopy examination are different.

Table 6.16 Sample 2 Parameters – FluidJet Polishing

Factor	Sample 2			
	1st Polishing Run - Fluid Jet	2nd Polishing Run - Fluid Jet	3rd Polishing Run - Fluid Jet	4th Polishing Run - Fluid Jet
Precess Angle (Deg)	10	10	10	10
Tool Offset (mm)	0.6	≈ 21	≈ 21	≈ 21
Tool Pressure (bar)	2	13-15	13-15	13-15
X-Y Spacing (mm)	0.4	0.4	0.4	0.4
Surface Feed (mm/min)	500	500	500	500
Tool Size	20mm radius bonnet	2.65mm diameter nozzle	2.65mm diameter nozzle	2.65mm diameter nozzle
Polishing Slurry	Silicon Carbide 44μm	Silicon Carbide 44μm	Silicon Carbide 44μm	Silicon Carbide 44μm

Some scratch marks caused by the cutting and ploughing action of abrasives can be observed after mechanical polishing in the hybrid technique of Sample 1 whereas considerable pits are found on the FluidJet polishing of Sample 2 without any new scratches found from the abrasive jet flow of slurry. In both cases turning signatures are still evident after the 1st stage of polishing as seen in the higher magnification images of Figure 6.18 although the signatures are harder to distinguish in Sample 2 than that of Sample 1.

Analysis of the 2nd polishing run as seen in Table 6.18 saw both samples polished with the same set of FluidJet parameters. The machine mark on sample 1 became very shallow and difficult to notice whereas on sample 2 they are still clearly visible. Again, it is noted that for Samples 1 and 2 the measured Sa values are were similar at 35.3nm and 37.8nm respectively.

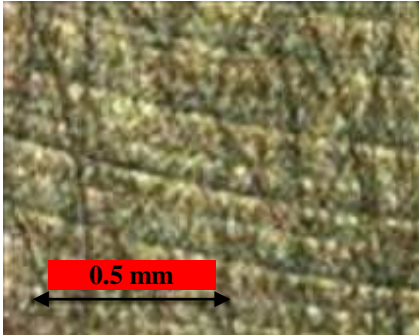
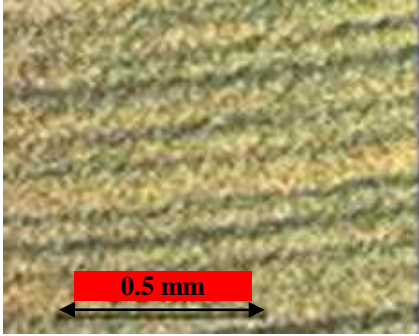
Visual / Measurement	After Stage 1 (Sample 1 Mechanical and Sample 2 Fluidjet)	
	Sample 1	Sample 2
Microscope Image		
Sa Value	48.7 nm	43.4 nm
Comments	Turning Signatures Easily Visible	Turning Signatures Less Visible

Table 6.17 Analysis after 1st Polishing Run for Samples 1 and 2

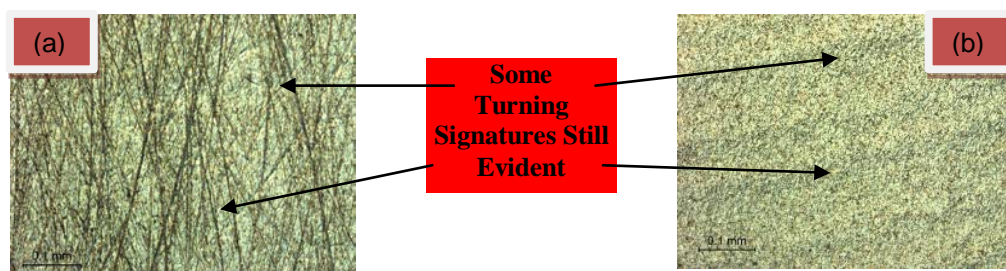


Figure 6.18 Microscope Images After 1st Run of Hybrid (a) and Fluidjet Only (b)

3rd and 4th polishing stages did not see much of significant change in Sa values with the final unfiltered Sa values recorded at 31.37nm for Sample 1 and 31.17nm for Sample 2 although microscope visuals shown in Table 6.19 show that Sample 1 (Hybrid Mechanical/FluidJet Process) has the turning signature marks removed whilst there are still evident in Sample 2 (Fluid Jet Process Only).

THE APPLICATION OF ZEEKO POLISHING TECHNOLOGY TO FREEFORM FEMORAL KNEE REPLACEMENT COMPONENT MANUFACTURE

Table 6.18 Analysis after 2nd Polishing Run for Samples 1 and 2

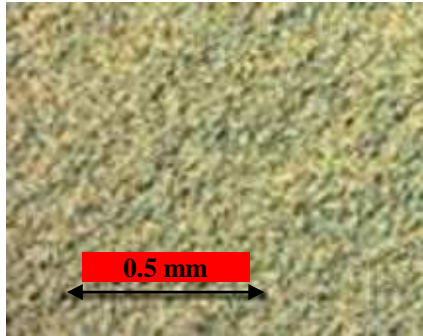
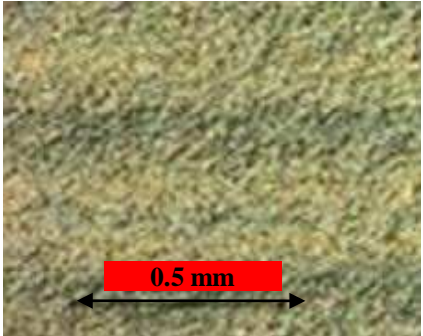
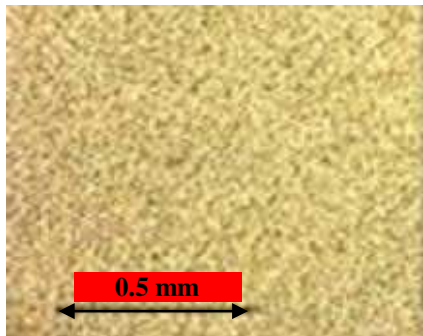
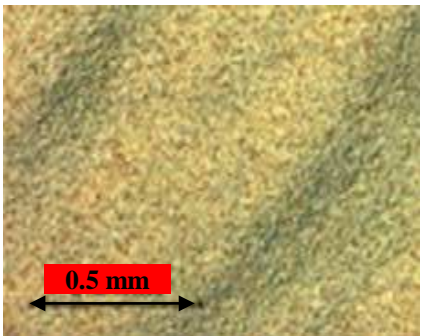
Visual / Measurement	After Stage 2 (Both Samples FluidJet Polished)	
	Sample 1	Sample 2
Microscope Image		
Sa Value	35.3 nm	37.8 nm
Comment	Turning Signatures Barely Visible	Turning Signatures Still Visible

Table 6.19 Analysis after 4th Polishing Run for Samples 1 and 2

Visual / Measurement	After Stage 4 (Both Samples FluidJet Polished)	
	Sample 1	Sample 2
Microscope Image		
Sa Value	31.37 nm	31.13 nm
Comment	Turning Signatures Barely Visible	Turning Signatures Still Visible

6.4 *Summary*

The trial and error method of optimising machine parameters to achieve the best quality output is seen as a costly exercise due to the time consuming effort it requires and the optimum result is not always achieved. An investigation using the Taguchi method was demonstrated to obtain an idea of the parameters that affect the 3D surface roughness parameter Sa. The Taguchi approach was affective in producing the parameters which have the greatest affect on filtered Sa with minimal amounts of testing. Using an L16b Taguchi array consisting of 16 individual tests, a two run average for a 12µm CR39 Glass mineral smoothing cloths was performed to outline the machine parameters which had the most effect on the Sa value of a polished 10mm aperture of Medical Grade 316L Stainless Steel.

Analysis using minitab v15.0 was carried out and proved that the two averages of the runs were not significantly different (student t-test). Although the filtered Sa values gave a good approximation of the parameters that affect the surface quality and essential wear resistance of the polished medical grade 316L Stainless Steel further investigations (Analysis of Mean (ANOM) and main effects plots for other 3D parameters that effect wear) were required to draw conclusions.

The effectiveness and advantages of the Taguchi testing were evident as results from the original analysis could be used as the measurement data file stored information on all the 3D surface roughness parameters. Using a total ranking score, calculated by the sum of the rankings for each 3D surface parameter (Sq, Spk, Sk and Svk) with scores ranging from 4 (Very significant) to 20 (No significance) dependant on the effect of the parameter in generating the best possible parameter value. Using this score system and adding a list of the values for parameters that produced the best results of the ANOM technique the findings were summarised as seen in Table 6.20.

THE APPLICATION OF ZEEKO POLISHING TECHNOLOGY TO FREEFORM FEMORAL KNEE REPLACEMENT COMPONENT MANUFACTURE

The knowledge gained from the Taguchi and ANOM techniques was used to access the polishing process on a harder Cobalt Chrome material used in orthopaedic implants. The polishing media needed to be stronger and therefore a bonded abrasive was used. The diamond bonded abrasive used caused a chemical reaction with the cobalt Chrome material with reasons that will be discussed in Chapter 9. An alternative was found but this also had its disadvantages which again are discussed in Chapter 9.

Throughout all the trials it became evident that in some cases the surface would have remaining machining marks from previous stages of polishing or pre-polish machining. An investigation of a hybrid process (combination of fluidjet and mechanical polishing) was trialed to see if occurrences of such marks could be eliminated. The introduction of a mechanical polishing stage at the beginning of the hybrid process proved influential in removing the machining marks from post polish turning process (further discussions in Chapter 9) compared to a full fluidjet polishing process albeit both surfaces had almost identical Sa values.

The process parameters between the two processes were difficult to compare as they are different for each process therefore a Taguchi process could not be applied although the outcome of using the fluidjet process to locate problem areas of a femoral knee implant identified in Chapter 5.4.5 was discovered.

Table 6.20 Summary of ANOM Technique Results

Parameter	Significance Ranking Order	Values that Generate Best 3D Surface Roughness				Comments
		Sq	Spk	Sk	Svk	
A – Head Speed (RPM)	1	2000	2000	2000	1000	2000 RPM predominant throughout the ANOM for Sq, Spk and Sk. In most cases the relationship is linear with values of the 3D surface roughness parameter decreasing as Head Speed increase from 500 to 2000 RPM. Hence a Head Speed of 2000 RPM should be fixed when using this polishing media for a best overall results for all parameters although a compromise of 1500 RPM could help increase SvK without compromising the other parameters
B – Head Pressure (Bar)	J2	1	1	0.5	1.5	No linear relationship evident but a fixed pressure of 1 Bar would produce the best overall result for all parameters us and contribute towards values that will reduce wear.
C – Precess Angle (°)	4	5	5	5	15	Most parameters show a pattern of a decrease in the parameter values from 0° to 5° and then a rise again for 10° and 15°. Although a 15° Precess Angle produced the best SvK value for a fixed precess angle of 5 ° ensures the best overall result for all parameters using this polishing media. .
D – X-Y Spacing (mm)	J2	0.1	0.1	0.1	0.4	Mainly a linear relationship. Processing times are increased dramatically using 0.1mm and although it produces the best result the advantage of saving process time compared to the small reduction in parameter values is not justifiable therefore a compromise of a smaller XY spacing maybe more appropriate as it increases the SvK value improving wear resistance.
E – Spot Size (mm)	3	6	6	6	6	The smallest Spot Size (6mm) produces the best results in a mainly linear relationship this maybe due to the fact that the variation and error of a smaller spot gives increased stability of uniform material removal.

CHAPTER 7: CORRECTIVE POLISHING METHOD

7 ZEEKO CORRECTIVE POLISHING METHOD

The key to developing conforming parts in a Total Knee Replacement (TKR) is the ability to machine investment cast near net shape femoral and tibial components to a form such that the typical clearances is within $600\mu\text{m}\pm 250\mu\text{m}$ (consultation with implant manufacturers) with the rationale that highly conforming smooth surfaces liberate less wear particles and last longer under synovial lubrication. To achieve these clearances the need to localise material removal on a pre-measured component is required. This can only be achieved if the material removal for a particular polishing media/slurry is predictable and repeatable.

The Zeeko corrective polishing method is made up of a series of steps: -

- Creation of an influence function or influence functions family to predict uniform material removal rate
- Measurement of component to be corrective polished on suitable metrology equipment e.g. CMM, Interferometer etc.
- Import CAD model in a NURBS format to allow close control of data points to drive the machine through the defined CNC tool path.

These steps are imported into the unique software developed by Zeeko Ltd. from where a CNC tool path is generated to correct the form of the component to the desired CAD model.

To date it should be noted that corrective polishing has not been demonstrated on bio-compatible metal materials. A summary of the freeform corrective polishing process can be seen in Figure 7.1

Basics of free form corrective polishing

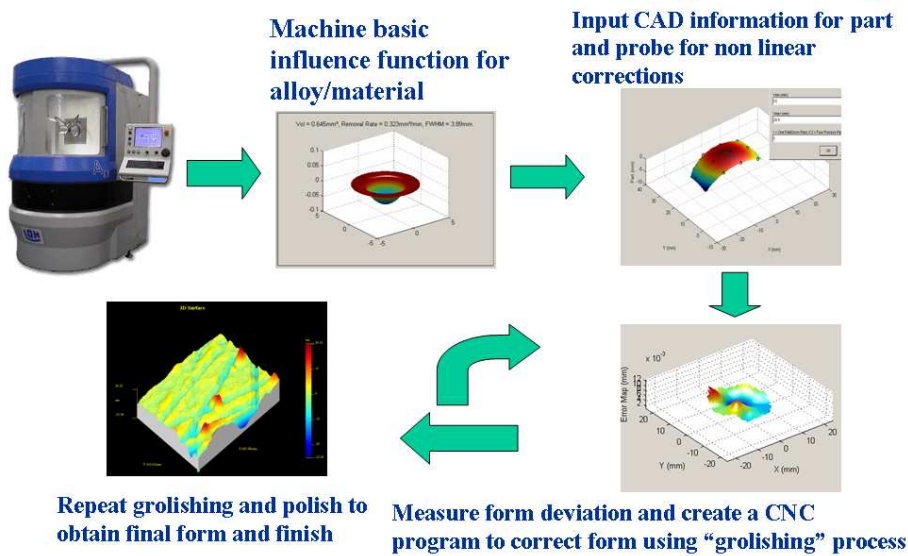


Figure 7.1 Basics of Freeform Corrective Polishing Procedure

7.1 Influence Function Creation

The influence function creation starts with a sample piece of material of the same mechanical/chemical properties of that which is to be corrected. The sample is placed on the machine in this case it is a flat 40mm diameter Plano of cobalt chrome. Inside the ZeeCAD software the Plano is generated using the design part button located in the tool box. Figure 7.2 shows the design new part function with the 40mm diameter Plano created.

It can be seen that the part was created using a rotationally symmetrical basic shape with a flat base and a radius of 20mm (40mm Diameter). The domain for the part was made slightly larger with $\pm X = 25\text{mm}$ and also $\pm Y = 25\text{mm}$. There were no offsets or tilt required. The part was then edged using a circular boundary function with X and Y centres at 0 and a selected radius of 20mm as the part will be located centrally on the machine using a self centred chuck. The part was now saved as a 3DP format so that it can be read back into the ZeeCAD software when required.

THE APPLICATION OF ZEEKO POLISHING TECHNOLOGY TO FREEFORM FEMORAL KNEE REPLACEMENT COMPONENT MANUFACTURE

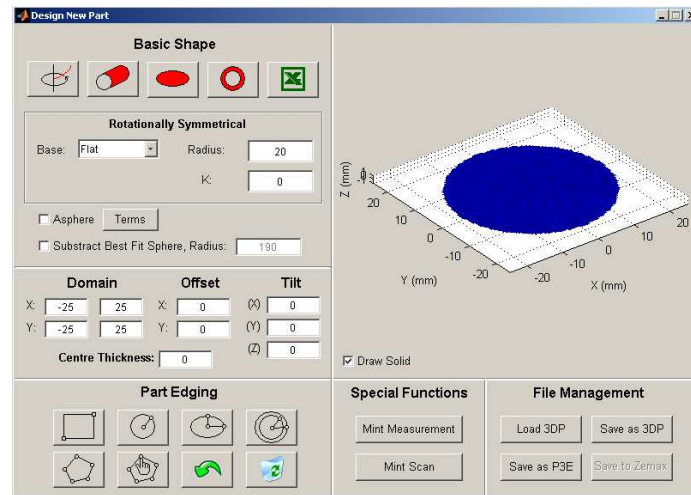


Figure 7.2 Design New Part Function with 40mm Flat Plano Design

The imported part can be seen in Figure 7.3 along with the inputted non linear correction data. The non linear process involves probing the part and compensating for the offset position and the geometry of the polishing bonnet. The average run out at different precess angles can be calculated. In this case only four probing points (2 in Y and 2 in X) were required as the part is flat although probing is required in four precess positions as the influence functions use all four precess to create its uniform Gaussian shape. The probing file is now created and feed into the Zeeko IRP200 CNC controller.

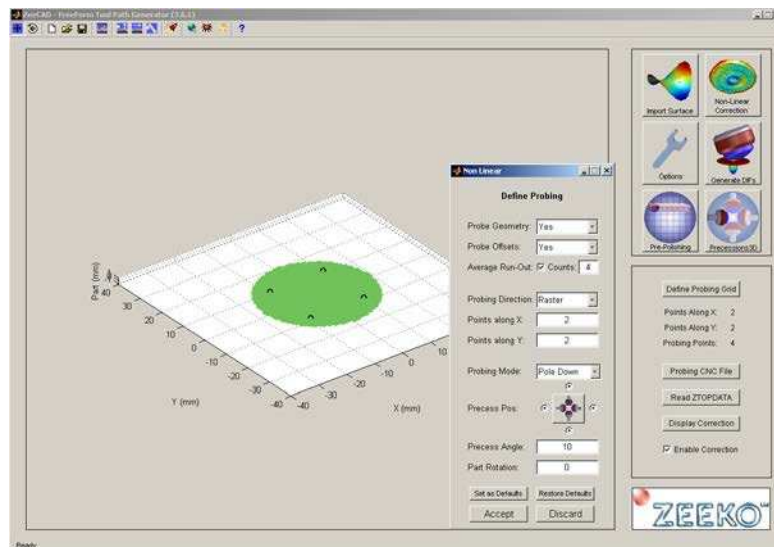


Figure 7.3 Imported Part in ZeeCAD with Non Linear Correction Parameters

THE APPLICATION OF ZEEKO POLISHING TECHNOLOGY TO FREEFORM FEMORAL KNEE REPLACEMENT COMPONENT MANUFACTURE

Each individual influence function has its own parameters (Head Speed, Spot Size and Process Angle). In this case of Figure 7.4 four influence functions are equally spaced not to overlap when the CNC machine manufactures them on the 40mm flat sample.

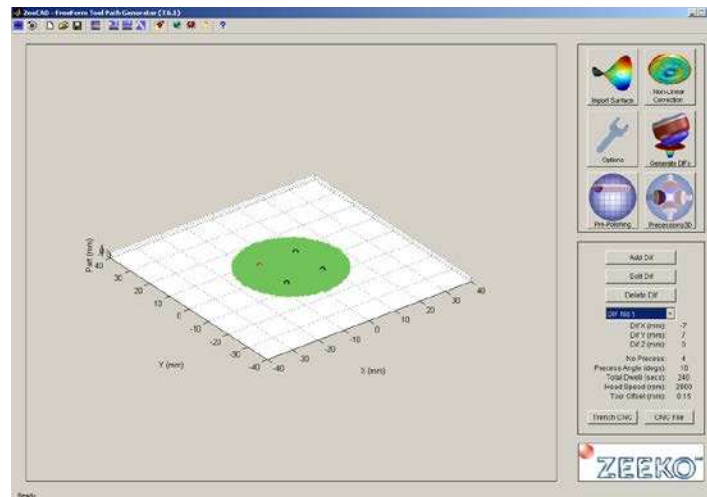


Figure 7.4 Generate DIF function in ZeeCAD

With the influence functions generated in ZeeCAD the CAD file could be generated and run on the Zeeko IRP200 machine. A digital image of the machined influence functions on the flat sample of cobalt chrome is shown in Figure 7.5.



Figure 7.5 Influence Functions on 40mm Plano Cobalt Chrome Sample

The machined influence functions were then measured on a 2D surface profiler although other metrology equipment can be used. A 2D surface profile of an influence function measured on a Somicronic Diamond Stylus Profiler is shown in Figure 7.6. Generation of the influence function allows deterministic knowledge of material removal to be gained.

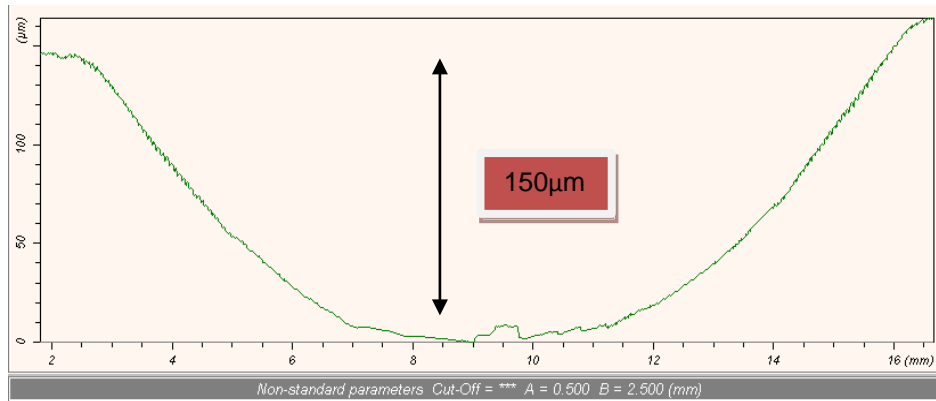


Figure 7.6 2D Surface Profile Measurement of a Machine Influence Function

The influence function used to predict the uniform material removal rate is Gaussian shape and has a removal rate depth of approximately 150µm for 240 seconds of dwell time. The information retrieved from the influence is saved and is ready to be imported into another piece of software called Precessions 3D from where the corrective polishing process will be generated and performed on the IRP200 machine.

7.2 Corrective Polish CNC file generation

With several influence functions manufactured on the IRP200 machine and measured on a 2D surface profiler the information collected can be combined into the corrective polishing process.

The data required by Precessions 3D software to generate a corrective polishing CNC program is: -

- Influence Function Data measured on 2D surface profiler or other surface metrology equipment.
- CAD model of desired manufactured finished component imported into Non Uniform Refined B-Spline (NURBS) format with only the required surface to be corrected and any residual components of the CAD model removed.
- Measured surface topography of the component to be corrected either from any type of surface metrology equipment e.g. CMM, WYKO or Taylor Hobson CCI.

7.2.1 *Influence Function Data*

The data that was retrieved from the 3D diamond stylus profiler is imported in the Precessions 3D. The software translates the data file and displays a 3D version of the influence function.

The displayed influence function can be seen in Figure 7.7. The Z-axis shows the depth of influence function matches that of 2D stylus measurement seen in Figure 7.6 with an approximate depth of 150um. The software can be used to moderate the influence function so that more or less material can be removed provided that other parameters are kept constant.

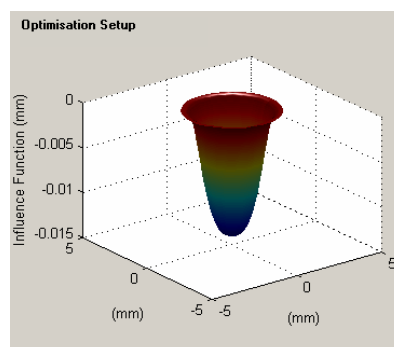


Figure 7.7 Imported Influence Function in Precessions 3D Software

7.2.2 CAD Model modification and NURBS conversion

A software package called Rhino CAD 3D designed for NURBS modelling was used to strip the CAD model from a STEP format to the trimmed surface required by removing the residual CAD model components and then converted into a NURBS model with additional control points used to control the polishing head across the work piece. The more control points used the more flexibility you have over the surface to be polished.

Figure 7.8 shows the NURBS surface imported into Precessions 3D which shows the desired finished component for which the software needs to create a CNC tool path to correct the pre cast / machined component too match that of the desired surface.

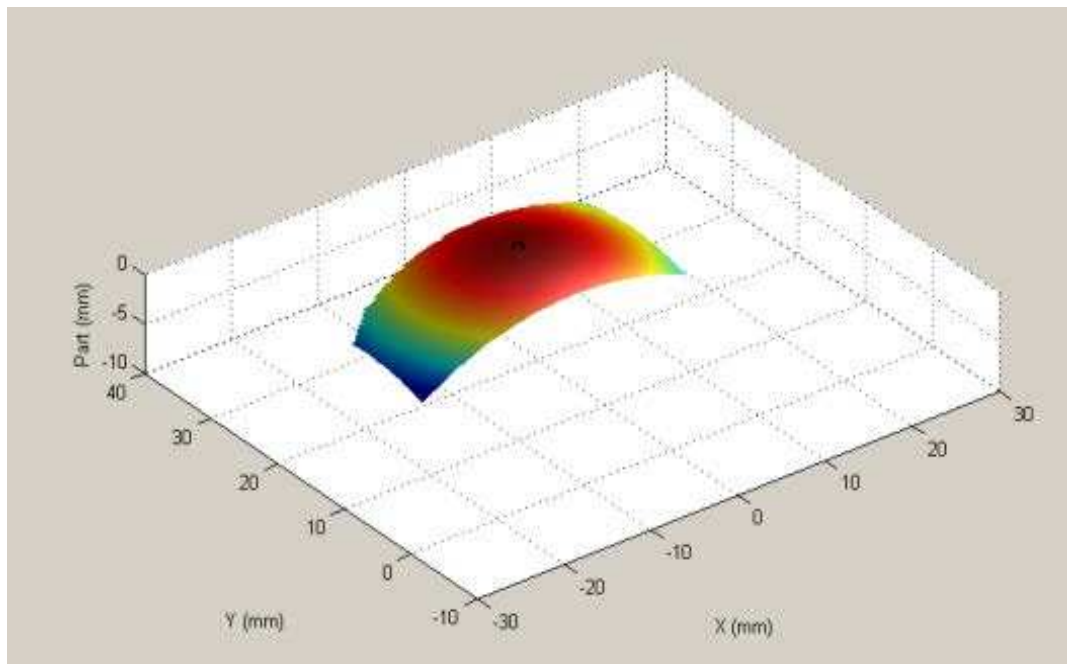


Figure 7.8 Desired geometry of a freeform femoral knee implant component section

7.2.3 Measured Surface Topography of Component to be corrected

To allow form error correction to be accomplished in Precessions 3D software an error map needs to be created from the pre-corrective polished component. The error map consists of a subtraction of the surface of the component to be corrected away from the desired CAD model. This will leave a residual surface which is known as the error map and this map is used by the software to calculate the dwell time needed by the polishing head over every section of the component to be corrected.



Figure 7.9 Taylor Hobson PGI 1240

In this case the section of the femoral knee implant component was measured on a Taylor Hobson PGI1240 diamond stylus profiler (Figure 7.9) fitted with a Y stage so that the surface of the component to be corrected by be scanned in 3D X,Y,Z co-ordinates. The X, Y, Z co-ordinates were then used to develop a map of the errors of the pre cast/machined and pre-polished component.

Figure 7.10 shows a Zeeko Metrology Toolkit image of the measured component with a colour coded scale to indicated form errors that will be corrected on the IRP200 machine after a CNC programme is generated in Precessions 3D. Area of red and yellow indicate high peaks that require longer polishing head dwell times and light and dark blues areas indicate lower peaks that require less polishing head dwell times.

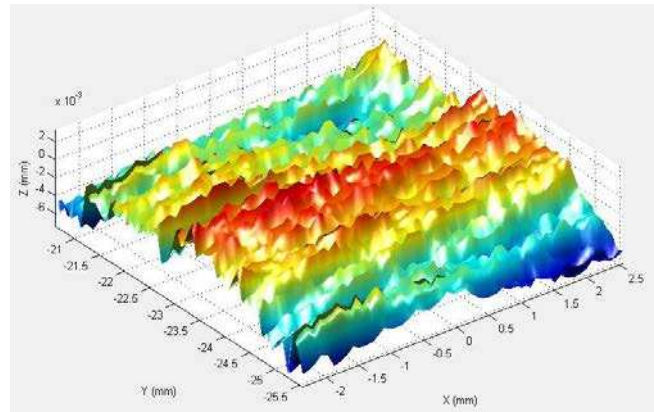


Figure 7.10 Error Map Imported to Metrology Toolkit from Taylor Hobson PGI 1240

7.3 Optimizing corrective polish procedure

With a predefined material removal (Influence Function), NURBS model (desired/control surface) and an error map (desired surface - metrology measured work piece) the information can be inputted to the Zeeko Precessions 3D software (Figure 7.11) together with the desired parameters from investigations in Chapter 6 to allow for the corrective polishing software to calculate an optimized result from which a CNC program can be generated.

It can be seen that the dwell time map shows areas of high dwell time (light blue and yellow) which have correspond to high peaks on the surface and low dwell time areas (dark blue) which correspond to lower peaks on the error map of the surface.

7.4 Form Correction of an area of a Freeform Femoral Knee Component

Before conducting corrective polishing, a part of the surface area of a single condole of a femoral knee component was measured. The measured data and the design surface were matched, from which an error map was generated, as shown in Figure 7.12. The upper part of Figure 7.12(a) shows the measured data and the design CAD model, and the lower part shows the form error map between the two sets of data.

THE APPLICATION OF ZEEKO POLISHING TECHNOLOGY TO FREEFORM FEMORAL KNEE REPLACEMENT COMPONENT MANUFACTURE

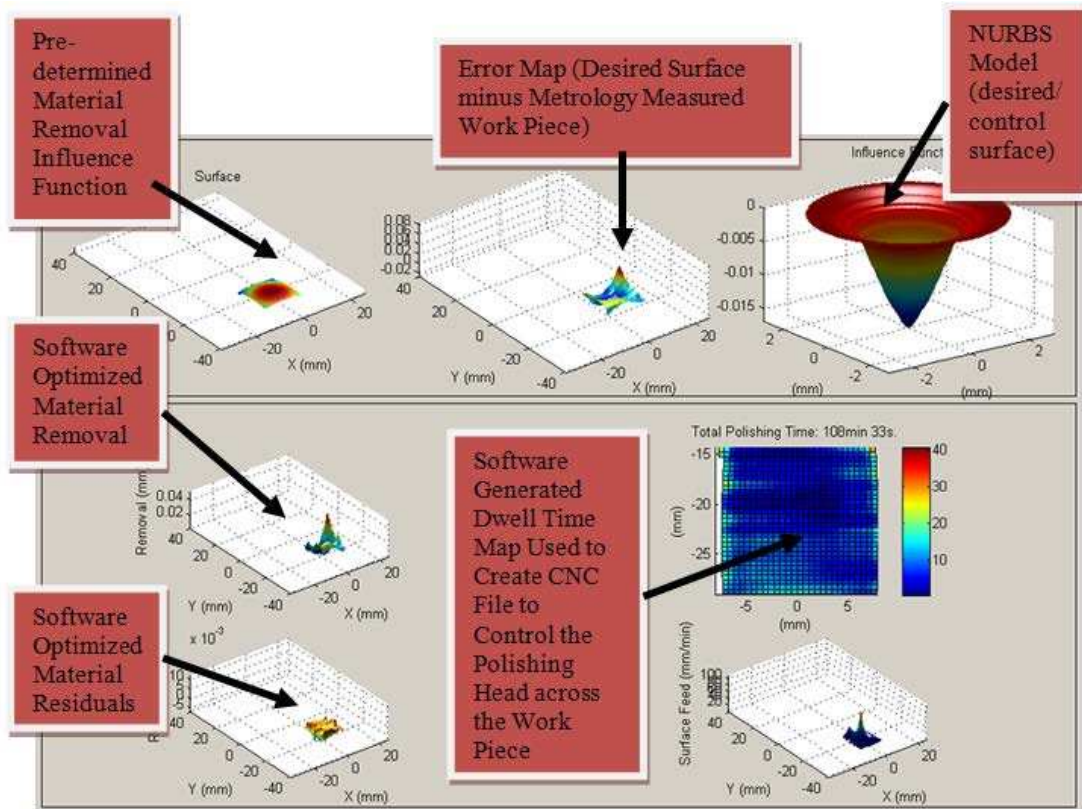


Figure 7.11 Precessions 3D Software for Optimised Corrective Polishing Process

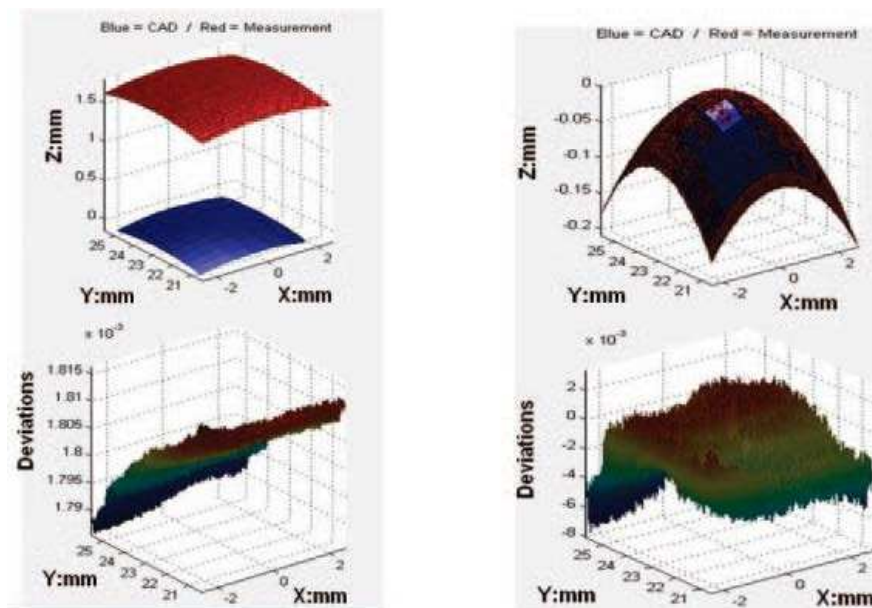


Figure 7.12 Measured Data (a) and Designed Surface Matching (b)

From the figure it is noted that, without matching of the measured data and design data, the error map will be meaningless. Therefore, data matching is necessary to obtain the real error map for corrective polishing. The data matching process is based on the least-squares method, which can be described as follows: -

$$F_{LS}(X) = \min \left(\sum_{i=1}^N |P_i^1 - P_i^2|^2 \right)$$

where $F_{LS}(X)$ is the least-squares target function, N is the number of sampled points, P_i^1 and P_i^2 are sampled points and the corresponding points in the design model, and $\min()$ is the minimization operator.

Equation 7.1: Least squares method for matching of data to generate error map

Equation 7.1 is optimized by minimizing the sum of the distance between the two sets of points within an acceptable threshold value. When the optimization process terminates, the measured data are matched to the designed surface model. The optimization of equation 7.1 usually requires the solution of a non-linear differential function set. For more precise matching, the minimum zone method is employed, which is carried out by minimizing the deviation zone between the sampled point set and the surface model. The function of the minimum zone method can be expressed as: -

$$F_{MZ}(X) = \min (|P_{\max}^+ - P_{\max}^-|)$$

Equation 7.2 Minimum zone method used to optimize surface matching

where $F_{MZ}(X)$ is the minimum zone target function, and P_{\max}^+ and P_{\max}^- are sampled points with the largest deviation in one direction from the mean surface and in the opposite direction respectively.

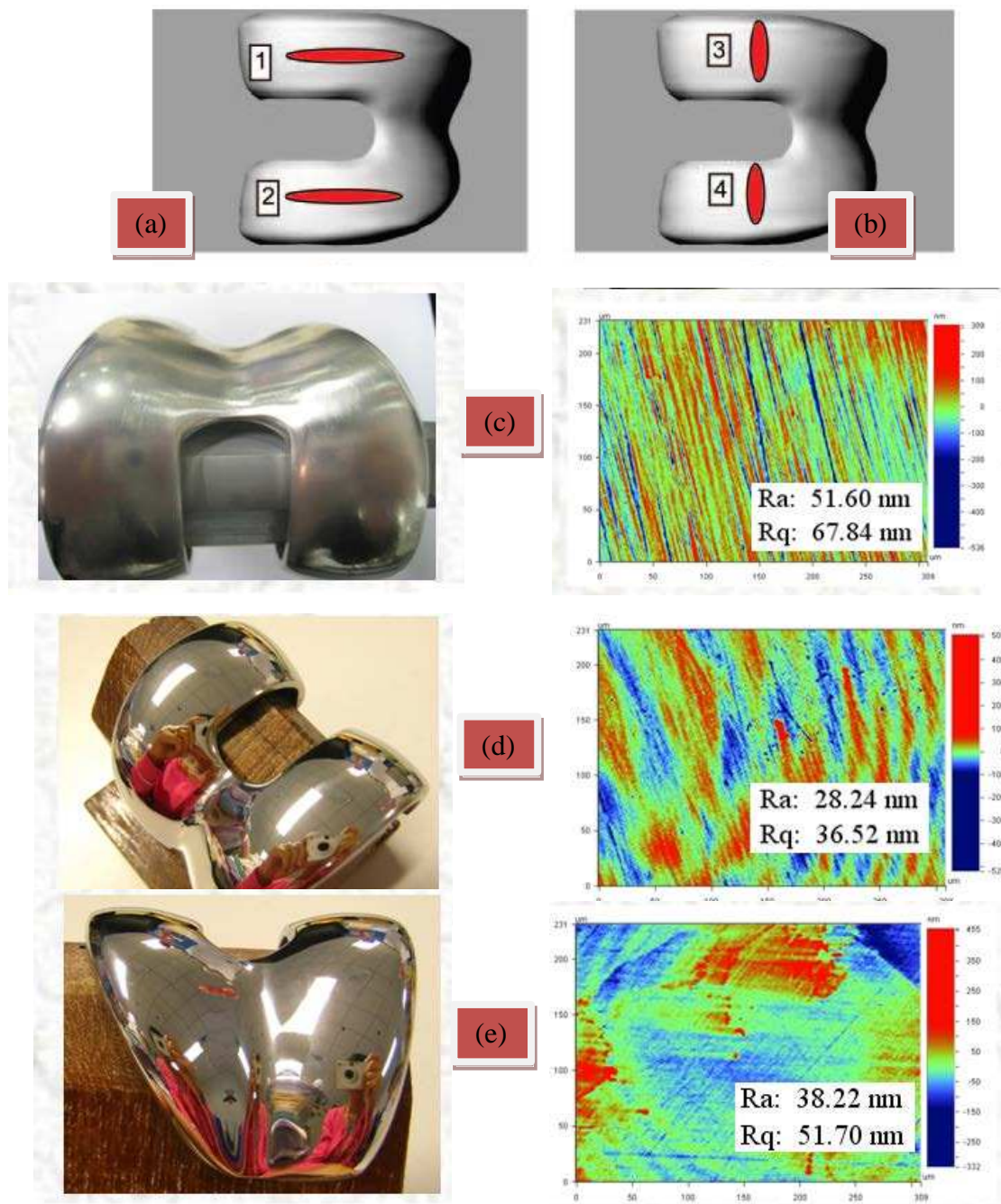
7.4.1 Corrective Polishing Results

After matching of the two surfaces and generating an influence function for the polishing of the CoCr implant using the parameters in Table 7.1, corrective polishing was conducted on the implant surface with an area of 33mm x 18mm (maximum measurement area due limitations of the measurement using a diamond stylus profiler) targeting the area most commonly associated with wear. The rest of the surface of the femoral knee implant was polished to blend in with the corrective polishing area the results of which can be seen in Table 7.2 and Figure 7.13 where measurements of 3D surface roughness Sa using a Wyko NT8000 white light interferometer were taken in areas within and outside the corrective polishing area before and after corrective polishing.

The results in Table 7.2 show after a series of polishing runs intended to blend the surface into the corrective polished area arithmetic mean roughness average in the four measured areas dropped from 145.4 nm to 9.51 nm within the 20nm stipulated in ISO standards after a series of blending and corrective polishing runs. Before blending and corrective polishing the range of surface roughness in different regions is very large (63.3nm – 309.5 nm), while that after blending/corrective polishing this is reduced significantly (8.2-10.4nm) indicating large surface roughness variations seen in different regions of the post blending/corrective polishing technique are significantly reduced using the procedure. The use of this technique and the appeared to be effective not only in bringing the surface roughness to a low value but also in making the surface roughness more homogeneous throughout the continuous freeform surface of the implant.

The PV values before and after corrective polishing were compared, as shown in Figure 7.14. It was observed that a tangible improvement in the form error (17.5%) is achieved within the central region (5mm x 5mm) of the polished area of the femoral knee condyle although there was no significant improvement outside of this central area.

THE APPLICATION OF ZEEKO POLISHING TECHNOLOGY TO FREEFORM FEMORAL KNEE REPLACEMENT COMPONENT MANUFACTURE



A: Horizontal Measurement Zones 1 & 2, B: Vertical Measurement Zones 3 & 4
 C: Femoral Knee Component (post cast and pre-polished) before Corrective Polishing
 D: Femoral Knee Component after Corrective Polishing, E: Commercial Equivalent Component

Figure 7.13 Measurement Areas Images Before and After Corrective Polishing

Table 7.1 Influence Function Parameters and Dwell Map for Corrective Polish

Parameters	
Slurry medium	17um SiC Paste
Path type	Raster
X spacing	0.5mm
Y spacing	0.5mm
Tool overhang	0mm
Tool offset	0.3mm
Head speed	2000rpm
Max. surface feed	500 mm/min
Max Dwell Time *	< 1 sec
Min Dwell Time *	≈ 30 sec

* Quoted as (0.5mm² x 0.5mm² area from X-Y Spacing)

Table 7.2 Surface Roughness Measurements Before and After Corrective Polishing

Area	3D Surface Roughness Sa (nm) Before Corrective Polishing (Rough Post Machined Femoral Surface)				3D Surface Roughness Sa (nm) After Blending / Corrective Polishing			
	1	2	3	AVG.	1	2	3	AVG.
1	50.7	69.7	168.2	96.2	10.9	12.1	8.3	10.4
2	84.5	142.3	110.7	112.5	10.3	10.3	10.4	10.3
3	438.1	262.7	227.7	309.5	10.2	9.6	7.5	9.1
4	62.8	57.8	69.4	63.3	7.6	9.6	7.3	8.2

In an attempt to justify the reason behind the lack of form improvement outside of the central area two sample pieces of CoCr with similar radius of curvature to that of the femoral knee joint component were manufactured. A set of 3 influence functions with identical parameters (Table 7.3) were generated on different areas of the surface of each of the samples as seen in

Figure 7.15. The influence functions were measured and generated within the Zeeko Software of which a summary can be seen Table 7.4.

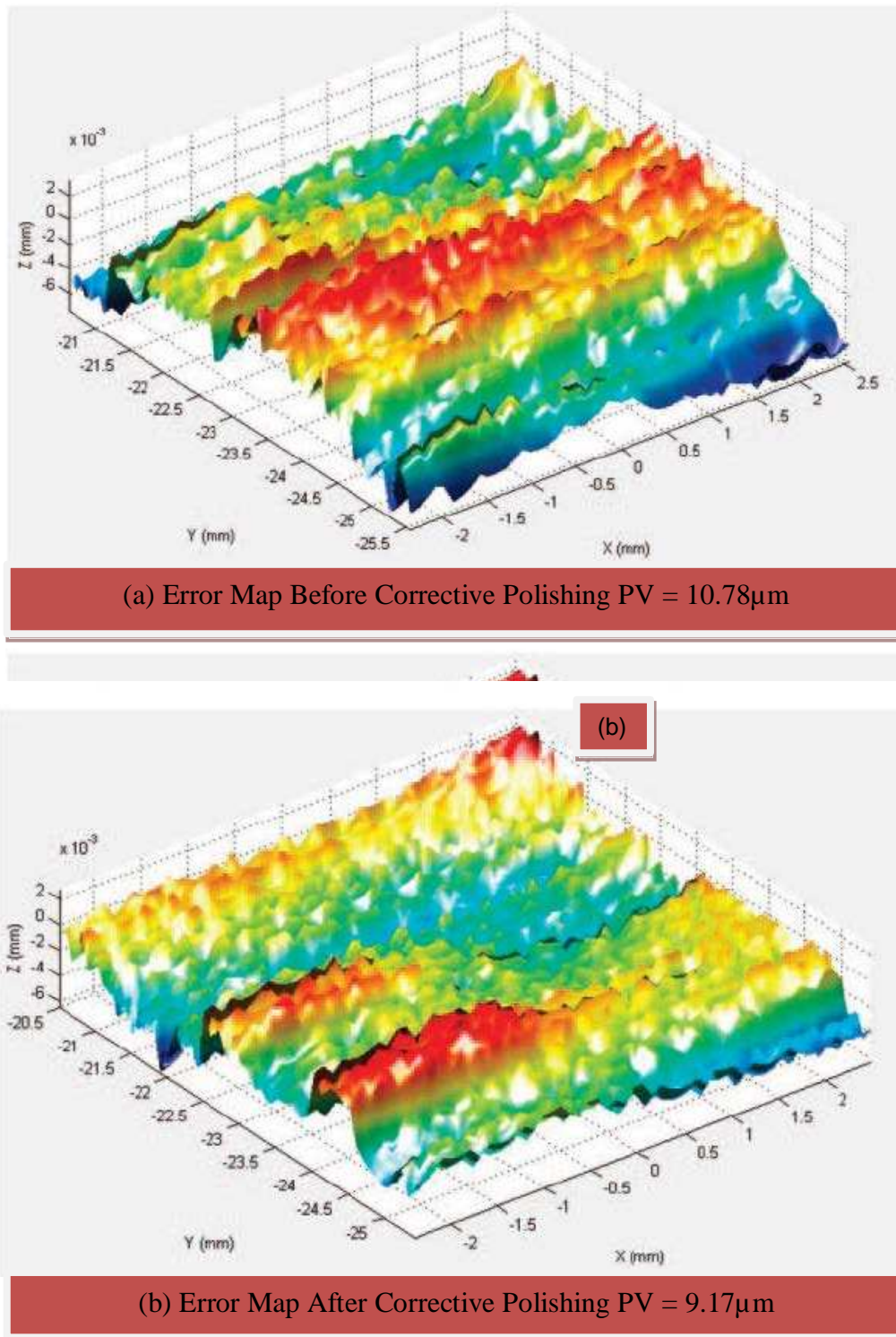


Figure 7.14 Error Maps Before (a) and After (b) Corrective Polishing Process

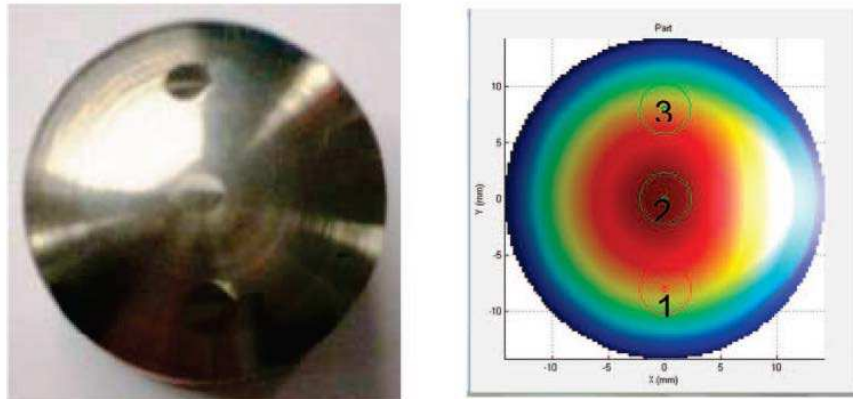
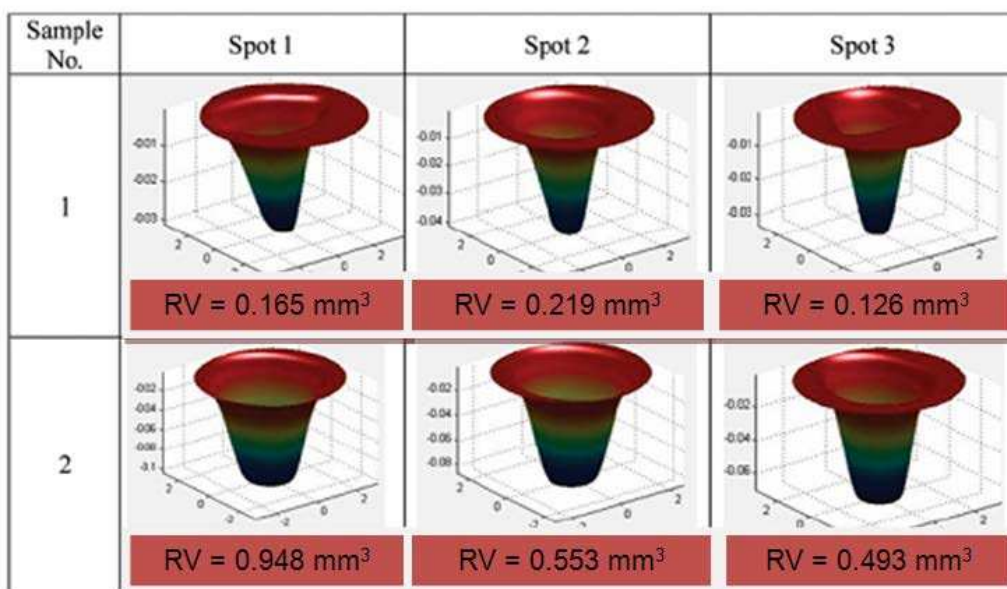


Figure 7.15 Influence Function Generations on CoCr Sample

Table 7.3 Parameters for Influence Functions on CoCr Curved Samples

Sample	Mechanical Polishing Parameters	
	1	2
Precess (no)	1	1
Total Dwell Time (s)	240	240
Head Speed (rpm)	2000	2000
Precess Angle (deg)	5	10
Compression offset (mm)	0.15	0.30
Tool pressure (bar)	2	2
Cloth Material	Zirconium oxide	Zirconium oxide
Slurry	SiC	SiC



RV = Removal Volume

Table 7.4 Influence functions Generated on Curved CoCr Sample Surface

7.5 *Summary*

The Zeeko corrective polishing procedure has been described with the steps required to perform a freeform corrective polishing procedure. The material removal process used in corrective polishing is a cross over between grinding and polishing as mentioned previously (Section 5.2) a new name for the process was termed ‘grolishing’ by the process patent holder Dr. David Walker.

The advanced software produced by Zeeko Ltd. in conjunction with NURBS software named Rhino CAD can produce a CNC program which controls the polishing head fitted with polishing media and a supply of slurry across the work piece to correct the form error using a pre-defined material removal mechanism (influence function). High spots on the error surface will be reduced by dwelling the polishing head for longer periods than that of low spots. In some cases 2nd and 3rd corrective polishing procedures are required when the surface has high quantities of peaks and valleys with each stage having a target error reduction level produced by offsetting the error map by a certain level.

The corrective polishing process was used in attempt to improve the PV error of a segment of a condyle of a freeform femoral knee implant component together with blending the surface around the corrected area using a hybrid process. The blended surface roughness was improved from a starting condition of $S_a = 145$ nm to that of $S_a = 9.5$ nm with the PV reduced from 10.78 to 9.17. Although the reduction of the PV is not a significantly large reduction (>20%) it has shown that the Zeeko IRP200 machine is capable of improving PV error without compromising the surface quality and the final blended surface is within ISO specifications. A further discussion of why the corrective polishing procedure only produced low PV improvements can be found in Chapter 9.

**CHAPTER 8:
PERFORMANCE OF
ZEEKO POLISHED
ORTHOPAEDIC
IMPLANT MATERIALS**

8 PERFORMANCE OF ZEEKO POLISHED ORTHOPAEDIC MATERIALS

To demonstrate the performance of orthopaedic implant materials polished on the 7-axis Zeeko IRP200 CNC polishing machine wear tests were performed on a series of specimens. The setup of the test incorporated multi-directional movement as seen in Figure 8.1.

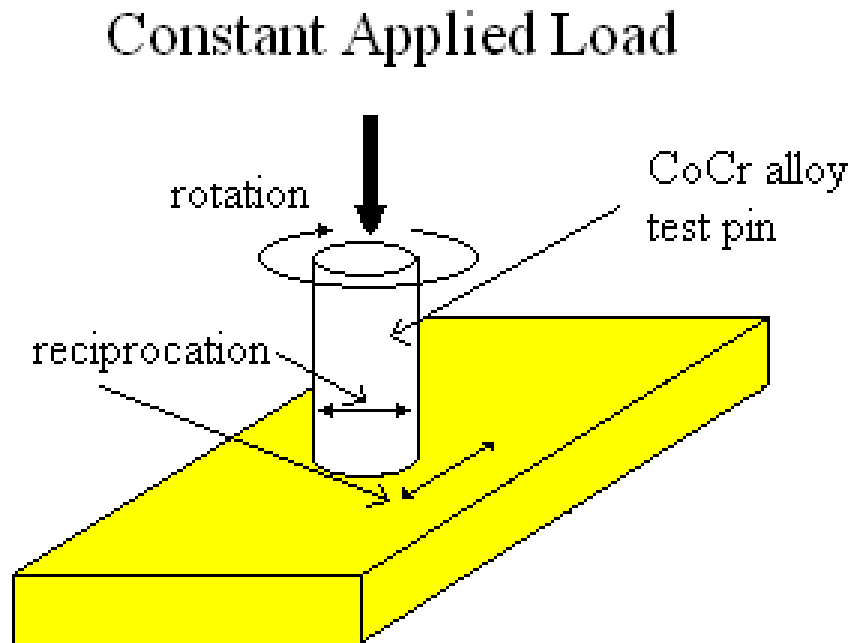


Figure 8.1 Schematic of Pin-on-Disc Wear Simulator Equipment

The two wear test strategies for assessing the wear performance of Zeeko IRP200 polished orthopaedic implant materials were as follows: -

- Wear Simulation of Zeeko Form Corrected Pins versus hand polished pins
- Modified Pin-on-Disc Testing of an Orthopaedic Implant Coating

Sample preparation, testing conditions and a review the results obtained will discussed in this Chapter of the thesis.

8.1 Zeeko form correction polished pins versus hand polished

The procedure to demonstrate the form correction of pins prior to finishing involves using the Zeeko IRP200 CNC polishing machine to prepare samples with the form error reduced using Precessions Software. The samples are then tested and compared to those of hand polished pins without form correction under a pre-determined set of parameters on a multi-directional pin-on-plate wear simulator.

8.1.1 Sample Preparation

The design for the cobalt chrome pin component used for pin on disc wear testing can be seen in Figure 8.2. These dimensions were machined to within tolerances where specified.

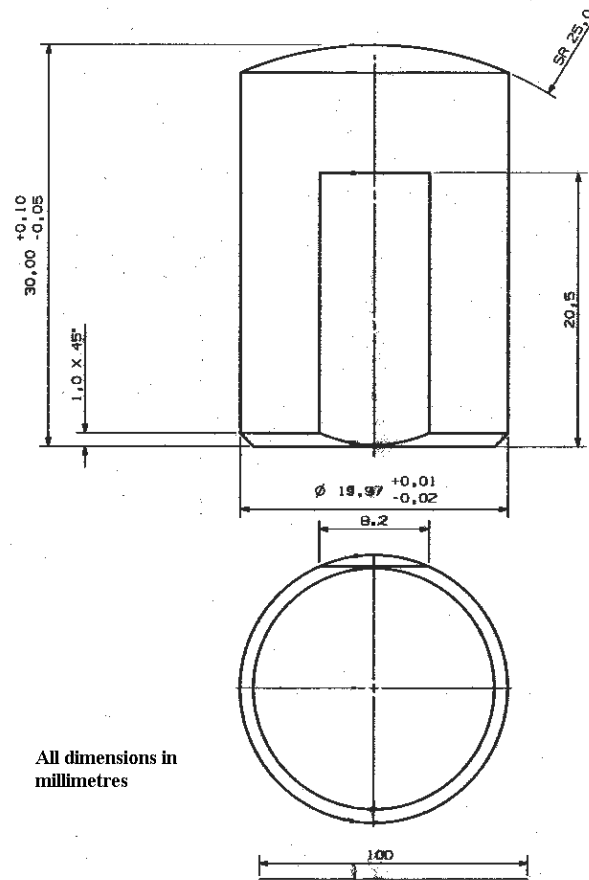


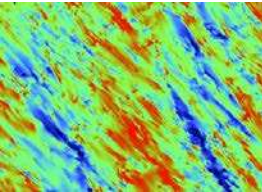
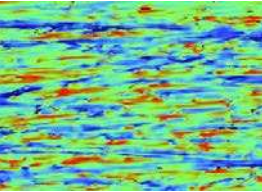
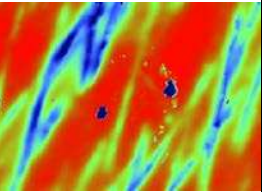
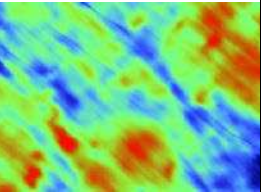
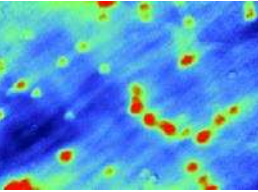
Figure 8.2 Cobalt chrome pin component CAD drawing showing dimensions

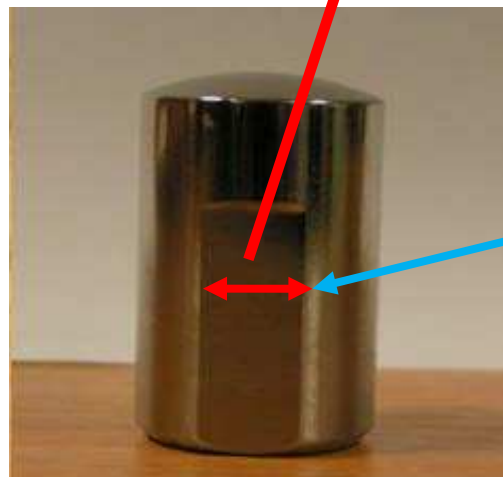
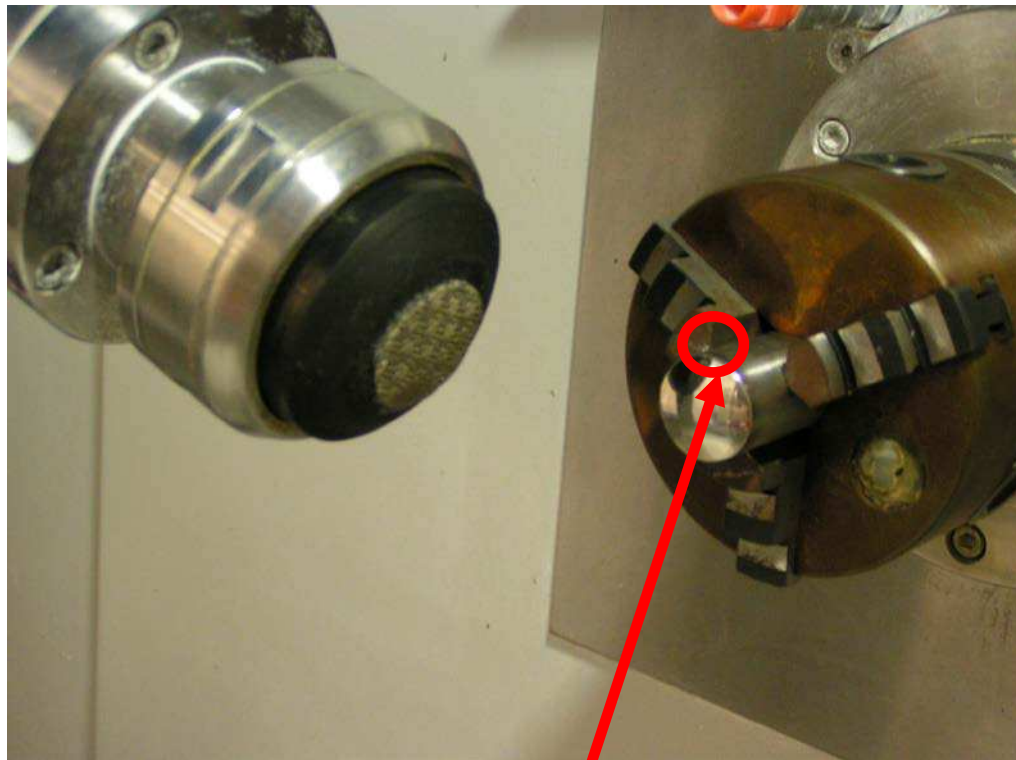
The radius of curvature for the top surface of the pins was targeted to be 25mm. All together 6 samples were prepared of which three samples were finished by hand using a range of various fixed and loose abrasives to achieve the best possible surface finish as near to industry standard ($R_a < 30$ nm) as possible. The other three samples were polished to the best possible finish including using the corrective polishing procedure (Chapter 7) at each stage of the polishing processes. The parameters and abrasives used for each of the Zeeko IRP200 polishing stages along with an example of surface measurements for one of the Zeeko polished pins are summarised in Table 8.1.

The parameters selected were determined from the optimisation of the polishing procedure outlined in Chapter 6 of the thesis. It should be noted that to limit the time to prepare the samples the X-Y spacing has been reduced from the optimum of 0.1mm - 0.2mm to between 0.3mm - 0.5mm reducing polishing runs to between 10-20 minutes. The polishing media was changed after each corrective polishing run thus not restricting the performance of polishing media during the corrective polishing process within the limits found in Chapter 6.2. An image of the polishing media used for each stage can be found in Figure 8.3 of the Appendix. Figure 8.4 shows an image of a pin held in position on the Zeeko IRP200 machine with a three jaw chuck in position a re-location key way was used to clock the pin into position ensuring the best relocation possible between polishing stages and measurements.

It can be noted that the form corrected radius of curvature measured using a Taylor Hobson Form Talysurf Diamond Stylus Profiler was improved slightly using the corrective polishing process as previously witness in Chapter 7.4 where the maximum Peak to Valley (PV) error of a femoral knee component was reduced using the corrective polishing technique whereas the radius of curvature for the hand polished pins had larger deviations from the desired 25 mm approximately $\pm 5\%$ compared to that of $\pm 2\%$ of the Zeeko IRP200 machine polished pins.

Table 8.1 Summary of Zeeko IRP200 Form Corrected Used in Wear Tests

	Stage 1	Stage 2	Stage 3	Stage 4	Stage 5
Polishing Media (FEPA Grit Size) N.B. Water used as a coolant in all Stages	Black Telum Nickel Bonded Diamond (120)	Red Telum Nickel Bonded Diamond (200)	Yellow Telum Resin Bonded Diamond (500)	Orange Telum Resin Bonded (4000)	Orange Telum Resin Bonded (4000)
H-Axis Head Speed (RPM)	2000	2000	2000	2000	2000
H-Ais Head Pressure (Bar)	0.5	0.5	0.5	0.5	0.5
X-Y Spacing (mm)	0.5	0.5	0.3	0.3	0.3
Spot Size (mm)	10	10	10	10	10
Precess Angle (°)	5	5	10	10	0 (pole Down)
Surface Roughness Image Wyko NT2000 White Light Interferometer (x20 Magnification (approx. 0.25mm x 0.25mm)					
Surface Roughness (Ra) nm	344.8	232.9	41.7	5.9	2.8
Form Corrected Radius of Curvature (m)	25.82	25.46	25.28	25.22	25.14
Comments	All post polishing machine marks removed although surface roughness increased	Form error reduced but polishing tracks evident	Form error reduced again surface roughness reduced significantly no polishing tracks	Surface roughness target achieved form reduction become less some evidence of carbide pullout.	Carbide pullout more evident surface roughness optimized and form target achieved to within 10%.



Clocking
Position

Pin With Relocation Key Way Used To Clock Pin in Jaw Accurately As Possible
Between Measurement and Polishing Runs

Figure 8.4 Positioning of Wear Test Pins in 3-Jaw Chuck on Zeeko IRP200 Machine

An average roughness value of Sa was recorded from 5 measurements (4 quadrants (0°, 90°, 180°, 270°) on the same radial arc and one measurement at the crown) using a Wyko NT 2000 white light interferometer. The average value of Sa for the three pins polished using the Zeeko IRP200 machine was equal to 9.4 nm compared to that of 22.6 nm of the conventional hand polished pins. A summary of the measurement results for the pins used in the wear test performance comparison of the techniques can be found in Table 8.2. Figure 8.5 shows a comparison between the best Hand Polished and Machine Polished Surfaces.

Table 8.2 Machine (MP) and Hand Polished (HP) Pin Surfaces Pre-Wear Testing

Interferometric Surface Measurement, Surface Roughness Ra (nm)						
Pin Number	Quadrant A	Quadrant B	Crown	Quadrant C	Quadrant D	Average
HP1	20.1	27.1	17.2	36.3	24.1	25.2
HP2	17.8	13.6	19.2	36.8	24.1	22.2
HP3	12.6	40.4	15.1	16.5	18.1	20.5
MP1	3.2	3.8	2.8	3.3	4.6	3.5
MP2	17.7	5.8	10.0	10.7	11.2	11.1
MP3	23.1	7.8	10.3	11.7	15.5	13.7

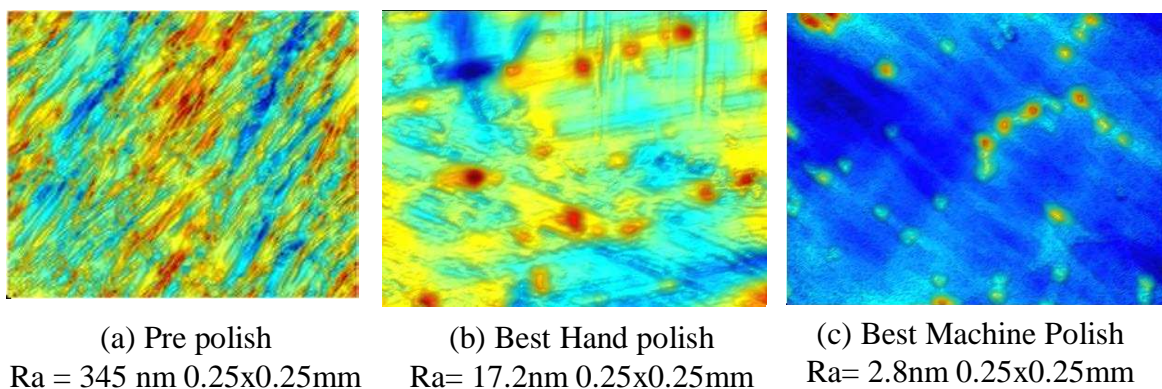


Figure 8.5 Best Machine and Hand Polished Pin Surfaces Pre-Wear Testing

It can be seen in Figure 8.5a that the surface is covered in uniform scratches in the direction of cutting from the 1200 Grit silicon carbide pre polish conditions before any hand or machine polishing of the pins was processed. The hand polished pin shows evidence of

carbide pullout where the work done in removing the 1200 grit scratches has caused removal of carbides from the surface due to the softer material carrying the carbide breaking down and releasing it. Also evident are residual scratches from previous stages. The Zeeko IRP200 machine polished surface has some carbide pullout with only a few random direction residual scratches. The reduction in residual scratches was predicted to enhance the wear performance of the Zeeko polished pins.

Table 8.2 shows a summary of repeatability of machine polish pins (MP) and the hand polished pins (HP). It is considered the larger variation in the machine polished results is caused by edge effects on the pins. Both sets of results show that for the machine polished pins the roughness obtained was within the bounds considered acceptable for these types of surfaces as stipulated in ISO standards of that of $R_a < 50$ nm.

8.1.2 Simulator Test Parameters

The pin-on-plate tests were performed at Stanmore UK one of the collaborative partners in conjunction with an Engineering Physical Sciences Research Council grant [304]. A constant load of 2.3kN (equivalent to three times body weight) was applied throughout the pin on disc testing. With this constant load applied to the pins the discs were reciprocated with a 10mm total travel and a radial motion of $\pm 5^\circ$. A 30% bovine serum solution was used as lubrication throughout the articulation of the bearing surfaces. At every million cycles the test was broken down and the following measurements taken:

- Surface profile of the pin surface including measurements of R_a , R_z and R_m .
- Weight loss of the UHMWPE.
- Penetration depth into the UHMWPE.
- Volumetric change in the wear track.

A blank disc of UHMWPE was used as a soak test left in the 30% bovine serum solution to compensate for the fluid absorption properties into the plastic polymer through a capillary action. The same keyway used for relocation of the pins on the Zeeko IRP200 machine between polishing runs and measurements was used to relocate the pin in the same location

on the pin-on-plate wear testing equipment between measurements taken at every one million cycles.

8.1.3 Analysis of Results

As seen in Table 8.2 the average Ra for the Zeeko IRP200 machine polished pins is lower than that for the hand polished pins. Analysis after two million cycles shows that both the hand polished and the CNC polished pins had become rougher, but there was still a difference with the CNC polished pins having a lower average Ra of 35nm compared to that 45nm of the hand polished pins as seen in Table 8.3

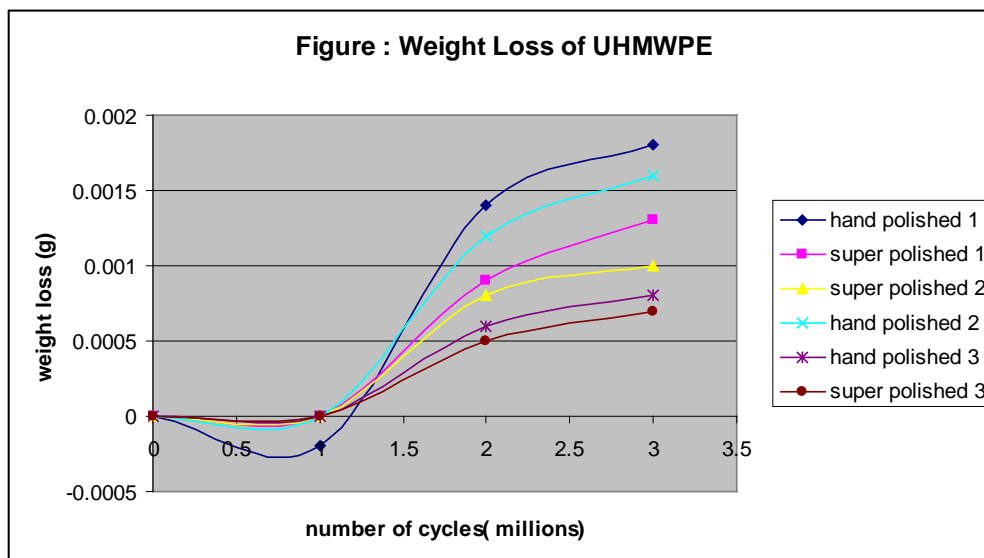


Figure 8.6 Weight Loss of UHMWPE (Plastic) during Co-Cr Pin on Disc Testing

There was no significant difference in the weight loss of the UHMWPE plates after two million cycles for discs that articulated against the hand polished cobalt chrome pins compared with the plastic articulating against the CNC polished pins (Figure 8.6). However on average CNC pins gave lower wear.

Gravimetric readings taken of the polyethylene discs at 2 million cycles showed that overall there is no statistical difference in the weight loss between polyethylene articulating with

CNC polished cobalt chrome and hand polished cobalt chrome. Although it can be seen that there is a trend to a more uniform and lower weight loss with the CNC polished pins between the 2 million and 3 million cycle points. Examination of the graph in Figure 8.6 shows that two out of three of the polyethylene discs articulating against hand polished plastic showed the greatest wear.

To demonstrate the penetration of the UHMWPE above the zero plane and also the effect of creep below the plane the profile of the wear tracks on the UHMWPE discs were measured by using a CMM.

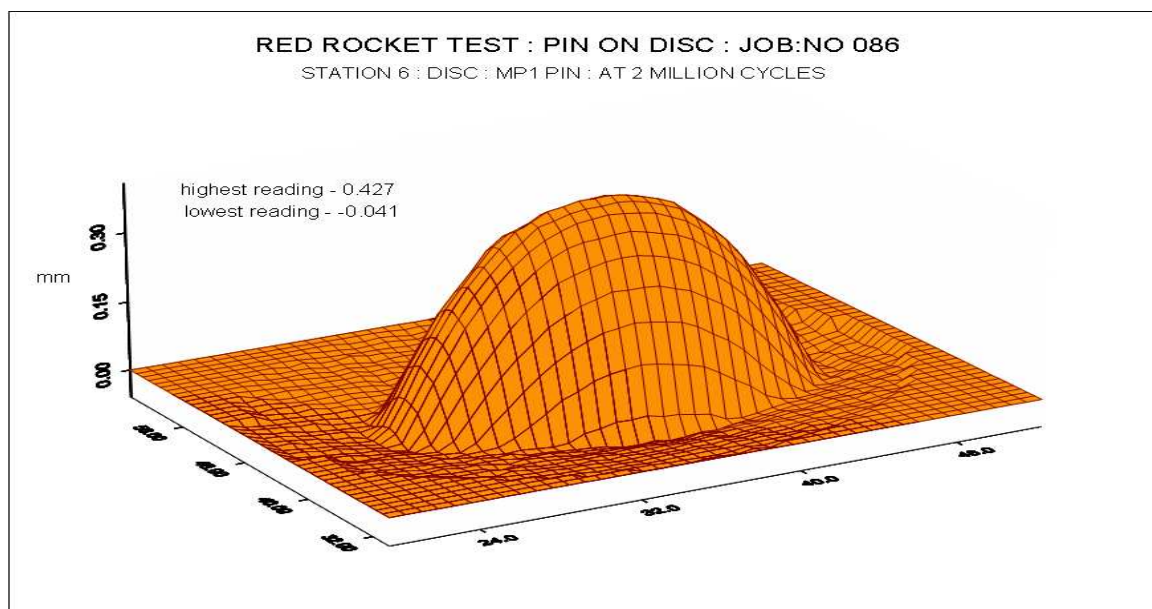


Figure 8.7 Inverse wear track profile of machine polished pin after 2 million cycles

Figures 8.7 and 8.8 show these measurements and indicate that a hand polished cobalt chrome articulating with a plastic disc showed a trend of overall greater penetration the figures show the inverse penetration for a better visual representation. The average penetration depth at 2 million cycles for the plastic articulating with the hand polished discs was 0.526mm (0.025SD) and the average penetration for the plastic articulating with the CNC polished discs was .485mm (0.052SD). All discs showed plastic creep with material thrown up at the margins of the wear track.

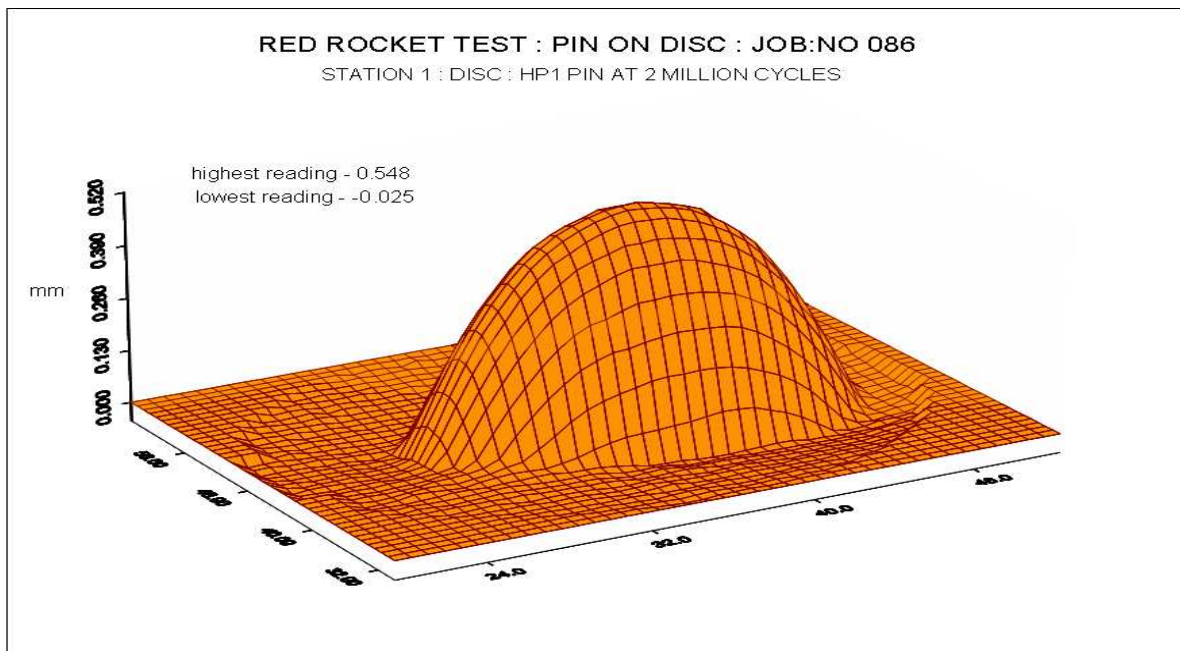


Figure 8.8 Inverse wear track profile of machine polished pin after 2 million cycles

Table 8.3 Summary of 2D Stylus Trace Averages for Pins after Wear Testing

2D Stylus Trace Parameter	Hand Polished Pins Average	Machine Polished Pins Average
Ra	45 nm	35 nm
Rz	162 nm	144 nm
Surface Material Ratio (S _{mr2}) after wear test	63 %	65%

The trend of increased wear may be associated with the increased roughness of the pin surfaces. Table 8.3 shows a summary of Ra, Rz and Sm average values of machine polished and hand polished cobalt chrome pins demonstrating it should be noted that all 3 hand polished pins measured a greater Ra, Rz and Rm values than that of the CNC polished pins.

In terms of radius of curvature the hand polished pin 3 which produced the lowest wear over 5 million cycles had the lowest form error with a radius of curvature of 25.08mm indicating that form control has a larger effect than surface roughness although the misalignment of the pins could have been a factor the spherical shape of the pin reduced this effect.

8.2 Pin on disc testing for Diamond Like Coatings (DLC's)

The procedure to demonstrate the performance of a polished DLC coating of pins utilizing the Zeeko IRP200 CNC polishing machine using a CNC program to polish un-coated discs of various radii and to various surface roughness values . The samples were then coated with a DLC and wear performance tested. The wear scar analysis from a modified multi-directional pin-on-plate wear simulator would determine the best surface quality for the DLC coating.

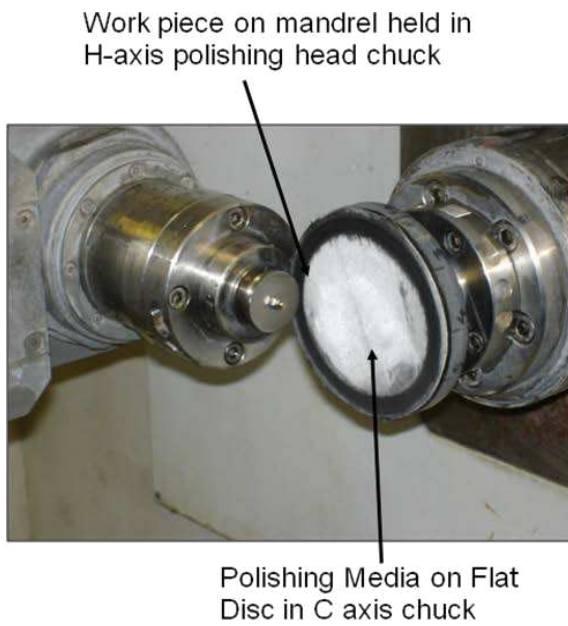
8.2.1 Sample Preperation

Rough cut discs were made from a 29mm diameter bar of cobalt chrome using a wire electro-discharge machining process with the edge of the disc being rounded on lathe using a forming tool as seen in Figure 8.8 a. This rough cut process produced an average surface finish of Ra= 317nm (SD 0.068) and an average radius of 28.560mm (SD 4.669) a sample disc can be seen in Figure 8.8.

Polishing pads of various silicon carbide grits and also diamond pastes on silk carrier cloths were attached to a 12cm diameter backing plate fixed into the C-axis of the Zeeko IRP200 machine allowing the plate to move in the X, Y, Z axis of the sample which was held at the virtual pivot (intersection of the centers of A and H axis of the machine) and could be rotated at a desired RPM speed. A setup of the disc loaded in the machine before being polished can be seen in Figure 8.9



Figure 8.8 Sample Disc Manufactured from Forming Tool



- 6 of the 7-axis used (A, C, X, Y and Z). Opposite function to normal polishing process where tool and workpiece have been inverted
- B-Axis kept stationary at 90 degrees
- A and Z-Axis used to control polishing head over the radius of the disc
- H-Axis polish head speed variation for 200-500 RPM
- X and Y used to control horizontal and vertical contact point on polishing media hence decreasing frequency of change due to wear
- C axis used to rotate polishing media for random surface contact hence improving surface finish

Figure 8.9 Setup for polishing sample discs on Zeeko IRP200 Machine

Using a co-ordinate transfer spreadsheet which could be loaded into the CNC the radius of the sample was followed by controlling the Z position of the component at intervals of X and Y across the component at a known angle of tilt of the sample being polished. The formula seen in equation 8.1 was derived elsewhere [305] to determine the Z position: -

$$z = R_d + \frac{\sqrt{(R_d - R_e)^2 + R_e^2 - (2(R_d - R_e)R_e \cos(\pi - \theta))}}{\cos \frac{\theta - (R_e \sin(\pi - \theta))}{\sqrt{(R_d - R_e)^2 + R_e^2 - (2(R_d - R_e)R_e \cos(\pi - \theta))}}} \quad (1)$$

(Where R_d = disc radius, R_e =radius at edge)

Equation 8.1 Formula for calculating Z position on surface of sample for known radii

A limiting factor regarding rounding of edges was discovered if the full range of the require radius was polished although the time frame for the experiments would not have allowed a solution to be derived therefore a more simplistic solution of using a fraction of the angle range used to cover the whole disc.

Once the required ISO standard surface finish ($R_a < 50$ nm) was achieved the surfaces were coated with a amorphous carbon coating using a Magnetron Ion Plating process giving an average coating thickness of $2.02\mu\text{m}$ and a microhardness value of 1795Kg/mm^2 (measured on a Fischerscope ultra low load microhardness tester with a maximum test load of 50mN).

8.2.2 Simulator Test Parameters

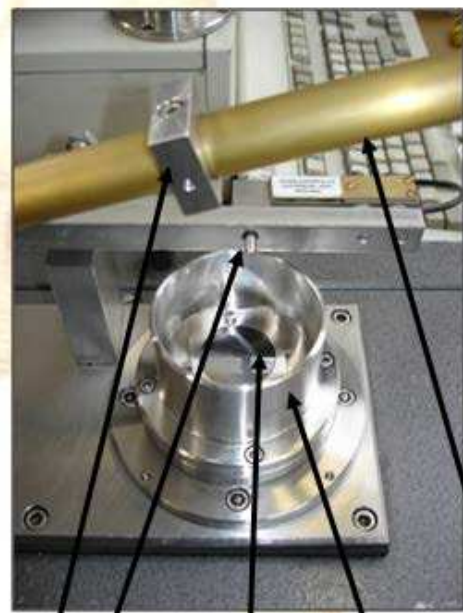
Pin on disc tests were carried out on a Teer Coatings Pin-on-Disc Wear Test Rig as seen in Figure 8.9. Due to the amount of samples to be tested the pin-on-plate test was modified from that seen in Figure 8.1 to that of Figure 8.11. Rotating the disc to a new coated surface area meant that several tests could be completed on one disc without affecting the load whereas using a pin would mean re-grinding and re-coating after each test with the decreased length of the pin affecting the applied load.

A load of 20N and a linear speed of 100mm/s inside a 25% bovine serum aqueous solution and a test time of one hour were applied. The counter face material was un-coated cobalt chrome with a surface finish of R_a less than 10nm . Two types of measurement of the wear scars were used to analyse the wear performance of the various radii and surface finishes.

The first method was a formula again derived elsewhere [305] which used a derivative involving measuring the wear scar diameter and secondly a Taylor Hobson CCI 6000 white light interferometer and Talymap software were used to calculate the wear volume of the scar the process of which can be seen in Figure 8.12. Frictional readings were also monitored throughout the wear tests.



Teer Coatings Ltd. Testing Rig



Counter-face disc
Load Arm
Load cell
Disc/pin holder
Lubricant holder

Figure 8.10 Teer Coatings Pin-on-Plate Wear Test Rig

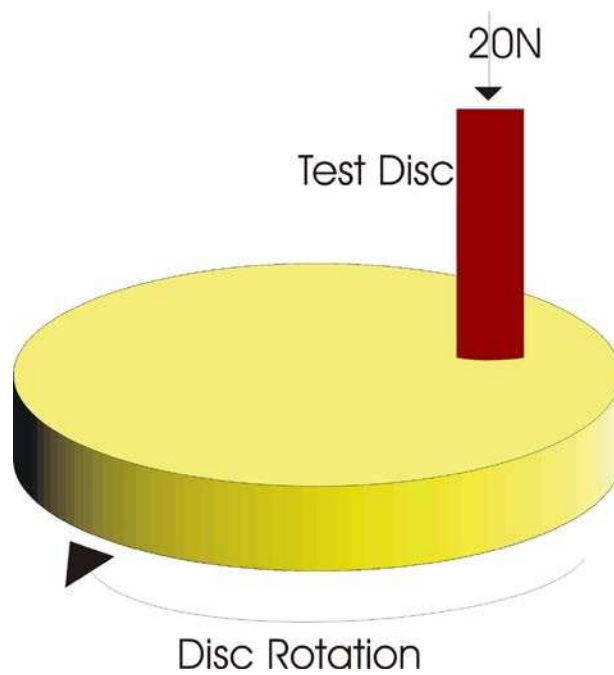


Figure 8.11 Modified Pin-on-Plate Wear Test Rig Setup

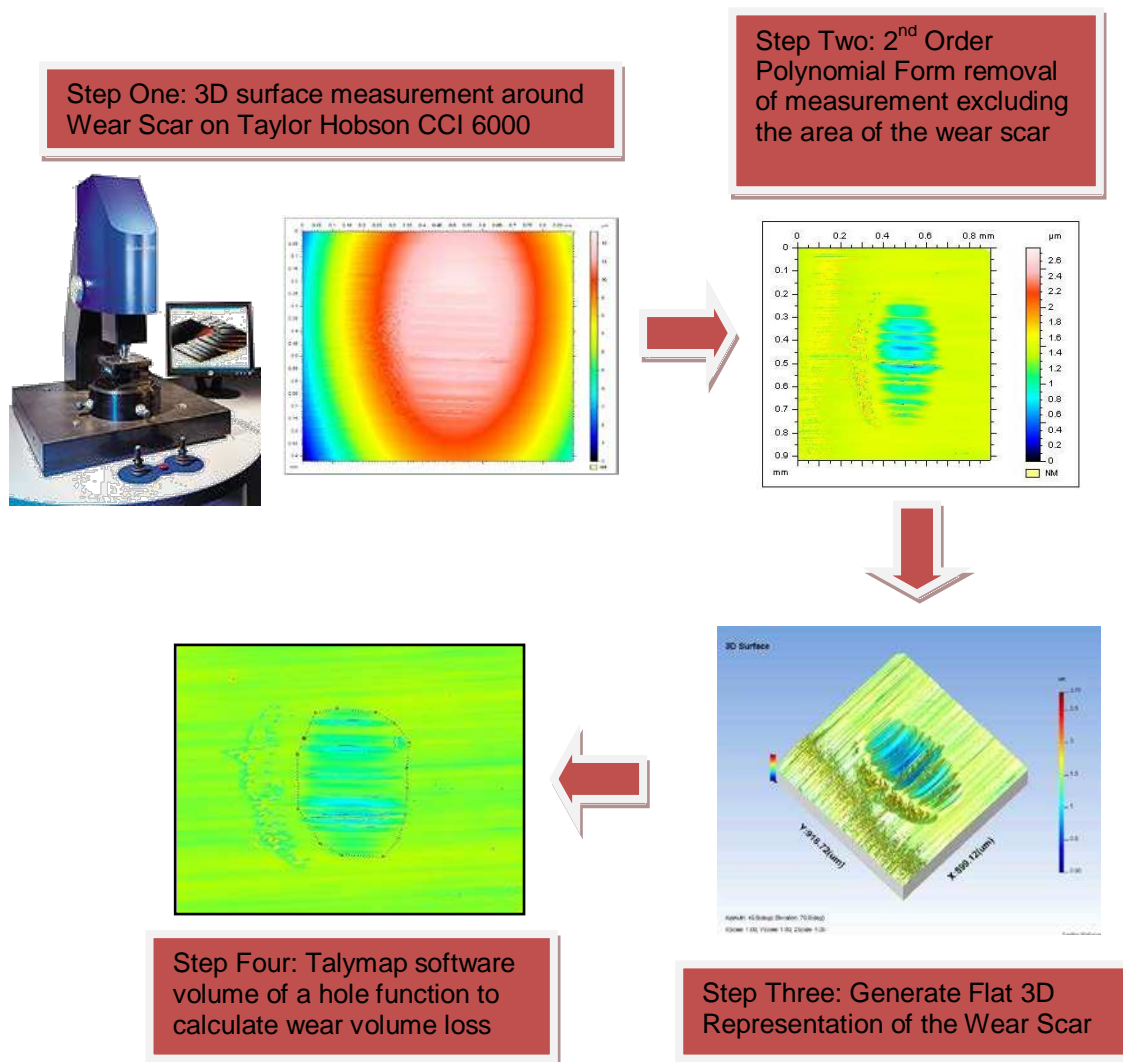


Figure 8.12 Interferometer process to determine wear volume loss of test discs

8.2.3 Analysis of Results

From the collected data an analysis of the effect of the disc radius and surface roughness on wear volumes could be performed. The results are shown in Figures 8.13 and 8.14 respectively.

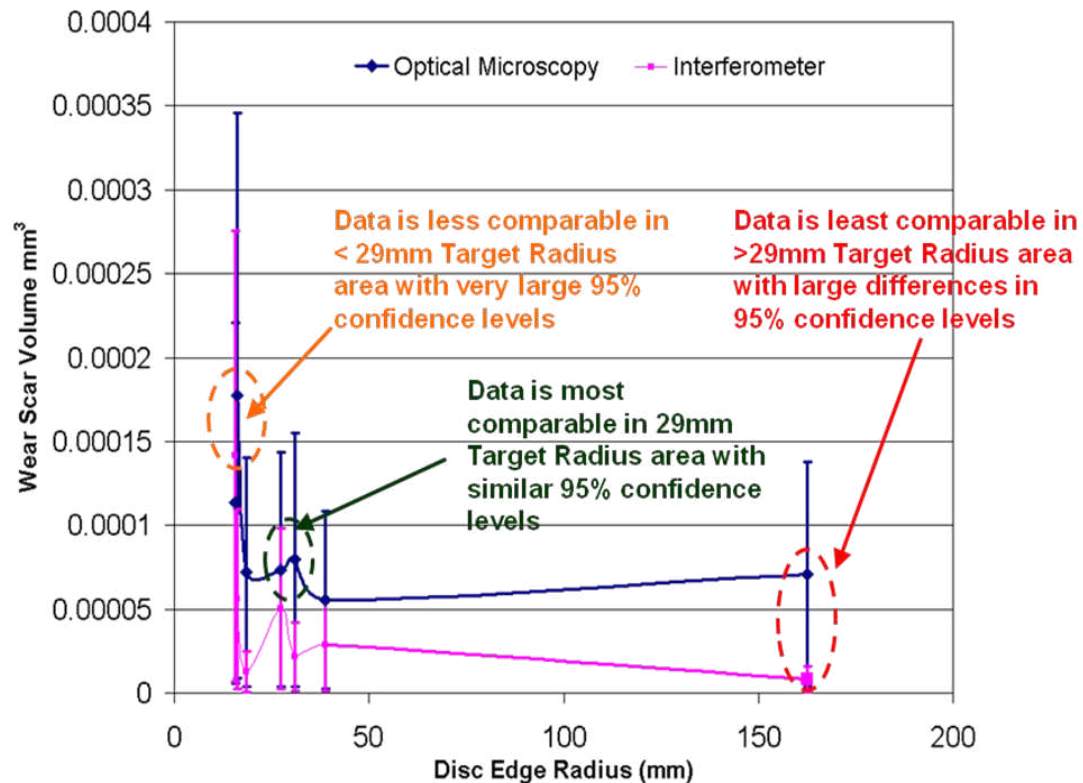


Figure 8.13 Comparison of methods for effect of disc edge radius on wear volumes

In the case of both methods the results of disc edge radius follow theory relating to an increase in disc edge radius can be seen to clearly decrease the wear rate due to a larger contact area hence producing a reduced contact pressure. The results are most comparable in the target roughness area of less than 20nm and the data becomes less comparable between the methods as the radius increases above the 29mm target with results least comparable when the radius is below the 29mm target.

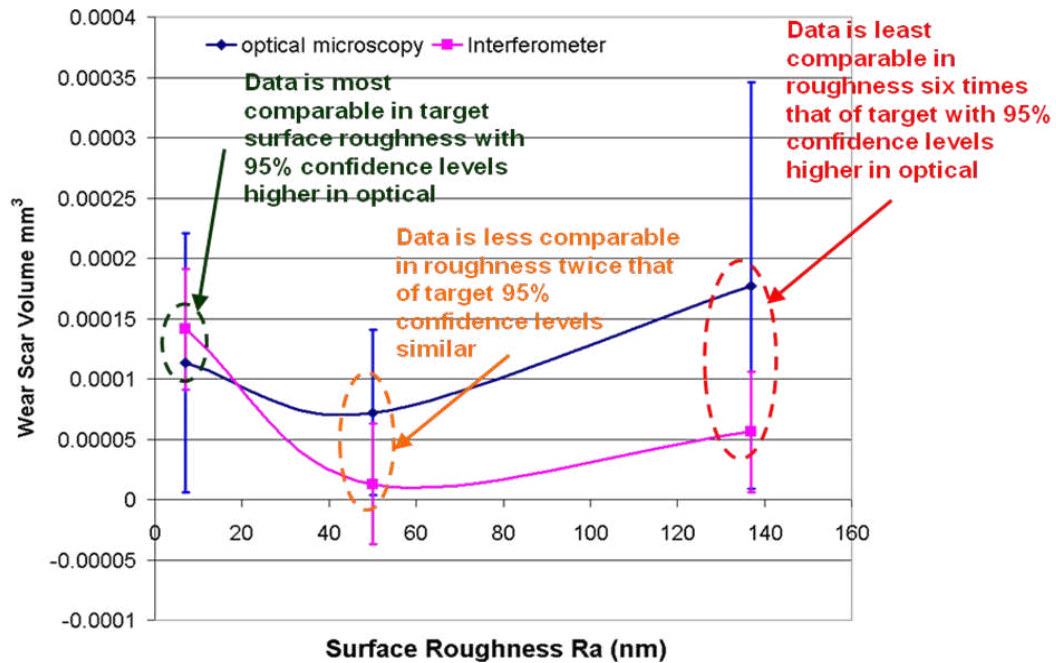


Figure 8.14 Comparison of methods for effect of surface roughness on wear volumes

Conflicting results are seen in the comparison of the methods for surface roughness compared to theory as it was anticipated that a smoother surface would lead to reduced wear; which is not a reflection of the wear test results. It is difficult to determine which method is best as Knox’s method assumes uniform wear across the scar which is not always the case whereas the effect of defining the boundary of the hole for software calculation can also affect the result. Knox later performed a paired t-test as part of his PhD thesis and the results show no significance difference ($p>0.05$) between the two methods within the target roughness and target radius results.

8.3 Summary

Through the use of pin-on-plate testing of form corrected pins using the Zeeko IRP200 polishing machine it has been proven that the process can match and even improve the wear performance of orthopaedic implant materials in comparison to that of conventional hand polished pins.

A comparison of two techniques to measure the wear volumes of scars produced on a modified pin-on-plate tester for testing coated orthopaedic implant was performed. Knox's visual inspection of the surface technique produced higher wear volumes to that of the interferometer technique due to the assumption of wear used in the mathematical calculations. The visual inspection proved the faster of the two processes due to further processing requirements of the interferometer data to obtain a wear volume value although when wear was low this technique overcome the difficulty associated with distinguishing wear using the visual method.

Through pin-on-plate testing it has been proven that the Zeeko IRP200 machine can produce coated and un-coated orthopaedic implant surfaces that perform well during wear test simulation further discussions on the limitations of the tests will be discussed in Chapter 9.

CHAPTER 9: OVERALL DISCUSSION

9 OVERALL DISCUSSION

The purpose of this thesis was to apply the Zeeko CNC Polishing technology from its original design of optics polishing to that of the orthopaedic implant component polishing especially targeting difficult to polish geometries associated with freeform femoral knees. At the beginning of the thesis it was unknown that application could be achieved. During this thesis there is certainly been indications that the application is feasibly possible although not without difficulties that have been encountered which will be discussed in this section of the thesis.

The discussions will cover the contributions to knowledge by discussing the following categories: -

- Surface Roughness Optimisation
- Form Correction of a Freeform Femoral Knee Implant Component
- Wear Performance of Zeeko Polished Implant Materials

9.1 *Surface Roughness Optimisation*

The optimization process itself was a difficult task although the initial testing proved that further investigation using Taguchi methods was required in order to reduce the time associated with trial and error techniques which are common in industry. This would not only quantify but also determine confidence in the findings associated with such testing.

It was discovered that certain machine parameters had a higher effect in the surface quality generated during the optimisation process. These parameters were found to be that of Head Speed, Head Pressure and to a certain extent X-Y Spacing. These factors were predominant in all types of analysis (Taguchi, ANOM and Main Effects Plots) investigated in Chapter 6, although the values for optimisation were dependant on the analysis being performed i.e.

optimisation of individual surface parameters produced different optimised levels of machine parameters under investigation.

Whereas the parameters of Precess Angle and Spot Size seemed to have little significance on the optimisation of surface roughness Sa and amplitude parameters Sq, Spk and Sk. Albeit they would almost certainly have an effect if other analysis were performed i.e. material removal volumes where increased precess angle and spot sizes would give a greater volume of material removal as witnessed in the influence function generation using various parameters (Tables 7.3 and 7.4 Chapter 7).

People unfamiliar with the finishing process of orthopaedic implants would be under the impression longer polishing times (governed by smaller X-Y spacing values) would improve surface finish. The results of the Taguchi tests and some background research proved this principle wrong.

Although the lowest X-Y spacing of 0.1 mm did produce the lowest values of Sa as well as the amplitude parameters of Sq, Spk and Sk (Table 6.13 Chapter 6) it was the highest value of 0.4 mm that produced the lowest Svk value. Svk determines the valley size of the surface after Spk has been removed. If the valleys are larger this may lead to added performance in the later stages of the lifetime of the implant. Larger valleys will trap lubricant and leave the implant in a lower friction state of the hydrodynamic regime reducing wear particle generation and entrapping any wear particles already generated reducing the risk of failures from aseptic loosening.

Further justification of this can be found in research that when polishing or grinding glass and metal materials used in the optics industry increasing processing time induces high and mid spatial frequencies on to the surface effectively decreasing the surface quality rather than improving it. Such an effect on the surfaces function was witnessed by Retherford et al (2001) [306] in the performance of calcium fluoride (CaF₂) as optics in eximer lasers and steeper lenses. It is certainly possible that this will affect the wear performance of implant materials although this is only assumed by the author from the background of Rutherford et al research.

Taking this knowledge into consideration then looking at the optimisation of processing time and the advantages offered from large S_{vk} values the trade off between the percentage of surface improvement of the parameters other than that of S_{vk} is not significant enough and using smaller X-Y spacing values prevails. This is provided that a head speed of 2000 RPM and 1 Bar is used to generate surface quality good enough to maintain the standards and current industrial practice associated with implant manufacture of $S_a < 20\text{nm}$.

Applying a 99.9% confidence level an optimised surface roughness of $S_a \approx 9 \text{ nm}$ could be achieved using a Head Speed of 2000 RPM, Head Pressure of 1 Bar, Precess Angle 0° , X-Y Spacing 0.3mm and spot size of 6 mm. Although the optimal values of the other surface roughness parameters S_q , S_{pk} , S_k and S_{vk} are not obtained using the parameters for the optimised S_a value they showed some similarities. Especially in the cases of Head Speed where higher head speeds produced better results and in Spot Size where smaller spot sizes produced better results.

The smaller spot size is most likely related to the fact that the variance of the spot size over the component differs less hence more uniform material removal is achieved than that of large spot sizes where it is more difficult to control the variance. The Head Speed is almost certainly related to the fact that in almost all machining processes high tool speeds relate to larger material removal hence removal of previous residual scratches and machining marks, leading to improved surface quality.

It may have also been of advantage to analyse surface parameters other than that of those related to amplitude i.e. S_{sk} a measurement of the surface skewness could have shown evidence of residual scratches. S_{al} the autocorrelation length could have been used to determine whether there was evidence of waviness in the surfaces of hybrid process from the Fluidjet pressure variation. Such variation led to the decision not to optimise the Fluidjet process using Taguchi process as the knowledge from the conventional technique showed that pressure was critical and the difficulty of controlling the fluctuation would almost certainly have affected the analysis.

The Taguchi method was of great assistance in indicating optimised parameters but the polishing media used in the testing would not be suitable for polishing of larger components (freeform femoral implants) due to its limited lifetime hence an alternative media solution was required.

Rather than repeat the Taguchi tests with another polishing media the challenge of choosing a suitable media to remove high amounts of material removal at reduced times in an attempt not to induce high spatial frequencies was decided to be a better option with the task also supplementing the corrective polishing process.

Medical Grade 316L Stainless Steel used in the Taguchi testing has been a popular material during the last 30 years of development but the advancement of hard-on-hard bearing materials have turned to metals with higher hardness values. The use of Cobalt Chrome (CoCr) alloys is becoming more popular especially in knee implants. Therefore an investigation of polishing media to achieve fast material removal on a CoCr alloy was performed in the purpose of developing the corrective polishing process from that of optics manufacture to that of femoral knee implants.

9.2 Form Correction of a Freeform Femoral Knee Implant Component

Although prior knowledge of a reaction between Cobalt Chrome and diamond used in single point diamond turning of hard to machine materials was known from research by Paul et al [307]. It was decided that the investigation of a nickel bonded diamond pad produced by KGS would be investigated after its performance was praised by a sales representative from the company. This and also the fact the larger contact of the polishing bonnet and the reduced speeds of a magnitude lower (up to 2000 RPM) in comparison to that of diamond turning up (up to 20000 RPM) would not provoke the increased localised surface temperatures that lead to the chemical aspects of the tool wear in diamond turning.

This assumption was proved wrong when influence functions for use in corrective polishing were generated for analysis of the potential of KGS cloths (Figure 6.19 Chapter 6). The first influence function produce rapid material removal but by the fourth it rapidly deteriorated. Through investigation of the cloths under a scanning electron microscope (SEM) it was evident that the condition of the cloth was provoking the chemical reactions that generated outer valance electron reactions described by Paul et al [307].

The reaction almost certainly involved the nickel bond material as a resin bonded diamond cloth produced positive results when used to polish the pins used in the pin-on-plate wear testing (Table 8.1 Chapter 8) of this thesis. The nickel bonded cloth was used on the pins for a short period of time not to invoke the chemical reactions and the pad was changed on regular intervals hence a good surface finish was achieved for the process when used in collaboration with the resin bonded diamond cloths.

The difference in performance of the nickel bonded cloth to that of the resin bonded cloth could be related to bonding toughness i.e. the resin bond would release the particles quicker than that of the nickel bond. Hence new sharp diamond particles would be revealed through a self sharpening process (Figure 3.6 Chapter 3) whereas the stronger bond of the nickel would created fractures of the diamond and frictional forces that would more likely provoke the chemical reaction inflicting the serious degradation of the cloths performance (Figures 6.16 and 6.17 Chapter 6).

Consultations with other suppliers of various abrasives lead to the trails of non-woven abrasive cloths supplied by Sia Abrasives which were embedded with silicon carbide and alumina oxide particles. Although these cloths produced significantly small variances between influence functions compared to that of the KGS diamond cloths (Figure 6.19 Chapter 6) there elasticity and lack of material removal compared to that of the initial influence functions of the nickel bonded diamond cloth proved their downfall. Non-linear probing required to generate a reliable and predictable influence function produced false values and upon commencement of a corrective polish the cloth was literally torn away from the bonnet upon contact leaving a gap between the surface and pad hence producing no material removal at all.

If a solution for this could have been found the low influence function depth would have increased grinding times substantially therefore the search for a non-diamond fixed abrasive substitute to decrease grinding process times was needed.

With the non predicted underperformance of fixed abrasives it was decided to use a loose abrasive (17 μ m grit silicon) for generation of influence functions. Without a total loss of confidence of fixed abrasives the silicon slurry would be applied through a controlled temperature (25°) delivery system to a pad with zirconium oxide particles embedded in it (37 μ m). This proved to be successful and the influence function generated using the knowledge obtained from the Taguchi testing could be used to generate a corrective polishing run to test the performance of the Zeeko machine in correcting form of a freeform femoral knee implant.

The results were neither of a negative nor of great positive nature with the PV error reduction of 17.5% from 10.78 μ m to 9.17 μ m (Figure 7.14 Chapter 7). The negativity being that the reduction was only witnessed in the central 5mm x 5mm of the maximum 33mm x 18mm measurement restricted by limitations of the Taylor Hobson PGI 1240 due to the stylus gauge range in the Z axis. Z measurement range was exceeded outside the maximum area due to the sharp radius of curvature increase of the freeform femoral knee implant. Although this restriction was in place it could have been resolved using a precision CMM (not available at the time of Corrective Polishing trials) the Talysurf Diamond Stylus Profiler produced a maximum measurement area better than that of a white light interferometer and would not require complicated stitching processes involved with such a non contact measurement principle. Based on such limitations of measurement due to the high radius of curvature the use of an interferometer technique for generation of an error map was almost impossible. The time consumption to measure the same size area of the component would be largely greater as the component would have to be located perfectly to aid stitching of small measurements for an accurate error map to be generated.

The matching of X-Y-Z co-ordinates on the Zeeko Machine to that of the measurements calculated for the form error on the form Talysurf PGI 1240 could have been related to the under performance of the corrective polishing although this should have been kept to a minimum from the anticipation of such a problem leading to the design of a fixture seen in chapter 5 (Figure 5.7).

The fitting technique used to generate the error map could also have caused an effect on the limited PV error reduction although a fitting technique (minimum zone) with a better performance of that of the Zeeko software fitting technique (least squares) was used limiting this error to as small as possible (Section 7.4 Chapter 7).

Another possibility was the freeform nature of the femoral knee component changed the shape of the influence function reducing or increasing material removal outside of the 5mm x 5mm PV improvement area. This was proved correct when tests on sample components with similar shapes to that of the freeform femoral component were used to generate influence functions using identical parameters. The influence function produced various material removal volumes in a trend where increased radius reduced volume due to the tool offset decreasing (movement away from surface) having an effect on the spot size in contact with component (Sample 1 in Tables 7.3 and 7.4 of Chapter 7). Although this was reversed when the precess angle was increased (Sample 2 in Tables 7.3 and 7.4 of Chapter 7) as this had the effect of increased velocity at the contact point which links to head speed (Ranked 1st) being more critical in the Taguchi analysis than that of spot size (Ranked 4th) itself (Table 6.13 Chapter 6).

With a small improvement in PV error from the corrective polishing process another question now arose in the progression of the application of the Zeeko IRP2000 polishing machine for correction of freeform femoral components. This would be is the machine capable of producing the surface finish to that of quality of current industry standards after form correction improvements.

This was achieved by using a series of processes including the development of tooling (Figure 5.8 Chapter 5) and the use of a fluidjet abrasive technique to produce a hybrid process (Section 6.3) implant to overcome problematic areas defined in Chapter 5 (Figure 5.9). Using the technique a surface quality of unfiltered Sa = 28.24 nm was achieved which was better than a equivalent industrial femoral component which had an unfiltered Sa value = 38.22 nm as seen in Figure 7.13 (Chapter 7).

9.3 Wear Performance of Zeeko Polished Implant Materials

Wear performance testing and analysis techniques (Tables 4.8 and 4.9 Chapter 4) of Zeeko polished implant materials were deemed a valid way of testing whether or not the wear produced by the manufacturing process of the bearing surfaces would perform better than that of current manufacturing processes.

Two tests were performed a multidirectional pin-on-plate test (Figure 8.1 Chapter 8) to analyse the performance of cobalt chrome pins polished by the Zeeko machine compared to those prepared to industrial standard articulating against UHMWPE in order to test one of most commonly used bearing surface combinations used in knee implants. The second test involved a modified test (Figure 8.11 Chapter 8) for reduction of testing times and preparation of material samples was used to analyse the performance of Zeeko pre-polished cobalt chrome DLC coated CoCr to improve wear performance.

Addressing the comparison of the Zeeko polished CoCr pins to that conventional hand polished pins outperformed hand polished pins in comparison of weight loss of the UHMWPE (Figure 8.6 Chapter 8). This is most likely related to the improved surface roughness and form correction of the Zeeko polished pins producing lower friction forces which produced lower average penetration (0.485mm to 0.586mm) and visual creep of the UHMWPE bearing surfaces after 2 million cycles (Figures 8.7 and 8.8 Chapter 8). The modified pin on plate-test compared two methods of wear measurement one of a visual technique and one of interferometer technique and the results showed no significant differences with a $P < 0.05$ returned from a student t-test of the average wear results obtained.

CHAPTER 10: CONCLUSIONS

10 CONCLUSIONS

At the beginning of the studies it was hypothesised that the Zeeko IRP200 Polishing Machine may be capable of improving surface quality and form of replacement knee implant components especially in the development of hard on hard bearing surfaces associated with reduced levels of wear particles that cause premature failures of implant components.

Development of the polishing process through Taguchi trials and statistical analysis techniques optimised machine parameters for 316L Stainless Steel using polishing media that was successful in the optics industry (CR39 Glass Mineral Smoothing Cloth 12 μ m grit). The surface parameter of Sa was optimised in conjunction with other amplitude parameters (Sq, Spk, Sk and Svk) that can be used to assess the performance of implant materials. An optimum Sa value of 9 nm was achieved with dominant factors being Highest Head Speed of 2000RPM and Head Pressures above 1 Bar.

The knowledge obtained from the Taguchi Analysis was applied to the development of influence function generation for predictive and repeatable material removal used to assist the corrective polishing process. Cobalt Chrome (CoCr) alloy and Titanium implant materials were used during the testing of a series of polishing consumables from fixed abrasives to loose abrasives. Identification of anticipated problems led to the development of a non-standard polishing tool, hybrid polishing technique (combination of classic bonnet tool and fluidjet polishing) and special fixturing to overcome problematic areas of a CoCr freeform femoral knee implant. The hard work prevailed when Peak to Valley error reduction of 17.5% was achieved through the corrective polishing process adapted from manufacture of precision optics.

Wear performance of Zeeko polished versus conventional hand polished pins using pin on plate testing produced positive results in the fact that the Zeeko polished pins produced less wear and penetration/creep of the UHMWPE bearing plate than that of the conventional hand polishing technique.

Further wear testing of a hard on hard combination of DLC coated CoCr articulated against uncoated CoCr produced results similar to that seen in other bearing combinations (metal-on-UHMWPE, ceramic-on-UHMWPE and uncoated metal on metal etc.)

The correlation of all the findings certainly indicates that the Zeeko IRP 200 7-Axis CNC polishing machine is capable of being used for form correction and surface improvements that can help generate better conformance of bearing components in advance of Hard-on-Hard combinations in the fight to further reduce wear rates and hence increase lifetimes of knee implants in the future.

The majority of this thesis was new research and the positive findings most certainly provide evidence that a continuation of the work would provide the ultimate answer i.e. full simulator testing to ISO standards to mimic natural joint movement during wear testing. This together with further understanding of the reactions between materials and polishing processes could lead to modelling the process to obtain optimised results on current and new materials available for the manufacture of knee implants.

The concern of time issues can be raised in industry although a definitive answer to the time required to corrective polish a femoral knee implant component was not determined it would be beneficial to work with orthopaedic implant manufactures to obtain such knowledge. With this in place a drive towards the Zeeko machine being used in future manufacturing processes in a fast developing orthopaedics market especially in the case of freeform geometries (knees, shoulders and finger joints). Such components are currently challenging even the most skilful operatives to control not so much surface finish but most definitely form by current manufacturing processes of manual and semi automatic buffing plants.

11 FUTURE WORK

Indications of future work almost certainly point towards better performance in the corrective polishing process.

The following areas should be addressed in future work: -

- Analysis of models by other researchers of material removal formulas to either find a suitable model or develop a current model that is more suited to the influence function generation on freeform femoral implant surfaces
- Investigation of other surface roughness parameters that may affect the performance of implant materials. Then use Taguchi testing and statistical analysis techniques to optimise these parameters in surface generation on the Zeeko IRP200 machine.
- Form correction and surface finish of full knee implant components using the Zeeko IRP200 machine. Then using a full joint simulator test to fully determine the hypothesis related to this thesis.
- Investigate the use of surface texture generation using fluidjet polishing for enhancing the functionality and performance of bio-materials other than that of orthopaedic implant bearing surfaces, i.e. bone to implant material integration for cement less fixation, cell cultivation and drug delivery etc.
- Develop processes and tooling for specific polishing applications to further enhancing the manufacture of freeform surfaces using the Zeeko IRP200 7 Axis CNC polishing machine.

REFERENCES

- [1] McGloughlin T.M., Kavanagh A.G.; Wear of ultra-high molecular weight polyethylene (UHMWPE) in total knee prostheses: A review of key influences, Proceedings of the Institution of Mechanical Engineers, Part H: Journal of Engineering in Medicine 2000 214: 349
- [2] McCann L. et al; An investigation of the effect of conformity of knee hemiarthroplasty designs on contact stress, friction and degeneration of articular cartilage: A tribological study, Journal of Biomechanics 42 (2009) 1326–1331
- [3] Osteoarthritis: National clinical guideline for care and management in adults, Developed by the National Collaborating Centre for Chronic Conditions at the Royal College of Physicians
- [4] <http://www.patient.co.uk/health/Osteoarthritis.htm>
- [5] Brandt, K.D.; Dieppe P.; Radin E.; Etiopathogenesis of Osteoarthritis. Med Clin N Am 93 (1): 1–24, 2008
- [6] Siddiqui F.H, Laborde J.M.; Osteoarthritis, <http://emedicine.medscape.com/article/1270114-Overview> (2008-09-12)
- [7] Pictures Courtesy of ADAMS quality.
- [8] Oiestad B.E. et al; Knee Osteoarthritis After Anterior Cruciate Ligament Injury-A Systematic Review, Am J Sports Med July 2009 vol. 37 no. 7 1434-1443
- [9] Burner T.W., Rosenthal A.K.; Diabetes and Rheumatic Diseases, Current Opinion in Rheumatology: January 2009 - Volume 21 - Issue 1 - p 50-54
- [10] Kaandorp C.J.E. et al; Risk factors for septic arthritis in patients with joint disease, Arthritis & Rheumatism, Volume 38 Issue 12, Pages 1819 – 1825
- [11] Sharma L. et al; The mechanism of the effect of obesity in knee osteoarthritis: The mediating role of malalignment, Arthritis & Rheumatism, Volume 43 Issue 3, Pages 568-575
- [12] National Joint Registry for England and Wales 4th Annual Report, ISSN 1753-9382
- [13] <http://news.bbc.co.uk/2/hi/health/3461585.stm>
- [14] <http://www.lawyersandsettlements.com/features/hip-knee-breaking.html>
- [15] Abu-Amer Y. et al.; Aseptic loosening of total joint replacements: mechanisms underlying osteolysis and potential therapies, Arthritis Research & Therapy 2007, 9 (Suppl 1):S6

- [16] R. M. Atkins, Bone Membrane Interface in Aseptic Loosening of Total Joint Arthroplasties, *The Journal of Arthroplasty* Vol. 12 No. 4 1997
- [17] Wimhurst J.A. et al; (ii) The pathogenesis of aseptic loosening, *Current Orthopaedics* (2002) 16, pp 407-410
- [18] Blumenfeld T.J., Bargar W.L., Early Aseptic Loosening of a Modern Acetabular Component Secondary to a Change in Manufacturing, *The Journal of Arthroplasty* Volume 21, Issue 5, August 2006, Pages 689-695
- [19] Miller M.D. et al; Early Aseptic Loosening of a Total Knee Arthroplasty Due to Gore-Tex Particle-Induced Osteolysis, *The Journal of Arthroplasty* Volume 21, Issue 5, August 2006, Pages 765-770
- [20] Reina R.J. et al.; Fixation and Osteolysis in Plasma-Sprayed Hemispherical Cups With Hybrid Total Hip Arthroplasty, *The Journal of Arthroplasty* Volume 22, Issue 4, June 2007, Pages 531- 534
- [21] Agarwal S., Osteolysis—basic science, incidence and diagnosis, *Current Orthopaedics* Volume 18, Issue 3, June 2004, Pages 220-231
- [22] http://www.totaljoints.info/Exp_osteolys_model.jpg
- [23] <http://liveonearth.livejournal.com/514105.html>
- [24] Koseki H. et al; Surface-engineered metal-on-metal bearings improve the friction and wear properties of local area contact in total joint arthroplasty, *Surface & Coatings Technology* 202 (2008), pp.4775–4779
- [25] Essner A. et al; Hip simulator wear comparison of metal-on-metal, ceramic-on-ceramic and crosslinked UHMWPE bearings, *Wear* 259 (2005) 992–995
- [26] Rosneck J. et al.; A Rare Complication of Ceramic-on-Ceramic Bearings in Total Hip Arthroplasty, *The Journal of Arthroplasty* Volume 23, Issue 2, February 2008, Pages 311-313
- [27] Blunt L., Thomas T.R., Wear ranking of hard on hard bearings for prosthetic hip joints *Wear* 257 (2004) 1208–1212
- [28] Beaulé P. E. et al; Bearing Surface: Metal on Metal, *Surgical Treatment of Hip Arthritis (First Edition)*, 2009, Pages 468-477
- [29] España F. A. et al; Design and fabrication of CoCrMo alloy based novel structures for load bearing implants using laser engineered net shaping Original Research Article *Materials Science and Engineering: C*, Volume 30, Issue 1, 1 January 2010, Pages 50-57
- [30] Mertl P. et al; Large diameter head metal-on-metal bearings total hip arthroplasty: Preliminary results Original Research Article *Orthopaedics & Traumatology: Surgery & Research*, Volume 96, Issue 1, February 2010, Pages 14-20

- [31] Joyce T. J. et al; A study of the wear of explanted metal-on-metal resurfacing hip prostheses Original Research Article Tribology International, Volume 44, Issue 5, May 2011, Pages 517-522
- [32] Hayter C. L. et al; Imaging of Metal-On-Metal Hip Resurfacing, Orthopedic Clinics of North America, Volume 42, Issue 2, April 2011, Pages 195-205
- [33] Landry ME et al; Morphology of in vitro generated ultrahigh molecular weight polyethylene wear particles as a function of contact conditions and material parameters, J Biomed Mater Res. 1999 Spring;48(1):61-9.
- [34] Lancaster J.G. et al; The wear of ultra-high molecular weight polyethylene sliding on metallic and ceramic counterfaces representative of current femoral surfaces in joint replacement, Proc Inst Mech Eng H. 1997;211(1):17-24
- [35] Galvin A. et al; Wear of crosslinked polyethylene under different tribological conditions, J Mater Sci Mater Med. 2006 Mar;17(3):235-43.
- [36] Price A. J. et al; Ten-year in vivo wear measurement of a fully congruent mobile bearing unicompartmental knee arthroplasty. J Bone Joint Surg (Br) 2005; 87 (11): 1493-7.
- [37] Wang F. C. et al; Lubrication and friction prediction in metal-on-metal hip implants, Phys. Med. Biol. 53 (2008) 1277–1293
- [38] Harrysson O.L.A. et al.; Direct metal fabrication of titanium implants with tailored materials and mechanical properties using electron beam melting technology Materials Science and Engineering: C Volume 28, Issue 3, 1 April 2008, Pages 366-373
- [39] Mitsuishi M. et al.; Determination of the Machining Characteristics of a Biomaterial Using a Machine Tool Designed for Total Knee Arthroplasty, CIRP Annals - Manufacturing Technology Volume 53, Issue 1, 2004, Pages 107-112
- [40] Novokov N.W. et al.; Finish diamond machining of ceramic femoral heads, Int J Adv Manuf Technol (2005) 25: 244–247
- [41] DeFrate L.E. et al; The 6 Degrees of Freedom Kinematics of the Knee After Anterior Cruciate Ligament Deficiency : An In-Vivo Imaging Analysis, Am J Sports Med 2006 34: 1240
- [42] Kurtz S.M.; UHMWPE Biomaterials Handbook, Second Edition: Ultra High Molecular Weight Polyethylene in Total Joint Replacement and Medical Devices, ISBN: 012374721X, pp385
- [43] Besier T.F. et al; Knee muscle forces during walking and running in patella femoral pain patients and pain-free controls, Journal of Biomechanics 42(2009)898–905

THE APPLICATION OF ZEEKO POLISHING TECHNOLOGY TO FREEFORM
FEMORAL KNEE REPLACEMENT COMPONENT MANUFACTURE

- [44] Henriksen M. et al; Increased joint loads during walking – A consequence of pain relief in knee osteoarthritis, *The Knee* 13 (2006) 445–450
- [45] Baliunas A. J. et al; Increased knee joint loads during walking are present in subjects with knee osteoarthritis, *Osteoarthritis and Cartilage* (2002) 10, 573–579
- [46] Kuster M.S. et al; Joint load considerations in total knee replacement, *J Bone Joint Surg [Br]* 1997; 79-B:109-13.
- [47] Costigan P.A. et al; Knee and hip kinetics during normal stair climbing, *Gait & Posture* Volume 16, Issue 1, August 2002, Pages 31-37
- [48] Christina K. and Cavanagh P.R.; Ground reaction forces and frictional demands during stair descent: effects of age and illumination, *Gait and Posture* 15 (2002) 153–158
- [49] Nisell R. and Ericsson M.; Patellar forces during isokinetic knee extension, *Clinical Biomechanics* Volume 7, Issue 2, May 1992, Pages 104-108
- [50] Rodosky, M.W et al (1989) The influence of chair height on lower limb mechanics during rising. *Journal of Orthopaedic Research* 7, 266-271.
- [51] *Biomechanics and Motor Control of Human Movement*, Second Edition. David A. Winter. Published by John Wiley & Sons, New York, 1990
- [52] <http://me.queensu.ca/people/deluzio/BiomedicalDataAnalysisTechniques.php>
- [53] Ishii et al; Gait analysis after total knee arthroplasty. Comparison of posterior cruciate retention and substitution, *J Orthop Sci* (1998) 3:310-317
- [54] http://www.totaljoints.info/Prehistory_GluckPean.htm
- [55] Claes L. et al.; Initial stability of fully and partially cemented femoral stems, *Clinical Biomechanics* 15 (2000) 750-755
- [56] Donkerwolckel M. et al.; Tissues and bone adhesives -historical aspects *Biomaterials* 19 (1998) 1461-1466
- [57] Lee T.Q. et al; Effects of screw types in cementless fixation of tibial tray implants: stability and strength assessment, *Clinical Biomechanics* 14 (1999) 258-264
- [58] Au A.G. et al.; A parametric analysis of fixation post shape in tibial knee prostheses, *Medical Engineering & Physics* 27 (2005) 123–134
- [59] Chockalingamu S., Scott G.; The outcome of cemented vs. cementless fixation of a femoral component in total knee replacement_TKR/with the identification of radiological signs for the prediction of failure, *The Knee* 7_2000.233]238
- [60] Kenneth A, Gustke, MD; Preoperative Planning for Revision Total Knee Arthroplasty. Avoiding Chaos, *The Journal of Arthroplasty* Vol. 20 No. 4 Suppl. 2 2005

THE APPLICATION OF ZEEKO POLISHING TECHNOLOGY TO FREEFORM
FEMORAL KNEE REPLACEMENT COMPONENT MANUFACTURE

- [61] Craig M. et al.; Component Asymmetry in Simultaneous Bilateral Total Knee Arthroplasty, *The Journal of Arthroplasty* Vol. 21 No. 5 2006
- [62] William D. Bugbee, MD et al., Does Implant Selection Affect Outcome of Revision Knee Arthroplasty? *The Journal of Arthroplasty* Vol. 16 No. 5 2001
- [63] Kalpana S. Katti, Biomaterials in total joint replacement, *Colloids and Surfaces B: Biointerfaces* 39 (2004) 133–142
- [64] H.F. El-Sheikh et al.; Material selection in the design of the femoral component of cemented total hip replacement, *Journal of Materials Processing Technology* 122 (2002) 309–317
- [65] David E. Hockman et al., Augments and Allografts in Revision Total Knee Arthroplasty Usage and Outcome Using One Modular Revision Prosthesis, *The Journal of Arthroplasty* Vol. 20 No. 1 2005
- [66] Young-Hoo Kim, MD, Jun-Shik Kim, MD; Revision Hip Arthroplasty Using Strut Allografts and Fully Porous-Coated Stems, *The Journal of Arthroplasty* Vol. 20 No. 4 2005
- [67] Ian McDermott, N.P. Thomas T; Tendon allografts in the knee, *The Knee* 12 (2005) 401–404
- [68] Shawn M. Brubaker DO et al; Treatment Options and Allograft Use in Revision Total Hip Arthroplasty The Acetabulum, *The Journal of Arthroplasty* Vol. 22 No. 7 Suppl. 3 2007
- [69] Viceconti M. et al; Primary stability of an anatomical cementless hip stem: A statistical analysis, *Journal of Biomechanics* 39 (2006) 1169–1179
- [70] Abdul-Kadir M.R et al; Finite element modelling of primary hip stem stability: The effect of interference fit, *Journal of Biomechanics* 41 (2008) 587–594
- [71] John R. Green et al; The Effect of Bone Compaction on Early Fixation of Porous-Coated Implants, *The Journal of Arthroplasty* Vol. 14 No. 1 1999
- [72] A. Grill; Diamond-like carbon coatings as biocompatible materials—an overview, *Diamond and Related Materials* 12 (2003) 166–170
- [73] Vincenzo Sollazzo et al; Zirconium oxide coating improves implant osseointegration in vivo, *dental materials* 24 (2008) 357–361
- [74] Breton P. et al; Biocompatible poly(methylidene malonate)-made materials for pharmaceutical and biomedical applications, *European Journal of Pharmaceutics and Biopharmaceutics* 68 (2008) 479–495
- [75] Roy M. et al; Laser processing of bioactive tricalcium phosphate coating on titanium for load-bearing implants, *Acta Biomaterialia* 4 (2008) 324–333

THE APPLICATION OF ZEEKO POLISHING TECHNOLOGY TO FREEFORM
FEMORAL KNEE REPLACEMENT COMPONENT MANUFACTURE

- [76] Frosch K-H. et al; Stem cell-coated titanium implants for the partial joint resurfacing of the knee, *Biomaterials* 27 (2006) 2542–2549
- [77] Katti K.S.; Biomaterials in total joint replacement, *Colloids and Surfaces B: Biointerfaces* 39 (2004) 133–142
- [78] Eynon-Lewis N. J. et al; Themistocles Gluck: an unrecognised genius, *BMJ* VOLUME 305 19-26 DECEMBER 1992, pp1534-1536
- [79] Walldius B. Arthroplasty of the knee using acrylic prosthesis. *Acta Orthop Scand* 1953; 23:121
- [80] Walldius B. Arthroplasty of the knee using an endoprosthesis. *Acta Orthop Scand* 1957; (Suppl): 24;
- [81] Walldius B. Arthroplasty of the knee using an endoprosthesis. *Acta Orthop Scand* 1960; 30:137
- [82] Walldius B. Arthroplasty of the knee using an endoprosthesis. *Sicot XI Congress, Mexico*; 447)
- [83] Burrows HJ. Major prosthetic replacement of knees: lessons learnt in 17 years *J Bone Joint Surg* 1968; 50B:225—22
- [84] Blundell-Jones C. Arthroplasty of the knee. *Mod Trends Orthop* 1972; 8:210
- [85] Gunston F.H.; Polycentric Knee Arthroplasty, *J Bone Joint Surg Br* Gunston 53-B (2): 272
- [86] Shetty A.A. et al; The evolution of total knee arthroplasty. Part II: the hinged knee replacement and the semi-constrained knee replacement, *Current Orthopaedics* (2003) 17, 403—407
- [87] <http://www.aori.org/tka/tkawhat.htm#history>
- [88] http://www.drlikover.com/oxford_knee.php
- [89] J Goodfellow et al, *Unicompartmental Athroplasty with the Oxford Knee*, Oxford University Press, May 2006
- [90] <http://i40.tinypic.com/2dqvhps.jpg>
- [91] Hyldahl H. C., MD et al; Does Metal Backing Improve Fixation of Tibial Component in Unicondylar Knee Arthroplasty? A Randomized Radiostereometric Analysis, *The Journal of Arthroplasty* Vol. 16 No. 2 2001
- [92] Regnér L, MD et al; Ceramic Coating Improves Tibial Component Fixation in Total Knee Arthroplasty, *The Journal of Arthroplasty* Vol. 13 No. 8 1998

THE APPLICATION OF ZEEKO POLISHING TECHNOLOGY TO FREEFORM
FEMORAL KNEE REPLACEMENT COMPONENT MANUFACTURE

- [93] Liau J-J. et al; The effect of malalignment on stresses in polyethylene component of total knee prostheses – a finite element analysis, *Clinical Biomechanics* 17 (2002) 140–146
- [94] Essner A. et al; The effect of sagittal conformity on knee wear, *Wear* 255 (2003) 1085–1092
- [95] Buechel, F.F. et al. “Twenty-year Evaluation of Meniscal bearing and rotating platform knee replacements.” *Clinical Orthopaedics & related Research*, 388 July 2001:41-50.
- [96] <http://www.endotec.com/Knee-Primary.htm>
- [97] National Joint Registry for England and Wales 6th Annual Report 2009, 6th Annual Report, ISSN1753-9374, www.njrcentre.org.uk
- [98] Sharkey P.F. et al; Insall Award Paper : Why Are Total Knee Arthroplasties Failing Today? *Clinical Orthopaedics And Related Research*, Number 404, November 2002, pp. 7–13
- [98] <http://www.zimmer.com/z/ctl/op/global/action/1/id/9387/template/MP/prcat/M3 /prod/y>
- [100] Savarino L. et al; Is wear debris responsible for failure in alumina-on-alumina implants? Clinical, histological and laboratory investigations of 30 revision cases with a median follow-up time of 8 years, *Acta Orthopaedica*, Volume 80, Issue 2 April 2009 , pages 162 – 167
- [101] http://www.totaljoints.info/TH_loose_DETAILS.htm
- [102] <http://radiology.usc.edu/knee/loosenin.htm>
- [103] Fehring TK, Valadie AL: Knee instability after total knee arthroplasty. *Clin Orthop* 299:157–162, 1994
- [104] Mitts K et al; Instability after total knee arthroplasty with the Miller-Galante II total knee: 5 to 7 year follow-up. *J Arthroplasty* 16:422–427, 2001
- [105] http://www.totaljoints.info/Instable_TK1.jpg
- [106] Koo K.H. ; Impregnation of vancomycin, gentamicin, and cefotaxime in a cement spacer for two-stage cementless reconstruction in infected total hip arthroplasty, *J Arthroplasty*. 2001 Oct;16(7):882-92
- [107] Letaif O.B. et al; Functional comparison between septic and aseptic knee arthroplasty review, *Acta Ortopédica Brasileira*, vol.17 no.3 São Paulo 2009, Print version ISSN 1413-7852
- [108] http://www.pansportmedical.ro/english/medical_imaging/Soft-tissues_changes_after_%20ACL_graft.html

THE APPLICATION OF ZEEKO POLISHING TECHNOLOGY TO FREEFORM
FEMORAL KNEE REPLACEMENT COMPONENT MANUFACTURE

- [109] Lotke P.A., Eckler M.L.; Influence of positioning of prosthesis in total knee replacement, *J Bone Joint Surg Am.* 1977;59:77-79.
- [110] Interventional Procedure Guidance (IPG) 345: Mini-incision surgery for total knee replacement, National Institute for Health and Clinical Excellence, ISBN 978-1-84936-247-4
- [111] Haaker R.G, Computer-Assisted Navigation Increases Precision of Component Placement in Total Knee Arthroplasty, *Clinical Orthopaedics and Related Research*: April 2005, Volume 433, pp 152-159
- [112] Nortmore-Ball M.D. et al; Sub-clinical rotational malposition: a potential cause of catastrophic wear in conforming condylar knee arthroplasty
- [113] <http://www.depuy.com/about-depuy/news-and-press/detail?tid=&year=&page=0>
- [114] Figueiredo-Pina C.G. et al; Understanding the differences between the wear of metal-on-metal and ceramic-on-metal total hip replacements, *Proceedings of the Institution of Mechanical Engineers, Part H: Journal of Engineering in Medicine* March 1, 2008 vol. 222 no. 3 285-296
- [115] Huiskes R. and Chao E. Y. S.; A survey of finite element analysis in orthopaedic biomechanics: The first decade, *J. Biomechanics*, Vol 16. No. 6 pp 385-409, 1983
- [116] I. Gibson, Editor, *Advanced Manufacturing Technology for Medical Applications*, J. Wiley & sons Ltd., London (2005).
- [117] Li B. et al; Combustion synthesis of CoCrMo orthopedic implant alloys: microstructure and properties, *Mat Res Innovat* (2003) 7:245–252
- [118] Short A. et al; A novel method for in vivo knee prosthesis wear measurement, *Journal of Biomechanics* 38 (2005) 315–322
- [119] Semlitsch, M. and Willert, H.-G. Clinical wear behaviour of ultra-high molecular weight polyethylene cups paired with metal and ceramic ball heads in comparison to metal-metal pairings of hip joint replacements. *Proc. Instn Mech. Engrs, Part H*: 1997, 211, 73–88.
- [120] McBryde C. W. et al; The Influence of Head Size and Sex on the Outcome of Birmingham Hip Resurfacing, *The Journal of Bone and Joint Surgery (American)*. 2010;92:105-112
- [121] Clarke M. T. et al; Levels of metal ions after small-and large diameter metal-on-metal hip arthroplasty, Vol. 85-B, No. 6, August 2003
- [122] <http://depuyhiprecall-info.com/2011/05/depuy-asr-pinnacle-hip-complications/>
- [123] Clarke I.C. et al; Ultra-low wear rates for rigid-on-rigid bearings in total hip replacements, *Proceedings of the Institution of Mechanical Engineers, Part H: Journal of Engineering in Medicine* 2000 214: 331

THE APPLICATION OF ZEEKO POLISHING TECHNOLOGY TO FREEFORM
FEMORAL KNEE REPLACEMENT COMPONENT MANUFACTURE

- [124] D'Antonio J. and Sutton K.; Ceramic Materials as Bearing Surfaces for Total Hip Arthroplasty, *J Am Acad Orthop Surg*.2009; 17: 63-68
- [125] Lawn B. Fracture of brittle solids. Cambridge solid state science series. 2nd ed. UK: Cambridge university press, 1993, p. 378.
- [126] Weisse B. et al; Failure analysis of in vivo fractured ceramic femoral heads, *Engineering Failure Analysis* 16 (2009) 1188–1194
- [127] Muchtar, A. and Lim, L. C.; Indentation fracture toughness of high purity sub-micron alumina. *Acta Mater.*, 1998, 46, 1683–1690.
- [128] Roy R.S. et al; Improved sliding wear-resistance of alumina with sub-micron grain size: A comparison with coarser grained material, *Journal of the European Ceramic Society* 27 (2007) 4737–4743
- [129] Sedel L. and Raould A.; Engineering aspect of alumina on alumina hip prosthesis, *Proceedings of the Institution of Mechanical Engineers, Part H: Journal of Engineering in Medicine*, olume 221, Number 1, 2007
- [130] Cales B. and Stefani Y.; Mechanical properties and surface analysis of retrieved zirconia hip joint heads after an implantation time of two to three years, *Journal of Materials Science: Materials in Medicine*, Volume 5, Numbers 6-7 / June, 1994,pp 376-380
- [131] Kumar P. et al; Low wear rate of UHMWPE against zirconia ceramic (Y-PSZ) in comparison to alumina ceramic and SUS 316L alloy, *Journal of Biomedical Materials Research*, Volume 25 Issue 7, Pages 813 - 828
- [132] Allain J. et al; Poor eight-year survival of cemented zirconia-polyethylene total hip replacements, *J Bone Joint Surg Br*. 1999 Sep;81(5):835-42
- [133] Tiefenbach A. et al; The use of impedance spectroscopy in damage detection in tetragonal zirconia polycrystals (TZP), *Ceramics International* 26 (2000), pp745-751
- [134] Oonishi H. et al; PE wear in ceramic/PE bearing surface in total knee arthroplasty: Clinical experiences of more than 24 years, *Bioceramics and Alternative Bearings in Joint Arthroplasty 11th BIOLOX® Symposium Rome*, June 30 – July 1, 2006 Proceedings, *Ceramics in Orthopaedics Session 4.1*, pp101-110
- [135] Yasuda K. et al; Low friction total knee arthroplasty with the alumina ceramic condylar prosthesis. *Bull Hosp Jt Dis*. 1993 Summer;53(2):15-21.
- [136] Hernigou Ph. Et al; Oxinium, a new alternative femoral bearing surface option for hip replacement, *Eur J Orthop Surg Traumatol* (2007) 17:243–246
- [137] Manilli M. et al; Profix-Oxniium Total Knee Replacement: Results of 110 Cases, *Journal of Bone and Joint Surgery - British Volume*, Vol 90-B, Issue SUPP_I, 174.

THE APPLICATION OF ZEEKO POLISHING TECHNOLOGY TO FREEFORM FEMORAL KNEE REPLACEMENT COMPONENT MANUFACTURE

- [138] Maccji F.; Alumina Ceramics in Joint Prosthesis, Journal of Bone and Joint Surgery - British Volume, Vol 87-B, Issue SUPP_I, 62-63.
- [139] Yoo J.J. et al; J Bone Joint Surg Am. 2005 Mar;87(3):530-5. Alumina-on-alumina total hip arthroplasty. A five-year minimum follow-up study.
- [140] Keurentjes J. C. et al; High Incidence of Squeaking in THAs with Alumina Ceramic-on-ceramic Bearings, Clin Orthop Relat Res. 2008 June; 466(6): 1438–1443.
- [141] Banchet, V., Fridrici, V., Abry, J.C., Kapsa, Ph., Short Communication: Wear and friction characterization of materials for hip prosthesis, Wear, Vol. 263, pp. 1066-1071 (2007)
- [142] Scholes, S.C., Unsworth, A., Hall, R.M., Scott, R., The Effects of Material Combination and Lubricant on the Friction of Total Hip Prostheses, Wear, Vol. 241, pp. 209-213 (2000)
- [143] Hall, R.M., Unsworth A., Review: Friction in Hip Prostheses, Biomaterials, Vol.18, pp. 1017-1025 (1997)
- [144] Friction Center Coefficient Database at Southern Illinois University 2005
- [145] http://www.ceramtec.com/index/divisions/medical_products/medical_professionals/products/knee_joint_components/biolox_delta_ceramic_knee_joint_components/04034,0125,0343,4024.php
- [146] Taeger G et al; Comparison of diamond-like carbon and alumina oxide articulating with polyethylene in total hip arthroplasty. Mat-wiss u Werkstofftech 2003;34:1094–1100.
- [147] Hauert R.; A review of modified DLC coatings for biological applications , Diamond and Related Materials, Volume 12, Issues 3-7, March-July 2003, Pages 583-589
- [148] Santos C.B. et al; Wear–Corrosion Resistance of DLC/CoCrMo System for Medical Implants with Different Surface Finishing, Tribol Lett (2010) 37:251–259
- [149] Alakoski E. et al; Load-Bearing Biomedical Applications of Diamond-Like Carbon Coatings- Current Status, The Open Orthopaedics Journal, 2008, 2, 43-50
- [150] Roy M.E. et al; Diamond-like carbon coatings enhance the hardness and resilience of bearing surfaces for use in joint arthroplasty, European Journal of cardiovascular Nursing Volume 6, Issue 4, Pages 1619-1624 (April 2010)
- [151] Roy R.K., Lee K-R.; Biomedical Applications of Diamond-Like Carbon Coatings:A Review, Journal of Biomedical Materials Research Part B: Applied Biomaterials, 2007 Oct;83(1):72-84.

THE APPLICATION OF ZEEKO POLISHING TECHNOLOGY TO FREEFORM FEMORAL KNEE REPLACEMENT COMPONENT MANUFACTURE

- [152] Thorwarth G. et al; Tribological behaviour of DLC-coated articulating joint implants, *Acta Biomaterialia* 6 (2010) 2335–2341
- [153] Thorwarth K. et al; Failure Mechanisms of DLC Coated Joint Replacements, *European Cells and Materials* Vol. 19. Suppl. 2, 2010 (page 24) ISSN 1473-2262
- [154] Heyse T.J. et al (2010); Retrieval Analysis of Femoral Zirconium Components in Total Knee Arthroplasty: Preliminary Results, *The Knee*, Article in Press, doi:10.1016/j.arth.2009.11.024
- [155] Heyse T.J. et al (2010); Matched-pair total knee arthroplasty retrieval analysis: Oxidized zirconium vs. CoCrMo, *The Knee*, Article in Press, doi:10.1016/j.knee.2010.08.011
- [156] Scholes S. C. , Unsworth A., Wear studies on the likely performance of CFR-PEEK/CoCrMo for use as artificial joint bearing materials, *J Mater Sci: Mater Med* (2009) 20:163–170
- [157] Gao L.M. et al; The effect of aspherical geometry and surface texturing on the elastohydrodynamic lubrication of metal-on-metal hip prostheses under physiological loading and motions, *Proc. IMechE* Vol. 224 Part C: J. Mechanical Engineering Science, pp 2627-2636.
- [158] <http://machinedesign.com/article/avoiding-stick-slip-chatter-in-low-speed-bearings-0410>
- [159] Stribeck, R. (1901), Kugellager für beliebige Belastungen (Ball Bearings for any Stress), *Zeitschrift des Vereins Deutscher Ingenieure* 45
- [160] <http://arnold-sommerfeld.co.tv/#Bibliography>
- [161] Smith S.L. et al; The lubrication of metal-on-metal total hip joints: a slide down the Stribeck curve, *Proc Instn Mech Engrs* Vol 215 Part J, pp 483-493
- [162] Murakami T. et al; The Adaptive Multimode Lubrication in Knee Prostheses with Artificial Cartilage during Walking , [Tribology Series, Volume 32](#), 1997, Pages 371-382
- [163] British Standards Institution; ISO 7207-1:2007 Implants for surgery -components for partial and total knee joint prostheses -- Part 1: Classification, definitions and designation of dimensions, Milton Keynes, BSI
- [164] British Standards Institution; ISO 7207-2:1998 Implants for surgery -Components for partial and total knee joint prostheses -- Part 2: Articulating surfaces made of metal, ceramic and plastics materials, Milton Keynes, BSI
- [165] Zhang H. et al; Influence of femoral stem surface finish on the apparent static shear strength at the stem–cement interface; *journal of the mechanical behaviour of biomedical materials* 1 (2008) 96-104

- [166] J.L. Tipper et al.; MINI-SYMPOSIUM: HIP REPLACEMENT (iv) The science of metal-on-metal articulation; *Current Orthopaedics* (2005) 19, 280–287
- [167] Cui F.Z., Li D.J.; A review of investigations on biocompatibility of diamond-like carbon and carbon nitride films; *Surface and Coatings Technology* 131 _2000. 481-487
- [168] Wall A., Heffron P. (Symmetry Medical Incorporated); Forgings and Orthopaedic Implants, BONEZONE, Summer 2004
- [169] <http://www.onlinetmd.com/tmd-0610-grinding-knee-implants-orthopedic-instruments.aspx>
- [170] <http://www.siemens.com/press/en/presspicture/?press=/en/presspicture/pictures-photonews/2010/pn201003.php>
- [171] Arola D.D. et al; Abrasive waterjet peening: A new method of surface preparation for metal orthopaedic implants, *Journal of Biomedical Materials Research* 20000901 53(5): 11
- [172] Lu X., Leng Y.; Electrochemical micromachining of titanium surfaces for biomedical applications, *Journal of Materials Processing Technology* 169 (2005) 173–178
- [173] Puijpe J.Cl.; Surface Treatments of Titanium Implants, *European Cells and Materials* Vol. 5. Suppl. 1, 2003 (pages 32-33)
- [174] http://www.ceramicindustry.com/CDA/Articles/Cover_Story/BNP_GUID_9-5-2006_A_10000000000000268338
- [175] Simpson D.J.; The effect of bearing congruency, thickness and alignment on the stresses in unicompartmental knee replacements, *Clinical Biomechanics* 23 (2008) 1148–1157
- [176] Kuster, M.S. et al; The effects of conformity and load in total knee replacement. *Clin. Orthop. Relat. Res.* 2000 (375), 302–312
- [177] British Standards Institution (1990-2003) ; BS 7251 / ISO 7206 Orthopaedic joint prostheses - Part 14: Components for partial and total knee-joint prostheses - Articulating surfaces made of metal, ceramic and plastics materials. Section 3
- [178] Baker B.; Face the future 3D software used to custom-build body parts damaged though injury or disease, *The Engineer* 14-27 July 2008
- [179] Samuels L.E.; *Metallographic Polishing by Mechanical Methods*, 4th Ed. 2003, ASM International, ISBN: 0871707799

THE APPLICATION OF ZEEKO POLISHING TECHNOLOGY TO FREEFORM FEMORAL KNEE REPLACEMENT COMPONENT MANUFACTURE

- [180] Davidson D.A.(Pegco Process Laboratories Inc., Bartlett, N.H., USA); Mass finishing processes, Metal Finishing Volume 99, Supplement 1, January 2001, Pages 110-124
- [181] Saad J.; Automating an encouraging bottom line: Robotics is at the forefront of the move to incorporate more value for metal parts that require buffing and polishing, Metal Finishing Volume 103, Issues 7-8, July-August 2005, Pages 19-24
- [182] Little M.; Eyeing Robotics, Products Finishing 2004, pp46-48
- [183] Bogue R.; Finishing Robots: a review of technologies and applications, Industrial Robot: An International Journal 2009, Volume 36, Issue 1, pp6-12
- [184] <http://www.pfonline.com/articles/pfd0509.html>
- [185] <http://www.odtmag.com/articles/2005/11/implant-manufacturers-robotics-are-finding-common-.php>
- [186] British Standards Institution; BS ISO 6344:1998 Parts 1 -3 Coated Abrasives Grain Size Analysis Parts
- [187] <http://horibalab.net/page.php?id=1073>
- [188] http://www.keihin-kogyo.co.jp/en/products/006_toishi_kousei.html
- [189] http://www.artifex-abrasives.com/en/DownloadCenter/DownloadFiles/metal/ARTIFEX_P_Plus_Datasheet.pdf
- [190] Zhang L. et al;An investigation of material removal in polishing with fixed abrasives, Proc Instn Mech Engrs Vol 216 Part B, pp103-112
- [191] Tam H-Y et al,Material removal by fixed abrasives following curved paths, Proc. Instn Mech. Engrs Vol. 218 Part B: J. Engineering Manufacture, pp713-720
- [192] Evans C.J. et al; Material Removal Mechanisms in Lapping and Polishing, CIRP Annals - Manufacturing Technology' Volume 52, Issue 2, 2003, Pages 611-633
- [193] http://www.aspe.net/publications/Annual_2000/PDF/POSTERS/METROL/SURFSUB/KANEEDA.PDF
- [194] <http://www.allproducts.com/manufacture98/chngn/Product-2007918113945.jpg>
- [195] <http://www.dmtsharp.com/general/whydiamond.htm>
- [196] http://www.microdiamant.com/diamondpowder/diatypes_rsyn.htm
- [197] <http://www.somtec.co.uk/tooling.asp>
- [198] <http://www.melloptics.com/shopping/shopdisplayproducts.asp?id=14>
<http://www.flatlap.co.uk/accessories.asp#pads>

REFERENCES

THE APPLICATION OF ZEEKO POLISHING TECHNOLOGY TO FREEFORM FEMORAL KNEE REPLACEMENT COMPONENT MANUFACTURE

- [199] http://solutions.3m.com/wps/portal/3M/en_WW/electronics/home/productsandservices/products/abrasives/TrizactAbrasives/
- [200] Image courtesy of Rhom and Haas
- [201] Image courtesy of KGS Diamond Group
- [202] Xie Y., Bhushan B; Effects of particle size, polishing pad and contact pressure in free abrasive polishing, *Wear* Volume 200, Issues 1-2, 1 December 1996, Pages 281-295
- [203] Trezona R.I. et al; Transitions between two-body and three-body abrasive wear: influence of test conditions in the microscale abrasive wear test, *Wear* 225–229 _1999. 205–214
- [204] http://www.askoxford.com/concise_oed/freeform?view=uk
- [205] http://www.askoxford.com/concise_oed/surface?view=uk
- [206] Vignesh R. et al; Development of CAD models from sketches: A case study for automotive applications, *Proc. IMechE Vol. 221 Part D: J. Automobile Engineering*, pp41-47
- [207] Lim E.E.M. et al; Integrated planning for precision machining of complex surfaces. Part 2: application to the machining of a turbine blade die, *Int. J. Mach. Tools Manufacture*. Vol. 37, No. I, pp. 77--91, 1997
- [208] Lin C.H., Hsu Y.L.; *The Strategy of Virtual Furniture Design in the Digital Architecture Era*, National Institute of Design, Swinburne University of Technology, Australia
- [209] <http://www.emeraldinsight.com/fig/0490300107001.png>
- [210] <http://www.replacementhip.co.uk/knee-replacement/images/knee-implant.jpg>
- [211] British Standards Institution; BS 7251-4:1997 Orthopaedic joint prostheses - Part 4: Specification for articulating surfaces made of metallic, ceramic and plastics materials of hip joint prostheses, Milton Keynes, BSI
- [212] British Standards Institution; BS 7251-14:1998 Orthopaedic joint prostheses Part 14: Components for partial and total knee-joint prostheses - Articulating surfaces made of metal, ceramic and plastics materials, Milton Keynes, BSI
- [213] Firkins, P. J. et al; Quantitative analysis of wear and wear debris from metal-on-metal hip prostheses tested in a physiological hip joint simulator. *Bio-Med. Mater. Engng*, 2001, 11, 143-157.
- [214] Büscher, R. Et al; Subsurface micro-structure of metal-on-metal hip joints and its relationship to wear particle generation. *J. Biomed. Mater. Res., Part B: Appl. Biomater.*, 2005, 72B, 206-214.

- [215] Reginald Lee, MS et al; Tribological Considerations in Primary and Revision Metal-on-Metal Arthroplasty, *The Journal of Bone and Joint Surgery (American)*. 2008;90:118-124.
- [216] Rieker C. Et al; Development and validation of a second-generation metal-on-metal bearing Laboratory studies and analysis of retrievals, *The Journal of Arthroplasty*, Volume 19, Issue 8, Pages 5-11
- [217] Sung H. et al; In vitro surface characterization of a biological patch fixed with a naturally occurring crosslinking agent, *Biomaterials*, Volume 21, Issue 13, July 2000, Pages 1353-1362
- [218] <http://www.tfhrc.gov/structur/pubs/04043/images/fig16.gif>
- [219] <http://www.azom.com/details.asp?ArticleID=4059>
- [220] Rieker C.B. et al; Influence of the clearance on in-vitro tribology of large diameter metal-on-metal articulations pertaining to resurfacing hip implants, *Orthop Clin North Am*. 2005 Apr;36(2):135- 42, vii
- [221] Kurtz S. M. Et al; Surface morphology and wear mechanisms of four clinically relevant biomaterials after hip simulator testing, *Journal of Biomedical Materials Research Part A*, Volume 52 Issue 3, Pages 447 - 459
- [222] Rieker C.B. et al; Clinical Wear Performance of Metal-on Metal Hip Arthroplasties, *Total Joint Replacement*, ASTM STP 1346, J.J. Jacobs and T.L. Craig, Eds., American Society for Testing and Materials 1998
- [223] Lakdawala A. Et al; The significance of surface changes on retrieved femoral components after total knee replacement, *Journal of Bone and Joint Surgery - British Volume*, Vol 87-B, Issue 6, 796-799.
- [224] McEwen H.J.M. et al; Wear of fixe bearing and rotating platform mobile bearing knes subjected to high levels of internal and external tibial rotation, *Journal of Materials Science : Materials in Medicine* 12 (2001) 1049-1052
- [225] Kennedy F.E. et al; Lubrication and Wear of Artificial Knee Joint Materials in a Rolling/Sliding Tribotester, *J. Tribol.* , April 2007, Volume 129, Issue 2, pp326
- [226] <http://www2.mitutoyo.de/en/coordinate-measuring-machines/products/sensors-and-changing-systems/touch-trigger-probes/umap-cmm/index.html>
- [227] <http://www.sme.org/cgi-bin/find-articles.pl?&ME05ART26&ME&20050509&&SME&#amp;article>
- [228] Bills P.J. et al; Development of a technique for accurately determining clinical wear in explanted total hip replacements, *Wear*, Volume 263, Issues 7-12, 10 September 2007, Pages 1133-1137, 16th International Conference on Wear of Materials

- [229] Spinelli M. et al; CMM-based procedure for polyethylene non-congruous unicompartmental knee prosthesis wear assessment, Volume 267, Issues 5-8, Pages, 683-1352 (15 June 2009), 17th International Conference on Wear of Materials, Las Vegas USA, 19-23 April 2009
- [230] <http://www.microscopyu.com/articles/interferometry/twobeam.html>
- [231] <http://www.mddionline.com/article/surface-metrology-stent-and-implant-manufacturing>
- [232] Raeymaekers B., Talke F.E.; The effect of laser polishing on fretting wear between a hemisphere and a flat plate, *Wear* 269 (2010) 416–423
- [233] Anonymous, American National Standards Institute (ANSI 1975) / International Standards Organisation (ISO 1985)
- [234] Williams J.M.; Wear improvement of surgical Ti-6Al-4V alloy by ion implantation, *Nuclear Instruments and Methods in Physics Research Section B: Beam Interactions with Materials and Atoms* Volumes 10-11, Part 1, 15 May 1985, Pages 539-544
- [235] Firkins P.J. et al; A novel low wearing differential hardness, ceramic-on-metal hip joint Prosthesis, *Journal of Biomechanics* 34 (2001) 1291–1298
- [236] Cristofolini L. et al; Comparative in vitro study on the long term performance of cemented hip stems: validation of a protocol to discriminate between “good” and “bad” designs, *Journal of Biomechanics* 36 (2003) 1603–1615
- [237] British Standards Institution; BS EN ISO 4287:1998 Geometrical product specification (GPS). Surface texture: Profile method. Terms, definitions and surface texture parameters, Milton Keynes, BSI
- [238] Moore G.E.; Cramming more components onto integrated circuits, *Electronics*, Volume 38, Number 8, April 19, 1965
- [239] *The First Electronic Computer, The Atanasoff Story*, Alice R. Burks and Arthur W. Burks, The University of Michigan Press, Ann Arbor, Michigan, 1988
- [240] Blunt L.A., Jiang X.; Advanced Techniques for Assessment Surface Topography Development of the the Basis for 3D Surface texture Standards “SURFSTAND” pp7, Kogan Page Science, 2003, ISBN 1-9039-611-2
- [241] Hilerio I. et al; 3D measurements of the knee prosthesis surfaces applied in optimizing of manufacturing process, *Wear* 257 (2004) 1230–1234
- [242] Fawzy A. S., El-Askary F.S; Effect acidic and alkaline/heat treatments on the bond strength of different luting cements to commercially pure titanium, *Journal of Dentistry*, Volume 37, Issue 4, April 2009, Pages 255-263

THE APPLICATION OF ZEEKO POLISHING TECHNOLOGY TO FREEFORM
FEMORAL KNEE REPLACEMENT COMPONENT MANUFACTURE

- [243] Rønold H.J., Ellingsen J .E.; Effect of micro-roughness produced by TiO₂ blasting—tensile testing of bone attachment by using coin-shaped implants, *Biomaterials* 23 (2002) 4211–4219
- [244] Rozenberg O.A. et al; Development of Research for Machining of Implants with Novel Materials for Bone Surgery, *IFMBE Proceedings, Volume 20*, pp156-159, 14th Nordic-Baltic Conference on Biomedical Engineering and Medical Physics NBC 2008 16–20 June 2008 Riga, Latvia
- [245] British Standards Institution; DD CEN ISO/TS 15530-3:2007 - Geometrical Product Specifications (GPS) — Coordinate measuring machines (CMM): Technique for determining the uncertainty of measurement - Part 3: Use of calibrated work pieces or standards, Milton Keynes, BSI
- [246] British Standards Institution; DD CEN ISO/TS 15530-4:2008 Geometrical product specifications (GPS). Coordinate measuring machines (CMM). Technique for determining the uncertainty of measurement. Evaluating task-specific measurement uncertainty using simulation, Milton Keynes, BSI
- [247] Savio E. , De Chiffre L.; An artefact for traceable freeform measurements on coordinate measuring machines, *Precision Engineering* 26 (2002) 58–68
- [248] Savio E. Et al; Approaches to the Calibration of Freeform Artefacts on Coordinate Measuring Machines, *CIRP Annals - Manufacturing Technology, Volume 51, Issue 1, 2002*, Pages 433-436
- [249] Zhang X. et al; A new free-form surface fitting method for precision coordinate metrology, *Wear* 266 (2009) 543–547
- [250] A.W. Fitzgibbon, Robust registration of 2D and 3D point sets, *Image Vision Comput.* 21 (13) (2003) 1145–1153.
- [251] Cheung C.F. et al; An integrated form characterization method for measuring ultra-precision freeform surfaces, *International Journal of Machine Tools & Manufacture* 47 (2007) 81–91
- [252] DesJardins J. D. et al; A direct comparison of patient and force-controlled simulator total knee replacement kinematics, *Journal of Biomechanics* 40 (2007) 3458–3466
- [253] Utzschneider S. et al; Wear of contemporary total knee replacements – A knee simulator study of six current designs, *Clinical Biomechanics* 24 (2009) 583–588
- [254] Burgess I.C. et al; Development of a six station knee wear simulator and preliminary wear results, *Proceedings of the Institution of Mechanical Engineers, Part H: Journal of Engineering in Medicine* Volume 211, Number 1 / 1997
- [255] <http://www.scielo.br/img/revistas/jbsmse/v28n3/30564f2.gif>

THE APPLICATION OF ZEEKO POLISHING TECHNOLOGY TO FREEFORM
FEMORAL KNEE REPLACEMENT COMPONENT MANUFACTURE

- [256] Streiker R, Schon R; Tribological behavior of various materials and surfaces against polyethylene. Presented at the 17th Meeting of the Society for Biomaterials, 1991
- [257] Sheeja D. et al; Feasibility of diamond-like carbon coatings for orthopaedic applications, *Diamond and Related Materials* 13 (2004) 184–190
- [258] C.R. Bragdon, D.O. O'Connor, J.D. Lowenstein and W.D. Synivta, The importance of multidirectional motion on the wear of polyethylene, *J. Eng. Med.* **210** (1996), 157–165
- [259] Joyce T.J. et al; A multi-directional wear screening device and preliminary results of UHMWPE articulating against stainless steel, *Bio-Medical Materials and Engineering* 10 (2000) 241–249 241
- [260] Saikko V.; A hip wear simulator with 100 test stations, *Proc. IMechE Vol. 219 Part H: J. Engineering in Medicine*, 309-318
- [261] Besong A. A. et al; Importance of pin geometry on pin-on-plate wear testing of hard-on-hard bearing materials for artificial hip joints, *Proceedings of the Institution of Mechanical Engineers, Part H: Journal of Engineering in Medicine*, Volume 215, Number 6 / 2001, pp605-610.
- [262] <http://www.prosim.co.uk/hip.shtml>
- [263] <http://www.prnewswire.com/news-releases/smith--nephew-receives-fda-510k-clearance-for-a-30-year-knee-91815029.html>
- [264] <http://www.shorewestern.com/Knee.html>
- [265] Platon F. et al; Tribological behaviour of DLC coatings compared to different materials used in hip joint prostheses, *Wear* 250 (2001) 227–236
- [266] British Standards Institution; BS ISO 14243-1:2002 Implants for Surgery - Wear of Total Knee-joint Prostheses - Part 1: Loading and Displacement Parameters for Wear-testing Machines with Load Control and Corresponding Environmental Conditions for Test
- [267] <http://www.world-trades.com/selling/699/710/weighing-measuring-apparatus-9.html>
- [268] Kretzer J.P., Heisel C.; A new method to quantitatively detect ultra low wear rates of metal-metal bearings in a simulator, Paper No. 21 • 6th Combined Meeting of the Orthopaedic Research Societies
- [269] Blunt L. et al; The role of tribology and metrology in the latest development of bio-materials, *Wear* 266 (2009) 424–431
- [270] Bills P. et al; A metrology solution for the orthopaedic industry, *Journal of Physics: Conference Series* 13 (2005) 316–319, 7th International Symposium on Measurement Technology and Intelligent Instruments.

THE APPLICATION OF ZEEKO POLISHING TECHNOLOGY TO FREEFORM FEMORAL KNEE REPLACEMENT COMPONENT MANUFACTURE

- [271] Walker P.S. et al; A knee simulating machine for performance evaluation of total knee replacements, *J. Biomechanics*, Vol. 30, No. 1, pp. 83 -89, 1997
- [272] Schwenke T. et al; Differences in wear between load and displacement control tested total knee replacements, *Wear* 267 (2009) 757–762
- [273] Saikko V., Calonius O.; Simulation of wear rates and mechanisms in total knee prostheses by ball-on-flat contact in a five-station, three-axis test rig, *Wear* 253 (2002) 424–429
- [274] Bingham R.G. et al; 'A Novel Automated Process for Aspheric Surfaces', *Proc. SPIE 45th Annual Meeting, the International Symposium on Optical Science and Technology, San Diego, Aug 2000* Vol. 4093 'Current Developments in Lens Optical Design and Engineering'; pp445-448
- [275] UK Intellectual Property Office; *Patents and Designs Journal* No. 6176., Zeeko Limited Computer controlled work tool method and apparatus, GB0716597.0, 24th Aug 2007.
- [276] Walker D.D.; 'Revolutionise aspheric polishing with the Zeeko IRP-series'. A Brochure distributed at the *Proc. SPIE 45th Annual Meeting, the International Symposium on Optical Science and Technology, San Diego, Aug 2000*
- [277] Martin H. M. et al; "Progress in the Stressed-lap Polishing of a 1.8m f/1 Mirror"; *Proc. SPIE* vol. 1236; pp. 682-690; 1990.
- [278] Kim S-W. et al; "OGLP-400: An Innovative Computer Controlled Polishing Machine"; *Proc. SPIE* vol. 2775; pp. 491-496; 1996.
- [279] Korhonen T., Lappalainen T.; "Computer Controlled Figuring and Testing"; *Proc. SPIE* vol. 1236; pp 691-695; 1990.
- [280] Images courtesy of Zeeko Ltd. from their Software Brochure
- [281] Walker D.D. et al; 'The Zeeko/UCL Process for Polishing Large Lenses and Prisms', *Proc Large Lenses and Mirrors conference, London, March 27-30 2001* pp106-111
- [282] Bely P.; *The Design and Construction of Large Optical Telescopes (Astronomy and Astrophysics Library)*, Springer Publications, 2003, pp 220, ISBN : 0387955127
- [283] Anderson T et al; "The Euro50 Extremely Large Telescope", *Proceedings SPIE Apr 2002* Vol. 4840 pp 214-225
- [284] Walker D.D. et al; 'The First Aspheric Form and Texture Results From a Production Machine Embodying the Precession Process', *Proc. SPIE 46th Annual Meeting, the International Symposium on Optical Science and Technology, San Diego, August, Vol. 4451*, pp267-276

THE APPLICATION OF ZEEKO POLISHING TECHNOLOGY TO FREEFORM FEMORAL KNEE REPLACEMENT COMPONENT MANUFACTURE

- [285] Walker D.D. et al; Novel CNC polishing process for control of form and texture on aspheric surfaces', Proc. SPIE 47th Annual Meeting, the International Symposium on Optical Science and Technology, Seattle, July 2002, Vol. 4451, pp267-276
- [286] Kim S-W. et al; Active profiling and polishing for efficient control of material removal from large precision surfaces with moderate asphericity, *Mechatronics* 13 (2003) 295–312
- [287] Walker D.D, Shore P.; Manufacture of Segments for Extremely Large Telescopes: a New Perspective, Proc. Second Backaskog Workshop on Extremely Large Telescopes, (Ardeberg A.L., Andersen T., Editors) July 2003, Pub. SPIE, Vol. 5382, pp. 277-284
- [288] Walker D.D. et al; 'The Precessions process for efficient production of aspheric optics for large telescopes and their instrumentation', Proc. SPIE Astronomical Telescopes and Instrumentation Meeting, Hawaii, August 2002, Vol. 4842, pp73-84
- [289] Walker D.D. et al; The 'Precessions' tooling for polishing and figuring flat, spherical and aspheric surfaces, *OPTICS EXPRESS*, Vol. 11, No. 8, 21 April 2003, pp958-964
- [290] Walker D.D. et al 'Precessions Aspheric Polishing - New Results from the Development Programme Proc SPIE 48th Annual Meeting San Diego August 2003 Vol 5180 pp15-28
- [291] Walker D.D. et al; 'New results from the Precessions Polishing Process Scaled to Larger Sizes'; Proc. SPIE Conference 'Optical Fabrication, Metrology and Materials Advancements for Telescopes, Glasgow, June 24,25, 2004, Volume 5494, pp71-80
- [292] Walker D.D. et al; 'New results extending the Precessions process to smoothing ground aspheres and producing freeform parts', Proc. SPIE Vol. 5869, San Diego, Aug. 2005, pp 79-87
- [293] Walker D.D. et al 'Zeeko 1 metre polishing system', 7th Int. Conf Lamdamap Cranfield, UK June 2005, p 240
- [294] Walker D.D. et al; 'Commissioning of the first Precessions 1.2m CNC Polishing Machines for Large Optics', Proc. SPIE Vol. 6288: Current Developments in Lens Design and Optical Engineering, San Diego Aug. 2006, 62880P, pp1-8
- [295] Walker D.D. et al; The Precessions Polishing and Hybrid Grolishing Processes - Implementation in a novel 1.2m Capacity Machine Tool, 8th International Conference and Exhibition on Laser Metrology, Machine Tool, CMM & Robotic Performance, Cardiff University, Wales, 25th June- 28th June 2007
- [296] Walker D.D. et al; 'Automated optical fabrication – First results from the new "Precessions" 1.2m CNC polishing machine', Proc. SPIE Vol. 6273: Optomechanical Technologies for Astronomy, Orlando, pp 627309-1 to 627309-8
- [297] Walker D.D. et al; 'A Quantitative Comparison of Three Grolishing Techniques for the Precessions TM Process', Proc. SPIE Optical Manufacturing and Testing Conference, San Diego, August 28, 29 2007, pp66711H-1 to H-9

THE APPLICATION OF ZEEKO POLISHING TECHNOLOGY TO FREEFORM
FEMORAL KNEE REPLACEMENT COMPONENT MANUFACTURE

- [298] Walker D.D. et al; 'First Results on Free-form Polishing Using the Precessions Process'; Proc. ASPE Winter Conference 'Freeform Optics, Design, Fabrication, Metrology, Assembly', Vol. 31, Chapel Hill, N. Carolina, February 4,5, 2004, pp29-34
- [299] Walker D.D. et al; 'Recent development of Precessions polishing of larger components and free-form surfaces', Proc. SPIE conference 'Current Developments in Lens Design and Optical Engineering V', Denver, Colorado, August 4,5, 2004, Volume 5523, pp281-289
- [300] Walker D.D., Hutchison M.; 'Matching Manufacturing and Measurements-solutions for Free-Form Surfaces', Euspen conference, Montpellier, France, May 9-12 2005, P28, Proceedings of the VisionOnline Seminar 'Ultra Precision Optics- Meeting the Manufacturing Challenge & The Metrology of Advanced Optics', May 2005.
- [301] Walker D.D. et al; 'Recent advances in the control of form and texture on free-form surfaces' (invited paper), Proc. SPIE conference 'Optical Fabrication, Testing and Metrology II', Jena, Vol. 5965, 13-15 May 2005
- [302] Walker D.D. et al; 'New Developments in the Precessions process for Manufacturing Freeform, Large-optical, and Precision-mechanical Surfaces', Proc. 2nd International Symposium on Advanced Optical Manufacturing and Testing Technology (AOMATT), plenary paper, Xian, 2005, pub SPIE Vol. 6148 pp 614805-1 to 614805-9
- [303] Engineering Physical Sciences Research Council, GR/S10209/01: From Optical Surfaces to Prosthetic Joint Lifetime (<http://gow.epsrc.ac.uk/ViewGrant.aspx?GrantRef=GR/S10209/01>)
- [304] Knox P.; Development of High Performance Tribological Coatings For Applications Onto Hip Joint Prostheses, PhD thesis, Wolverhampton University, December 2009
- [305] Retherford S.R. et al; Effect of surface quality on transmission performance for (111) CaF₂, Applied Surface Science, Volume 183, Issues 3-4, 28 November 2001, Pages 264-269
- [306] Paul E. et al; Chemical aspects of tool wear in single point diamond turning, Precision Engineering, Volume 18, Issue 1, January 1996, Pages 4-19

SELECTED LIST OF PUBLICATIONS

- 1. Chi Fai Cheung, Wing Bun Lee, P. Charlton, S. To; A Study of Wear Characteristics of Superpolished Orthopaedic Implant Materials Using Ultra-Precision Polishing, Key Engineering Materials, 447-448, 111, 2010**

Ultra-precision polishing is an emerging technology for producing superfinishing surfaces with sub-micrometer form accuracy and surface finish in nanometer range. It has been applied in superpolishing the freeform bearing surfaces of orthopaedic implants. It is believed that the superfinished surfaces are capable of prolonging the life of the implants. In this paper, an experimental investigation of ultra-precision polishing of orthopaedic implants and the study of the wear characteristics of the superfinished surfaces using a multi-directional pin-on-plate wear test simulator have been conducted. Tests were carried out over 3 million cycles using Zeeko IRP200 superfinished cobalt chrome pins articulating against cross-linked UHMWPE plates. The results were compared to that of manually polished pins articulated against the same UHMWPE material. The results show that the Zeeko IRP200 polished pins produced better wear performance than that of the manually polished pins

- 2. Cheung C. F., Ho L. T. Charlton P., Kong L. B., To S., Lee W.B.; Analysis of surface generation in the ultraprecision polishing of freeform surfaces, Proceedings of the Institution of Mechanical Engineers, Part B: Journal of Engineering Manufacture, Volume 224, Number 1 / 2010 , pp 59-73. (Winner of the Sir Joseph Whitworth Prize 2010). A Copy of the full paper can be found in Appendix.**

Abstract

The use of freeform designs in engineering surfaces has become increasingly popular over the last decade. Applications of freeform shapes range from aesthetics of components to the bending of light rays through advanced optic designs. The fabrication of the components for these applications requires submicrometre form accuracy, in some cases with surface roughness at nanometric levels. Ultraprecision polishing is an emerging technology for the

THE APPLICATION OF ZEEKO POLISHING TECHNOLOGY TO FREEFORM FEMORAL KNEE REPLACEMENT COMPONENT MANUFACTURE

fabrication of high-precision and high-quality freeform surfaces. However, the factors affecting nanosurface generation in ultraprecision polishing have received relatively little attention. Moreover, the quality of the polished surface relies heavily on appropriate selection of process conditions and polishing strategies. This paper presents an analytical study of the factors affecting surface generation in ultraprecision polishing. A series of polishing experiments have been designed and undertaken, allowing the relationships between various factors and the surface quality of the workpiece to be determined. The results of the study provide a better understanding of nanosurface generation, as well as the strategy for optimizing surface quality, in the ultraprecision polishing of freeform surfaces.

- 3. P.A. Knox, P.Charlton, T.Laoui, Gillian Pearce, Liam Blunt; The significance of sample preparation when testing surface coatings for orthopaedic implants; 8th International Conference and Exhibition on Laser Metrology, Machine Tool, CMM & Robotic Performance p.270-278, Cardiff University, Wales , 25th-28th June 2007**

Abstract

In the UK there are over 50,000 hip replacement operations annually, of which approximately 10% are revision surgeries, most commonly necessitated by aseptic loosening. By improving implant design the number of risky and costly revision surgeries can be significantly reduced. Aseptic loosening is mainly caused by osteolysis, a condition that occurs when the body attempts to break down wear particles produced from the articulation of the artificial joint; the chemicals used by the body have limited effect on the wear particles but do start to cause the bone to reabsorb. By reducing the production of wear particles and making those that are produced as biocompatible as possible, the incidence of aseptic loosening can be reduced. Surface coatings are prime candidates for achieving this.

By modifying the surface of the implant using coatings, it is possible to modify the tribology of the joint while retaining the bulk properties. This not only enables the increase of wear resistance of the joint but introduces a barrier between the blood and the metal components which are causing increased concern among medical professionals who are worried about the toxic effect of metal ions being released into the body.

For orthopaedic implants to reach the market, stringent testing is required. Joint simulators are used for testing, machines that attempt to mimic the movement and loading expected in the body. Unfortunately tests can take months to complete; this is unsuitable for initial development of coatings numerous iterations of which can be produced in a few days. Consequently preliminary testing is carried out using other techniques, such as pin on disc, which sacrifices elements of the simulation of the joint movement for speed.

Initial pin on disc tests used to identify potential coating candidates identified a need to accurately control the geometry and surface characteristics of the test samples used for short tests (<1 day) so as to be able to accurately measure the small amounts of wear created by the measurement techniques described within this paper. Control of surface finish was also important to ensure that there were no significant surface defects which may act as stress concentrators and result in premature failing of the coating.

By using a 7 axis CNC Zeeko polishing machine, it has been possible to accurately control the surface roughness and form of samples and characterise their effect on the wear of surface coatings that are being developed for orthopaedic applications.

4. P. Charlton, L. Blunt, Surface and form metrology of polished “freeform” biological surfaces, *Wear* (2007), doi:[10.1016/j.wear.2006.08.043](https://doi.org/10.1016/j.wear.2006.08.043)

Abstract

It is a well documented fact that in the developed world the general population is aging and the percentage of elderly persons within the total population is growing rapidly. This demographic change has massively increased healthcare demands. In aging persons osteo-arthritis has been shown to be particularly problematic. Osteo-arthritis is the progressive degeneration of the natural cartilage tissue which plays a critical part in the load bearing function of hip and knee joints. Solutions to the problems caused by this tissue breakdown are administration of anti-inflammatory drugs or more normally and especially in advanced cases is the replacement of all or part of the joint with artificial joints. Worldwide, the total number of implant procedures is around 800,000. Today the life expectancy of such systems is 5–15

years. This paper outlines the development of a new technique which has been adapted to polish free form knee joint surfaces. The manufacturing route utilises a seven axes CNC Zeeko polishing machine to polish knee joint surfaces to the required form and finish. The paper discusses the process constraints and optimal settings and the surface generation.

- 5. P.Charlton, L.Blunt, A.Beaucamp; Machining of "Freeform" Biological Surfaces on an Advanced 7-axis CNC Polishing Machine; 3rd International Congress of Precision Machining 2005 p.95-102; Festivity Hall – Festsaal, Vienna University of Technology, Vienna, Austria; October 18th-19th, 2005.**

Abstract

It is a well documented fact that in the developed world the general population is aging and the percentage of elderly persons within the total population is growing rapidly. The result of this demographic change is an increasing demand on healthcare.

In aging persons Oesteo-arthritis has been shown to be particularly problematic. Oesteo-arthritis is the progressive degeneration of the natural cartilage tissue which plays a critical part in the load bearing function of hip and knee joints. Solutions to the problems caused by this tissue breakdown are administration of anti-inflammatory drugs or more normally and especially in advanced cases is the replacement of all or part of the joint with artificial joints. Worldwide, the total number of implants is around 800,000. Today the life expectancy of such systems is 5-15 years.

The thrust of much research in the field of hip replacement has been to use a hard on hard bearing couple of metal on metal or ceramic on ceramic. To enable this combination extremely low surface roughness' and excellent conformances of the part is necessary. This can be achieved in the case of hips though with some difficulty. For knee systems the use of hard on hard bearings has up till now been precluded by the need to obtain the conformance and roughness constraints on the effectively free form knee surfaces.

The present paper outlines techniques which have the ability to bridge this gap. The manufacturing route utilises a 7 axis CNC Zeeko polishing machine to polish knee joint surfaces to the required form and finish. The paper discusses the machine constraints and optimal settings and the surface generation process to overcome the challenges of conformance and create smooth surfaces hence reducing wear and increasing lifetimes of prosthetic joints.

6. P.Charlton, L.Blunt; Polishing “Freeform” Biological Surfaces using a 7-axis CNC Polishing Machine; 7th International Conference and Exhibition on Laser Metrology, Machine Tool, CMM & Robotic Performance p., Cranfield Management Development Centre, Cranfield, Bedfordshire, UK, 27th-30th June 2005

It is a well documented fact that in the developed world the general population is aging and the percentage of elderly persons within the total population is growing rapidly. The result of this demographic change is an increasing demand on healthcare.

In aging persons Oesteo-arthritis has been shown to be particularly problematic. Oesteo-arthritis is the progressive degeneration of the natural cartilage tissue which plays a critical part in the load bearing function of hip and knee joints. Solutions to the problems caused by this tissue breakdown are administration of anti-inflammatory drugs or more normally and especially in advanced cases is the replacement of all or part of the joint with artificial joints. In the UK alone, over 40,000 hips and 30,000 knees are replaced each year at a cost of approximately £350 million per annum. Worldwide, the total number of implants is around 800,000. Over many years considerable research has been conducted concerning the design and function of artificial joint systems and today the life expectancy of such systems is 5-15 years.

Current replacement knee systems comprise a metallic femoral component running on a polymeric bearing surface. Throughout the joint life wear occurs though this is normally within acceptable levels However in a considerable proportion of joints (10%) a process of aseptic loosening occurs causing joint failure.

THE APPLICATION OF ZEEKO POLISHING TECHNOLOGY TO FREEFORM FEMORAL KNEE REPLACEMENT COMPONENT MANUFACTURE

During the life of these joints considerable wear occurs at this interface generating wear particles which in turn trigger an immune response which attacks and loosens the joint. At this stage the joint is deemed to have failed and is replaced prematurely. The thrust of much research in the field of hip replacement has been to use a hard on hard bearing couple of metal on metal or ceramic on ceramic. To enable this combination extremely low surface roughness' and excellent conformances of the part is necessary. This can be achieved in the case of hips though with some difficulty. For knee systems the use of hard on hard bearings has up till now been precluded by the need to obtain the conformance and roughness constraints on the effectively free form knee surfaces.

The present paper outlines techniques which have the ability to bridge this gap. The manufacturing route utilises a 7 axis CNC Zeeko polishing machine to polish knee joint surfaces to the required form and finish. The paper discusses the machine constraints and optimal settings and the surface generation process. The resulting surface is then discussed in terms of its fitness for purpose as a functioning implant bearing surface.

APPENDIX

THE APPLICATION OF ZEEKO POLISHING TECHNOLOGY TO FREEFORM
FEMORAL KNEE REPLACEMENT COMPONENT MANUFACTURE

APPENDIX

Taguchi Designs

n/k	3	4	5	6	7	10	11	12	13	15	21	22	26	27	31	40	63
4		L4 2															
8					L8 2												
9		L9 3															
12								L12 2									
16			L16b 4							L16 2							
18					L18 3.6												
25				L25 5													
27									L27 3.2								
32						L32b 4.2										L32 2	
36												L36 3		L36b 3.2			
50								L50 5.2									
54														L54 3.2			
64													L64b 2				L64 4
81																	L81 3

n = number of tests k = number of factors

Figure 6.1 Taguchi Orthogonal Array Selection Table

Factor	Level 1	Level 2	Level 3	Level 4
H-Axis Head Speed (RPM)	500	1000	1500	2000
Head Pressure (Bar)	0.5	1	1.5	2
Precess Angle (Degrees)	0	5	10	15
X-Y Spacing (mm)	0.1	0.2	0.3	0.4
Spot Size (mm)	6	8	10	12

THE APPLICATION OF ZEEKO POLISHING TECHNOLOGY TO FREEFORM
FEMORAL KNEE REPLACEMENT COMPONENT MANUFACTURE

Test Number	Column					Approx. Process Time (mins.)
	1	2	3	4	5	
1	1	1	1	1	1	28
2	1	2	2	2	2	16
3	1	3	3	3	3	11
4	1	4	4	4	4	9
5	2	1	2	3	4	11
6	2	2	1	4	3	9
7	2	3	4	1	2	28
8	2	4	3	2	1	16
9	3	1	3	4	2	9
10	3	2	4	3	1	11
11	3	3	1	2	4	16
12	3	4	2	1	3	28
13	4	1	4	2	3	16
14	4	2	3	1	4	28
15	4	3	2	4	1	9
16	4	4	1	3	2	11

Table 6.2 Taguchi L16b Orthogonal Array with Factors Assigned to Columns

THE APPLICATION OF ZEEKO POLISHING TECHNOLOGY TO FREEFORM
FEMORAL KNEE REPLACEMENT COMPONENT MANUFACTURE

		Wyko Measurement Run 1 (4 Quadrant Surface Roughness Sa)				
Random Run No.	Test Number	Run 1qA Sa	Run 1qB Sa	Run 1qC Sa	Run 1qD Sa	Average Sa Run 1
4	1	9.68	7.01	9.27	10.92	9.22
14	2	9.26	9.07	10.08	9.68	9.47
12	3	11.45	14.85	13.72	14.01	13.34
6	4	16.09	13.55	11.17	9.54	13.60
8	5	8.17	8.60	8.43	10.21	8.40
13	6	10.40	11.03	10.67	10.47	10.70
2	7	10.07	9.81	10.76	11.04	10.22
15	8	7.19	7.40	9.40	12.00	8.00
10	9	7.84	8.74	10.20	9.60	9.09
7	10	11.07	7.35	6.89	7.39	8.17
3	11	14.09	8.61	8.40	8.48	9.90
16	12	8.72	7.51	7.12	8.13	7.87
11	13	7.31	7.58	6.17	7.79	7.21
5	14	4.75	4.96	5.62	5.94	5.32
9	15	8.31	4.47	9.89	8.08	7.69
1	16	6.77	7.22	8.09	6.29	7.09

		Wyko Measurement Run 2 (4 Quadrant Surface Roughness Sa)				
Random Run No.	Test Number	Run 2qA Sa	Run 2qB Sa	Run 2qC Sa	Run 2qD Sa	Average Sa Run 2
2	1	7.29	11.87	12.30	15.35	11.70
15	2	13.79	13.13	14.35	11.35	13.16
7	3	9.71	10.43	11.68	6.98	9.70
16	4	9.78	8.68	11.65	8.97	9.77
12	5	10.65	11.86	10.81	9.62	10.73
9	6	11.85	8.78	9.62	6.22	9.12
4	7	9.71	10.33	11.67	12.18	10.97
8	8	9.94	9.45	7.31	12.93	9.91
1	9	12.48	13.80	9.94	11.99	12.05
15	10	9.71	6.47	9.29	11.32	9.20
9	11	10.22	9.22	9.20	9.12	9.44
6	12	11.55	12.52	14.33	16.73	13.79
10	13	10.08	12.47	11.82	11.41	11.44
11	14	9.29	12.52	12.68	9.38	10.97
3	15	15.63	7.02	8.18	5.40	9.06
5	16	6.17	7.46	8.72	7.34	7.42

Table 6.3 Random Run Number, Test Number & Filtered Sa Values for Taguchi Tests

THE APPLICATION OF ZEEKO POLISHING TECHNOLOGY TO FREEFORM FEMORAL KNEE REPLACEMENT COMPONENT MANUFACTURE

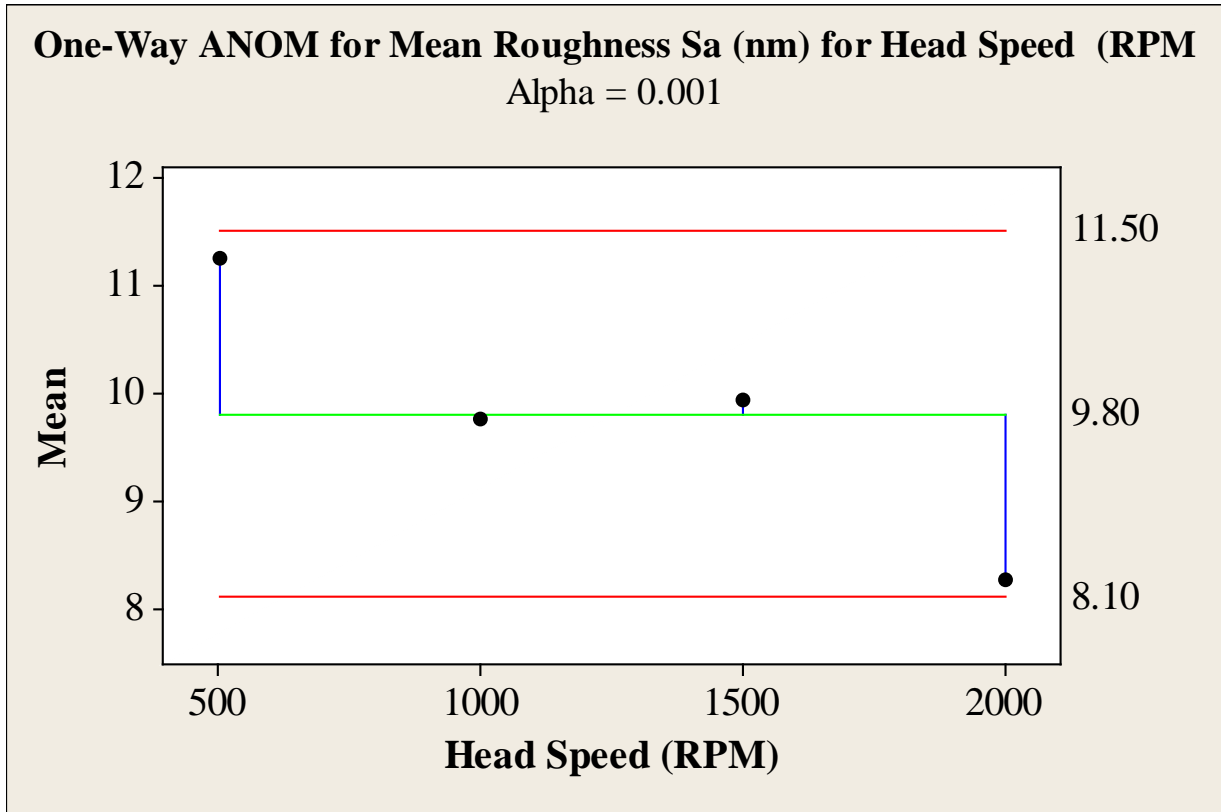


Figure 6.4 One way ANOM of 3D Surface Roughness Sa (nm) for Head Speed (RPM)

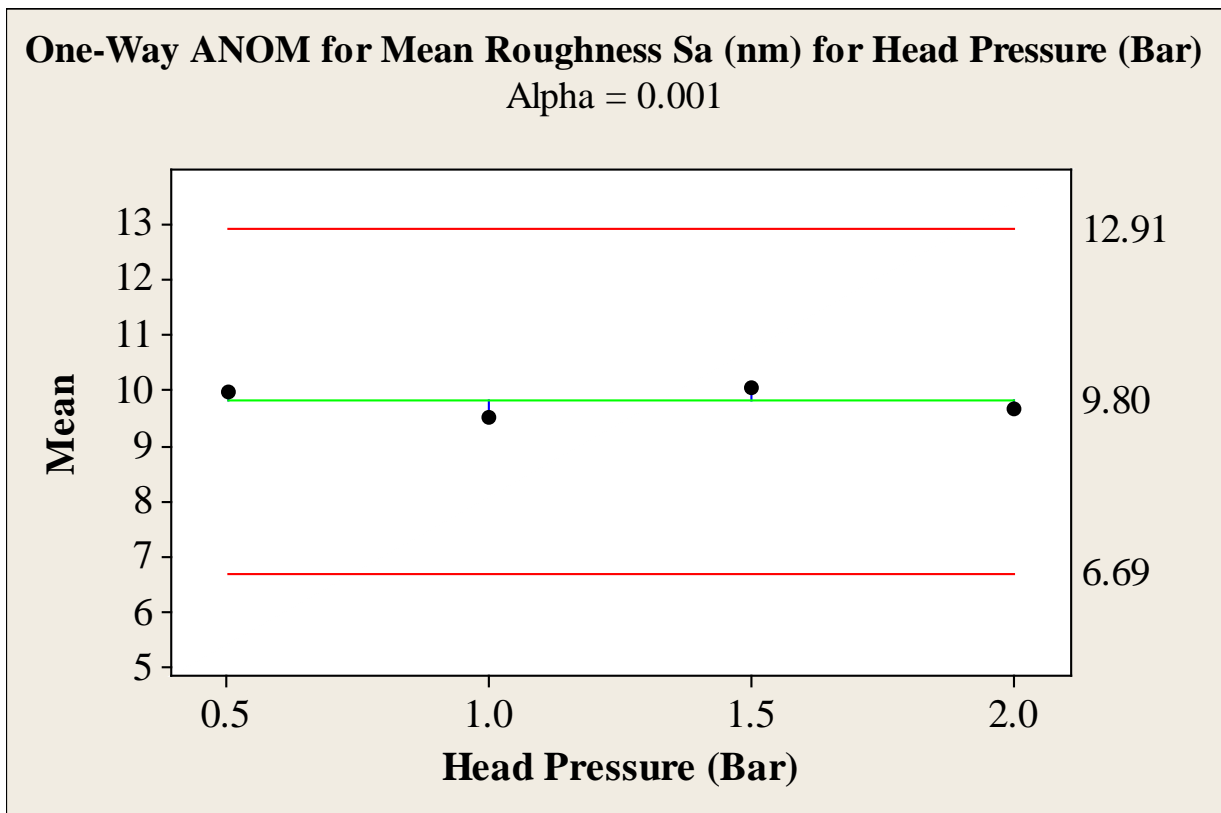


Figure 6.5 One way ANOM of 3D Surface Roughness Sa (nm) for Head Pressure (Bar)

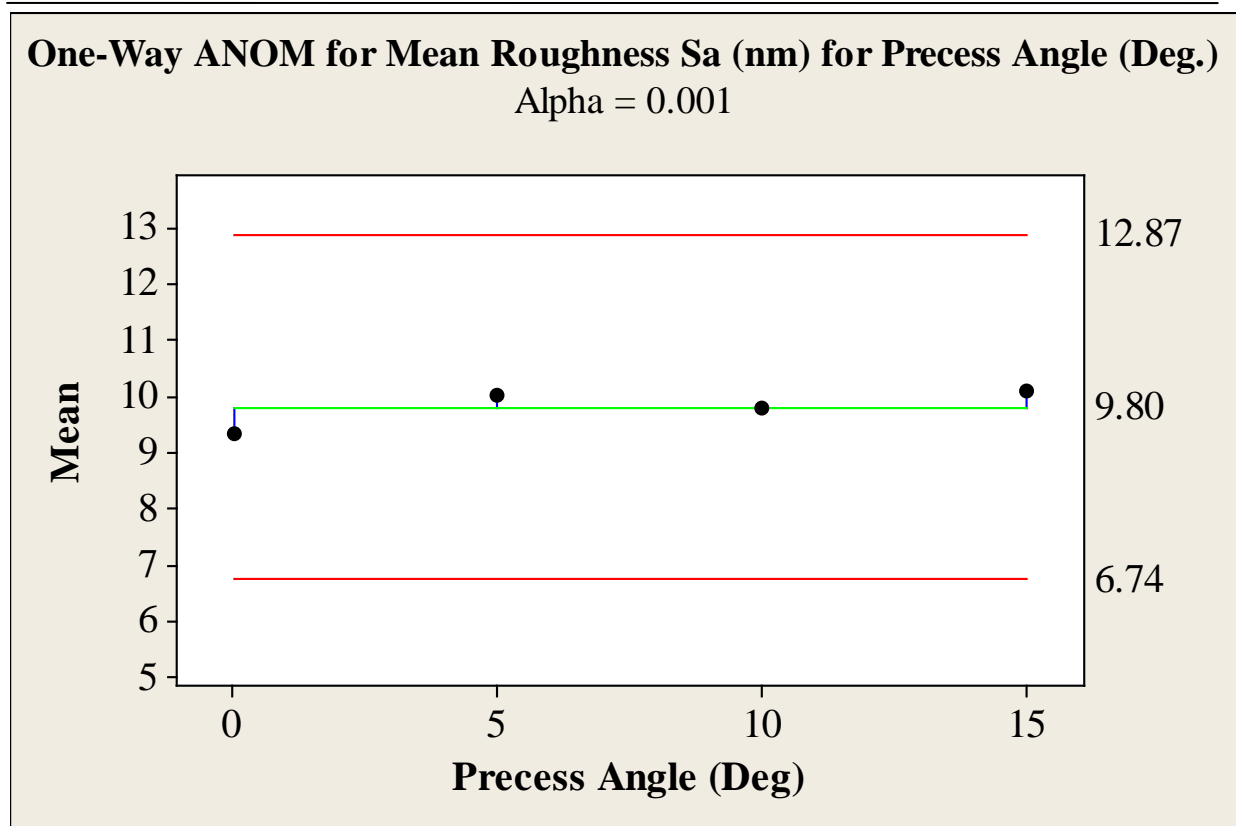


Figure 6.6 One way ANOM of 3D Surface Roughness Sa (nm) for Precess Angle (°)

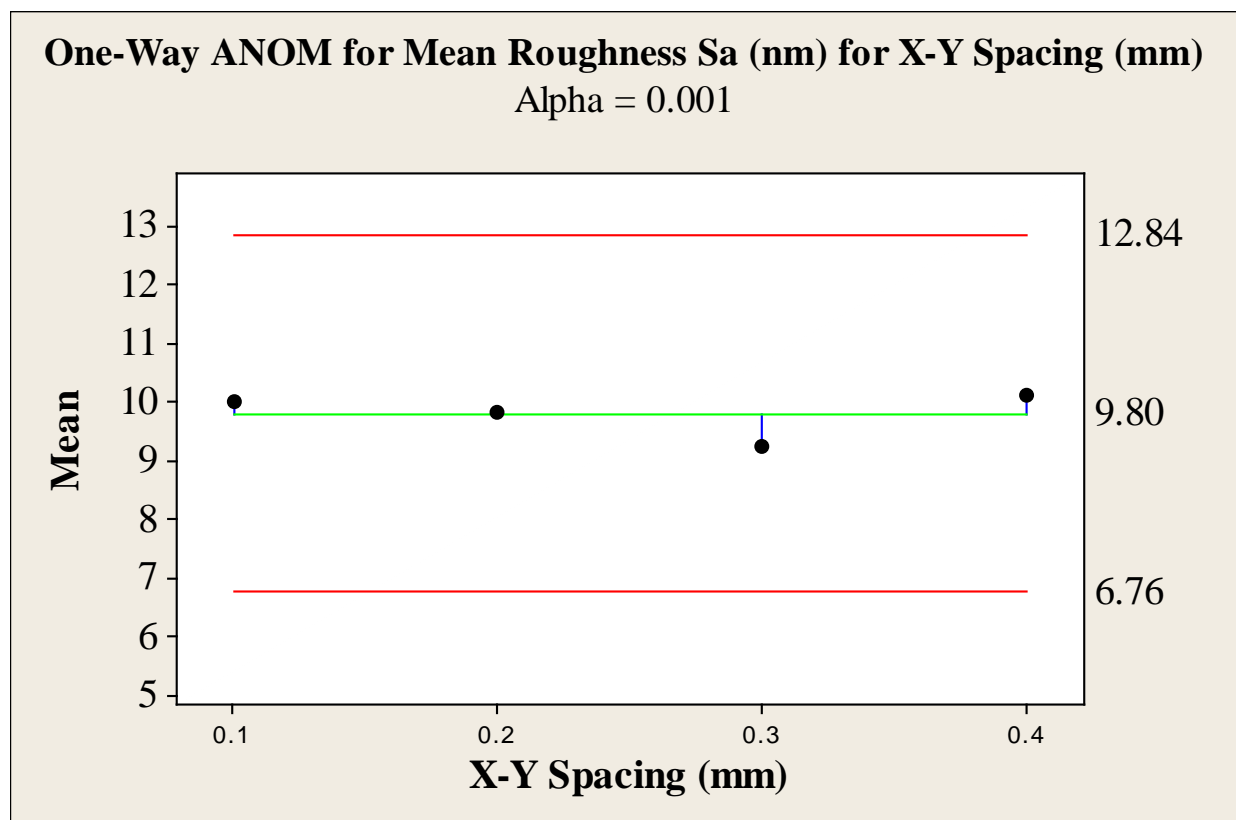


Figure 6.7 One way ANOM of 3D Surface Roughness Sa (nm) for X-Y Spacing (mm)

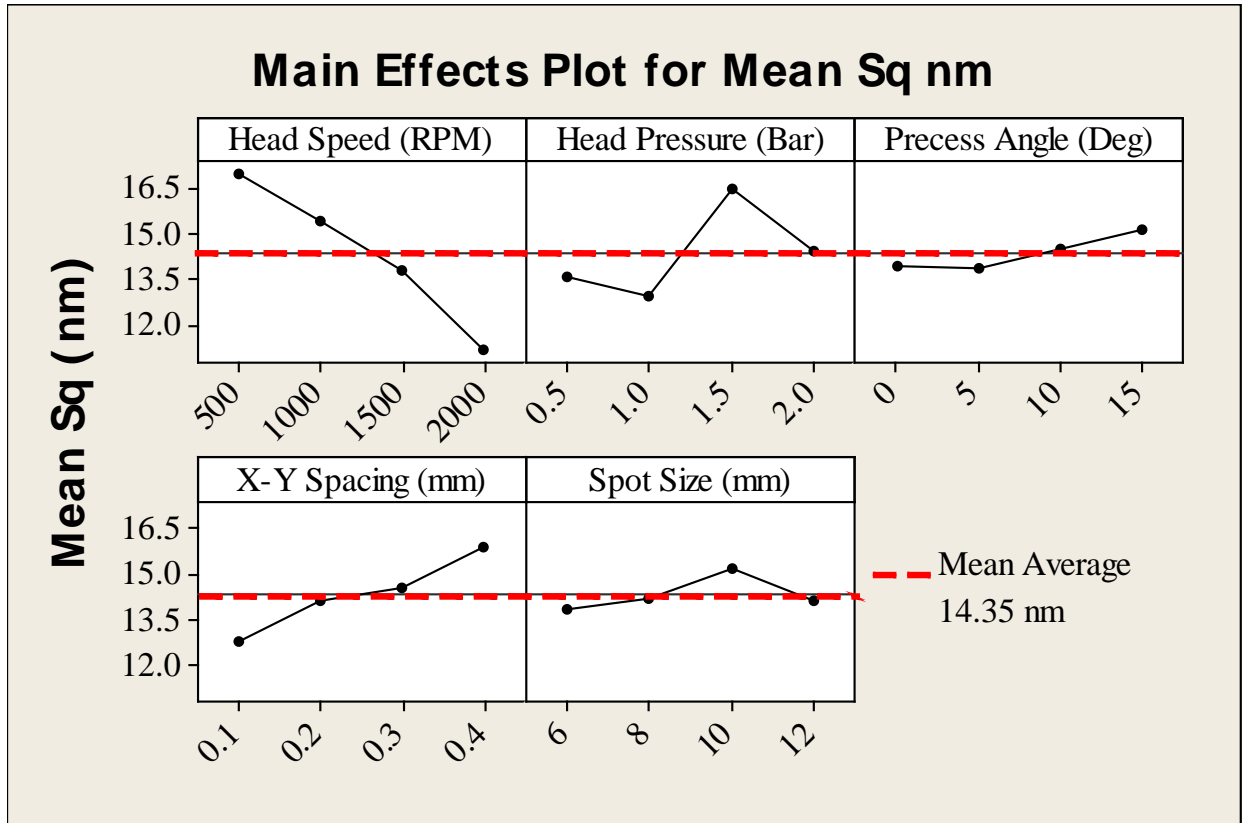


Figure 6.8 Main effects Plot of Sq

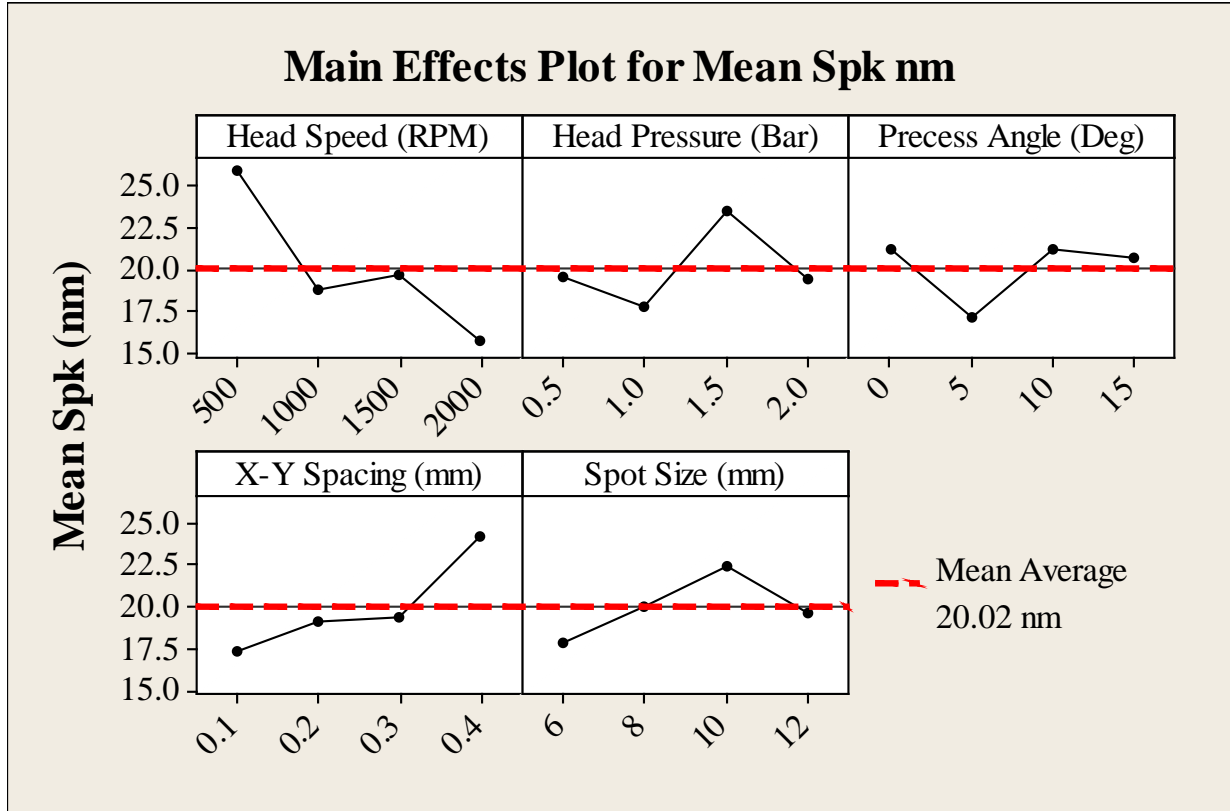


Figure 6.9 Main effects Plot of Spk

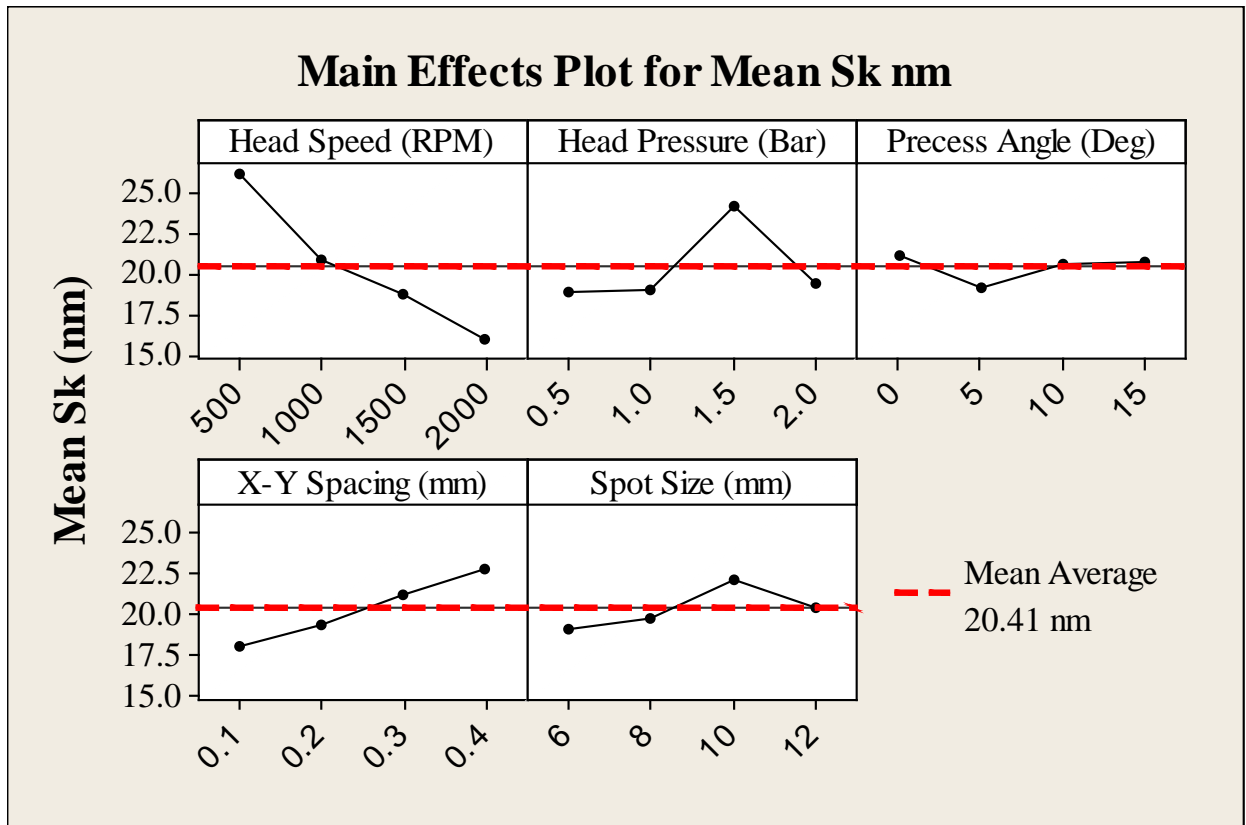


Figure 6.10 Main Effects Plot of Sk

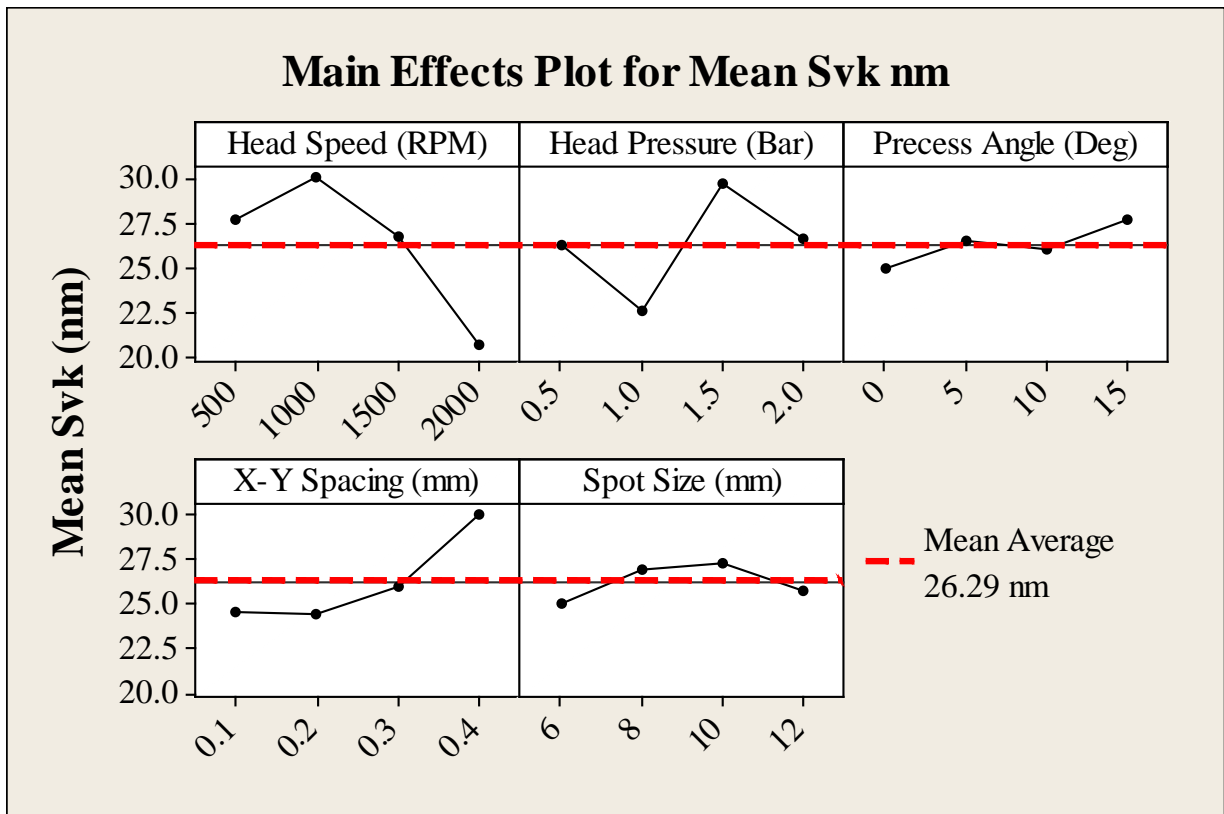


Figure 6.11 Main Effects Plot of Sv_k

THE APPLICATION OF ZEEKO POLISHING TECHNOLOGY TO FREEFORM FEMORAL KNEE REPLACEMENT COMPONENT MANUFACTURE

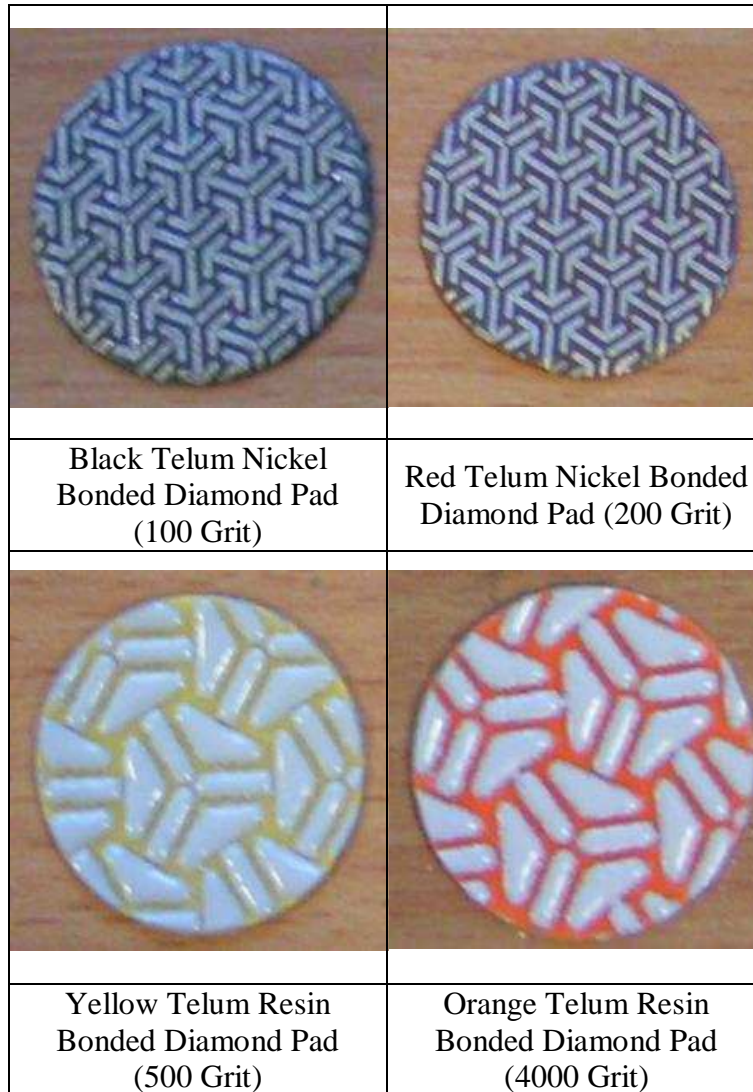


Figure 8.3 Polishing Media Used in Corrective Polishing of Wear Test Pins

Analysis of surface generation in the ultraprecision polishing of freeform surfaces

C F Cheung^{1*}, L T Ho¹, P Charlton², L B Kong¹, S To¹, and W B Lee¹

¹Department of Industrial and Systems Engineering, The Hong Kong Polytechnic University, Kowloon, People's Republic of China

²Centre for Precision Technologies, University of Huddersfield, UK

The manuscript was received on 9 March 2009 and was accepted after revision for publication on 18 June 2009.

DOI: 10.1243/09544054JEM1563

Abstract: The use of freeform designs in engineering surfaces has become increasingly popular over the last decade. Applications of freeform shapes range from aesthetics of components to the bending of light rays through advanced optic designs. The fabrication of the components for these applications requires submicrometre form accuracy, in some cases with surface roughness at nanometric levels. Ultraprecision polishing is an emerging technology for the fabrication of high-precision and high-quality freeform surfaces. However, the factors affecting nanosurface generation in ultraprecision polishing have received relatively little attention. Moreover, the quality of the polished surface relies heavily on appropriate selection of process conditions and polishing strategies. This paper presents an analytical study of the factors affecting surface generation in ultraprecision polishing. A series of polishing experiments have been designed and undertaken, allowing the relationships between various factors and the surface quality of the workpiece to be determined. The results of the study provide a better understanding of nanosurface generation, as well as the strategy for optimizing surface quality, in the ultraprecision polishing of freeform surfaces.

Keywords: surface generation, ultraprecision machining, freeform surfaces, polishing, orthopaedic implants, optimization

1 INTRODUCTION

The use of freeform surfaces in engineering is increasing greatly. Its application is moving rapidly in the automotive industry from aesthetics of car body panels and interiors [1] to advanced optical reflectors for use with LED lighting [2]. The biomedical engineering sector uses freeform femoral knee components with matching freeform tibial inserts to create a load-bearing surface that mimics the movement of the human knee joint [3]. The conformance between these bearing surfaces, their surface finish, and the form of such components can reduce the effect of wear mechanisms, hence increasing the lifetime of the medical implant [4]. The aforementioned com-

ponents are often made from difficult-to-machine materials such as Ti-6Al-4V ELI, titanium, and, in the case of optical moulds, NiCu alloys that have a hardness and tensile strength enabling them to withstand the press forces applied to the mould during the manufacture of components.

Polishing of these kinds of component with submicrometre form accuracy and surface finish in the nanometric range is thought of as the most complicated of all machining processes. As a result, knowledge of the removal mechanisms [5] and the factors that affect these removal mechanisms [6], which in turn determine the surface quality and form control within the polishing process, is essential in achieving the ever increasing tolerances and demands for high-precision optical [7], biomedical [8], and automotive components [9].

Most research involving the material removal mechanisms involved in polishing relates to classical polishing methods such as belt polishing [10], free

*Corresponding author: Department of Industrial and Systems Engineering, The Hong Kong Polytechnic University, Hung Hom, Kowloon, Hong Kong, People's Republic of China.
email: mfbenny@inet.polyu.edu.hk

abrasive polishing [11], fixed abrasive polishing [12], chemical mechanical polishing [13], fluid jet polishing [14], etc. Although these polishing processes have been investigated, present understanding of the removal mechanism is still far from complete. This is particularly true of ultraprecision, multiaxis, freeform polishing, which is a kind of non-conventional polishing method that has been used for machining ultraprecision freeform components that require precise control and accuracy across the polishing surface to maintain the form and achieve nanometre surface finishes, which improve the functionality of the components. In the present study, an experimental investigation of surface generation in ultraprecision freeform polishing is undertaken. The results provide an important means for optimizing surface generation and hence the surface quality in the ultraprecision polishing of freeform surfaces.

2 FACTORS AFFECTING SURFACE GENERATION IN ULTRAPRECISION FREEFORM POLISHING

Ultraprecision freeform polishing is a kind of computer-controlled polishing (CCP). In the present study, CCP is undertaken using an IRP200 ultraprecision, multiaxis, freeform polishing machine (Zeeko™ Ltd, UK) [15], as shown in Fig. 1(a). The machine has seven axes of motion, four of which control the workpiece motion, while the other three control the polishing head, as shown in Fig. 1(b). The machine uses a point called the virtual pivot which is located at the centre of the A and B axes of the machine and which, when combined with the tool radius, controls the contact point on the surface, enabling the CNC controller to know its exact location in machine coordinates and hence its capability accurately to follow the freeform contours. Originally designed for the polishing of aspheric optics applications [16], the Zeeko IRP series of precision,

multiaxis, freeform polishers have found their way into various other markets including mould press and die manufacture, electronic blank wafer production and orthopaedic joint replacements [17], etc. These markets present a challenge owing to the lack of knowledge about material removal from the Zeeko process on metal, composite, and ceramic materials used in the manufacture of such components.

Computer-controlled polishing is a broadly used, high-precision finishing technology that produces a high-quality surface [7]. It is a process that is characterized by the polishing tool removal characteristic and the error profile of the workpiece surface [9]. As shown in Fig. 2, the mechanical polishing employs a polymer membrane bonnet covered with a polishing cloth to perform the polishing process.

Figure 3 shows the cutting geometry for ultraprecision freeform polishing. The factors affecting the surface generation in ultraprecision freeform polishing are basically composed of process factors and material factors. The former include surface feed, precess position, precess angle, head speed, head pressure, tool radius, tool offset, tool overhang, workpiece radius, etc. The latter includes cloth material, slurry medium, workpiece material, slurry temperature, slurry specific gravity, etc. As shown in Fig. 4, the surface quality is also affected by the polishing strategies, which include raster, spiral, and random modes, etc.



Fig. 2 Polishing tools for mechanical polishing

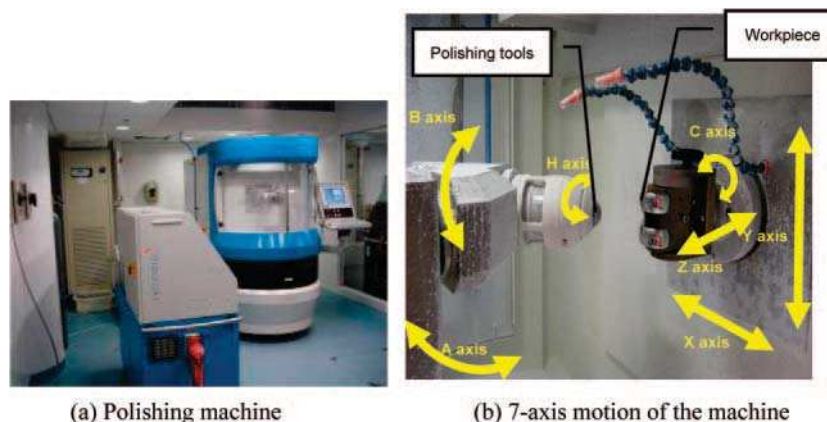


Fig. 1 Ultraprecision freeform polishing machine (Zeeko IRP200 from the UK)

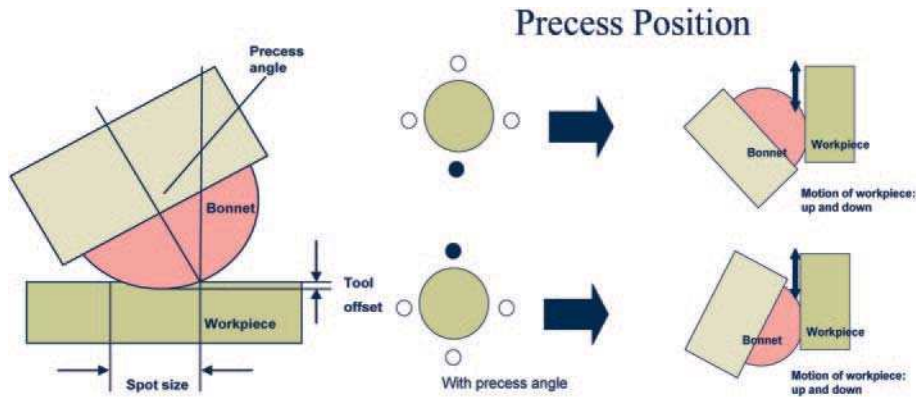


Fig. 3 Cutting geometry for mechanical polishing

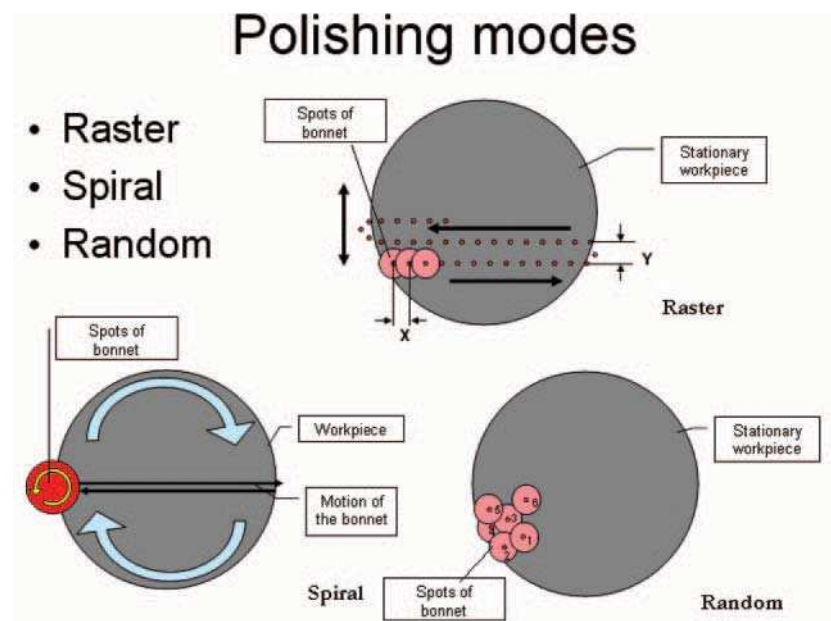


Fig. 4 Polishing strategies

In ultraprecision freeform polishing, the surface error profile and the tool removal characteristic are necessary. The removal characteristic of the polishing tool is also known as the removal function [10] and the influence function. Measurements are included in the acquisition of these data. It is essential to develop influence functions for different workpiece materials, tool materials, and workpiece geometries in corrective polishing. The influence function is incorporated into both the process and material factors. It is a tool that is used in calibration, prediction, or correction. During determination of the influence function process, a spot is polished on the surface and information about the spot is extracted by the measuring system which identifies the properties of the polished spot under a set of predetermined process parameters for optimization, calibration, and form correction. Figure 5 shows a magnified flat surface that contains some peaks and

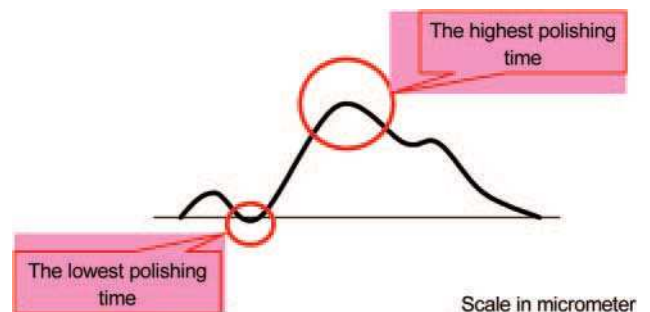


Fig. 5 Importance of influence functions

valleys. To ensure the flatness of the surface, the time for polishing different areas must be known. Based on the error map of the surface, the influence function indicates where the polishing tool should stay for a longer or shorter time in order to remove more or less material from the surface. In the present study,

the influence function is generated by the influence function generator, as shown in Fig. 6.

3 EXPERIMENTAL

Basically, the experimental work is divided into four parts – A, B, C, and D. Part A focuses on the effect of process parameters on surface generation. Part B investigates the characteristics of the influence function in mechanical polishing. In part C, polishing experiments are conducted to study corrective polishing in order to increase the form accuracy of an orthopaedic implant. In part D, polishing experiments are conducted to study the polishing strategy for improving the surface roughness in the mechanical polishing of an orthopaedic implant.

3.1 Part A: Study of the effect of process factors on surface generation

The Taguchi method is one of several ways of using design of experiments quickly to analyse the parameters in a process and to determine which parameters have less or more effect on the desired result, with minimal testing [18]. In the present study, a more advanced Taguchi array is used to test other materials and optimize the polishing process for final finishing of materials such as nickel–copper (NiCu). The array is used to analyse the machine parameters and polishing media used in Zeeko mechanical polishing with a bulged polymer head in contact with the surface. A Taguchi array of seven factors (A to G), one two-levelled factor, and six three-levelled factors was chosen for optimizing the machine tool parameters and polishing media, as summarized in Tables 1 and 2. Optimization of machine tool and polishing medium parameters is undertaken to obtain the best surface finish using the Zeeko bulged polymer head polishing

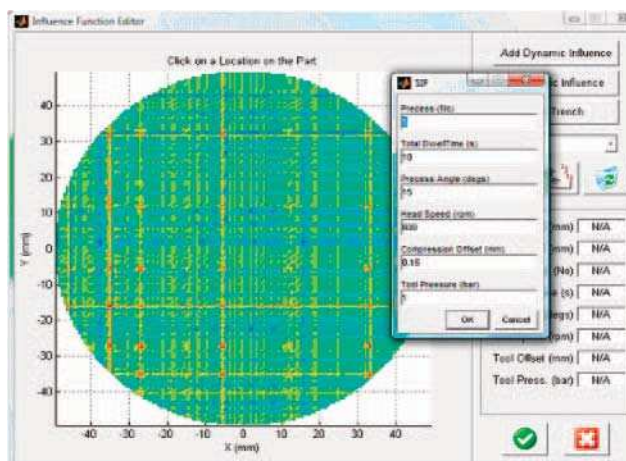


Fig. 6 Influence function generator

process on flat NiCu workpieces. The three-dimensional (3D) arithmetic roughness parameter S_a is used to analyse the results. The surface measurement is carried out on a Wyko NT8000 optical profiling system.

A specially designed workpiece consisting of 12 square pads was manufactured from NiCu, as shown in Fig. 7. Each of the square pads has an area of 12 mm × 12 mm (see Fig. 8) and are rough cut by raster milling using a nanoform 705G ultraprecision freeform machine from Precitech Inc. The rough

Table 1 Factors and levels selected for the study

Factors	Level		
	1	2	3
A. Cloth (durometer hardness D)	Hard (37)	Soft (25)	
B. Head speed (r/min)	2000	1500	1000
C. Bonnet pressure (bar)	2	1	0.5
D. Tool offset (mm)	0.6	0.4	0.2
E. Feed rate (mm/min)	1500	1000	500
F. Slurry (grit size)	Coarse (44 μm)	Medium (20 μm)	Fine (10 μm)
G. Precess angle (deg)	10	5	0

Table 2 Experimental design with L_{16} orthogonal array used

Trial	Cloth	Head speed	Bonnet pressure	Tool offset	Feed rate	Slurry	Precess angle
1	Hard	2000	2	0.6	1500	Coarse	10
2	Hard	2000	1	0.4	1000	Medium	5
3	Hard	2000	0.5	0.2	500	Fine	0
4	Hard	1500	2	0.6	1000	Medium	0
5	Hard	1500	1	0.4	500	Fine	10
6	Hard	1500	0.5	0.2	1500	Coarse	5
7	Hard	1000	2	0.4	1500	Fine	5
8	Hard	1000	1	0.2	1000	Coarse	0
9	Hard	1000	0.5	0.6	500	Medium	10
10	Soft	2000	2	0.2	500	Medium	5
11	Soft	2000	1	0.6	1500	Fine	0
12	Soft	2000	0.5	0.4	1000	Coarse	10
13	Soft	1500	2	0.4	500	Coarse	0
14	Soft	1500	1	0.2	1500	Medium	10
15	Soft	1500	0.5	0.6	1000	Fine	5
16	Soft	1000	2	0.2	1000	Fine	10
17	Soft	1000	1	0.6	500	Coarse	5
18	Soft	1000	0.5	0.4	1500	Medium	0



Fig. 7 Workpiece for machine mark removal study

cutting conditions include a spindle speed of 4000 r/min, a feed rate of 300 mm/min, a depth of cut of 10 μm , and a step distance of 200 μm . Figure 9 shows a micrograph of the surface and the surface topography measured by a Wyko NT8000 non-contact profiler system. It is shown that raster cusp surface marks are formed on the workpiece after raster milling. Table 2 shows the process conditions used in the experiment, and the polishing parameters are listed below:

Number of samples	18 (see Figs 7 and 8)
Sample size	12 mm \times 12 mm
Polished sample size	8 mm \times 8 mm
Sample material	Nickel copper
Polishing tool	Bonnet
Tool size	20 mm radius
Cloth	Zirconium oxide with hardness 25 and 37 (soft and hard in Table 1)
Slurries	Silicon carbide with Everflo
Grit sizes	320 mesh (10 μm , fine), 600 mesh (20 μm , medium), 1200 mesh (44 μm , hard)

The following parameters are set as constant:

XY spacing	0.4 mm
Precess position (number)	4
Tool overhang	3 mm

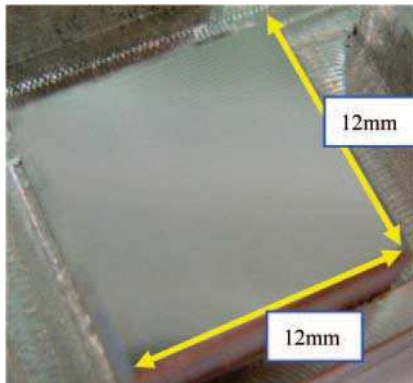


Fig. 8 Surface after raster milling

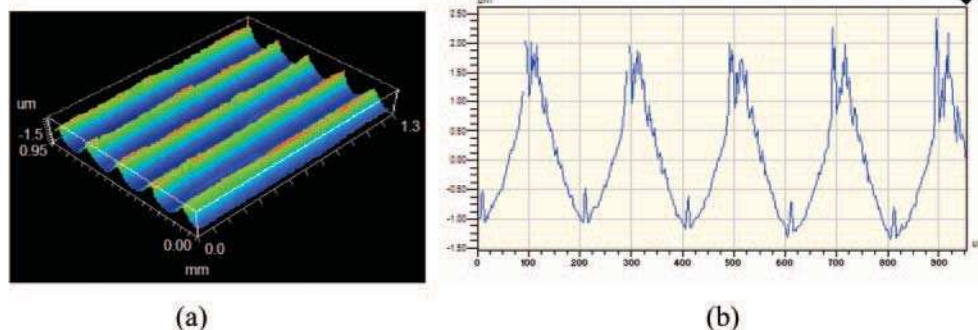


Fig. 9 (a) 3D view of the surface topology after raster milling and before polishing under Wyko (5 \times), and (b) cross-sectional view of the surface roughness profile in the Y direction

3.2 Part B: Study of influence functions

An experiment is conducted to investigate the difference in influence functions and relationships at different positions on the same workpiece. As shown in Fig. 10(a), the workpiece being machined is a convex surface with a diameter of 14.4 mm that is made of Ti-6Al-4V ELI. The radius of curvature of the convex surface is 30 mm. Figure 10(b) shows the position of spots machined on the workpiece. The workpiece is machined by the Zeeko IPR200 seven-axis ultraprecision polishing machine. The cloth material used in the experiment was zirconium oxide with a hardness D 37 (durometer hardness), and the slurry medium was silicon carbide paste with a 62 μm grit size; a bonnet tool of 20 mm radius is used in the experiment. Two samples were polished under different conditions, as summarized in Table 3. The influence functions at each of the three specific positions of the workpiece were obtained and compared to determine the effect of the workpiece geometry on material removal.

3.3 Part C: Study of corrective polishing of the bearing surface for the orthopaedic implant

To study the corrective polishing process, the influence function is analysed. The results of the experiment form the basis for determination of the material removal rate in corrective polishing. Hence, corrective polishing of a small area on the implant is undertaken. The surface data of a small area of the implant were first measured with a Form Talysurf PGI1240 freeform surface measurement system, and the error map between the design surface and measured surface was determined. The material being polished was cobalt-chromium-molybdenum (CoCrMo), which is a common biomedical material for implant manufacturing. Table 4 gives the conditions used in the corrective polishing process. Hence, corrective polishing was undertaken on the basis of the error map and influence

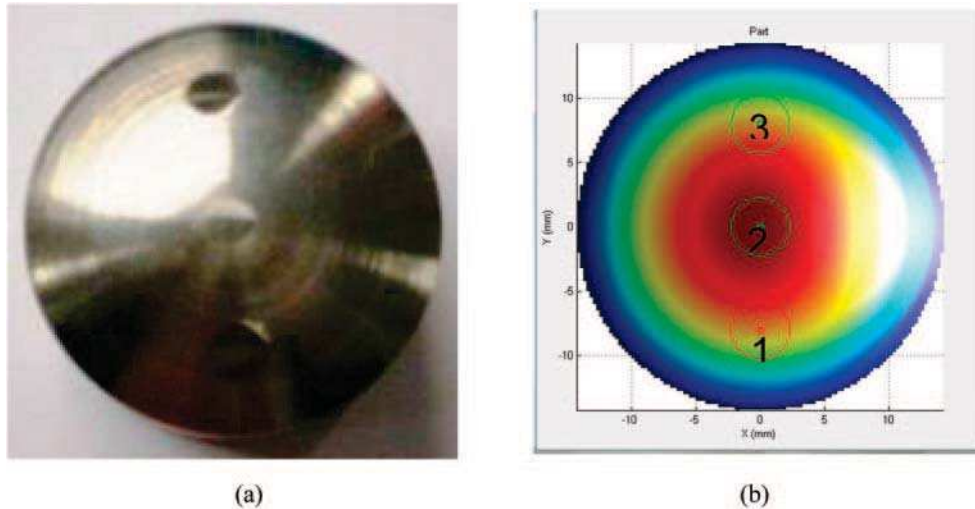


Fig. 10 (a) Geometry of the workpiece and (b) position of the spots being polished

Table 3 Influence function parameters

	Mechanical polishing parameters	
Sample	1	2
Precess (number)	1	1
Total dwell time (s)	240	240
Head speed (r/min)	2000	2000
Precess angle (deg)	5	10
Compression offset (mm)	0.15	0.30
Tool pressure (bar)	2	2
Cloth material	Zirconium oxide	Zirconium oxide
Slurry	SiC	SiC

Table 4 Parameter settings

Parameters	
Slurry medium	SiC paste 17 μm
Path type	Raster
X spacing	0.5 mm
Y spacing	0.5 mm
Tool overhang	0 mm
Tool offset	0.3 mm
Head speed	2000 r/min
Maximum surface feed	500 mm/min

Table 5 Polishing conditions, parameters, and schedule for the experiment in part D

Polishing schedule		Step 1	Step 2	Step 3
Polishing materials	Polishing abrasive	SiC	SiC	Alumina
	Grit size (μm)	30	12	1
	Polishing cloth	Zirconium oxide	Zirconium oxide	3M Multi-tex
	Mode	Raster	Raster	Raster
Process parameters	Precess angle (deg)	15	15	15
	Head speed (r/min)	1000	1000	1000
	Tool offset (mm)	0.3	0.3	0.3
	Tool overhang (mm)	0.5	0.5	0.5
	Pressure (bar)	1	1	1
	XY spacing (mm)	0.3	0.3	0.2
	Surface feed (mm/min)	100	100	100
	Precess position (number)	3	3	3

function. The form errors before and after the compensation polishing are evaluated and compared.

3.4 Part D: Study of effect of polishing strategy on surface generation

The effect of polishing strategy on surface generation was studied. The polishing strategy studied the use of different polishing materials and process para-

eters at different stages of the polishing process. The polishing was conducted by the ultraprecision freeform polishing machine on an orthopaedic implant made of cobalt–chromium–molybdenum (CoCrMo). The polishing conditions and polishing schedule are given in Table 5. The surface roughness and surface topography in different regions of the implant before and after polishing are compared and analysed in Fig. 11.

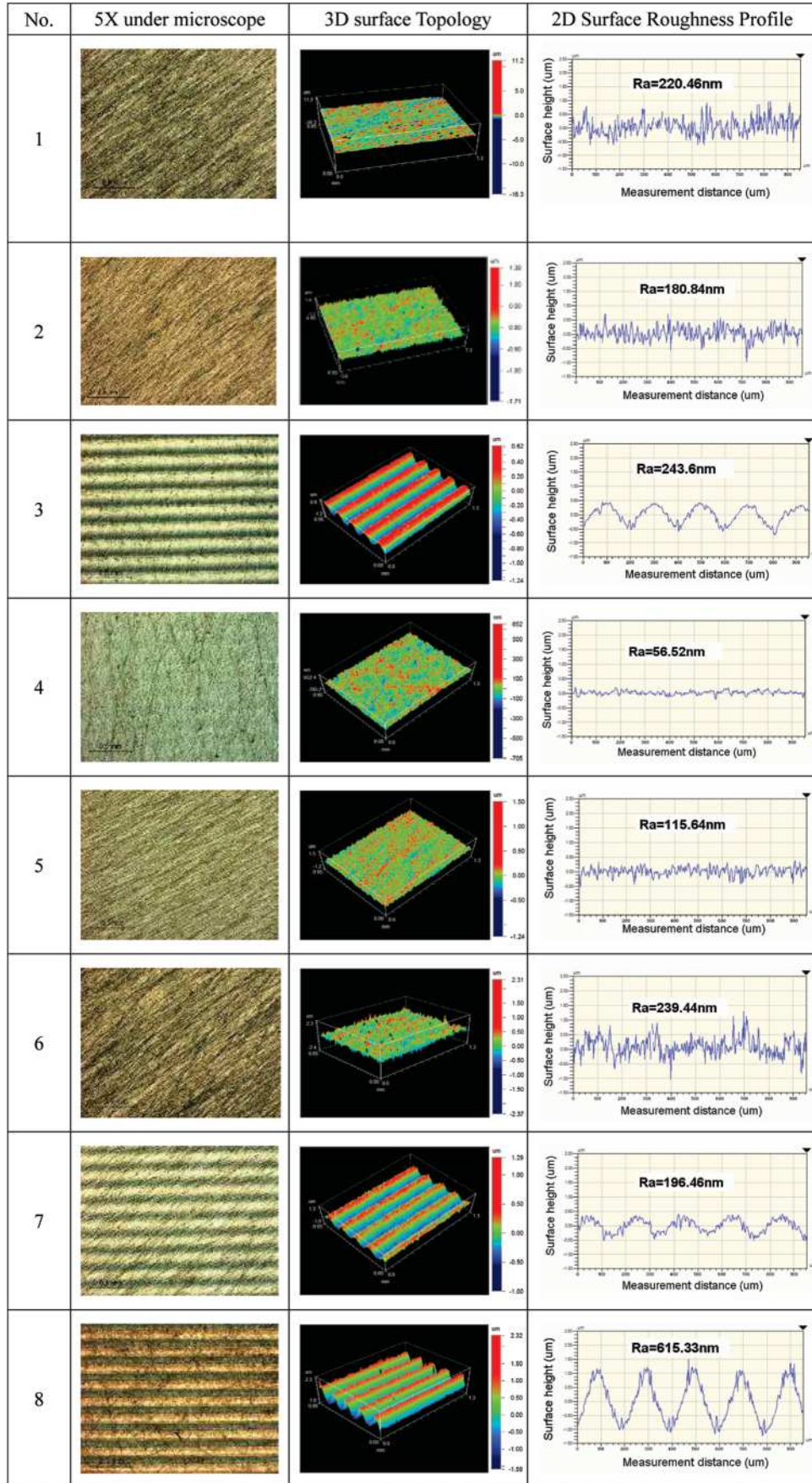


Fig. 11 Continued

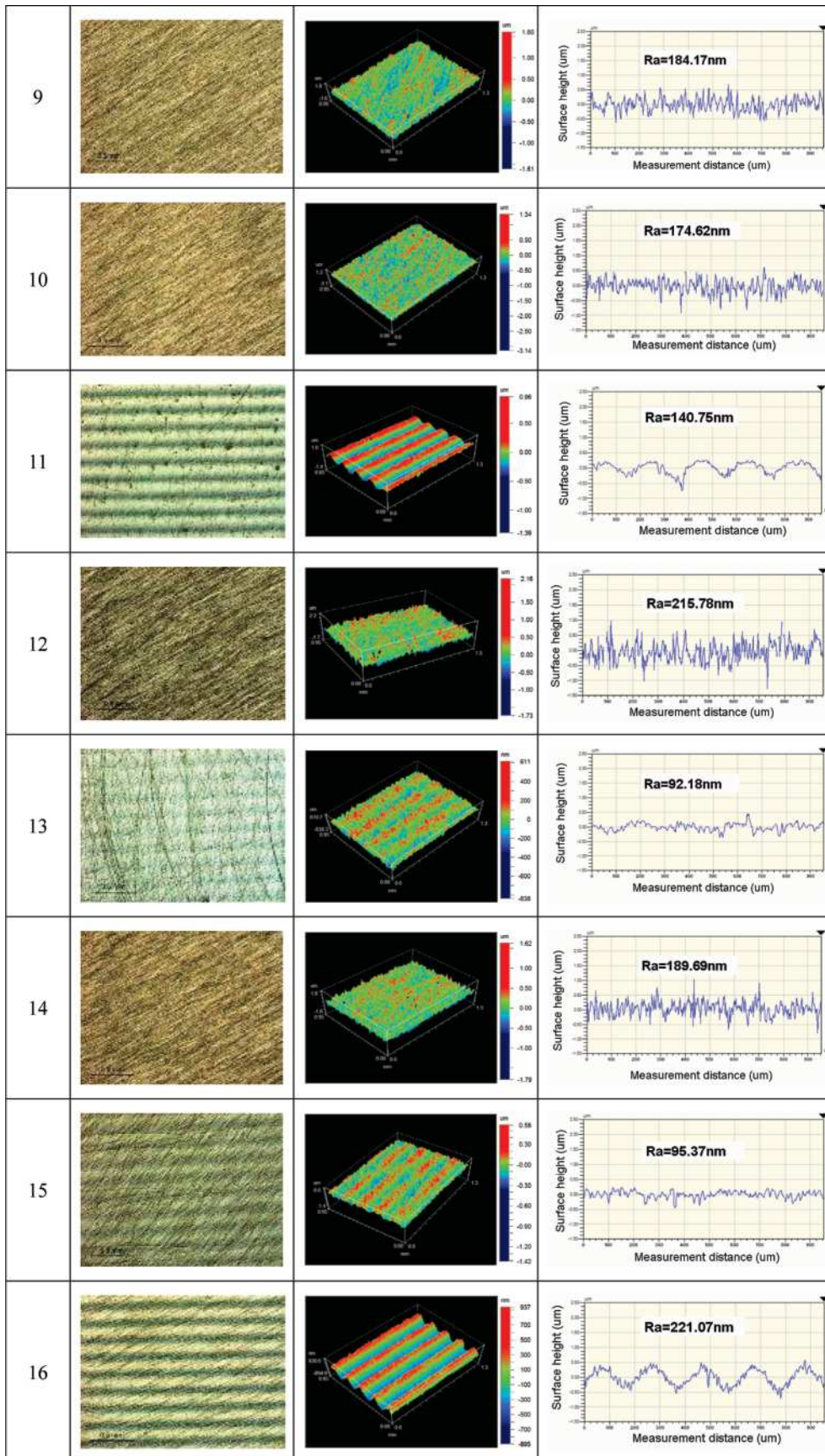


Fig. 11 Continued

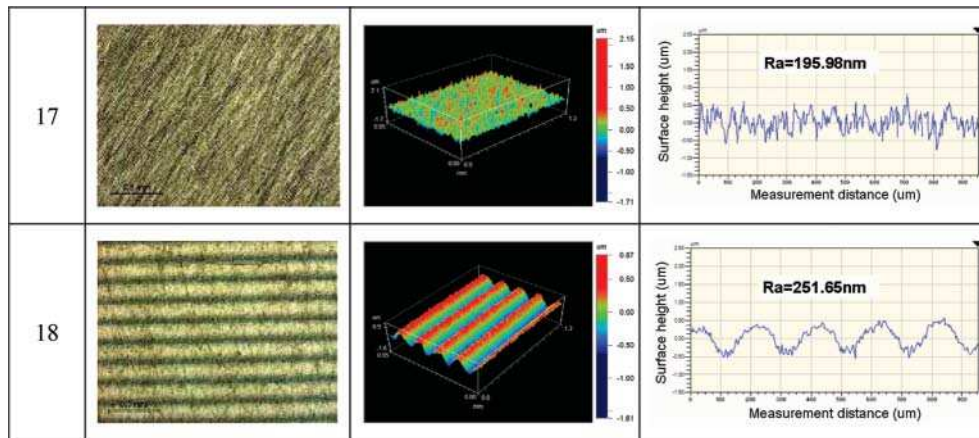


Fig. 11 Effect of process parameters on machine mark removal

4 RESULTS AND DISCUSSION

4.1 Part A: Effect of process factors on surface generation

The results of surface roughness measurement in part A are shown in Table 6. Figure 11 shows the variation in surface texture, surface topography, and surface roughness profile under various conditions. It is interesting to note that there are some combinations of polishing conditions that produce better surface generation in terms of surface texture, surface topography, surface roughness, and surface roughness profile. Condition 4 produces a surface with the smallest surface roughness; raster milling tool marks are almost completely removed, and thus the surface topology is better. In other words, the surface generation is strongly affected by the process conditions being used, and the surface roughness improvement is much greater for some combinations of polishing conditions.

A Taguchi analysis was conducted to minimize the number of polishing tests for identification of the optimal polishing conditions that can produce low surface roughness and surface topology with preferred random textures, i.e. removal of the raster milling machine marks on the surface. Based on the results of the Taguchi analysis, as shown in Table 7, the optimum polishing conditions are identified (see Table 8). A polishing test was conducted under the optimum conditions, and the results are shown in Fig. 12. By comparing the results before and after polishing, it is found that surface generation after optimizing the machine parameters using Taguchi techniques reduced surface roughness from 693 to 117 nm, with visual and microscopic inspection showing evidence that the process removed post-raster milling marks from the rough cut preparation of the samples. After polishing, the texture changed to a random texture. The Taguchi analysis is

Table 6 Results of surface roughness measurement

No.	R_a before polishing (R_a before) (nm)	R_a after polishing (R_a after) (nm)	Improvement $\Delta R_a = (R_a$ before $- R_a$ after) (nm)	Effectiveness % = $(\Delta R_a / R_a$ before) $\times 100\%$
1	770.14	226.47	543.67	70.59
2	770.69	185.92	584.77	75.88
3	726.77	243.60	483.17	66.48
4	729.11	55.45	673.66	92.39
5	733.44	110.39	623.05	84.95
6	769.21	226.12	543.09	70.60
7	776.67	190.46	586.21	75.48
8	716.91	615.33	101.58	14.17
9	764.73	186.63	578.10	75.60
10	776.02	169.87	606.15	78.11
11	760.79	143.06	617.73	81.20
12	772.34	219.40	552.94	71.59
13	758.36	81.78	676.58	89.22
14	725.06	188.05	537.01	74.06
15	765.26	95.37	669.89	87.54
16	720.55	222.86	497.69	69.07
17	713.06	189.63	523.43	73.41
18	755.99	247.97	508.02	67.20

demonstrated to provide a useful means of determining the optimum conditions for polishing so that the number of time-consuming and costly trial polishing experiments can be significantly reduced.

4.2 Part B: Study of influence functions

The results in part B are shown in Fig. 13. Spots 1 and 3 were at similar geometrical positions, but they gave slightly different material removal rates. The maximum removal rate is found at the centre position of the workpiece, i.e. spot 2. It appears that the removal rate is not consistent at different positions of the workpiece. Also, it is interesting to note that a greater tool offset and precess angle are likely to give a larger material removal rate. Tool offset and precess angle may change rapidly for CNC control at high feed rates to compensate for freeform surfaces. Hence, more or

Table 7 Signal-to-noise ratio after analysis

Level	Cloth	Head speed	Bonnet pressure	Tool offset	Feed rate	Slurry	Precess angle
1	-45.54	-47.87	-45.76	-47.94	-43.74	-46.77	-44.61
2	-44.25	-41.03	-46.03	-44.13	-44.9	-43.94	-44.64
3		-45.79	-42.9	-42.61	-46.04	-43.97	-45.44
Rank* (effectiveness)	6	1	3	2	5	4	7

*Contribution of factors to R_a ('1' indicates the greatest contribution, '7' the smallest contribution).

Table 8 Optimum conditions determined by the Taguchi method

Factor	Level description	Level
Cloth	Soft	2
Head speed	1500	2
Bonnet pressure	2	1
Tool offset	0.6	1
Feed rate	500	3
Slurry	Fine	3
Precess angle	5	2

less material is removed, depending on the work-piece geometry.

4.3 Part C: Results of corrective polishing

Before conducting corrective polishing, a part of the surface area was measured. The measured data and the design surface were matched, and the error map was generated, as shown in Fig. 14. The upper part of Fig. 14(a) shows the measured data and the design CAD model, and the lower part shows the form error map between the two sets of data. From the figure it is noted that, without matching of the measured data and design data, the error map will be meaningless. Therefore, data matching is necessary to obtain the real error map for corrective polishing. The data matching process is based on the least-squares method, which can be described as follows

$$F_{LS}(X) = \min \left(\sum_{i=1}^N |P_i^1 - P_i^2|^2 \right) \quad (1)$$

where $F_{LS}(X)$ is the least-squares target function, N is the number of sampled points, P_i^1 and P_i^2 are sampled points and the corresponding points in the design model, and $\min()$ is the minimization operator.

Equation (1) is optimized by minimizing the sum of the distance between the two sets of points within an acceptable threshold value. When the optimization process terminates, the measured data are matched to the designed surface model. The optimization of equation (1) usually requires the solution of a non-linear differential function set.

For more precise matching, the minimum zone method will be employed, which is carried out by minimizing the deviation zone between the sampled

point set and the surface model. The function of the minimum zone method can be expressed as

$$F_{MZ}(X) = \min(|P_{\max}^+ - P_{\max}^-|) \quad (2)$$

where $F_{MZ}(X)$ is the minimum zone target function, and P_{\max}^+ and P_{\max}^- are sampled points with the largest deviation in one direction from the mean surface and in the opposite direction respectively.

Figure 14(b) shows the measured data and the design CAD model (upper part) and the error map (lower part) after the data matching process.

After matching of the two surfaces and generating the influence function for the polishing of the CoCr implant, corrective polishing is conducted on the implant surface with an area of $33 \text{ mm} \times 18 \text{ mm}$. The PV values before and after polishing were compared, as shown in Fig. 15. It can be seen that a tangible improvement in the form error was achieved.

4.4 Part D: Study of the effect of polishing strategy on surface generation

An orthopaedic implant is polished and the surface roughness results in different regions of the implant (see Fig. 16) are analysed. The results of surface roughness analysis in the ultraprecision polishing of an orthopaedic implant are summarized in Table 9. Figure 17 shows the surface quality before and after polishing. The arithmetic mean roughness after fine polishing for the two areas is 9.51 nm.

It is found that surface roughness is significantly reduced after a series of polishing steps applied on the implant. The arithmetic mean roughness drops from 145.4 to 9.5 nm after two steps of compensation polishing. It is interesting to note that the variation in surface roughness in different regions is very large, although after polishing this variation was reduced significantly. In other words, large surface roughness variations seen in different regions of the non-corrective technique are significantly reduced using the corrective polishing technique. The use of compensation polishing and the influence function appear to be effective not only in bringing the surface roughness to a low value but also in making the surface roughness more homogeneous throughout the continuous freeform surface of the implant.

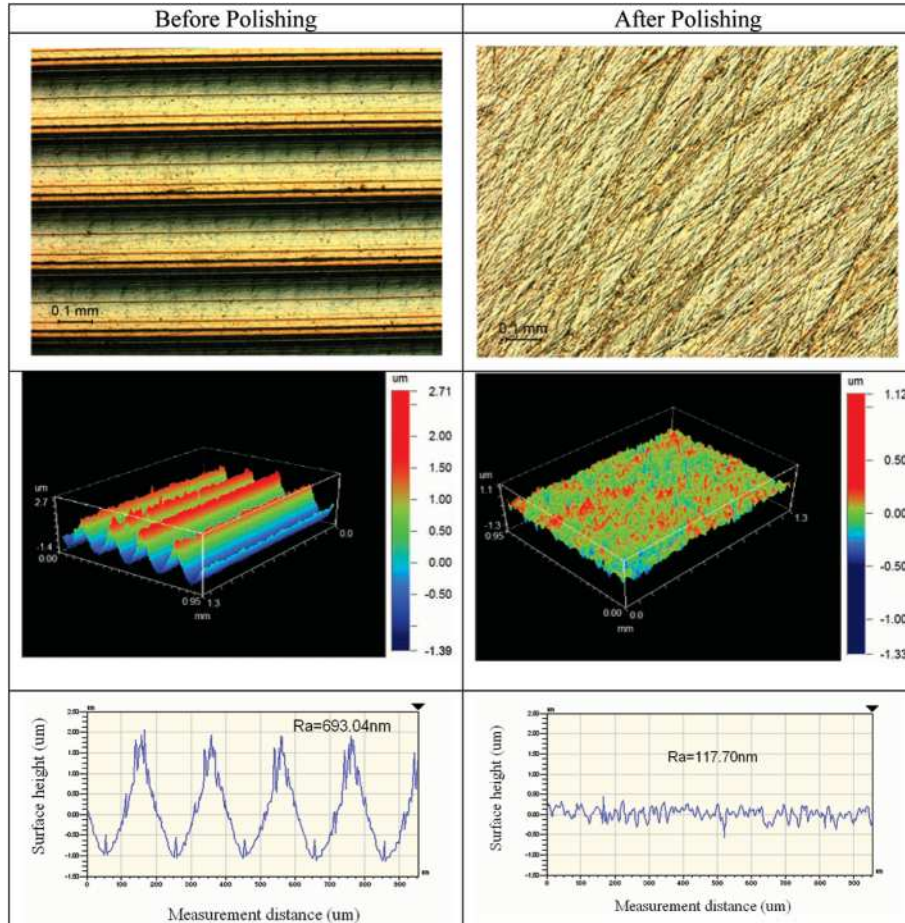


Fig. 12 Results of polishing using the optimum conditions

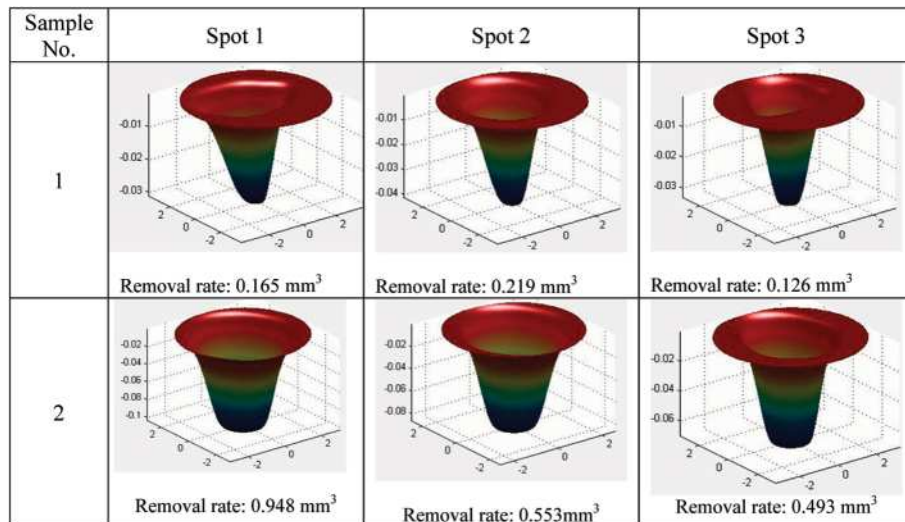


Fig. 13 Influence functions at different positions for sample 1 and sample 2

5 DISCUSSION AND FUTURE WORK

The present study focuses on experimental studies, which are not only helpful for a better understanding of the polishing mechanisms but also provides an

important means for future study. This lays the foundation for future work as proposed below:

1. *Mathematical modelling of the material removal function.* It is interesting to note that previous

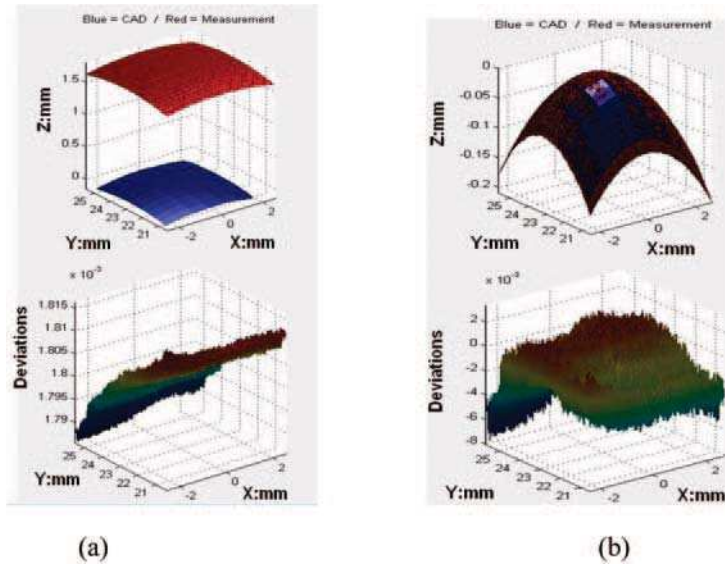
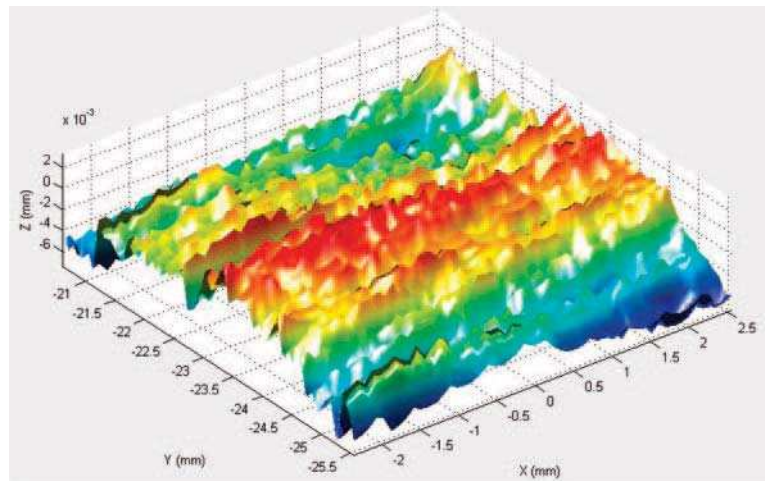
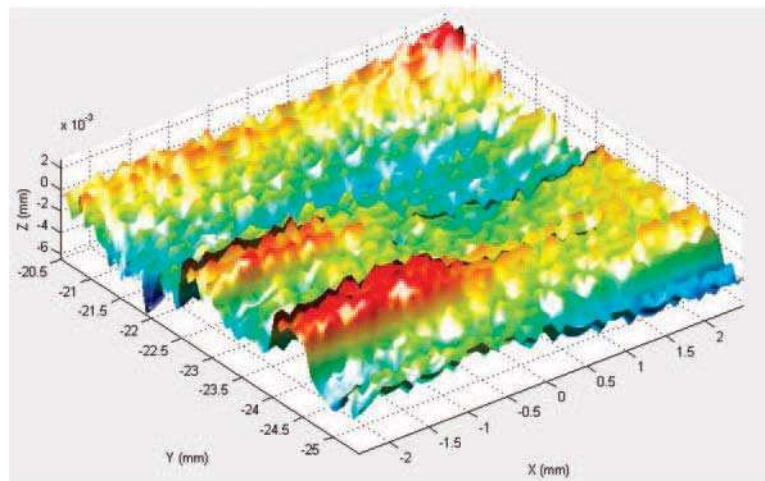


Fig. 14 (a) Before and (b) matching the measured surface and the designed surface



(a) Error map before polishing with PV 10.7756 (5mmX5mm)



(b) Error map after polishing with PV 9.1703 (5mmX5mm)

Fig. 15 Form error (a) before and (b) after polishing of the implants

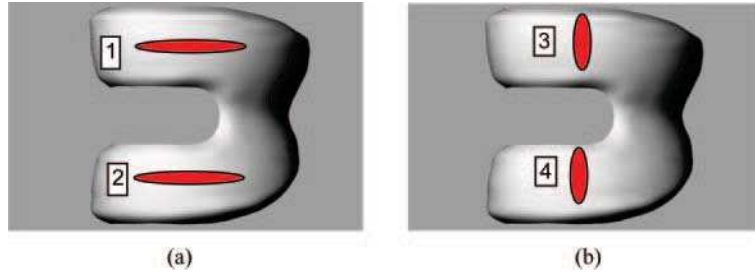


Fig. 16 Regions of analysis (a) before and (b) after corrective polishing



Fig. 17 Surface quality of the orthopaedic implant (a) before and (b) after polishing

Table 9 Results of surface roughness before and after corrective polishing

Area	Before polishing after preprocessing				After all polishing steps			
	R_a (nm)		Average (nm)		R_a (nm)		Average (nm)	
1	50.7	69.7	168.2	96.2	10.9	12.1	8.3	10.4
2	84.5	142.3	110.7	112.5	10.3	10.3	10.4	10.3
3	438.1	262.7	227.7	309.5	10.2	9.6	7.5	9.1
4	62.8	57.8	69.4	63.3	7.6	9.6	7.3	8.2

work has been conducted by Zhang and Tam [19], Zhang *et al.* [20], and Tam *et al.* [21, 22] based on analytical analysis of the material removal in polishing by fixed abrasives. This led to further study of the mathematical modelling of the material removal function. According to Preston’s theory [23], the depth of material removal at point $A(r)$ (see Fig. 18) can be expressed as

$$D(r) = k \cdot P(r) \cdot V(r) \tag{3}$$

where k is Preston’s constant, which is related to the operating conditions, $P(r)$ is the contact pressure between the polishing tool and the workpiece at point $A(r)$, and $V(r)$ is the relative velocity of the tool to the workpiece.

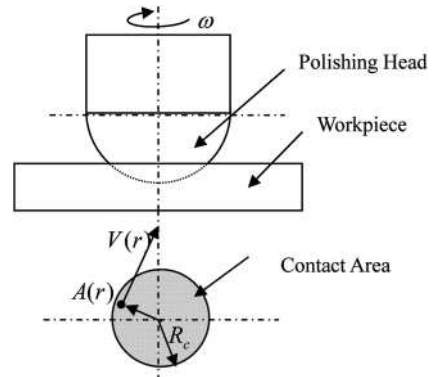


Fig. 18 Graphical illustration of the material removal function for bonnet polishing

As a result, the material removal function during a certain cycle T for a contact area of radius R_c can be expressed as

$$E = \frac{1}{T} \int_0^T \int_0^{R_c} D(r) dr dt = \frac{1}{T} \int_0^T \int_0^{R_c} k \cdot P(r) \cdot V(r) dr dt \tag{4}$$

This mathematical model of the material removal function will be further investigated in future research work.

2. *Power spectrum analysis of surface generation.* Analysis of the power spectrum of the surface roughness profiles in ultraprecision freeform polishing will be based on previous work by the present authors [24]. This allows the characteristics of the material removal function in polishing to be analysed. According to Parseval's theorem [25], surface error (R_q ; root-mean-square) over the same frequency intervals is expressed as

$$R_q = \sqrt{(\Delta f) \times \sum_{i=1}^N \text{PSD}(f_i)} \quad (5)$$

where $\text{PSD}(f_i)$ is the power spectral density of the material removal function at a specified frequency f_i , which is defined as

$$\text{PSD}(f_i) = \frac{[W(f_i)]^2}{\Delta f} \quad (6)$$

where Δf is the increment between frequencies, and $W(f_i)$ is the discrete Fourier amplitude at frequency f_i , which can be expressed by Fourier transform over the total length D

$$W(f_i) = \int_0^D E(x) \exp(-ifx) dx \quad (7)$$

3. *Process modelling.* Achieving the desired surface quality in ultraprecision freeform polishing involves the use of different polishing schedules and process parameters. It is suggested that a case-based process planning model be developed that can provide appropriate recommendations for planning of the polishing processes and polishing schedule and for using the optimum combination of machining parameters for ultraprecision polishing of different types of surface made of different materials.

6 CONCLUSIONS

In this paper, a study of factors affecting the surface generation in ultraprecision freeform polishing has been presented. A series of polishing experiments have been undertaken, and the relationships between various factors and the surface quality of the work-piece have been determined. It has been found that surface generation in ultraprecision freeform polishing is significantly affected by the influence function and process parameters. There are optimum polishing conditions with which better surface generation and surface quality are obtained. Moreover, Taguchi

analysis is demonstrated to provide a useful means for determining the optimum conditions for polishing, so that the number of time-consuming and costly trial polishing experiments can be significantly reduced. On the other hand, the influence function is found to depend on the geometry of the surface being polished. Hence, the process flow for the determination and use of the influence function has been experimentally verified and proven to be effective for corrective polishing. It is also interesting to note that the polishing strategy, in terms of the number of steps and the conditions used at each step, plays an important role in ensuring surface quality in ultraprecision freeform polishing. On the whole, the results in the present study provide an important means for a better understanding of the factors affecting nanosurface generation in ultraprecision freeform polishing and hence the fabrication of superfinished orthopaedic implants for biomedical applications.

ACKNOWLEDGEMENTS

The authors would like to express their sincere thanks to the Research Committee of Hong Kong Polytechnic University and to the Technology Commission of the Government of the Hong Kong Special Administrative Region of the People's Republic of China for financial support of the research work under project numbers G-YF55 and GHP/052/06 respectively. Many thanks are also due to Zeeko Ltd for technical support, and to Universal Photonics for providing polishing materials for the research work.

© Authors 2010

REFERENCES

- 1 **Qin, S., Wright, D. K., Kang, J., and Prieto, P. A.** Use of three-dimensional body motion to freeform surface design. *Proc. IMechE, Part B: J. Engineering Manufacture*, 2006, **220**(B2), 335–339. DOI: 10.1243/095440506X77616.
- 2 **Yin, D., Liu, X., Zheng, Z. R., and Gu, P. F.** Secondary optical design for LED illumination using a freeform lens. In Proceedings of SPIE, Glasgow, UK, 2 September 2008, 2008, vol. 7103, pp. 71 030–71 038 (SPIE, The International Society for Optical Engineering, USA).
- 3 **Curodeau, A., Sachs, E., and Caldarise, S.** Design and fabrication of cast orthopedic implants with freeform surface textures from 3-D printed ceramic shell. *J. Biomed. Mater. Res.*, 2000, **53**, 525–535.
- 4 **Blunn, G. W., Joshi, A. B., Minns, R. J., Lidgren, L., Lilley, P., Ryd, L., Engelbrecht, E., and Walker, P. S.** Wear in retrieved condylar knee arthroplasties. A comparison of wear in different designs of 280 retrieved

- condylar knee prostheses. *J. Arthroplasty*, 1997, **12**, 281–290.
- 5 Evans, C. J., Paul, E., Dornfield, D., Lucca, D. A., Byrne, G., Tricard, M., Klocke, F., Dambon, O., and Mullany, B. A. Material removal mechanisms in lapping and polishing. *Ann. CIRP – Mfg Technol.*, 2003, **52**, 611–633.
- 6 Xie, Y. S. and Bhushan, B. Effects of particle size, polishing pad and contact pressure in free abrasive polishing. *Wear*, 1996, **200**, 281–295.
- 7 Jacobs, S. D. Manipulating mechanics and chemistry in precision optics finishing. *Sci. Technol. Advd Mater.*, 2007, **8**, 153–157.
- 8 Hilerio, I., Mathia, T., and Alepee, C. 3D measurements of the knee prosthesis surfaces applied in optimizing of manufacturing process. *Wear*, 2004, **257**, 1230–1234.
- 9 Chang, K. H. and Tang, P. S. Integration of design and manufacturing for structural shape optimization. *Adv. Engng Software*, 2001, **32**, 555–567.
- 10 Axinte, D. A., Kritmanorot, M., Axinte, M., and Gindy, N. N. Z. Investigations on belt polishing of heat-resistant titanium alloys. *J. Mater. Processing Technol.*, 2005, **166**, 398–404.
- 11 Gharbia, Y. A. and Katupitiya, J. Loose abrasive blasting as an alternative to slurry polishing of optical fibre end faces. *Int. J. Mach. Tools Mf.*, 2003, **43**, 1413–1418.
- 12 Choi, J. Y. and Jeon, H. A study on polishing of molds using hydrophilic fixed abrasive pad. *Int. J. Mach. Tools Mf.*, 2004, **44**, 1163–1169.
- 13 Seo, Y. J., Kim, N. H., and Lee, W. S. Temperature effects of pad conditioning process on oxide CMP: polishing pad, slurry characteristics, and surface reactions. *Microelectronic Engng*, 2006, **83**, 362–370.
- 14 Kim, J. D., Kang, Y. H., Bae, Y. H., and Lee, S. W. Development of a magnetic abrasive jet machining system for precision internal polishing of circular tubes. *J. Mater. Processing Technol.*, 1997, **71**, 384–393.
- 15 Zeeko Ltd. Products, IRP200. Available from http://www.zeeko.co.uk/index.php?option=com_content&task=view&id=19&Itemid=82 (access date January 2009).
- 16 Bingham, R. G., Walker, D. D., Kim, D. H., Brooks, D., Freeman, R., and Riley, D. Novel automated process for aspheric surfaces. In Proceedings of SPIE, San Diego, California, 2–4 August 2000, 2008, vol. 4093, pp. 445–450 (SPIE – The International Society for Optical Engineering, USA).
- 17 Charlton, P. and Blunt, L. Surface and form metrology of polished ‘freeform’ biological surfaces. *Wear*, 2009, **264**, 394–399.
- 18 Lewandowski, H. S. and Lindeke, R. R. An automated method for the preparation of orthogonal arrays for use in Taguchi designed experiments. *Comput. Ind. Enging*, 1989, **17**, 502–507.
- 19 Zhang, L. and Tam, H. Y. Prediction of materials removal in polishing free-form surfaces with fixed abrasives. *Key Engng Mater.*, 2004, **257–258**, 423–428.
- 20 Zhang, L., Tam, H. Y., Yuan, C. M., Chen, Y. P., and Zhou, Z. D. An investigation of materials removal in polishing with fixed abrasives. *Proc. IMechE, Part B: J. Engineering Manufacture*, 2002, **216**(B1), 103–112. DOI: 10.1243/0954405021519591.
- 21 Tam, H. Y., Zhang, L., and Hua, M. Material removal by fixed abrasives following curved paths. *Proc. IMechE, Part B: J. Engineering Manufacture*, 2004, **218**(B7), 713–720.
- 22 Tam, H. Y., Hau, M., and Zhang, L. Aspheric surface finishing by fixed abrasives. *Int. J. Advd Mfg Technol.*, 2007, **34**(5–6), 483–490.
- 23 Preston, F. W. The theory and design of plate glass polishing machines. *J. Soc. Glass Technol.*, 1927, **11**, 214–256.
- 24 Cheung, C. F., Chan, K. C., and Lee, W. B. A power spectrum analysis of surface generation in ultraprecision machining of Al/SiC metal matrix composites. *Mater. Mfg Processes*, 2003, **18**(6), 929–942.
- 25 Wikipedia, Parseval’s theorem. Available from [http://en.wikipedia.org/wiki/Parseval’s_theorem](http://en.wikipedia.org/wiki/Parseval's_theorem) (access date May 2009).